This is to certify that the
dissertation entitled

CHANGES IN ATMOSPHERIC CIRCULATION OVER EUROPE AND THE RELATIONSHIP TO TEMPERATURE EXTREMES IN BULGARIA

presented by

Galina Stefanova Guentchev

has been accepted towards fulfillment
of the requirements for the

Doctoral degree in Geography

Major Professor's Signature

August 2, 2007

Date

DATE DUE	DATE DUE	DATE DUE

CHANGES IN ATMOSPHERIC CIRCULATION OVER EUROPE AND THE RELATIONSHIP TO TEMPERATURE EXTREMES IN BULGARIA

Volume I

By

Galina Stefanova Guentchev

A DISSERTATION

Submitted to
Michigan State University
in partial fulfillment of the requirements
for the degree of

DOCTOR OF PHILOSOPHY

Department of Geography

2007

CH

relat

major

circula

secon

assoc

classi

doma

of the

basel

detai

resea

2004

domi

persis

in rep

locat

ABSTRACT

CHANGES IN ATMOSPHERIC CIRCULATION OVER EUROPE AND THE RELATIONSHIP TO TEMPERATURE EXTREMES IN BULGARIA

By

Galina Stefanova Guentchev

Large-scale atmospheric circulation patterns over Europe and their relationships to extreme temperature events in Bulgaria were investigated. The major goals were to 1) develop a classification scheme of sea-level pressure circulation patterns, 2) identify changes in temperature extremes during the second half of the 20th century, and 3) determine the circulation patterns associated with the temperature extremes. A comprehensive two-tier classification of the atmospheric circulation for the European/North-Atlantic domain was developed using principal components and cluster analysis. One tier of the classification comprises 'supertype' patterns and is appropriate for baseline analysis of circulation frequency and persistence. The second, more detailed, tier consists of 'circulation types' and can be used to address applied research questions. Changes in the frequency of the supertypes during 1951-2004 were evident for all seasons except for spring. In general, the supertypes dominated by anticyclones or positive anomalies increased in frequency and persistence, whereas the supertypes dominated by cyclonic features decreased in frequency and persistence.

Significant changes in indices of temperature extremes at several locations in Bulgaria have occurred in two sub-periods of the 20th century, defined

as the

negati

tempe

durati

degre

and a

for th

perio

maxi

for th

indic

unorg

dum

insig

as the early (1951-1979) and late (1973-1999) sub-periods. In 1951-1979, negative trends were observed in the magnitude of the extreme maximum temperature in fall, annual and summer daily temperature range, number and duration of heat waves, average length of cold spells, and number of cooling degree days, for example. A positive trend was observed in the magnitude of the annual and springtime extreme minimum temperature. For most indices, trends for the late sub-period have opposite signs compared to those for the early sub-period. In addition, projected return levels were higher for indices derived from maximum temperature and lower for those derived from minimum temperature, for the late period compared to the early period.

A comparison of the circulation types with the temperature extremes indicated that heat waves in summer occur when Bulgaria is located within an unorganized zone of higher pressure or a thermal low, while cold spells occurred during northerly or easterly airflow. The derived classification presents useful insights on the circulation responsible for temperature extremes in Bulgaria.

DEDICATION

To

My family,

who made all of this possible,

with their endless encouragement and patience.

ACKNOWLEDGEMENTS

It has been a special pleasure working with the faculty, staff and students of the department of Geography at the Michigan State University during my tenure as a doctoral student. This work would never have been possible were it not for the guidance, invaluable assistance and support of my advisor, Dr. Julie Winkler. I would like to particularly thank Dr. Andresen, Dr. Nurnberger and Dr. Pigozzi for their kind attention, for their helpful advice and most of all for their patience. I would also like to thank Dr. Black for agreeing to become a member of my committee on a short notice. I was very fortunate to have established contacts with Dr. Wijngaard, Dr. Gilleland, Dr. Choulakian and Dr. Stephens, who offered counsel during the preparation of this dissertation. Also, I would like to thank Ms. Sharon Ruggles for her utmost professionalism, her assistance on any perplexing matter the graduate studies might offer and her kind encouragement throughout the years. I am extremely geatful to Mr. Jim Brown and Mr. Wilson Ndovie for their help on any computer-related issues that appeared. Finally, I would like to say a heartfelt "Thank you" to Jeanne Bisanz, Krerk Piromsopa, Claudia Walters and Jenni Van Ravensway for being great friends and supporting me through this challenging process, and to all of my professors who taught me trough the years at MSU.

Chap

1. M
2. P
3. C

Chap

1. I
1
1

2. D

3. M

3

3
3
3
3

3

3
3
3
3
3
3

3

3

3

4. R
4

Table of Contents

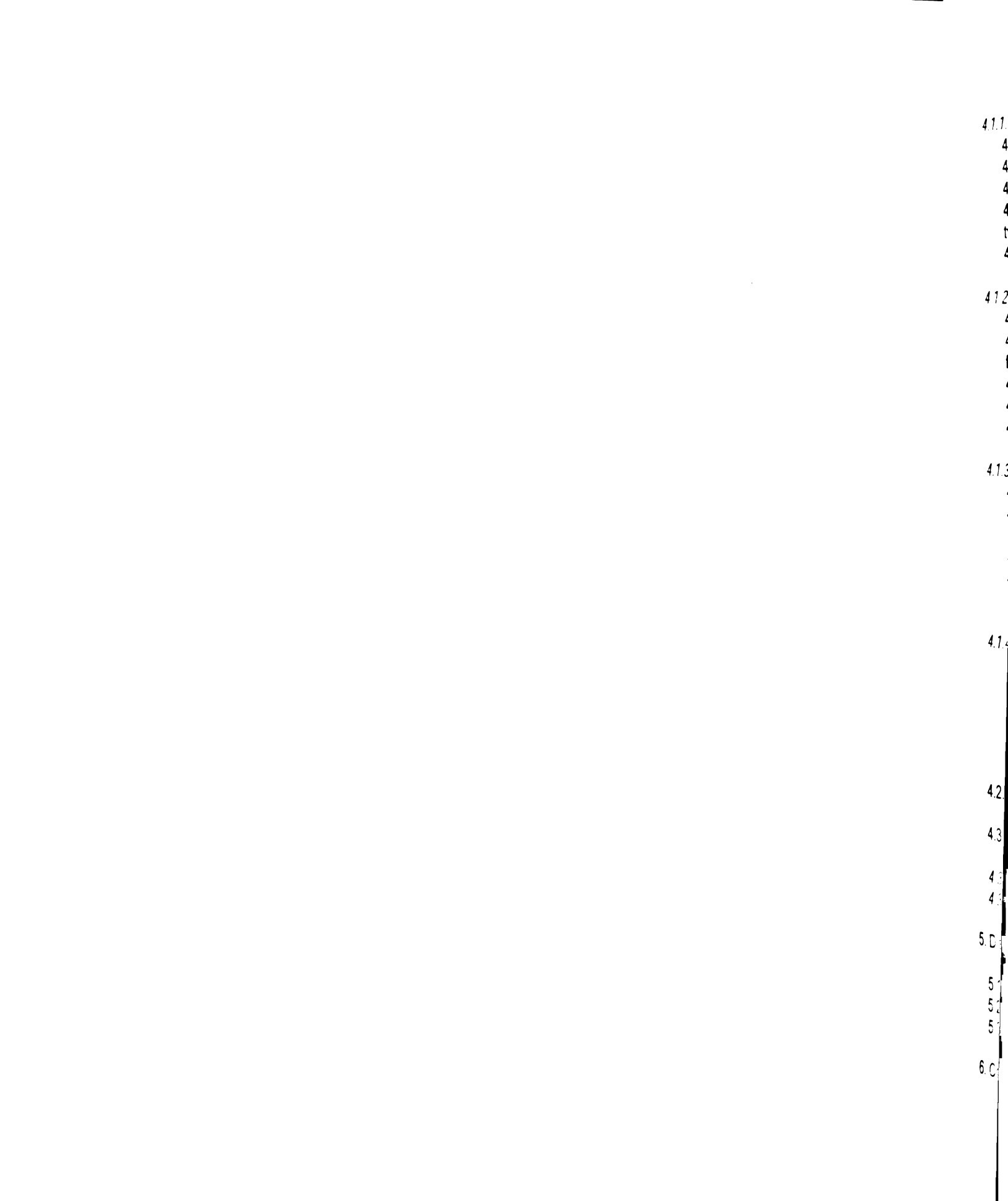

Chap
Buga

1. I
1
1
1
1
1

2. S
2
2

3. C

4. H
4
4
4
4
4
4
4
4
4
4

5. S

6. C

7. M
late
7
7

List of Tables

List of Figures

Cha

Exam
the 19
centur
trend
estima
2007).
for the
increas
occurre
means
the mea
over sp

change
events
natural
limited
Human
damage
In addi
extreme

Chapter 1 – Introduction

Climate fluctuations affect extensive regions if not the entire planet. Examples since the pre-industrial era (the 1880s) are the warming observed in the 1940s and the cooling of the 1960s. However, the last decades of the 20th century and the beginning of the 21st century are characterized by a warming trend that is unprecedented in recent history. Global mean temperature is estimated to have increased by 0.74°C from 1906 through 2005 (IPCC FAR, 2007). Moreover, the trend over the last 50 years is almost twice as large as that for the last 100 years (0.13°C/decade, IPCC, FAR, 2007). The observed increases in mean temperature on global and regional scales could affect the occurrence of extreme temperature events. Since the relationships between the means and the extremes of a distribution are nonlinear, even a small change in the mean can result in a large change in the frequency of temperature values over specified thresholds (Mearns et al., 1984).

Many researchers (e.g., Easterling et al., 2000a) are concerned that changes in the frequency and intensity of the extreme weather and climate events could greatly affect human society and the environment. Society and the natural environment have adjusted to the mean climate and can tolerate well a limited range of deviations around the mean (Salinger and Griffiths, 2001). Human and natural systems, however, are less able to adapt without stress and damage to increasingly extreme climatic conditions (Salinger and Griffiths, 2001). In addition, over the last decades, human society has become more vulnerable to extreme weather (Kunkel et al., 1999) since population has increased in areas

susce

2000b

result

for exa

1995, a

temper

import

extrem

change

affect t

scale a

exampl

underly

importa

addition

tempera

changes

tempera

these ex

atmosph

circulatio

area of ir

susceptible to extremes such as extreme temperature events (Easterling et al., 2000b). In recent years, catastrophic extreme temperature events have occurred resulting in high human mortality rates (Easterling et al., 2000a). These include, for example, the heat waves in Europe in 1994 and 1995, the U.S. heat wave of 1995, and the intense heat wave in western Europe in 2003. Thus, research on temperature extremes and their regional and local implications is of utmost importance, especially for areas identified as being vulnerable to climatic extremes. It is imperative to explore not only the historical characteristics and changes in temperature extreme events, but also the underlying factors which affect the spatial and temporal distribution of these extremes.

Temperature extremes occur as a result of the interaction between large-scale atmospheric circulation and the local characteristics of a place (for example, topographical features and altitude). To better understand the underlying causes for the occurrence of temperature extreme events, it is important to identify the circulation patterns associated with these events. In addition, baseline knowledge of the historical temporal and spatial variations of temperature extremes has to be established in order to relate the observed changes in atmospheric circulation to trends in the frequency and intensity of temperature extremes, and also to be able to assess potential future changes in these extremes. To address the questions about the relationships between the atmospheric circulation and temperature extreme events, an atmospheric circulation catalogue is needed which is spatially and temporally relevant to the area of interest and to the period of study.

specifi

singled

Panel

impact

capaci

2001).

econor

during

impacts

transitio

Mediter

comple

of their

the curr

occurre

1. Majo

T

atmosph

three ma

Th

that can

The area of interest in this research is the Balkan Peninsula, and more specifically Bulgaria. This choice was prompted by the fact that the Balkans were singled out in the Third Assessment Report (TAR) by the Intergovernmental Panel on Climate Change (IPCC) as one of the areas where more adverse impacts of potential climate change could be expected due to lesser adaptive capacity resulting from a lower level of economic development (Cramer et al., 2001). Bulgaria is undergoing a difficult transition from a centrally planned economy towards an open market economy, and the difficulties encountered during this transitional period may be aggravated even more by the adverse impacts of temperature extremes. Furthermore, the country is located on the transition between two climate zones, temperate continental in the north and Mediterranean continental climate in the south, which contribute to the complexity of the temporal and spatial distribution of temperature extremes and of their relationships with atmospheric circulation. Hence, an important focus of the current study is to identify atmospheric circulation patterns which favor the occurrence of temperature extreme events in Bulgaria.

1. Major research objectives and specific questions

The broad goal of this research is to better understand the changes in atmospheric circulation and temperature extremes in Bulgaria. The study has three major objectives.

The first major objective is to develop a Europe-wide classification scheme that can be applicable to different research agendas and various regions in

Europ

these

betwe

the ex

locate

catalo

the La

(Jone

(1957

classif

Simon

weste

Europe

classif

classif

distribu

(2000)

airflow

catalog

relation

Howeve

relative

Europe. Although atmospheric circulation catalogues are currently available, these classifications are not appropriate for investigating the relationships between atmospheric circulation and temperature extremes in Bulgaria. Most of the existing classifications were developed for limited areas spatially, often located far from Bulgaria. Examples include: a) the Hess-Brezowsky subjective catalogue (1969) which emphasizes circulation conditions over central Europe; b) the Lamb airflow types (1972) and the automated version of Lamb's classification (Jones et al., 1993) which focus on the British Isles; c) Péczely classification (1957) that was derived specifically for Hungary; d) Schüepp's synoptic classification (1979) of circulation patterns for the Alpine region; e) the Plaut and Simonnet (2001) classification of wintertime circulation for France, the Alps and western Europe; and f) the classification of Esteban et al. (2006) for western Europe. In addition to these classification schemes, two relatively recent classifications were developed for areas located close to Bulgaria. These classification schemes, however, are defined in terms of sea level pressure distribution and airflow anomalies specifically over Greece (Maheras et al. (2000) and/or combine location-specific surface air mass conditions with the airflow characteristics (Kassomenos et al. 2003).

Given the lack of available classifications relevant to Bulgaria, a circulation catalogue needed to be developed in order to be able to address the relationships between circulation and temperature extremes in Bulgaria. However, instead of deriving circulation patterns applicable only to research relative to Bulgaria, a broader objective emerged. That is, to develop a

compr

and di

suppor

the cor

needed

betwee

importa

project

'Harmo

regions

method

Europea

T

tempera

On a co

extreme

tempera

years (E

comprehensive, generalized classification for use for various research agendas and different regions in Europe. The need for a Europe-wide classification is supported by the fact that the variety of existing classifications hampers greatly the comparison of research outcomes between studies. A unified framework is needed, instead, for a consistent approach to studies considering relationships between circulation patterns and local or regional climates in Europe. The importance of this issue is further emphasized by the existence of a current project under the auspices of the European Science Foundation regarding the "Harmonization and applications of weather type classifications for European regions". The main purpose of this project is "to achieve a general numerical method for assessing, comparing and classifying typical weather situations in European regions" (COST action 733, http://www.cost733.org/).

Specific questions ensuing from the first major objective of this study are:

- What are the main circulation patterns that characterize the climate of Europe during each season?
- How has the frequency and persistence of the circulation patterns changed during the historical period?

The second major objective is to identify changes in the temporal trends of temperature extreme events in Bulgaria during the later half of the 20th century. On a continental scale, significant changes in temperature and temperature extremes have occurred during the 20th century in Europe. The annual mean temperature over the continent has increased about 0.95°C during the last 100 years (EEA, 2004). The number of cold and frost days has diminished, while the

freq

wav

evid

usin

1975

mini

the f

temp

temp

incre

extre

(Klein

during

tempe

higher

from 1

resultin

addition

(Heino

the colo

two in H

number

frequency of hot summer days (defined as temperature above 25°C) and heat waves has increased for the continent as a whole (EEA, 2004). Differences are evident when sub-periods are considered. For example, Klein Tank et al. (2003), using 86 stations around the continent, determined that during the cooler 1946-1975 sub-period, the frequency of warm extremes (defined as maximum and minimum temperatures above the 90th percentile) decreased. At the same time, the frequency of the cold extremes (defined as maximum and minimum temperatures below the 10th percentile) did not change, which resulted in lower temperature variability in Europe. Subsequently, in 1976-1999 the rate of increase of warm extremes was much greater than the rate of decline of the cold extremes for the entire continent, inducing a further rise in temperature variability (Klein Tank et al., 2003).

Historical changes in the temperature extremes have also been observed during the 20th century on a regional scale. Daily maximum and minimum temperatures have increased with the minimum temperature changing at a higher rate than maximum temperatures in both northern Europe (based on data from 11 stations) and central Europe (based on data from 9 stations), thus resulting in a decline in the diurnal temperature range (Heino et al., 1999). In addition, the number of frost days has declined in northern and central Europe (Heino et al., 1999). Other regional changes include a decrease in the length of the cold season in central Europe as estimated from one station in Poland and two in Hungary (Domonkos and Piotrovicz, 1998). At a finer spatial scale, the number of frost days has declined, and the duration of heat waves has

increas

Bardos

investi

researc

associa

Althoug

atmosp

relation

been la

atmosp

of count

wintertim

occurred

occurred

1998). In

under ar

increased, at the majority of stations in western Germany (Hundecha and Bardossy, 2005).

In terms of current and past climate, no research to date has explicitly investigated historical trends in temperature extremes in Bulgaria. Specific research questions, related to the second major objective, are:

- Are the temperature series obtained from Bulgarian temperature stations homogeneous and suitable for trend analysis and the analysis of return levels?
- What are the historical changes in temperature extreme events in terms of past trends and changes in projected return levels?

The third major objective is to determine the circulation patterns associated with the occurrence of temperature extremes in Bulgaria. Although some references to connections between climate in Bulgaria and atmospheric circulation characteristics exist (e.g., Velev, 1996, 1998), the relationships between circulation patterns and temperature extreme events have been largely neglected. Some associations, however, between large-scale atmospheric circulation patterns over parts of Europe and temperature extremes of countries neighboring Bulgaria, have been established. For example, wintertime extreme cold temperature events at three stations in Hungary occurred under anticyclonic conditions, while warm temperature anomalies occurred with circulation patterns with southerly or westerly flow (Domonkos, 1998). In summer, over the same region, extreme warm anomalies occurred under anticyclonic conditions, while extreme cold anomalies were more likely

with circulation patterns characterized by northerly airflow. Extreme cold events at 11 stations in south-central Europe occurred under a variety of airflow patterns including easterly airflow, northerly airflow and anticyclonic conditions, while warm extreme events occurred with southerly airflow or persistent anticyclones (Domonkos et al., 2003), Similarly, almost 75% of the heat waves at Prague-Klementinum, Czech Republic, occurred when an anticyclone was present over central Europe or over Fennoscandia, or during southwesterly or southeasterly airflow (Kysely, 2002a). Periods with summertime extreme high temperatures at 12 stations in nearby Greece occurred under westerly or northwesterly airflow or anticyclonic conditions (Katsoulis et al., 2005).

The specific research questions, related to the third major objective, are:

- Which are the circulation patterns contributing to the occurrence of temperature extreme events in Bulgaria?
- How do the changes in the frequency or persistence in the circulation patterns relate to the changes in the temperature extreme events?
- How does the atmospheric circulation classification derived as part of the first major objective perform when addressing a specific research question regarding the relationships between circulation patterns and temperature extremes in Bulgaria?

2. Phy

B

approxi

by Rom

southw

and Mo

Bulgari

meters

the top

made u

remain

location

(from n

Planina

and the

lowland

part of

of Rila a

Planina

Bulgaria

cold air

are cons

Bulgaria

2. Physiographic overview of Bulgaria

Bulgaria is situated on the Balkan Peninsula in southeast Europe between approximately 41° - 44° N and 22° - 29° E. The country is bounded to the north by Romania, to the east by the Black Sea, to the southeast by Turkey, to the southwest by Greece, and to the west by the Republic of Macedonia and Serbia and Montenegro (Figure 1-1). The area of Bulgaria is 110,993 sq km (NSI, 2004). Bulgaria's topography is quite diverse. The average altitude in Bulgaria is 470 meters (source: http://www.exploitz.com/Bulgaria-Topography-cg.php). Although the topography varies across the country, more than two-thirds of the land area is made up of plains, plateaus, or hilly land at an altitude less than 600 meters. The remainder is made up of mountainous topography with elevations in some locations greater than 1,500 meters.

The main features of the topography form latitudinal belts represented (from north to south) by the Danube Plain, the Predbalkan mountains, the Stara Planina (Balkan) mountains, the Zadbalkan valleys, the Upper-Tracian lowland, and the Rhodopi mountains (Figure 1-1). To the east of the Upper-Tracian lowland are the Sakar and Strandja mountains located in the southeastern most part of Bulgaria. Several medium high mountains as well as the high mountains of Rila and Pirin are located in the southwestern corner of Bulgaria. The Stara Planina mountain range separates the country into almost equally sized Northern Bulgaria and Southern Bulgaria, and serves as a natural barrier to the intrusion of cold air into the southern half of the country. The Rila and Rhodopi mountains are considerable obstacles to the advection of warm air into the northern half of Bulgaria.

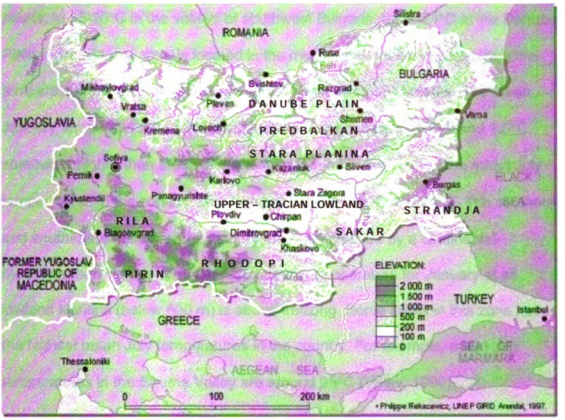

Figure 1-1 – Map of Bulgaria, from http://www.grida.no/db/maps/prod/level3/id_1264.htm - source: The Times Atlas of the World, UNEP GRID-Arendal.

The climate of Bulgaria is strongly influenced by its latitudinal extension, the altitude of the various regions, topographic features, proximity to large water bodies and the predominant atmospheric circulation (Koleva et al., 1996). The country is situated on the transition between the temperate continental climate and the Mediterranean climate. Much of Bulgaria (predominantly the territory to the north of the Stara Planina mountain and some of the valleys and mountains in southwest Bulgaria) has a temperate continental climate. The average January temperatures vary between -1°C and -8°C with the latter measured at the highest

mountai

peaks. t

Plain. A

tempera

January

somew

tempera

and sou

Mediterr

lowland

the highe

temperat

3. Orga

Th

describe

specific re

backgrou

discussion

discussion

literature;

classificati

and the ar

Chapter 3

mountain peaks. Mean July temperatures vary from 8-9°C at the high mountain peaks, to 18-20°C in the valleys of southwest Bulgaria, to 22-24°C in the Danube Plain. A transitional zone is located in the middle of the country separating the temperate continental and the continental Mediterranean climates. The mean January temperatures in the transitional zone are between –1.5°C and 1.5°C, somewhat higher than those of the temperate continental zone. The mean July temperatures in the zone of transition are between 22°C and 24°C. The southern and southeastern parts of the country are characterized by a continental-Mediterranean climate. The average monthly temperature for January at all lowland stations (below 600 m) is above freezing. Some areas in this zone have the highest mean July temperatures in the country. For example, mean July temperatures in the Struma Valley are around 25°C (Velev, 1990).

3. Organization of the dissertation

The dissertation is organized around the three major research objectives described above. Each chapter includes: a) an introduction that presents the specific research questions and elaborates on their significance; b) a background/literature review that summarizes the relevant past research; c) a discussion of the methodology; d) a presentation of the research findings; e) a discussion section that presents the results from this study in terms of relevant literature; and f) a conclusion section. Chapter 2 describes the derivation of a classification scheme of the atmospheric circulation for the European continent and the analysis of the frequency and persistence of the circulation patterns. Chapter 3 is concerned with the homogeneity analysis and the investigation of

the chan

extreme

between

temperat

and the

the changes in the temperature extremes in Bulgaria using trend analysis and extreme value analysis. Chapter 4 includes the analysis of the association between the frequency and trends in the circulation patterns and those of the temperature extremes in Bulgaria. Chapter 5 contains the overall conclusions and the directions for future work.

Chapter 2 – Atmospheric circulation classification for Europe

1. Introduction

The main centers of action[1] and elements of the atmospheric circulation that influence the European climate are the mid-latitude westerlies, the Icelandic Low, the Azores High, the Siberian High, the Mediterranean cyclones and the Asian thermal Low. It is well established that the main circulation features demonstrate seasonality of occurrence and/or intensity over Europe and the North Atlantic. The westerlies result from the strong pressure differences between the tropical and the polar regions. These winds steer the cyclonic and anticyclonic synoptic systems, thus affecting the everyday local weather over the continent, and are more than twice as strong in winter than in summer (Barry and Chorley, 2003). Although the Azores High and the Icelandic Low are evident on sea level pressure (SLP) maps throughout the year, the Azores Anticyclone is most prominent and expands over the largest area during summer (Sahsamanoglou, 1990). In contrast, the Icelandic Low displays highest intensity during winter (Serreze et al., 1997). The Gulf of Genoa is a seasonal cyclogenesis area producing the most intense Mediterranean cyclones in winter (Maheras et al., 2001). Another seasonal center is the Siberian Anticyclone which is active and well developed during the winter months. A center of action evident on the SLP maps in summer is the extension of the Asian thermal cyclone over the Arabic Peninsula and the Persian Gulf.

[1] Semi-permanent highs or lows that appear on mean charts of sea level pressure (SLP), Glossary of Meteorology, 2000, p. 122.

Th

spatial v

atmosph

of autho

recent y

atmosph

about ob

1.1. Ex

T

approac

was wid

approac

manual a

upper-le

objective

require s

known ex

Brezowsk

In additio

classifica

(Domonk

encompas

between a

The impact of the large-scale atmospheric circulation on the temporal and spatial variability of the local weather has long been of great interest. The atmospheric circulation patterns over Europe have been examined by a number of authors in the past (Hess and Brezowsky, 1969; Lamb, 1972, for example). In recent years, resurgence of the research focusing on relationships between atmospheric circulation and local climate has occurred due to increased concern about observed and future climate changes.

1.1. Existing atmospheric circulation classifications

The two main approaches to circulation classification are: a) a manual approach which depends on the subjective assessment of the researcher and was widely used before the advent of computers; and b) a computer-assisted approach, which is faster to apply and the results of which are reproducible. The manual approach is based on visual comparison of thousands of SLP and/or upper-level weather maps. The computer-assisted, sometimes referred to as objective, approach is based mostly on statistical grouping methods but also require subjective input during different stages of the classification process. Well known examples of the manual, or subjective classifications are the Hess-Brezowsky classification (1969) and the Lamb's Airflow Types (1972) for Europe. In addition, some other subjective classifications, e.g., the Schüepp's synoptic classification (Stefanicki et al., 1998) or the Péczely macrocirculation types (Domonkos, 1998) exist for Europe. The computer-assisted approach encompasses a variety of methods. Goodess and Palutikof (1998) differentiate between: a) automated classifications based on existing subjective circulation-

types cata

distinguis

numerica

grouping

analysis a

Th

the circul

recently (

the period

hPa geop

between

distinguis

meridiona

comprise

(GWL) pe

years and

artificial b

its limited

to Bulgari

boundary

The

subjective

wind direc

types catalogues (e.g. the Lamb catalogue), where parameters used to distinguish between types are represented via mathematical equations or numerical values within a given range; and b) classifications based on statistical grouping methods (i.e. principal component analysis, principal component analysis and cluster analysis, neural networks, to name a few).

The Hess-Brezowsky (1969) *Grosswetterlagen* classification emphasizes the circulation patterns over central Europe. The catalogue was expanded recently (Gerstengarbe and Werner, 1993; Gerstengarbe et al., 1999) and covers the period 1881-1998. The circulation patterns were derived using SLP and 500 hPa geopotential height (Z500) maps for an area extending approximately between 40° W – 25° E and 40° – 70° N. The classification is nested. The authors distinguish three major groups of circulation (zonal, half-meridional and meridional), subdivided into ten major types (Grosswettertypen, GWT) which comprise a total of 29 types (Grosswetterlagen, GWL). Any circulation type (GWL) persists for at least 3 days. The GWL classification was revised in recent years and is considered to be homogeneous (Gerstengarbe et al., 1999), i.e., no artificial biases or trends are present. A major disadvantage of this catalogue is its limited spatial extent. More specifically, the circulation types are not relevant to Bulgaria because a portion of the country falls outside the easternmost boundary of the Hess-Brezowsky classification.

The Lamb (1972) 'airflow types' over the British Isles were derived by subjectively classifying SLP weather maps according to pressure distribution, wind direction and observed weather. The catalogue was expanded by Hulme

and Barro

area cons

60° N. E

British Isl

unspecifi

pressure

with a de

unclassif

2001). Li

Sweeney

circulatio

systems

large scal

Isles, sma

regions.

Ad

The Pécze

Károssy, 1

of cyclonic

Schüepp's

1945-1994

direction,

surface. U

and Barrow and covers the period 1881-1995 (Hulme and Barrow, 1997). The area considered in this classification extends between 10° W – 2° E and 50° – 60° N. Eight major directional types were determined based on airflow over the British Isles, and each was further subdivided into anticyclonic, cyclonic and unspecified categories. The anticyclonic category includes days with a high pressure area dominating over the British Isles; the cyclonic consists of the days with a depression crossing or stagnating over the British Isles; and the unclassified category depicts weak and chaotic patterns (Barry and Carelton, 2001). Limitation of the Lamb classification scheme, according to O'Hare and Sweeney (1993), is its inability to categorize complex and transitional synoptic circulations. In addition, the authors point out that the size of the synoptic systems affects the weather patterns over the British Isles. For example, while large scale systems would generally bring uniform conditions over the British Isles, smaller scale cyclones would bring contrasting conditions to different regions.

Additional subjective classifications focused on limited areas in Europe. The Péczely classification of macrocirculation types (Péczely, 1957; updated by Károssy, 1987), developed for the period 1901-1991, was based on the locations of cyclonic and anticyclonic SLP centers closest to Hungary (Domonkos, 1998). Schüepp's synoptic weather types (1979) were derived for the central Alps for 1945-1994 based on the surface pressure distribution, geostrophic wind direction, upper-level wind speed and direction, and the height of the 500 hPa surface. Unlike the Hess-Brezowsky classification, Schüepp's synoptic weather

types or

(Stefani

A

Collison

thresho

al. (199

the Brit

Lamb's

and Pal

They fo

patterns

the sche

S

combina

patterns

and Gre

are that

that othe

(Esteba

(Kasson

characte

use of th

types only take into account the meteorological conditions on the considered day (Stefanicki et al., 1998).

An objective classification scheme was developed by Jenkinson and Collison (1977) which uses rules for pattern differentiation based on chosen threshold values of sea-level airflow and vorticity over the British Isles. Jones et al. (1993) used the scheme to classify SLP air flow direction and curvature over the British Isles from 1880 to 1989, and to compare the objective scheme to Lamb's airflow types. The same objective scheme was also applied by Goodess and Palutikof (1998) to classify SLP data for 1956-1989 for southeast Spain. They found that the threshold values used for differentiation of circulation patterns over the British Isles may not be appropriate for other regions. Hence, the scheme is not easily transferable.

Several researchers have applied principal component analysis (PCA) in combination with cluster analysis to derive classifications of SLP or upper-air patterns for western Europe (Plaut and Simonnet, 2001; Esteban et al., 2006) and Greece (Kassomenos et al., 2003). Disadvantages of these classifications are that some are limited to one season (e.g., Plaut and Simonnet, 2001), and that others have limited spatial extent covering only western Europe or Greece (Esteban et al., 2006; Kassomenos et al., 2003). Also, some classifications (Kassomenos et al., 2003) combine synoptic conditions with surface air mass characteristics at single location (for example, Athens, Greece) which limits the use of that classification to the location for which it was derived.

T

poin:s ir

catalogu

geopote

Accordi

any regi

Disadva

results o

influence

In

represen

focused

Maheras

cover per

specific s

classifica

to other r

they were

in cyclon

grouped t

circulation

The spatial methods of topology and geometry to define high and low points in a circulation field have also been used to derive atmospheric circulation catalogues, such as the automated classification of SLP and 500 hPa geopotential height (Z500) for Greece created by Maheras et al. (2000). Accordign to the authors, the advantage of the method is that it can be used for any region and to classify circulation at any level of the atmosphere. Disadvantages are that: a) the method is not absolutely objective; and b) the results of the classification and the frequencies of the circulation types might be influenced by trends in the data (Maheras et al., 2000).

In sum, the classifications available to date offer incomplete representations of the circulation conditions over Europe because they are focused on limited areas (Hess-Brezowsky, 1969; Lamb, 1972; Schüepp, 1979; Maheras et al., 2000, for example). Also, most of the existing patterns catalogues cover periods extending only through the 1990s, or were developed for only specific seasons (e.g., Plaut and Simmonet, 2001). In addition, some proposed classification schemes (Jenkinson and Collison, 1977) are not easily transferable to other regions. A problem with some of the earlier classifications is, also, that they were too detailed to be used to address some research questions or trends in cyclonic and anticyclonic airflow. In these cases, researchers often subjectively grouped the detailed circulation types into larger groups. Since the grouping of circulation patterns is study specific the results are difficult to compare.

1.2. Ob

directed

classifi

appropr

allow fo

compre

used to

tempera

frequen

Europe.

2. Data

the mai

Bulgaria

1996. Ki

2.5° long

ESRL/PS

reanalys

data from

and othe

this datas

unchange

(Kalnay e

1.2. Objectives

The limitations of the existing classification catalogues and schemes directed the current study towards the development of a new circulation classification that is applicable for the entire continent but general enough to be appropriate for different research agendas. A standard approach would also allow for comparison. The main objective of this part of the study is to develop a comprehensive atmospheric circulation classification for Europe which will be used to compare the changes in circulation patterns and their relationships to temperature extremes in Bulgaria. An additional objective is to investigate the frequency, persistence and trends of the derived circulation patterns over Europe.

2. Data sources and Study area

The circulation classification was based on SLP data in order to elucidate the main circulation features that influence the temperature extreme events in Bulgaria. Daily mean SLP data from the NCEP/NCAR Reanalysis (Kalnay et al., 1996, Kistler et al., 2001) were used. The Reanalysis data have a 2.5 ° latitude x 2.5° longitude spatial resolution. The data were obtained from the NOAA-CIRES ESRL/PSD Climate Diagnostics branch website at http://www.cdc.noaa.gov. The reanalysis database contains global analyses of atmospheric fields based on data from land surface observations, ship, rawinsonde, pibal, aircraft, satellite and other sources. The historical data (January 1, 1948 to present) gathered in this database are quality controlled and assimilated using a frozen (i.e., kept unchanged over the reanalysis period) "state-of-the-art analysis/forecast system" (Kalnay et al., 1996, Kistler et al., 2001). The output variables are classified in

four classe

observatio

"A" variabl

The

December

temperatu

componen

temperatu

In a

obtained fr

compare th

level circula

The

longitudina

70°N (Figur

features ov

that used in

Jones et al

Trigo et al.

four classes according to the extent to which they are influenced by the observations or the model. For example, mean SLP and geopotential height are "A" variables and are strongly influenced by observed data.

The reanalysis data used in the study extends from January 1, 1951 until December 31, 2004. The study period was determined by the availability of temperature observations for Bulgaria (starting in 1951), since an important component of this research is the investigation of the relationships between temperature extremes in Bulgaria and large-scale circulation patterns.

In addition, daily 500 hPa geopotential height (Z500) data were also obtained from the NCEP/NCAR Reanalysis. The Z500 data were used to compare the consistency between the derived patterns at SLP and the upper-level circulation features.

The study area, represented by 777 grid points (21 latitudinal rows by 37 longitudinal columns), is enclosed between 40° W and 50° E, and 20° N and 70°N (Figure 2-1). This areal extent was chosen to capture the major circulation features over the European continent and is comparable in size and location to that used in previous studies (Slonosky et al., 2000; Goodess and Jones, 2002; Jones et al., 1999; Quadrelli et al., 2001; Wibig, 1999; Maheras et al., 1999; Trigo et al., 2004; Huth, 2000; etc.).

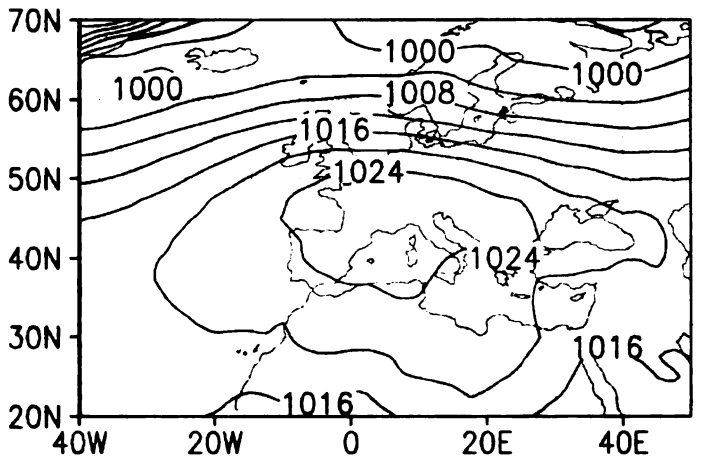

Figure 2-1 A SLP composite map illustrating the total study area

3. Methods

The combination of a principal component analysis (PCA) and a cluster analysis is one of the most frequently and successfully used classification approaches in climatological research. PCA and cluster analysis were used also in this study. The region of interest encompasses mostly mid-latitude areas, which are characterized by diverse and vigorous atmospheric circulation during most of the year. Because of the dissimilarity in circulation characteristics for the separate seasons, the PCA and the cluster analysis were applied to seasonal datasets, where winter comprised December, January and February, spring included March, April and May, summer June, July and August, and fall was represented by September, October and November.

3.1. Principal Component Analysis

Principal Component Analysis (PCA) is a technique that identifies "patterns of simultaneous variation" (von Storch and Zwiers, 1999, p.293). PCA

was used in the study to decrease the dimensionality of the data as well as to elicit the primary circulation modes of variability.

3.1. a. Input data preparation

There is divergence in the climatological literature on whether raw data, anomalies or standardized data (normalized anomalies) should be used in a PCA for a subsequent classification. Many authors have used anomalies (Quadrelli et al., 2001; Tomozeiu et al., 2002; Trigo et al., 2004; Hannachi et al., 2006; Preisendorfer 1988; etc.). Another large group of researchers have applied PCA to normalized anomalies or standardized data (Esteban et al., 2005; Maheras et al., 1999; Maheras et al., 2004; Xoplaki et al., 2000; Yarnal, 1993, among others). Huth (1995) argues that when using anomalies in PCA "the time-mean pattern is unclassifiable, and patterns close to the time mean are classified unreliably" (p. 155). Wilks (1995) indicates that unstandardized anomalies "tend to exaggerate the importance of departures in high-variability regions, and mask the importance of anomalies in low-variability regions" (p. 86). Bjornsson and Venegas (1997) point out that "strictly speaking you can find EOFs without removing any mean" (p. 8).

Disagreement exists also about the type of standardization or scaling of the data. Circulation data are usually normalized either by time or by space. Time scaling was used, for example, by Quadrelli et al. (2001), Tomozeiu et al. (2002), Maheras et al. (1999), Hannachi et al. (2006), Bjornsson and Venegas (1997), Maheras et al. (2004), Xoplaki et al. (2000), Huth (1995), Preisendorfer (1988),

and space scaling was applied by Esteban et al. (2005), Bretherton (2000), Trigo et al. (2004), and Yarnal (1993), to name a few. Space standardization scales all the grid points to have the same variance, although stationarity will not be attained if analysis is done on an annual basis as the data will still display seasonality. Time standardization results in a stationary process since all the days are forced to have the same variance for each grid point. The spatial differences of the high and low latitudes, i.e. the "space" variability, are retained.

Normalized (or standardized) anomalies were used in this study. This choice was prompted by the concern that unstandardized anomalies tend to amplify or to obscure the importance of departures in regions with diverse variability. The normalized anomalies were obtained by subtracting from each value the sample mean of the SLP series and dividing by the sample standard deviation. Initially, the SLP daily data were standardized separately by time and by space. PCA analyses were run on both datasets and compared. The outcome of this comparison is discussed later in the text.

3.1. b. Mode of decomposition and dispersion matrix

Although six possible modes of decomposition exist for PCA (Rummel, 1967), in synoptic climatology the most commonly used modes are "P" and "S" (Yarnal, 1993). P-mode analyzes a set of variables changing over time and is used mainly for synoptic typing, whereas S-mode focuses on one variable varying over space and is applied in map-pattern classification and regionalization (Yarnal, 1993). In some recent publications, Huth (1995, 2000)

recomm

and the

patterns

of T-mo

dispropo

cases.

G

using ar

columns

decision

choice c

S

althoug

previous

types ha

Jones e

Huth, 19

and Gra

similarit

intensity

covarian

data in s

areas w

recommended the use of PCA in a T-mode (where the gridpoints are the rows and the daily patterns are the columns) for the classification of circulation patterns. In a later study (Huth, 2001), however, he indicated that the application of T-mode PCA to very large data sets is difficult, probably because of the disproportionately larger number of variables in comparison to the number of cases.

Given the objectives of this study, the SLP data were subjected to a PCA using an S-mode decomposition, where the rows were the days or cases and the columns were the gridpoints or the variables. Another consideration in this decision was the very large data set for the study period, which eliminated the choice of a T-mode PCA.

S-mode PCA can be performed on different types of similarity matrices, although most often correlation or covariance matrices are used. The majority of previous studies concerned with the frequency and persistence of circulation types have used correlation matrices (Slonosky et al., 2000; McGinnis, 2000; Jones et al., 1999; Esteban, et al., 2005; Tomozeiu et al., 2002; Wibig, 1999; Huth, 1995, 1997; Barnston and Livezey, 1987; Galambosi et al., 1996; Slonosky and Graham, 2005, for example). According to Yarnal (1993), when a correlation similarity matrix is used, only map-pattern shapes are generated, and the intensity of the features is not considered. On the other hand, the use of a covariance matrix, while more accurate in displaying the actual deviations of the data in space, will lead to a concentration of the pressure or height centers in the areas with maximum variance (Yarnal, 1993) and also may lead to ingnoring of

meaningful dimensions. Based on an analysis of circulation types from synthetic data, Huth (1995) found that the solutions using correlation and covariance matrices were very similar and that the choice of a covariance or correlation matrix has little impact on the results. Galambosi et al. (1996), however, recommend that different dispersion matrices be used depending on the type of data scaling. They suggested using a product or second moment matrix with no scaling of the data, a covariance matrix with anomalies, and a correlation matrix with standardized data. This study uses a correlation similarity matrix calculated from the standardized SLP gridpoint values. The correlation matrix is used because the focus in this study is primarily on the shape and placement of the circulation features rather than their intensity.

3.1. c. Rotation

Many authors (Horel, 1981; Yarnal, 1993; Wilks, 1995, among others) agree that a rotation (orthogonal or oblique) allows for easier interpretation of the retained principal components in terms of circulation modes. Moreover, Richman (1986) warns that unrotated Empirical Orthogonal Functions (EOF[2]) or PCA patterns are domain shape dependent (i.e., the patterns are determined by the shape of the domain rather than the covariation among the data) and characterized by sub domain instability. Sub domain instability means that the component patterns identified for Northern Hemisphere may not be reproducible if a sub region is analyzed. Richman also states that unrotated solutions have

[2] The terms 'EOF analysis' and 'PCA' "refer to the same set of procedures", Wilks, 1995, p.373.

sampl

becom

than a

unrota

the da

unrota

orthog

since i

Varima

facilita

of subj

3.1. d

rotate.

princip

explain

that ex

and Ri

compo

leads t

more s

by dist

sampling errors, in other words "the information from population patterns can become mixed up when samples are drawn with eigenvalues separated by less than a specific value" (Richman, 1986, p. 298). Richman also argues that the unrotated solutions are unable to portray accurately the physical relationships of the data matrix. Richman (1986) demonstrates that the disadvantages of unrotated solutions can be minimized by rotation. Although different types of orthogonal rotations exist, Varimax orthogonal rotation was used for this study since it is the most widely applied in climatological research. In addition, the Varimax rotation maximizes the variance of the loadings of the variables, thereby facilitating interpretation. Oblique rotation was not considered due to the number of subjective decisions that need to be made during its application.

3.1. d. How many PCs to retain?

There are several considerations for choosing the number of PCs to rotate, but the two most frequently used in climatology are to: a) rotate all principal components (PCs) with eigenvalues > 1 since each retained PC explains the variance equivalent ot at least one variable, and b) include all PCs that explain at least 5 percent of the total variance. However, both Stone (1989) and Richman (1986) caution that it is better to over factor than to retain too few components. O'Lenic and Livezey (1988) also point out that while over factoring leads to "excessive regionalization of large-scale patterns", under factoring is a more serious problem because of the "loss of signal which is often accompanied by distortion of the patterns".

compo

used a

then ro

rotated

compo

were n

occurre

compo

examin

associa

numbe

(Table

over fa

compa

retaine

with the

compo

several

An iterative approach was used to select the number of rotated components for this study. The number of components with eigenvalues > 1 was used as the initial estimate of how many PCs to retain. These components were then rotated and the loadings of the original variables (i.e., grid points) on the rotated components were examined. The variable loadings for several components were small (defined as < 0.5), suggesting that these components were not strongly associated with any grid point and that over factoring had occurred. The rotation was then performed with a smaller number of components, and again the variable loadings for each rotated component were examined to ensure that at least one grid point was moderately (loading > 0.5) associated with each component. This process continued until the maximum number of rotated components each with at least one loading > 0.5 was identified (Table 2-1). This approach attempted to balance the desire to error on the side of over factoring yet retain components that are physically interpretable. In comparison, a considerably larger number of components would have been retained using the "eigenvalue > 1" rule, but many with only small correlations with the grid points, suggesting over factoring. On the other hand, all the components extracted using the "variance greater than 5 percent" rule had several very high (greater than 0.80) loadings, suggesting under factoring.

Table
exp

Rule
Eigen
5% e
var
Rotat
with l
>

revealin
standar
fields. I
similarit
most pr
to contir

3.2. Clu

T

the maps
importan

Table 2-1 Example of number of PCs to be retained according to the different rules (% of explained total variance given in parentheses) using time-standardized data matrix

Rule/Season	Winter	Spring	Summer	Autumn
Eigenvalues > 1	31 (97.3%)	36 (96.9%)	44 (96.3%)	35 (97.1%)
5% explained variance	6 (71.7%)	6 (66.1%)	6 (61%)	6 (68.4%)
Rotated PCs with loadings > 0.5	11 (86.9%)	14 (87.9%)	16 (85.3%)	9 (80.8%)

The loadings were mapped for each of the rotated principal components, revealing spatial modes of SLP variation. The maps based on the time-standardized SLP fields were compared to those based on space-standardized fields. In spite of a difference in the number of retained components, a close similarity between the patterns was found. This correspondence, and the fact that most previous authors have used time-standardized data, prompted the decision to continue the research with the time-standardized SLP data only.

3.2. Cluster Analysis

The component loadings maps are not actual pressure surfaces. Instead, the maps represent modes of low-frequency variability, and some illustrate important teleconnections patterns. To identify circulation types, the scores of the

daily grids on the retained components need to be subjected to a cluster analysis in order for the most common combinations (i.e. circulation types) to be determined (Yarnal, 1993).

Cluster analysis groups data based on a given measure of similarity or dissimilarity between the individual values and/or groups of values. The main objective of this technique is to obtain high within-cluster homogeneity and high between-cluster heterogeneity (Hair et al., 1998). There are many subjective decisions that are made during a clustering process which introduce uncertainty in the results.

3.2. a. Choice of clustering algorithm

Whether hierarchical or non-hierarchical clustering techniques should be used depends to a great extent on the research objectives. Hierarchical methods combine the data in such a way that the groups at a given stage are nested within the groups of the subsequent stages of the clustering process (Hair et al., 1998). On the other hand, non-hierarchical methods distribute the data into a predefined number of clusters according to the similarity or dissimilarity of the values to initial cluster seeds. Both groups of methods have advantages and disadvantages. One of the main shortcomings of the hierarchical methods is that the cluster membership cannot be changed later in the process. A drawback of the non-hierarchical methods is their dependence on the initial choice of seeds for the clusters. Frequently, in order to overcome the shortcomings of both methods, a combination of hierarchical and non-hierarchical procedures is employed. The hierarchical procedure is used to suggest the number of seeds or

clusters

groupin

A

study. F

minimur

method

perhaps

reason

have bia

of cluste

Ward's

member

similarity

were ap

standard

because

the point

the anal

multiplie

standard

clusters, and then the non-hierarchical method is used to arrive at the final groupings.

A combined hierarchical/non-hierarchical approach was also used for this study. First, two well known hierarchical methods (average-distance and Ward's minimum variance methods) were applied to the component scores. Both methods are widely used in climatology, with the average distance method perhaps the most frequently employed clustering procedure (Wilks, 1995). The reason that more than one hierarchical procedure was used is that both methods have biases. While the average-linkage method is "biased toward the production of clusters with approximately the same variance" (Hair et al., 1998, p.496), the Ward's method is biased toward producing clusters with almost equal number of members. For both methods, Euclidean distance was used as the measure of similarity between the observations. The two hierarchical clustering procedures were applied to non-standardized PC scores. According to Johnson (1998), non-standardized rather than standardized scores should be used in cluster analysis because standardized scores do not realistically represent the distances between the points (observations). Since SAS (the statistical software package used for the analysis) only outputs standardized components scores, the scores were multiplied by the square root of the corresponding eigenvalue to obtain the non-standardized scores.

3.2. b

resear

have b

[1985]

use at

(Kalkst

among

.

the out

hierarch

a

packag

appropr

than 3 (

b

1998). T

clusters

1998). C

c

on a plo

applied

best per

Calinski

3.2. b. Stopping rules

Selecting the level of detail, i.e., the number of clusters for a specific research question has always been a difficult decision. A variety of stopping rules have been developed (see Cooper and Milligan [1984], and Miligan and Cooper [1985] for a relatively complete listing of stopping criteria), and many researchers use at least one objective criterion to choose the final number of clusters (Kalkstein et al., 1987, Wilks, 1995; Fovell and Fovell, 1993; Johnson, 1998, among others).

The choice of the stopping rules in this study was in part determined by the output available from the SAS statistical package for the Ward's and Average hierarchical methods. The stopping criteria used here are:

a) the Cubic Clustering Criterion (CCC, Ray (1982), proprietary to the SAS package). The CCC is usually plotted against the number of clusters. On this plot appropriate numbers of clusters will correspond to peaks with CC criterion larger than 3 (Johnson, 1998).

b) the Hotelling Pseudo-t^2 statistic (PST2, recommended by Johnson, 1998). The Hotelling PST2 statistic evaluates the means of two clusters. The two clusters could be combined if the means are not significantly different (Johnson, 1998). Choose the level before a relatively large PST2 value is observed.

c) the combined Pseudo-F and Pseudo-T^2 statistics. A stopping rule based on a plot of the Pseudo-F statistic in combination with the Pseudo-T^2 statistic, as applied by Fovell and Fovell (1993), was used as well. This rule unites the two best performing, according to Milligan and Cooper (1985), stopping rules: the Calinski and Harabasz, and the Duda and Hart criteria. The Calinski and

Haraba
sum of
The Du
sum of
can be
with th
followe
clusteri
1987; D
clusteri
Fovell a
betwee
betwee
betwee
such a
plots of
these p
multiple
yielded

Harabasz (1974) "pseudo-F" criterion is based on the among- and within-cluster sum of squares, as well as the number of objects and the number of clusters. The Duda and Hart (1973) "Je(2) / Je(1)" criterion is a ratio of the within-cluster sum of squared errors before and after the grouping of two clusters. This criterion can be transformed into the "Pseudo-T^2" statistic which is plotted in combination with the Pseudo-F statistic. Look for local peaks in the pseudo-F statistic that are followed by sudden jumps in the pseudo-t^2 for the next clustering level. Choose clustering levels that precede particularly large or disparate mergers.

d) the R^2 or the proportion of the explained variance (Kalkstein et al., 1987; Davis and Kalkstein, 1990). The explained variance is plotted against the clustering step. The clustering procedure is terminated before a sharp drop in R^2.

e) the distance between the clusters merged at each step (Wilks, 1995; Fovell and Fovell, 1993). At the beginning of the clustering process the distances between merged clusters are small at each step. A point where the distances between grouped clusters jump sharply is indicative of increased dissimilarity between the clusters, and the clustering process should be terminated before such an abrupt increase.

As noted above, most of the rules recommend finding local peaks in the plots of the criteria and considering the cluster steps corresponding to or before these peaks as the appropriate numbers of clusters. Many of the plots feature multiple peaks at different levels of detail, so the stopping rules used in this study yielded multiple candidate numbers of clusters per criterion for each hierarchical

clustering

given in Fi

Table 2-2

Stoppin rules
1. CCC Plot
2. Hotelling Pseudo-t statistic – PST2 Plot

clustering method (Table 2-2). The stopping criteria plots for all the seasons are given in Figure 2-2, Figure 2-3, Figure 2-4 and Figure 2-5.

Table 2-2 Results of the application of different stopping rules for the cluster analysis for all the seasons
(The numbers for each season indicate the candidate numbers of clusters)

Stopping rules	Suggested clustering level by Average method	Suggested clustering level by Ward method	Comments / Description of selection criterion
1. CCC Plot	WINTER - 6, 10, 15, 19, 26, 33 SPRING – 8, 18, 46 SUMMER – 14, 19, 28 AUTUMN – 19, 29, 34, 36, 47	WINTER – 8, 13, 20, 27 SPRING – 11, 22, 28, 43 SUMMER – 12, 39 AUTUMN – 9, 19, 26, 32	Available in the SAS output. **Peaks on the plot that have CCC > 3 are supposed to correspond to an appropriate number of clusters.** (Johnson, 1998)
2. Hotelling's Pseudo-t^2 statistic – PST2 Plot	WINTER – 6, 10, 12, 15, 19, 27, 33 SPRING – 5, 8, 12, 23, 46 SUMMER – 3, 14, 19, 28, 41 AUTUMN – 19, 21, 29	WINTER – 5, 11 SPRING – 6, 8 SUMMER – 5, 9 AUTUMN – 7, 12, 18	Available in the SAS output. If PST2 is large, the two clusters should not be combined; **Choose the level before a relatively large PST2 value is observed.** (Johnson, 1998)

Table 2-2 Continued

Stopping rules	Suggested clustering level by Average method	Suggested clustering level by Ward method	Comments / Description of selection criterion
3. Combined Pseudo-F and Pseudo T^2 criterion Plot	WINTER - 6, 15, 19, 27, 33 SPRING – 5, 8, 12, 23, 46 SUMMER – 3, 14, 19, 28, 41 AUTUMN – 17, 19, 29	WINTER, SPRING, SUMMER, AUTUMN - Plot is not informative.	Pseudo F = [A/W] * [(n-k) / (k-1)], where A and W are the among- and within-cluster sum of squares, n is the number of objects; k is the number of existing clusters. Plot Pseudo-F and t^2 statistics against the cluster level; the pseudo- t^2 value plotted to be the change in the value between steps. **Look for local peaks in the pseudo-F test that are followed by sudden jumps in the pseudo-t^2 for the next clustering level. Choose clustering levels that precede particularly large or disparate mergers.** (Fovell and Fovell, 1993)
4. R^2 Plot of explained variance vs clustering step	WINTER - 6, 10, 14, 15, 19, 27 SPRING – 5, 8, 12, 23, 46 SUMMER – 19 AUTUMN – 17, 18, 19, 29	WINTER, SPRING, SUMMER, AUTUMN - Plot is not informative.	Proportion of variance explained by the current number of clusters. **Find where the coefficient drops more sharply. Terminate before the more dramatic drop.** (Kalkstein et al., 1987; Davis and Kalkstein, 1990)
5. Plot distance between the clusters merged at each step	WINTER - 5, 7, 13 SPRING – 5, 6, 13, 23 SUMMER – 3, 8, 11 AUTUMN – 4, 10, 20	WINTER, SPRING, SUMMER, AUTUMN - No distance info available in the output.	If a point can be discerned where the distances between merged clusters jumps markedly, the **process can be stopped just before these distances become large. Look for plateaus or natural breaks.** (Wilks, 1995; Fovell and Fovell, 1993)

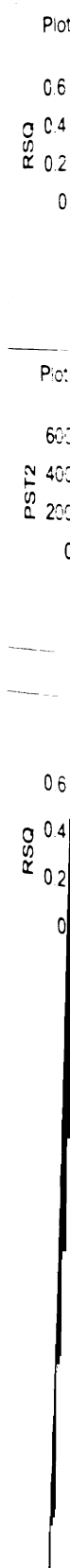
Plot
0.6
RSQ 0.4
0.2
0
Plot
PST2
RSQ

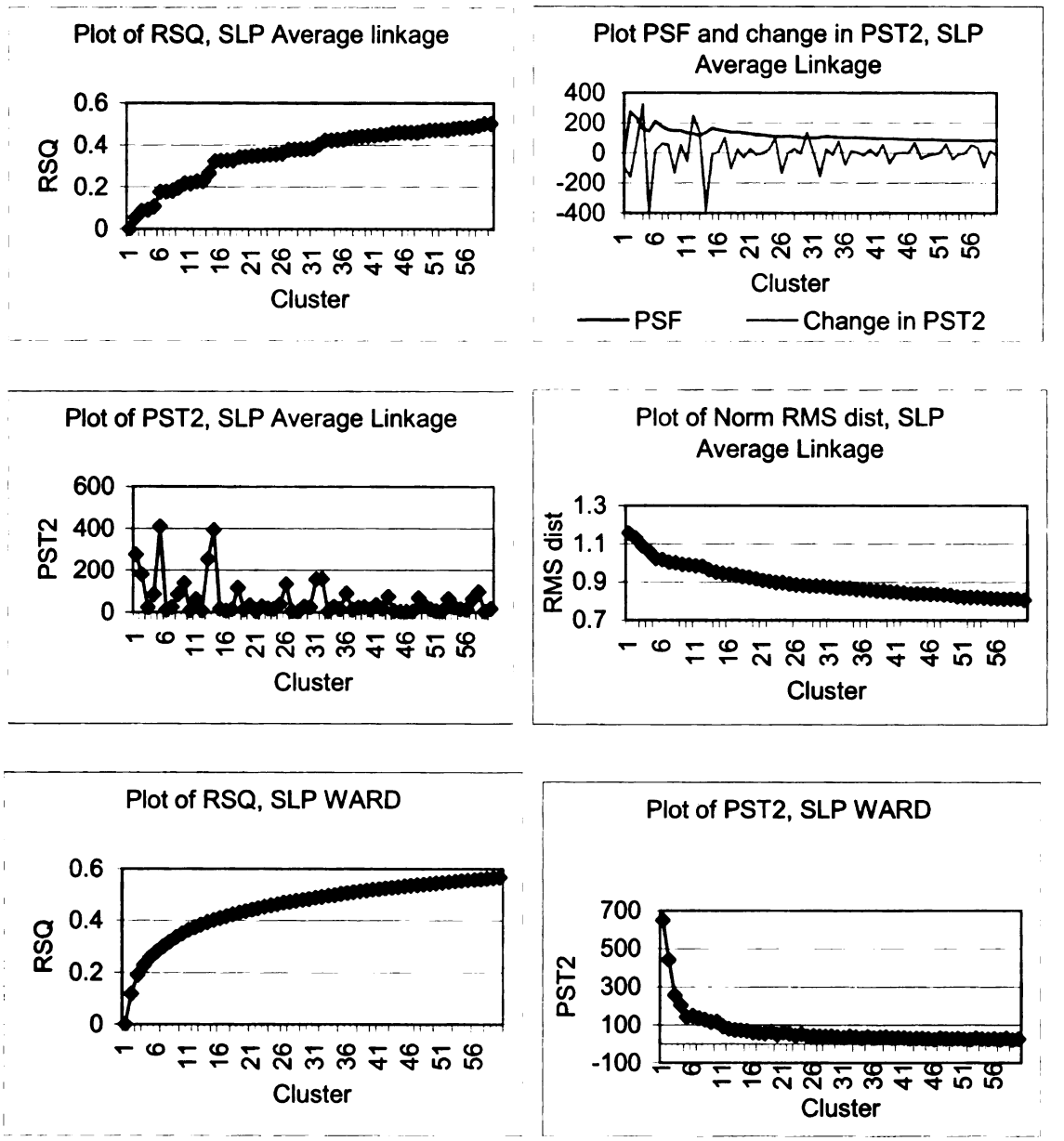

Figure 2-2 Plots of the stopping rules, winter, SLP 1951-2004

RSQ
PST2
RSQ

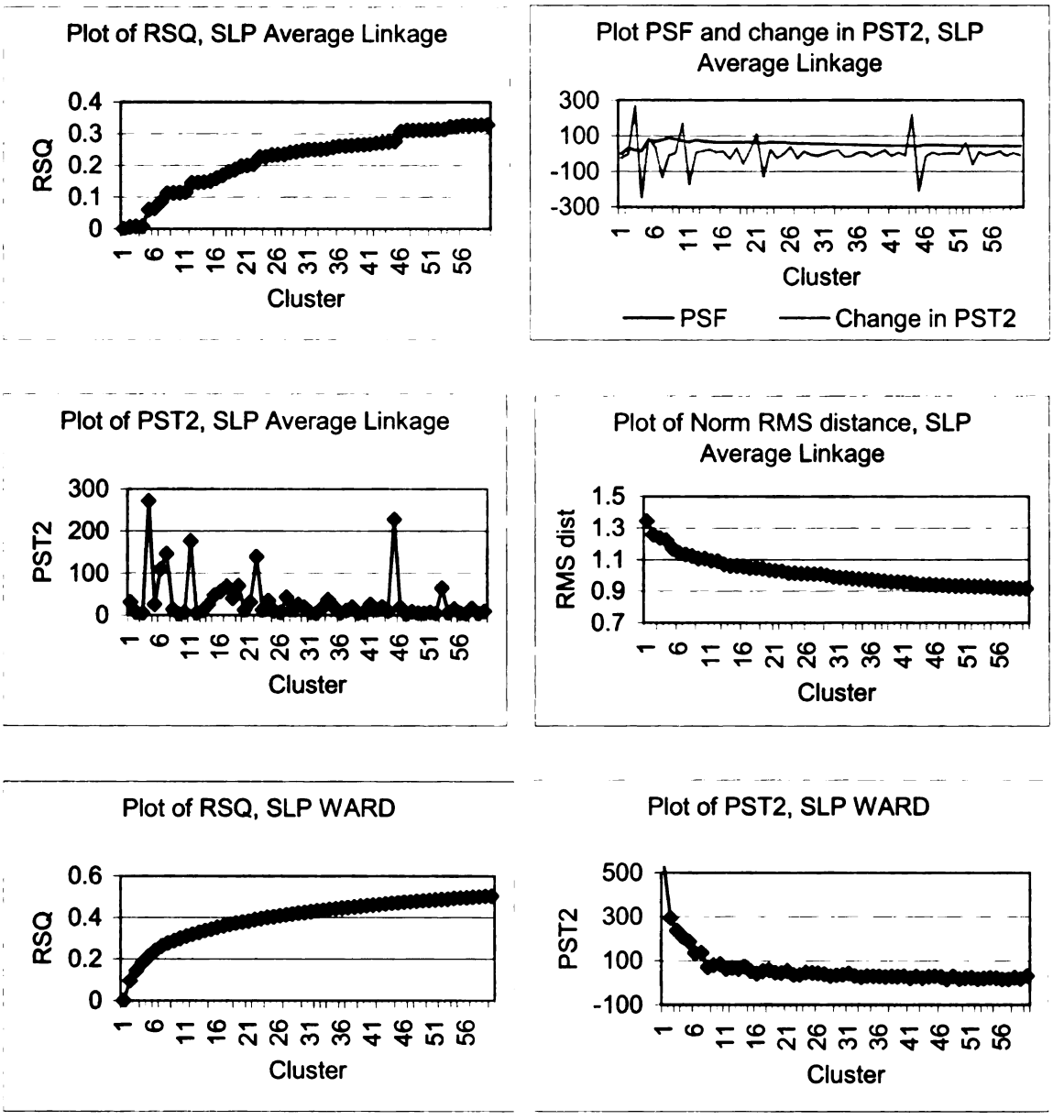

Figure 2-3 Plots of the stopping rules, spring, SLP 1951-2004

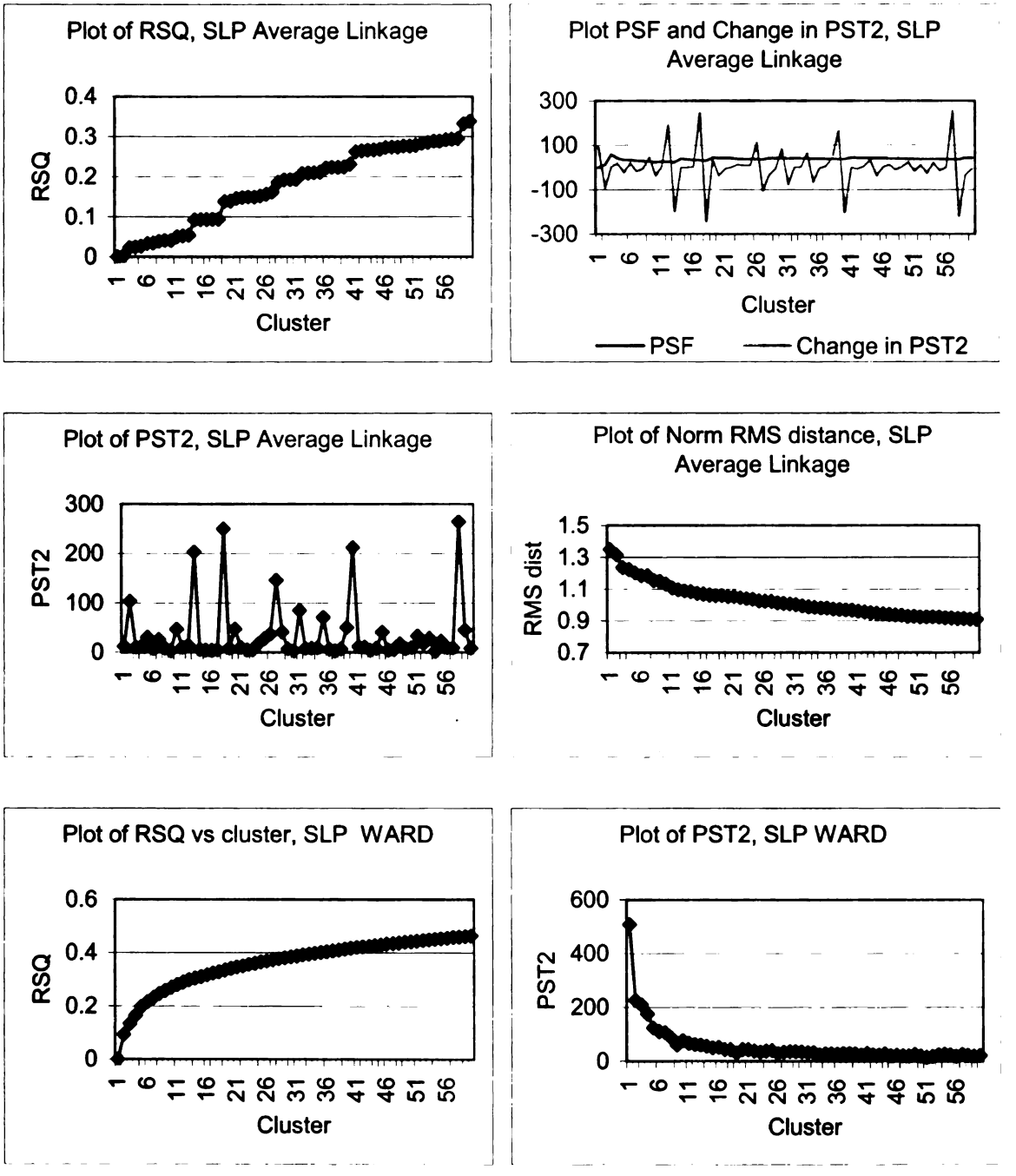

Figure 2-4 Plots of the stopping rules, summer, SLP 1951-2004

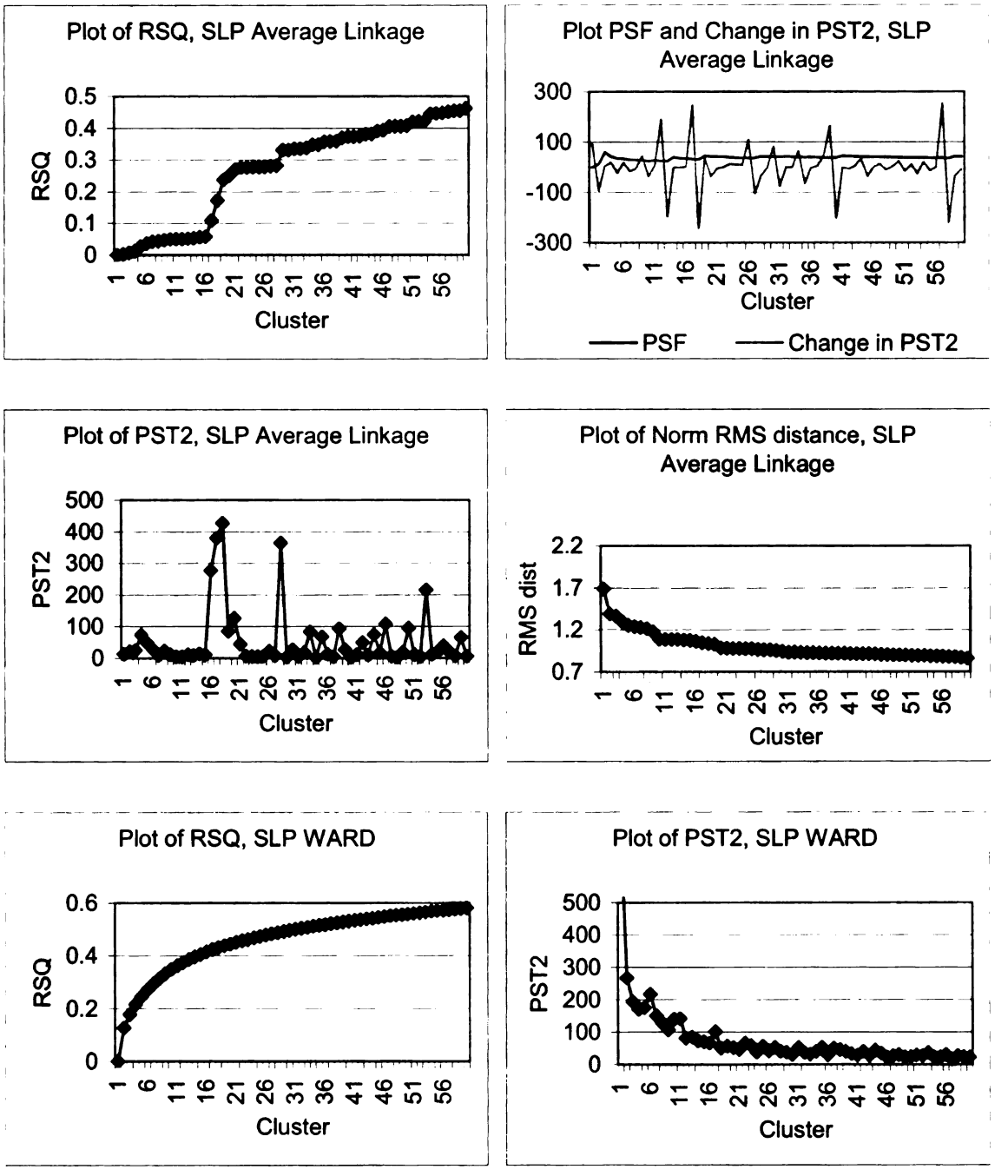

Figure 2-5 Plots of the stopping rules, fall, SLP 1951-2004

The candidate numbers of clusters were used in the SAS FASTCLUS procedure to obtain multiple non-hierarchical clustering solutions. The clustering solutions were compared using Beale's Pseudo-F criterion in order to determine objectively which levels of grouping are most adequate for the data in hand. The application and outcome for each season of the Beale's testing are discussed in section 3.2.d. A two level final clustering solution is sought after. The two solutions with different level of detail will be used to answer different research questions. The solution that consists of a small number of clusters can be used to address baseline questions about the temporal characteristics of the derived patterns. The second more detailed level, which consists of a larger number of clusters, can be used for more in depth analysis of the relationships of the derived patterns and the local climate, or in this study, the temperature extremes in Bulgaria.

3.2. c. Options of the FASTCLUS procedure

The non-hierarchical FASTCLUS algorithm was run multiple times with the different number of seeds suggested from the hierarchical clusterings. Any one run of this procedure may include up to four steps. For three of the steps, the researcher has the opportunity of managing the process by specifying different options.

By default, the FASTCLUS procedure selects the first *n* consecutive observations as initial estimates of the means of the clusters, or initial seeds, where *n* is the number of clusters determined from the hierarchical procedures (SAS, 1995). Since the choice of these initial seeds is influenced by the ordering

of the data (Johnson, 1998), a randomization option was applied that allowed the selection of a pseudo-random sample of observations as the initial cluster seeds (SAS, 1995).

After the cluster seeds are chosen, the default is for the seeds to remain constant until all the observations are assigned to the nearest cluster seed. The "drift" option used in this analysis, however, allowed for adjustment of the seeds in order to reach optimal clustering solution. With each new assignment to a cluster, the corresponding cluster seed was recalculated as the mean of the cluster. After all observations are assigned to the nearest cluster seed, the seeds are once again recalculated as the means of the clusters.

The process can be iterative, with the maximum number of iterations supplied by the user. At the beginning of iteration, the recalculated cluster seeds from the end of the previous iteration are used as initial seeds. The iterations cease when the changes in the values of the seeds become less than or equal to a given convergence criterion (the default criterion was used in this study). After multiple trials it was determined that 30 - 50 iterations were necessary to attain convergence of the clustering solution.

3.2. d. Beale's Pseudo F statistic

Since multiple clustering solutions were obtained, an objective procedure was needed to determine which solutions to choose as the final solutions. Following Johnson (1998), every pair of cluster solutions based on consecutive candidate numbers of cluster seeds was evaluated with the Beale's Pseudo *F*

statistic

statistic

other. T

sum of

availabl

are con

number

their US

with larg

smaller

chosen.

critical v

For exan

7. 8. 10,

step. eac

number

winter 6

concludi

solution.

In this ex

Beale's

clusters

residual

statistic. For two clustering solutions with a different number of clusters, this statistic determines if a given grouping represents an improvement over the other. The Pseudo *F* statistic was computed using Beale's intracluster residual sum of squares (USS) of the distances of the data points from the cluster means, available from the FASTCLUS procedure in SAS. When two clustering solutions are considered, one with a smaller number of clusters and another with a larger number of clusters, the solution with the smaller number of clusters is chosen if their USS values are quite similar (Jonhson, 1998). If the USS for the solution with larger number of clusters is much smaller than the USS of the solution with smaller number of clusters, then the solution with the larger number of clusters is chosen. The Pseudo *F* statistic for every pair of solutions was compared to critical values from the *F*-distribution with the appropriate degrees of freedom. For example, for the winter season, the hierarchical procedures suggested 5, 6, 7, 8, 10, 11, 12, 13, 14, 15, 19, 20, 26, 27, and 33 numbers of clusters. As a first step, each cluster solution was compared to the solution based on the lowest number of clusters, 5 in this case, using the Beale's Pseudo-F statistic. The winter 6 cluster solution was compared to the 5 cluster solution, and after concluding that the 5 cluster solution is an improvement over the 6 cluster solution, the 7 cluster solution was compared to the 5 cluster solution, and so on. In this example, the 5 cluster solution was an improvement, according to the Beale's Pseudo-F statistic, over the solutions with 6, 7, 8, 10, 11, 12 and 13 clusters (Table 2-3). However, the 14 cluster solution for winter had a lower residual sum of squares compared to the 5 cluster solution and was considered

as bet

20 clus

cluster

solutio

tier sol

Tab

| Stop
ru |
| --- |
| Beale s
Pseudo
criteno
obtain
from th
FASTC
proced
applied
based
cluster
from th
averag
the Wa
method |

3.2. e

The s

as better. The 14 cluster solution was also an improvement over the 15, 18, and 20 clusters solutions. In sum, the first tier of the classification consisted of the 5 cluster solution, while the second, more detailed tier, consisted of the 14 cluster solution. The clustering solutions, found to be an improvement over the second tier solutions for each season, were too detailed to be useful.

Table 2-3 Results of the application of Beale's Pseudo-F statistic for all the seasons

Stopping rule	Results from the application of the Beale's Pseudo-F statistic	Comments / Description of selection criterion
Beale's Pseudo-F criterion (obtained from the FASTCLUS procedure applied based on cluster seeds from the average and the Ward methods)	WINTER – 5 is significantly better than 6, 7, 8, 10, 11, 12, 13; 14 is better than 5, 15, 19, 20; 26 is better than 14, 27, 33; **5 and 14 clusters chosen.** SPRING – 5 is better than 6, 8, 11, 12, 13; 18 is better than 5, 22, 23, 28; 43 is better than 18, 46; **5 and 18 clusters chosen.** SUMMER – 3 is better than 5, 8, 9, 11, 12, 14; 19 is better than 3, 28; 39 is better than 19, 28, 41. **3 and 19 clusters chosen.** FALL – 4 is significantly better than 7, 9, 10 and 12; 17 is better than 4, 18, 19, 20, 21 and 26; 29 is better than 17, 32, 34, 36, 37; 47 is better than 29. **4 and 17 clusters chosen.**	Compares sums of squares (W1 and W2) of within cluster distances computed from the cluster means for two separate clustering solutions. If W1 is close to W2, for simplicity choose the clustering with fewer number of clusters, since the two clustering solutions are equally good. If W1 is much smaller than W2, then could be said that the first clustering is an improvement over the second, and we will choose the 1st one. Can be calculated after applying FastClus in SAS and obtaining the USS value for each compared clustering solution. (Johnson, 1998)

3.2. e. The final clustering solution

The sequence of procedures in the cluster analysis is summarized in

Figure 2-6.

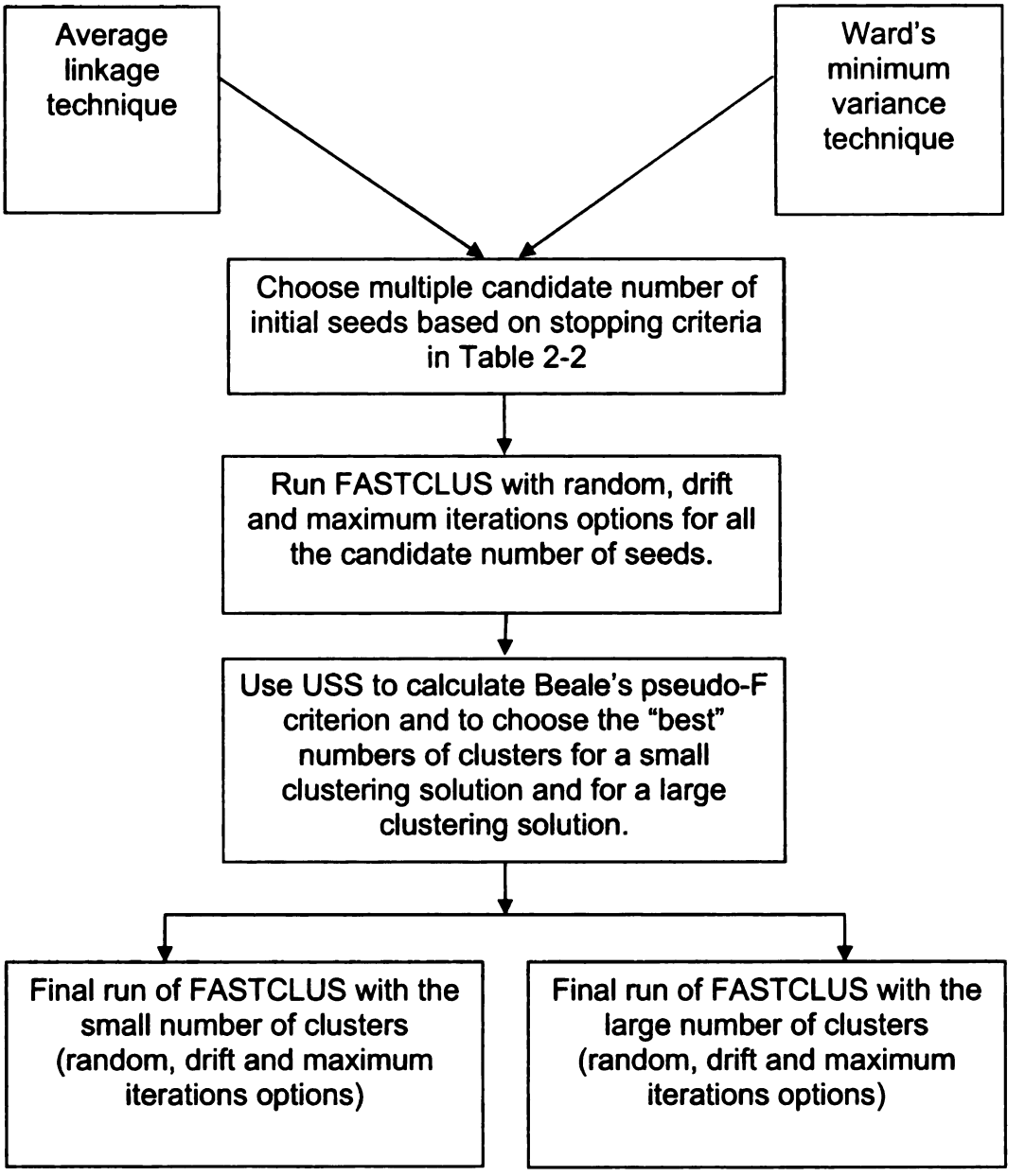

Figure 2-6 Cluster analysis flow chart

Based on the objective procedure, discussed above, a two-tier classification for every season was established (Table 2-4) – one tier (A) with a small number of clusters, and another tier (B) with a larger number of clusters.

The circulation patterns obtained from the small cluster solution are termed "supertypes" and are composed of the primary features of the atmospheric circulation over the region. The patterns from the more detailed clusterings are referred to as "types" and, as will be shown below, represent nuances in positioning and intensity of the features seen in the supertypes. The supertype patterns derived for every season are similar and illustrate the evolution of circulation conditions during the year. It should be acknowledged that due to the application of the cluster analysis by season, there might exist seasonal boundary problems.

Some authors (Galambosi et al., 1996; Huth, 2001; Kysely and Huth, 2006), after using a computer assisted classification to group circulation patterns, relied on subjective decisions to aggregate the clusters into larger groups. The aggregation of the circulation patterns into supergroups was defended by the authors as a necessary step, since the obtained clusters were too detailed for some applications. In contrast to these authors, in this study the supertypes were established objectively, based on the above described statistical evaluation.

Table 2-4 – Seasonal clustering solutions – number of clusters

Solution/Season	Winter	Spring	Summer	Autumn
A	5	5	3	4
B	14	18	19	17

It is important to note that a "type" is not necessarily strictly associated with a single supertype, since the clustering method was non-hierarchical rather than hierarchical. Rather, types can be associated with several supertypes. This is considered advantageous, as transition in atmospheric circulation can be better detected. To assess the correspondence between the types and the supertypes, the dates of overlap were compared for every season. Most of the types are strongly associated with only one of the supertypes, although a few types are associated with two, and in rare occasions, three supertypes. The results for the correspondence between the supertypes and the types for all the seasons are presented below (Table 2-5, Table 2-6, Table 2-7, and Table 2-8).

The clusters can not be mapped directly (Yarnal, 1993). However, since each day is assigned to only one cluster from the small clustering solution and to one cluster from the large clustering solution, the grids from each cluster for each solution were averaged to produce composite pressure maps. Composite maps were also plotted for the standardized anomalies of the circulation patterns. These plots reveal the main anomaly centers characterizing given supertype or type. For a given season, the standardized anomalies were calculated by subtracting from every daily grid point value the seasonal average for that grid point, and dividing by the grid point seasonal standard deviation. The standardized anomaly patterns for each cluster from each solution were averaged to obtain the composite patterns for each supertype and type. The composite analysis of the supertypes and the types for each season is the end product of the map-pattern classification.

Table 2-5 Overlap between the small and the large clustering solutions, WINTER 1951-2004 (total number of days and percent of days for a given cluster from the large clustering solution in common with a given cluster from the small clustering solution; the numbers in bold show the highest percentage of overlap for given clusters)

Count 5 – defined as the total number of days classified as cluster 1 through 5
Count14 – defined as the total number of days classified as cluster 1 through 14
J – number of clusters for the small clustering solution
K – number of clusters for the large clustering solution

	Count 14	357	237	364	289	277	409	453	408	386	404	340	358	332	246
Count 5	j/k	**1**	**2**	**3**	**4**	**5**	**6**	**7**	**8**	**9**	**10**	**11**	**12**	**13**	**14**
1011	**1**	0	2	100	225	4	65	18	0	0	246	25	325	0	1
	%	0	1	27	**78**	1	16	4	0	0	**61**	7	**91**	0	0
1021	**2**	17	41	228	13	250	1	197	0	0	2	98	7	163	4
	%	5	17	**63**	4	**90**	0	43	0	0	0	29	2	49	2
1092	**3**	0	1	2	0	0	86	195	39	379	102	198	26	9	55
	%	0	0	1	0	0	21	43	10	**98**	25	**58**	7	3	22
868	**4**	2	189	0	0	0	1	43	369	7	1	2	0	131	123
	%	1	**80**	0	0	0	0	9	**90**	2	0	1	0	39	**50**
868	**5**	338	4	34	51	23	256	0	0	0	53	17	0	29	63
	%	**95**	2	9	18	8	**63**	0	0	0	13	5	0	9	26

Table 2-6 Same as above for SPRING 1951-2004

Count 5 – the total number of days classified as cluster 1 through 5, Count18 – the total number of days classified as cluster 1 through 18
J – number of clusters for the small clustering solution, K – number of clusters for the large clustering solution

	Count18	230	348	371	245	454	293	255	167	311	328	112	216	356	245	197	192	360	288
Count5	j/k	**1**	**2**	**3**	**4**	**5**	**6**	**7**	**8**	**9**	**10**	**11**	**12**	**13**	**14**	**15**	**16**	**17**	**18**
1056	**1**	28	244	35	12	73	0	0	0	281	1	0	4	209	0	0	36	31	102
	%	12	**70**	9	5	16	0	0	0	**90**	0	0	2	**59**	0	0	19	9	35
1030	**2**	13	2	12	6	217	244	35	116	0	21	111	0	0	188	44	12	9	0
	%	6	1	3	2	**48**	**83**	14	**69**	0	6	**99**	0	0	**77**	22	6	2	0
967	**3**	17	98	1	0	11	0	4	0	3	201	0	7	22	54	0	62	302	185
	%	7	28	0	0	2	0	2	0	1	**61**	0	3	6	22	0	32	**84**	**64**
993	**4**	62	0	1	120	143	1	216	51	0	18	0	195	124	0	44	0	18	0
	%	27	0	0	**49**	31	0	**85**	31	0	5	0	**90**	35	0	22	0	5	0
922	**5**	110	4	322	107	10	48	0	0	27	87	1	10	1	3	109	82	0	1
	%	**48**	1	**87**	**44**	2	16	0	0	9	27	1	5	0	1	**55**	**43**	0	0

Table 2-7 Same as above for SUMMER 1951-2004

Count 3 – the total number of days classified as cluster 1 through 3, Count19 – the total number of days classified as cluster 1 through 19
J – number of clusters for the small clustering solution, K – number of clusters for the large clustering solution

	Count 19	282	287	278	263	227	283	211	248	188	298	297	194	291	301	281	301	277	133	328
Count 3	j/k	**1**	**2**	**3**	**4**	**5**	**6**	**7**	**8**	**9**	**10**	**11**	**12**	**13**	**14**	**15**	**16**	**17**	**18**	**19**
1577	**1**	0	79	3	0	204	210	76	0	43	23	0	176	0	19	214	48	265	133	84
	%	0	28	1	0	**90**	**74**	36	0	23	8	0	**91**	0	6	**76**	16	**96**	**100**	26
1646	**2**	0	102	240	190	22	41	117	11	17	25	175	18	272	84	63	253	0	0	16
	%	0	36	**86**	**72**	10	14	**55**	4	9	8	**59**	9	**93**	28	22	**84**	0	0	5
1745	**3**	282	106	35	73	1	32	18	237	128	250	122	0	19	198	4	0	12	0	228
	%	**100**	37	13	28	0	11	9	**96**	**68**	**84**	41	0	7	**66**	1	0	4	0	**70**

Table 2-8 Same as above for FALL 1951-2004

Count 4– the total number of days classified as cluster 1 through 4, Count17– the total number of days classified as cluster 1 through 17
J – number of clusters for the small clustering solution, K – number of clusters for the large clustering solution

	Count17	366	236	327	200	248	276	204	271	509	240	199	239	327	286	376	320	290
Count4	j/k	**1**	**2**	**3**	**4**	**5**	**6**	**7**	**8**	**9**	**10**	**11**	**12**	**13**	**14**	**15**	**16**	**17**
1781	**1**	285	2	181	0	9	0	0	42	416	0	3	0	46	64	376	190	167
	%	**78**	1	**55**	0	4	0	0	15	**82**	0	2	0	14	22	**100**	**59**	**58**
1100	**2**	62	48	23	144	0	268	99	124	0	7	50	0	168	4	0	0	103
	%	17	20	7	**72**	0	**97**	**49**	**46**	0	3	25	0	**51**	1	0	0	36
1047	**3**	1	29	69	41	121	7	1	0	92	14	142	239	112	160	0	1	18
	%	0	12	21	20	**49**	3	0	0	18	6	**71**	**100**	34	**56**	0	0	6
986	**4**	18	157	54	15	118	1	104	105	1	219	4	0	1	58	0	129	2
	%	5	**67**	17	8	**48**	0	**51**	39	0	**91**	2	0	0	20	0	40	1

3.2. f. Comparison with upper level airflow

For the dates belonging to the supertypes, the Z500 data were averaged and composite 500 hPa geopotential height maps were produced as well. The combination of surface and upper-air maps allows for a more comprehensive representation of the circulation conditions over the study domain.

3.3. Analysis of the frequency and persistence of the supertypes and types

The frequency of occurrence of the supertype patterns was investigated. The seasonal frequency (in %) was calculated relative to the total number of days of a given season for the period 1951-2004. The monthly occurrence (in %) was computed relative to the number of days for a given month, again for the entire period.

The number of consecutive days during which a given supertype dominates the study domain (or the 'persistence' of this supertype) is of particular interest since it directly affects the local climate of the different regions. The persistence characteristics summarized over the entire period are termed 'total persistence' in this study. Following Huth (1997), three main parameters were the focus of the analysis of the total persistence characteristics for every supertype: a) the number of 1-day, or transitional, events; b) the percentage of days included in events lasting 4 days or longer; and c) the average event length in days. An 'event' was considered to be the uninterrupted sequence of days classified with the same supertype. The percentage of days included in events lasting 4 days or more was calculated as the ratio of the number of days within

events lasting 4 or more days for a certain supertype to the total number of days classified with the same supertype. The average event length was calculated by dividing the total number of days classified with a given supertype by the total number of events of any length for this supertype.

The Mann-Kendall test for the existence of trends was used to study the interannual changes in the persistence of the following parameters: a) the average length of all events per supertype; b) the number of transitional (1-day) events, by pentads (non-overlapping five year periods starting in 1951); c) the frequency of events lasting 2-4 days, by pentads; d) the frequency of events lasting more than 4 days, by pentads; e) the average length of the events lasting more than 4 days, by pentads; and f) the total number of days in events lasting more than 4 days, by pentads. Pentadal values were used instead of the annual values since one of the requirements of the Mann-Kendall test for existence of trend is that at least one value per time period (day, month, or year) should be observed in order for this test to be valid. Some of the persistence characteristics were not available for every year, because they were based on truncated series, including only the data values for events lasting 4 days or longer. In these cases, the totals or averages by pentads were used following Changnon and Changnon (1992).

3.3.1. Break point tests

The interannual changes in the seasonal frequency of the circulation patterns were assessed using break point tests and nonparametric trend analysis

tests. The nonparametric Pettit test (Pettit, 1979) and the Standard Normal Homogeneity Test for a single break (SNHT, Alexandersson, 1986) were used to identify change points or step changes in series of interest. The SNHT assumes that the values of the series of interest are normally distributed, while the Pettit test does not make this assumption. The Pettit test is less sensitive to outliers compared to the SNHT, since it is based on ranks rather than actual values of the series. The SNHT is more sensitive to breaks in the beginning and end of the series. In contrast, the Pettit test is sensitive to breaks in the middle of the tested period. This test is affected also by existence of trends in the series, which leads to frequent rejection of the null hypothesis (Busuioc and von Storch, 1996). In this study, following Busuioc and von Storch (1996), the SNHT was employed together with the Pettit test. To be considered a break point, both tests have to indicate a statistically significant change point in the same year or quite close to the same year (within a 2-3 years difference).

The null hypothesis for this analysis is that there are no changes or breaks in the series. The alternative hypothesis states that a step-like shift exists in the series of interest. The tests were applied initially to the entire 1951-2004 period. If a break point was detected by the tests, following Kysely and Domonkos (2006), only the sub-periods larger than 20 years determined by this break point were tested in turn for breaks.

3.3.1. a. Details of the Pettit test

If $Y_1, Y_2, \ldots, Y_n$ is the series of interest, and $r_1, r_2, \ldots, r_n$ are the ranks of the values, we can calculate the statistic:

and n is

The ma

original

exceed

significa

3.3.1. b

T

the first

statistic

w

$\bar{Z}_1$

Y_i are th

and s is

maximu

plotted

$$X_k = 2\sum_{i=1}^{k} r_i - k(n+1) \quad \text{, where } k = 1, \ldots, n,$$

and n is the total number of years. X_k is plotted against the years of the period. The maximum or minimum of the calculated X_k values signify a break in the original series if a critical value for a given length of the original series is exceeded at pre-specified significance level. The critical values for given levels of significance are given in Pettit (1979).

3.3.1. b. Details of the SNHT

The $T(k)$ statistic of the SNHT allows for the comparison of the mean for the first k years of the period to the mean for the n-k years of the period. The $T(k)$ statistic is calculated as follows:

$$T(k) = k\bar{z}_1^2 + (n-k)\bar{z}_2^2 \quad , \; k = 1, \ldots, n$$

where

$$\bar{z}_1 = \frac{1}{k}\sum_{i=1}^{k}(Y - \bar{Y})/s \quad \text{and} \quad \bar{z}_2 = \frac{1}{n-k}\sum_{i=k+1}^{n}(Y_i - \bar{Y})/s$$

Y_i are the values from the series of interest, $\bar{Y}$ is the mean of the original series, and s is the standard deviation. If a break exists in a given year, $T(k)$ has a maximum value near that year. For convenience and better visualization, $T(k)$ is plotted against year. The test statistic T_0 is found from:

$$T_0 = \max_{1 \le k < n} T(k)$$

The nu

the pe

2003).

3.3.2.

nonpar

2004 p

3.3.2. a

missing

values f

length c

statistic

Gilbert (

a

b)

c

The null hypothesis is rejected if T_0 is above the critical value for certain length of the period at a pre-selected significance level (see Table III, Wijngaard et al., 2003).

3.3.2. Nonparametric trend tests

The Mann Kendall trend test for existence of trends and the Sen's nonparametric estimate of slope (Gilbert, 1987) were applied to the entire 1951-2004 period, as well as to the sub periods determined by the break points tests.

3.3.2. a. Mann Kendall nonparametric test for existence of trend

The Mann Kendall nonparametric trend test allows for the existence of missing data in the series and does not assume a specific distribution of the values for the period of interest. The test varies somewhat depending on the length of the series. If the period of interest comprises 40 values or less then the statistic S is computed using the following procedure, described in full detail in Gilbert (1987, p.209):

a) list the data in the order they were obtained over time, i.e. $x_1, x_2, \ldots, x_n$, where x is the data value and $i=1,\ldots n$ is the time.

b) determine the sign of all $n(n-1)/2$ possible differences of $x_j - x_k$, where $j>k$.

c) if $x_j - x_k > 0$ then $\text{sgn}(x_j - x_k) = 1$, if $x_j - x_k < 0$ then $\text{sgn}(x_j - x_k) = -1$, if $x_j = x_k$ then $\text{sgn}(x_j - x_k) = 0$, where *sgn* indicates which value

d

T

tested a

when S

p.272) c

significa

a downv

the absc

specified

Excel an

W

period 19

approxim

approxim

presence

above.

was assigned to the $x_j - x_k$ difference in the cases when the difference is negative, positive or equal to zero.

d) compute the S statistic using the formula

$$S = \sum_{k=1}^{n-1} \sum_{j=k+1}^{n} \operatorname{sgn}\left(x_j - x_k\right)$$

The null hypothesis states that there is no trend in the series. If the null is tested against the alternative hypothesis of an upward trend, the null is rejected when S is positive and the probability value in table A18 (see Gilbert, 1987, p.272) corresponding to the computed S is less than an *a priori* specified significance level α. When the null is tested against an alternative hypothesis for a downward trend, the null is rejected if S is negative and the probability value for the absolute value of S from table A18 (Gilbert, 1987) is less than the beforehand specified significance level α. The calculations of the S statistics were done in Excel and also using the program of Helsel, Mueller and Slack (2006).

When the data series contains more than 40 values, (for this study the period 1951-2004 consisting of 54 data values was used), the normal approximation test can be applied (Gilbert, 1987, p.211). The normal approximation test takes into account the variance of the S statistic and the presence of ties (equal values) in the series. The S statistic is computed as above. The variance of S is calculated using the formula:

where

group.

A positi

alternat

alternat

and its

used to

3.3.2. b.

S

(1950).

gross da

$$VAR(S) = \frac{1}{18}\left[n(n-1)(2n+5) - \sum_{p=1}^{q} t_p (t_p - 1)(2t_p + 5) \right],$$

where q is the number of tied groups, t_p is the number of data values in the pth group. Subsequently S and VAR(S) are used to calculate the test statistic Z:

$$Z = (S - 1)/[\text{VAR}(S)]^{1/2} \qquad \text{if } S > 0,$$

$$Z = 0 \qquad \text{if } S = 0$$

$$Z = (S + 1)/[\text{VAR}(S)]^{1/2} \qquad \text{if } S < 0.$$

A positive (negative) value of Z indicates a positive (negative) trend. If the alternative hypothesis is for an upward trend, the null is rejected if $Z > Z_{1-\alpha}$. If the alternative hypothesis is for a downward trend, the null is rejected if Z is negative and its absolute value is greater than $Z_{1-\alpha/2}$.The standard normal tables can be used to assess the statistical significance of the Z statistic.

3.3.2. b. Sen's nonparametric estimator of slope

Sen's (1968) method for calculation of the slope builds on a test by Theil (1950). Sen's test is not affected by the existence of missing values, outliers or gross data errors. The slope estimates are calculated using the formula:

$$Q = \frac{X_{i'} - X_i}{i' - i}$$

where

numb

of slo

4. Re

namin

pressu

Low" p

a well

conve

labels

The tw

patter

4.1. C

4.1.1.

4.1.1.

identif

repres

two lar

normal

analys

where $x_{i'}$ and x_i are the values during times i' and i, and $i' > i$. If the N' is the number of data pairs for which $i' > i$, the median of the N' values is the estimator of slope.

4. Results

In order to maintain consistency between the different seasons, the naming of the circulation patterns was based on the most prominent sea level pressure anomaly centers. For example, the "Scandinavian High-Mediterranean Low" pattern features a strong positive SLP anomaly area over Scandinavia and a well developed negative anomaly over the Mediterranean. This naming convention allows for an immediate association to be made between the pattern labels and the pressure configurations over the continent and the North Atlantic. The two maps presented for each circulation pattern include the composite pattern and the composite anomaly pattern.

4.1. Circulation catalog

4.1.1. Wintertime circulation

4.1.1. a. Winter SLP supertypes

Five main sea-level circulation patterns, referred to as "supertypes", were identified for winter. Each supertype is characterized by one or more centers represented by positive or negative SLP anomalies. The first supertype features two large anomaly areas (Figure 2-7). A large negative anomaly, indicating below normal SLP values, is located over the northern and northeastern portion of the analysis domain, particularly over the arctic regions of Scandinavia. Higher than

norma

with th

Medite

"Voeik

locatio

pattern

abbrev

stronge

strong l

higher t

normal

superty

MLwin).

negative

eastwar

Mediter

circulati

T

for the n

High (M

[1] The nam
extension
Atlantic we
Kontinent

normal SLP values are found over the southern portion of the analysis domain with the largest positive anomalies seen over northern Africa and the Mediterranean. This extended area of generally higher pressure resembles the "Voeikov axis", earlier described by Giles and Balafoutis (1992). Based on the location and relative magnitude of the two anomaly centers, this circulation pattern is labeled the **Arctic Low-Voeikov Belt**[3] (AL-VBwin) supertype (the abbreviations of the supertypes names are presented in Table 2-9). The strongest pressure gradients are found between 45° and 55° N resulting in a strong low-level zonal flow over the British Isles and northern Europe.

The second supertype is approximately the mirror image of the first, with higher than normal SLP over the arctic regions of Scandinavia and lower than normal SLP over the Mediterranean and northern Africa. This circulation supertype is referred to as the **Scandinavian High-Mediterranean Low** (SH-MLwin). The positive anomaly over Scandinavia is stronger compared to the negative anomaly over the Mediterranean and North Africa, and extends eastward towards Siberia. This pattern emphasizes the influence of the Mediterranean cyclones and the Siberian anticyclone on the wintertime circulation over Europe.

The Mediterranean Low is also present in the composite anomaly analysis for the next supertype, referred to as the **Mediterranean Low-North Atlantic High** (ML-NAHwin). Here the negative anomaly center over North Africa and the

[3] The name "Voeikov Belt" was influenced by a 1992 article of Giles and Balafoutis, where the extension of the Siberian Anticyclone westward to connect with an anticyclone over the eastern Atlantic was referred to as the Voeikov axis. This feature has been termed also '*der Axe des Kontinents*' by van Bebber and Koppen (1885).

Mediterr

area of

anomali

positive

NAHwin

cyclone

T

The sup

higher-th

a ridge c

into Sca

eastern

large neg

Atlantic.

large neg

pressure

Western

the Iberia

Mediterranean is considerably larger in extent compared to the negative anomaly area of the previous SH-MLwin supertype. Also, the northern area of positive anomalies is displaced southwestward over the British Isles, and the average positive anomalies are not as large as for the SH-MLwin supertype. The ML-NAHwin configuration reflects the importance of the Gulf of Genoa area of cyclogenesis during winter.

The next two supertypes are characterized by single anomaly centers. The supertype referred to as the **European High** (EHwin) is characterized by higher-than-normal SLP values across most of the analysis domain. In particular, a ridge of higher pressure extends from North Africa north and northeastward into Scandinavia. This pattern is conducive to meridional circulation in the eastern portions of the analysis region. The last supertype is characterized by a large negative anomaly situated over the British Isles and the northeastern Atlantic. This supertype is named the **Icelandic Low** (ILwin), even though the large negative anomaly is displaced somewhat eastward from Iceland. Strong pressure gradients are seen over much of Europe but particularly in extreme Western Europe. Low-level airflow over much of Europe, with the exception of the Iberian Peninsula, would have on average a southerly component.

Table 2-9 Table of abbreviations of the supertypes

Abbreviation	Meaning
VB	Voeikov Belt
AL	Arctic Low
AH	Azores High
EL	European Low
EH	European High
ML	Mediterranean Low
ASR	Azores-Scandinavian Ridge
IL	Icelandic Low
PGL	Persian Gulf Low
NAH	North Atlantic High
SH	Scandinavian High
WPGL	Weak Persian Gulf Low


70N
60N
50N
40N
30N
20N
40W

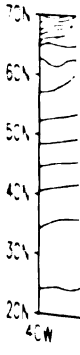
70N
60N
50N
40N
30N
20N
40W


70N
60N
50N
40N
30N
20N
40W

Figu

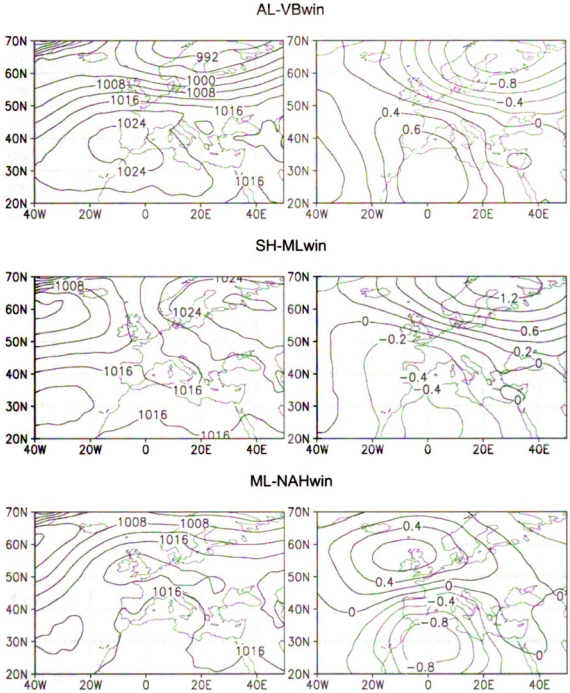

Figure 2-7 Supertype composites for winter – pressure patterns (left column) and standardized anomaly patterns (right column)

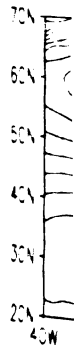

4.1.1. b

T

superty

abbrevi

the sea

the type

type ha

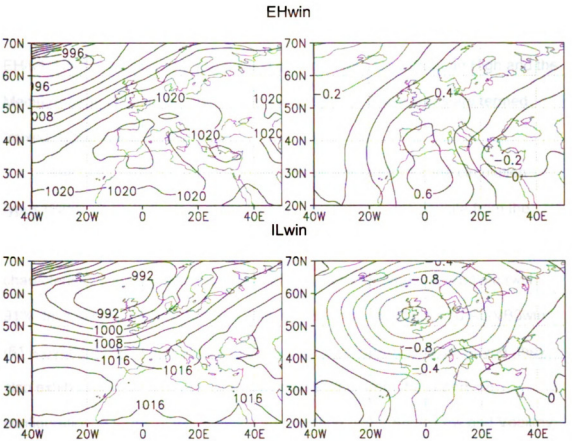

Figure 2-7 continued

4.1.1. b. Relationships between wintertime supertypes and types

The name designation for the circulation types that overlap with a given supertype on over 49% of the days of occurrence is made up of the supertype abbreviation, a sequential number for the type, and a three-letter abbreviation for the season (for example, AL-VB1win, Table 2-10). The sequential placement of the type depends on the percentage days in common with the supertype, i.e., the type having the highest overlap with the supertype is labeled "1". For types

overlapp

abbrevia

EHML-M

Mediterr

"mixed"

T

types (Fi

supertyp

characte

91% day

(61% ove

also exhi

configura

Belt. For

is more i

In contra

and the

terms of

Low wea

to the ve

overlapping with two or more supertypes, the name is represented by the abbreviations of the supertypes to which the pattern is related (for example, EH/ML-NAH is a pattern having days in common with the European High and the Mediterranean Low-North Atlantic High supertypes). These types are termed "mixed" types in this study.

The composite maps of the standardized anomalies for the circulation types (Figure 2-8), indicate that most of the circulation types deviate from the supertype configurations in terms of the intensity or the location of the characteristic anomaly features. Although the maps for types AL-VB1win (with 91% days in common), AL-VB2win (having 78% days overlap), and AL-VB3win (61% overlap) clearly are similar to the Arctic Low-Voeikov Belt supertype, they also exhibit some differences. The composites differ from the supertype configuration in terms of the intensity and position of the Arctic Low and Voeikov Belt. For AL-VB1win, the positive anomaly in the southern portions of the domain is more intense and extends somewhat further northward over western Europe. In contrast, the Voeikov Belt positive anomaly is much weaker for AL-VB2win and the negative anomaly in the Arctic is stronger. Type AL-VB3win differs in terms of both positioning and intensity of the anomaly centers, with the Arctic Low weaker and displaced southward and the Voeikov Belt stronger but limited to the very southern areas.

Table 2-10 Classification of the atmospheric circulation over Europe – Association between the supertypes and circulation types for winter
*** Mixed types have less than 50% days overlap with any one supertype.**

Type abbreviation	Associated supertype	Overlap with supertype(s) %
AL-VB1win	Arctic Low- Voeikov Belt (AL-VBwin)	91%
AL-VB2win		78%
AL-VB3win		61%
ML-NAH1win	Mediterranean Low-North Atlantic High (ML-NAHwin)	90%
ML-NAH2win		63%
EH1win	European High (EHwin)	98%
EH2win		58%
SH-ML1win	Scandinavian High-Mediterranean Low (SH-MLwin)	90%
SH-ML2win		80%
SH-ML3win		50%
IL1win	Icelandic Low (ILwin)	95%
IL2win		63%
ML-NAH/SH-MLwin	Mixed* between ML-NAHwin and SH-MLwin	49%/39%
ML-NAH/EHwin	Mixed between ML-NAHwin and EHwin	43%/43%

Closely related to the Mediterranean Low-North Atlantic High supertype are types ML-NAH1win (90% days in common) and ML-NAH2win (63% days overlap). The composite for type ML-NAH1win deviates from the supertype pattern by the less intense positive anomaly shifted to the southwest and by the stronger negative anomaly. For type ML-NAH2win, the negative anomaly

extends over most of eastern Europe and Scandinavia, and the strong positive anomaly is shifted northwest over Iceland and is more intense.

The European High supertype has days of overlap with types EH1win (98% days in common) and EH2win (58% overlap). For type EH1win, the intensity of the anomaly areas is higher and a second center of higher than normal SLP exists over Scandinavia. A spatially limited, closed positive anomaly area is found over central and western Europe for type EH2win.

Closest to the Scandinavian High-Mediterranean Low supertype are types SH-ML1win (90% overlap), SH-ML2win (80% of days in common), and SH-ML3win (50% of days in common). These types differ from the supertype by: a) a more intense positive anomaly and a shift of the negative anomaly northwestward towards Iceland (SH-ML1win); b) a stronger negative anomaly and less intense positive anomaly shifted westward over Iceland (SH-ML2win); and c) a much stronger negative anomaly shifted to the west over the Atlantic ocean (SH-ML3win).

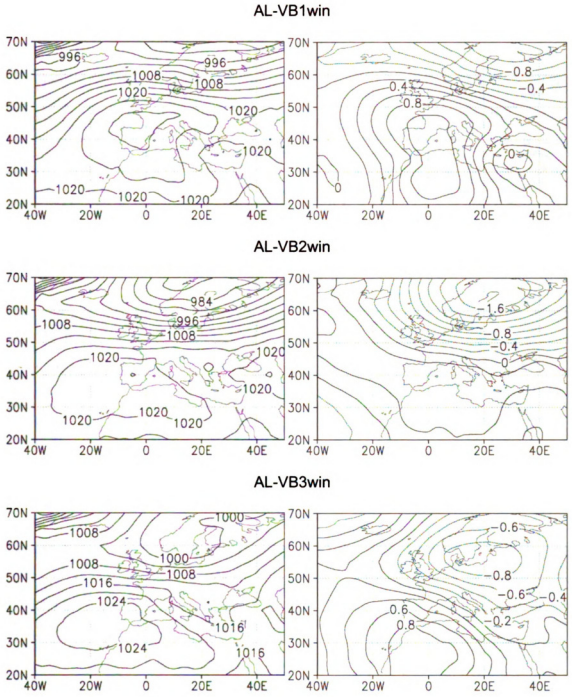

Figure 2-8 Winter types composites - pressure patterns and standardized anomalies The left column presents the SLP patterns, while the right column displays the standardized anomaly patterns

ML-NAH1win

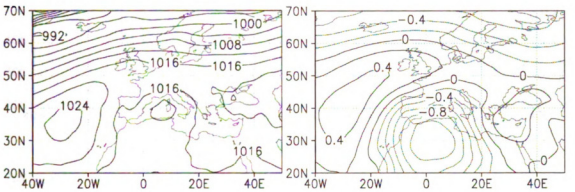

ML-NAH2win

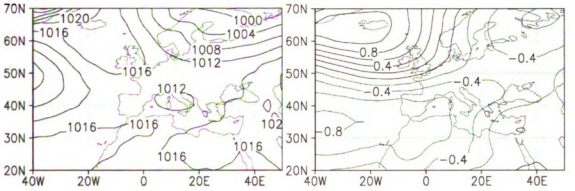

EH1win

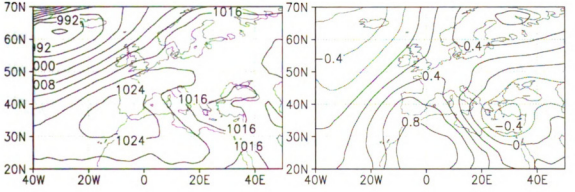

Figure 2-8 continued

EH2win

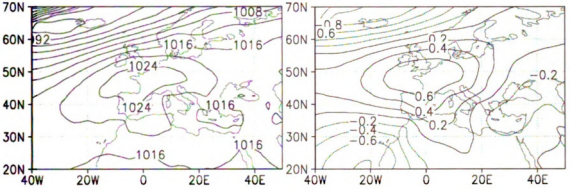

SH-ML1win

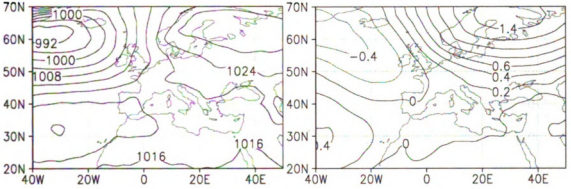

SH-ML2win

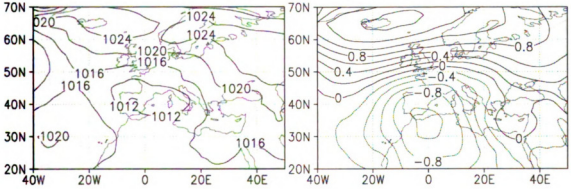

Figure 2-8 continued

SH-ML3win

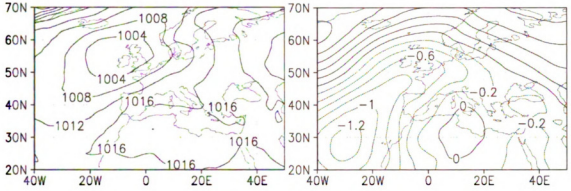

IL1win

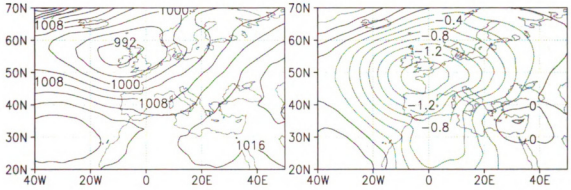

IL2win

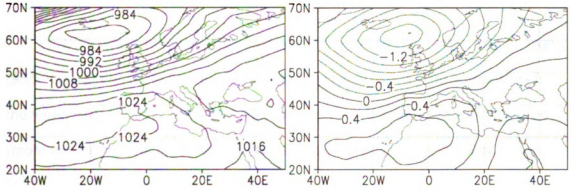

Figure 2-8 continued

ML-NAH/SH-MLwin

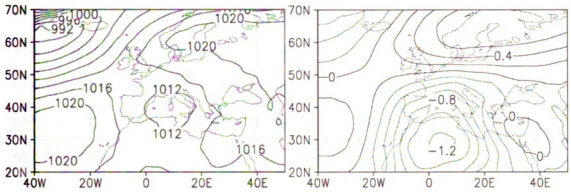

ML-NAH/EHwin

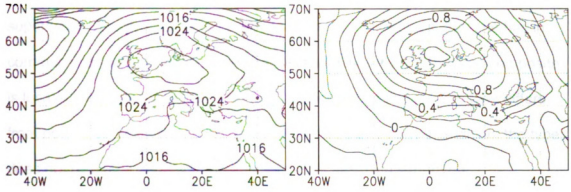

Figure 2-8 continued

Two types are highly associated with the Icelandic Low supertype: IL1win (95% days in common) and the IL2win (63% overlap) types. The composites for the types vary from the supertype by the intensity of the negative anomaly area (more intense in both cases and shifted to the northwest between Iceland and the British Isles for IL2win),

Some types are not clearly identified with only one particular supertype. Two mixed types exist in winter. Type ML-NAH/SH-MLwin is intermediate between the Mediterranean Low-North Atlantic High (49% overlap) and the

Scandinavian High-Mediterranean Low (39% days in common). The type shares with both supertypes the positive anomaly in the northern portion and the negative anomaly in the southern portion of the study domain. It differs from both supertypes by the more intense negative anomaly to the south. In addition, the type varies from the SH-MLwin supertype by the less intense positive anomaly over Scandinavia.

Type ML-NAH/EHwin is classified as a combination of the Mediterranean Low-North Atlantic High (43% days in common), and the European High (43%) supertypes. Clearly a transition between these two supertypes, the type has in common with both supertypes the positive anomaly, which in the type composite is located between the British Isles and southern Scandinavia. The type differs from both supertypes by the higher intensity of the anomaly. In addition, the type does not display a negative anomaly as the ML-NAHwin supertype.

4.1.1. c. Frequency of the winter supertypes

Although the supertypes exhibit relatively similar frequencies during the winter season, the EHwin supertype is present on the largest number of winter days (22.5%, Figure 2-9). The ML-NAHwin and the AL-VBwin supertypes are the next most frequent patterns with frequencies of 21.0% and 20.8%, respectively. The SH-MLwin and the ILwin supertypes are least frequent, both with seasonal frequencies of 17.9%.

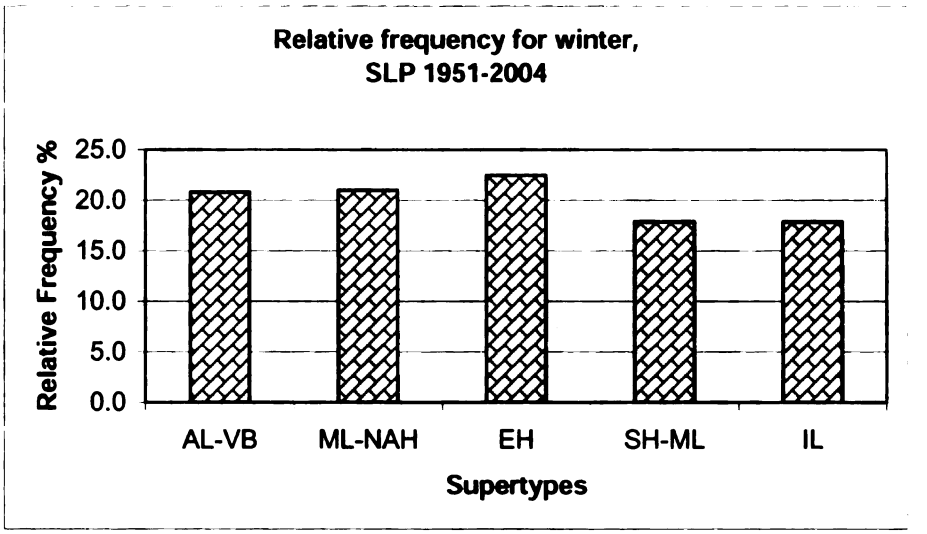

Figure 2-9 Relative frequency of the winter supertypes compared to the total number of winter days in the period (%)

The monthly distributions of the circulation patterns are of particular interest since they reveal the intra-seasonal evolution of the circulation conditions during winter. Typical of December are the AL-VBwin supertype with 23.2% occurrence, the EHwin supertype with 22.7%, and the ML-NAHwin supertype with 22.0% occurrence (Figure 2-10). The SH-MLwin supertype occurs least often (13.8%) in December compared to the other supertypes.

In January, the EHwin supertype occurs most often (26.3%). The AL-VBwin supertype is also frequent, occurring on 22.3% of all January days. The other supertypes are less frequent during this month, occurring during 16.8% (ML-NAHwin) to 17.5% (SH-MLwin) of the winter days.

The amplification of the land-sea contrasts in February, compared to the previous months, is evident in the predominance of the ML-NAHwin (24.6%) and the SH-MLwin supertypes (22.8%). The zonal flow characterizing the AL-VBwin supertype is least important during February with only a 16.5% frequency.

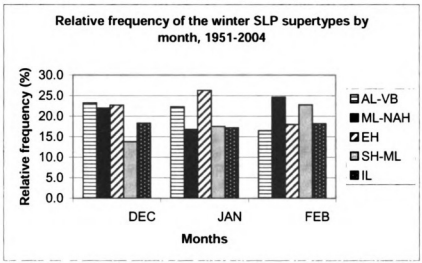

Figure 2-10 Relative frequencies of the winter supertypes compared to the total number of days in each month for the overall period (%)

4.1.1. d. Seasonal and monthly distributions of the winter circulation types

The frequency of the circulation types during winter ranges from 4.9% to 9.3% (Table 2-11). The types highly associated with the most frequent winter supertype, EHwin, although quite frequent are not prevalent. For example, EH1win occurred on 7.9% of the winter days and EH2win on 7.0% of the winter days. The mixed type ML-NAH/EHwin, however, which has high percentage of overlap with the EHwin supertype (43%), is the most recurrent (9.3%) in winter. Hence, the mixed type contributes significantly to the overall maximum winter frequency of the EHwin supertype. The SH-ML2win (4.9%) and SH-ML3win (5.1%) types are least frequent in winter similar to the supertype to which they are related, SH-MLwin.

Table 2-11 Relative frequency of the winter types compared to the total number of winter days in the period (%)

Type	IL1	SH-ML2	ML-NAH2	AL-VB2	ML-NAH1	IL2	ML-NAH/EH
Seasonal frequency	7.3	4.9	7.5	5.9	5.7	8.4	9.3

Type	SH-ML1	EH1	AL-VB3	EH2	AL-VB1	ML-NAH/SH-ML	SH-ML3
Seasonal frequency	8.4	7.9	8.3	7.0	7.4	6.8	5.1

The circulation types are fairly evenly distributed throughout the winter months, with most of the types occurring on 3.2% to 10.8% of the days in a month (Table 2-12). The most recurrent types, ML-NAH/EHwin (10.8% in February), EH1win (10.6% in January) and ML-NAH/SH-MLwin (10.6% in February), follow the monthly distribution of the supertypes with which they are associated. These types have maximum incidence in the same months in which the respective supertypes with which they are associated have their maximum. This correspondence between the monthly frequencies of the supertypes and the related types holds true for the rest of the types as well.

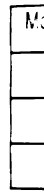

4.1.1

corre

troug

defin

are e

the d

2-11)

comp

flow

north

prom

a tro

Spi

Table 2-12 Relative frequencies of the winter types compared to the period number of days for each month (%)

Month/Type	IL1	SH-ML2	ML-NAH2	AL-VB2	ML-NAH1	IL2	ML-NAH/EH
DEC	6.7	3.2	9.0	7.0	6.5	9.6	8.0
JAN	6.5	5.0	6.2	6.0	4.4	8.4	9.3
FEB	9.1	6.5	7.3	4.7	6.3	7.2	10.8

Month/Type	SH-ML1	EH1	AL-VB3	EH2	AL-VB1	ML-NAH/SH-ML	SH-ML3
DEC	8.5	8.0	9.3	9.0	7.4	4.3	3.6
JAN	7.2	10.6	9.7	6.0	8.7	6.0	6.0
FEB	9.6	4.9	5.8	5.8	5.8	10.6	5.6

4.1.1. e. Winter Z500 composites characteristics

The Z500 composite maps created for the supertypes show a clear correspondence to the respective SLP patterns. A low amplitude ridge and trough in the southern portion of the European/North Atlantic region, a well-defined zonal flow to the north, and weak troughing over northern Scandinavia, are evident on the composite created from averaging the Z500 daily patterns for the dates classified as having the Arctic Low-Voeikov Belt supertype (Figure 2-11). An intense Z500 gradient, and a split flow characterize the Z500 composite for the Mediterranean Low-North Atlantic High supertype. The split flow features a ridge over the Atlantic and a trough over the continent in the north, and a ridge and a trough with much higher amplitude in the south. A prominent mid-tropospheric ridge over western, central and northern Europe and a trough over eastern Europe, are associated with the European High supertype. Split flow, manifested by mostly zonal circulation in the southern parts of the

region with weak troughing over the Mediterranean, and a distinct trough to the west of Iceland and a prominent ridge over northern Europe in the northern flow, is associated with the Scandinavian High-Mediterranean Low SLP pattern. The Icelandic Low Z500 composite is characterized by a combination of a ridge to the south and trough at the northern portions of the Atlantic and mostly zonal flow over the continent. All of the Z500 composites represent upper-air configurations that relate strongly to the SLP features of the supertypes.

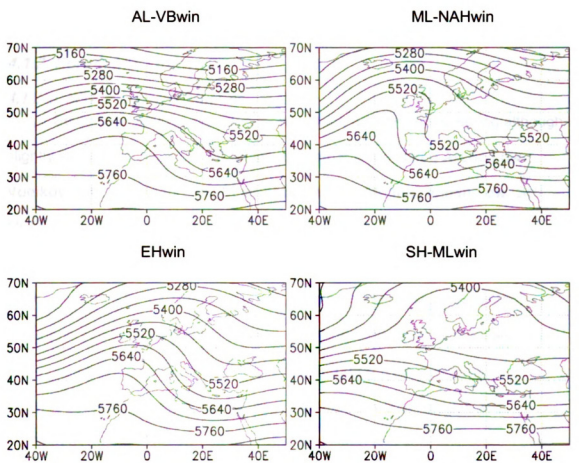

Figure 2-11 Z500 supertypes composites, Winter

ILwin

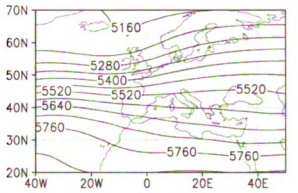

Figure 2-11 Continued

4.1.2. Springtime circulation

4.1.2. a. Spring supertype patterns

Several supertypes identified for winter are also present in spring although slightly modified. Similar to their winter counterparts, the spring **Arctic Low-Voeikov Belt**[4] (AL-VBspr) and **Scandinavian High-Mediterranean Low** (SH-MLspr) supertypes feature two anomaly centers of opposite sign over the northern and the southern areas of the study domain (Figure 2-12). Although the anomaly centers for AL-VBspr are similar in intensity to those in the winter supertype with the same name, the area with higher than normal pressure is shifted to the north and is located over central Europe. This supertype, in general, produces mostly westerly (zonal) surface flow over western and northern Europe and northwesterly flow over eastern and southeastern Europe. Southwestern Europe is characterized by anticyclonic conditions.

[4] The supertypes have the same names in two seasons, if the location and the sign of the anomalies they feature are similar.

The mirror image to the AL-VBspr anomaly pattern, is the SH-MLspr anomaly pattern. It features a strong positive anomaly over Scandinavia and a less intense, compared to winter, negative anomaly centered over Spain. The spring supertype is similar to the winter supertype with the same name, with the exception that the anomalies are weaker. The low-level air flow is predominantly easterly-northeasterly over most of Europe.

The main feature of the composite for the **Icelandic Low** (ILspr) supertype, like the ILwin supertype, is the well developed negative anomaly over Ireland. In addition, however, an area of higher than normal SLP is evident over the Mediterranean and the southeastern portions of the study domain, with the largest positive anomaly located south of Italy. Most of Europe is affected by southerly airflow under this supertype.

Another supertype in spring which features two anomaly centers is the **European Low** (ELspr), which, in contrast to the above configurations, does not have a winter counterpart. This pattern is characterized by an extensive negative anomaly located over central Europe, affecting the entire continent. A weak positive anomaly is centered south of Iceland. The European Low configuration is clearly conducive to meridional low-level circulation: from the north-northwest over western Europe and from the south over southeastern and central Europe.

The only supertype dominated by a single anomaly center is the **Azores-Scandinavian Ridge** (ASRspr), which is also a springtime pattern without a winter counterpart. This supertype is dominated by an elongated area of higher than normal SLP extending in a northeasterly direction from the tropical latitudes

of the Atlantic towards the British Isles and Scandinavia. The largest positive anomaly is centered over Denmark. The strongest pressure gradient is seen over Iceland. Most of the continent is dominated by anticyclonic conditions under this supertype.

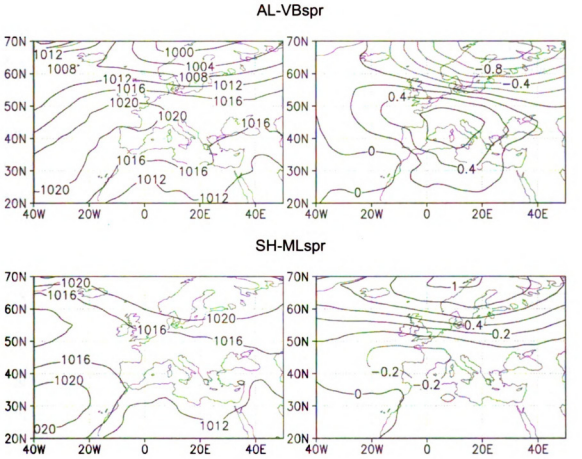

Figure 2-12 Supertypes composites for spring – pressure patterns (left column) and standardized anomaly patterns (right column)

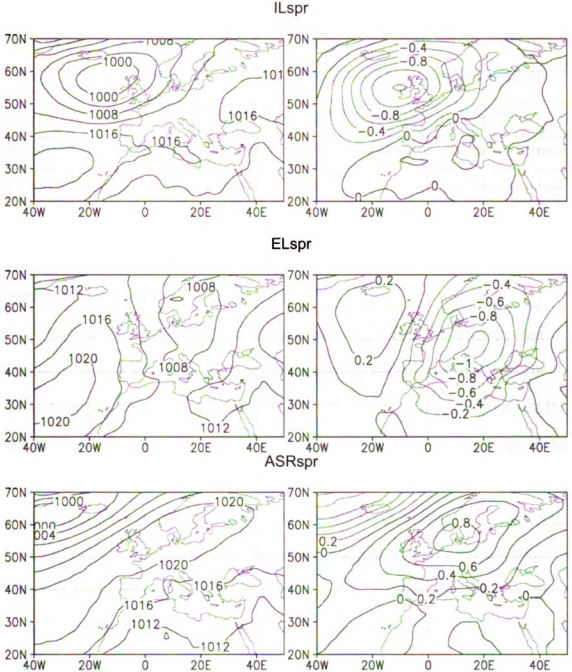

Figure 2-12 continued

4.1.2. b. Relationships between the supertypes and the circulation types for spring[5]

The Scandinavian High-Mediterranean Low supertype has the strongest association with types SH-ML1spr (90% of days in common), SH-ML2spr (70% overlap), and SH-ML3spr (59% overlap, Table 2-13). The composite maps for types SH-ML1spr and SH-ML2spr differ from that of the supertype by the intensity of the negative anomaly (higher in both cases) and by the displacement of the positive anomaly to the south for SH-ML1spr and of the negative anomaly to the northwest for SH-ML2spr. For type SH-ML3spr, the negative anomaly is stronger and shifted to the east, and the positive anomaly is weaker and displaced to the west (Figure 2-13).

Several types are strongly associated with the Arctic Low-Voeikov Belt supertype. They are type AL-VB1spr (99% days in common), type AL-VB2spr (83%), type AL-VB3spr (77%), and type AL-VB4spr (69%). The composite SLP pattern for AL-VB1spr shows more intense anomaly centers in comparison to the supertype pattern. The AL-VB2spr type features less intense anomalies and, in addition, a second positive anomaly center southwest of Iceland. The composite for AL-VB3spr illustrates a more intense area of higher SLP over the continent compared to the supertype, and a negative anomaly shifted westward over the Atlantic. AL-VB4spr portrays a more intense negative anomaly shifted somewhat to the south and an elongated less intense positive anomaly extending into the southwestern portion of the study domain.

[5] The types composite maps are arranged according to the sequence in which they are addressed in the text.

Table 2-13 Classification of the atmospheric circulation over Europe - Spring types
Association between the types and supertypes
*** Mixed types have less than 50% days overlap with any one supertype.**

Type abbreviation	Associated supertype	Overlap with supertype(s) %
SH-ML1spr	Scandinavian High-Mediterranean Low (SH-MLspr)	90%
SH-ML2spr		70%
SH-ML3spr		59%
AL-VB1spr	Arctic Low- Voeikov Belt (AL-VBspr)	99%
AL-VB2spr		83%
AL-VB3spr		77%
AL-VB4spr		69%
ASR1spr	Azores-Scandinavian Ridge (ASRspr)	84%
ASR2spr		64%
ASR3spr		61%
EL1spr	European Low (ELspr)	90%
EL2spr		85%
IL1spr	Icelandic Low (ILspr)	87%
IL2spr		55%
AL-VB/ELspr	*Mixed between AL-VBspr and ELspr	48%/31%
EL/ILspr	Mixed between ELspr and ILspr	49%/44%
IL/ELspr	Mixed between ILspr and ELspr	48%/27%
IL/ASRspr	Mixed between ILspr and ASRspr	43%/32%

The Azores-Scandinavian Ridge supertype is related to several types.

Type ASR1spr (84% days in common) is dominated by a large and more intense

positive anomaly over the British Isles compared to the supertype. An additional negative anomaly is evident to the southwest of Spain. Type ASR2spr, with 64% of days of overlap with the supertype pattern, differs from it by a more intense positive anomaly that is shifted northeastward. An additional positive anomaly center, not present in the supertype composite, is seen in the southwestern portion of the study domain, and the negative anomaly over Greenland extends to the southeast. ASR3spr has 61% days in common with the supertype and features a stronger negative anomaly over Iceland, and a zone of less intense positive anomalies located to the south of the positive anomaly in the supertype.

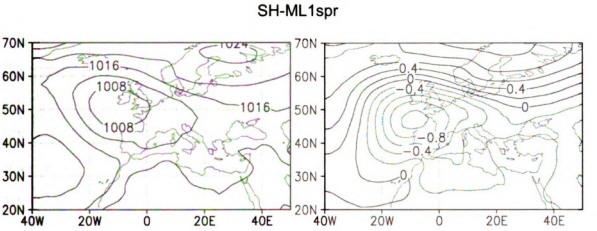

Figure 2-13 Spring types composites – pressure patterns and standardized anomalies The left column presents the SLP patterns, while the right column displays the standardized anomaly patterns

70N
60N
50N
40N
30N
20N
40W

70N
60N
50N
40N
30N
20N
40W

70N
60N
50N
40N
30N
20N

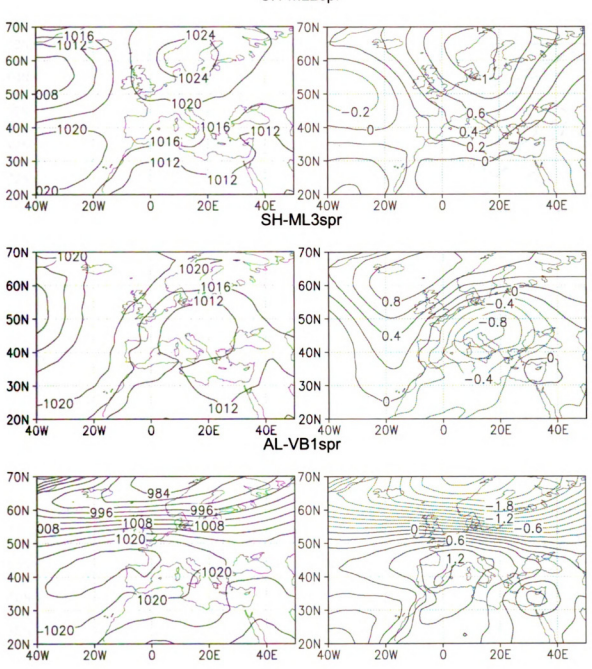

Figure 2-13 continued

AL-VB2spr

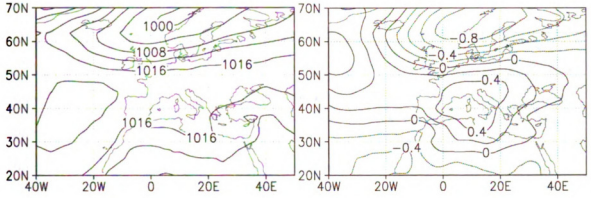

AL-VB3spr

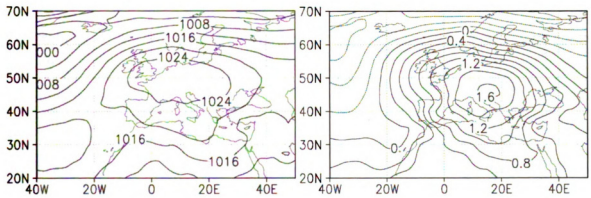

AL-VB4spr

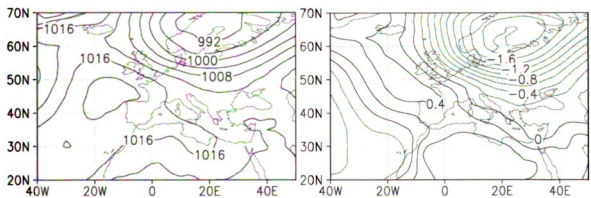

Figure 2-13 continued

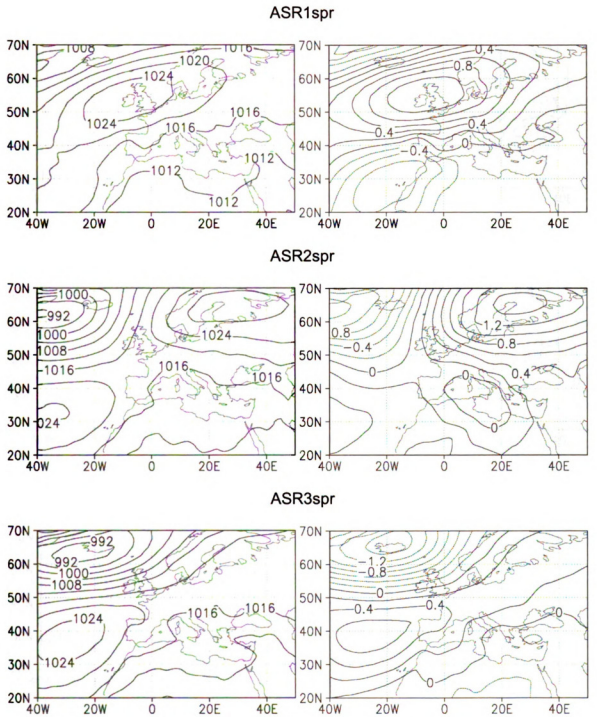

Figure 2-13 continued.

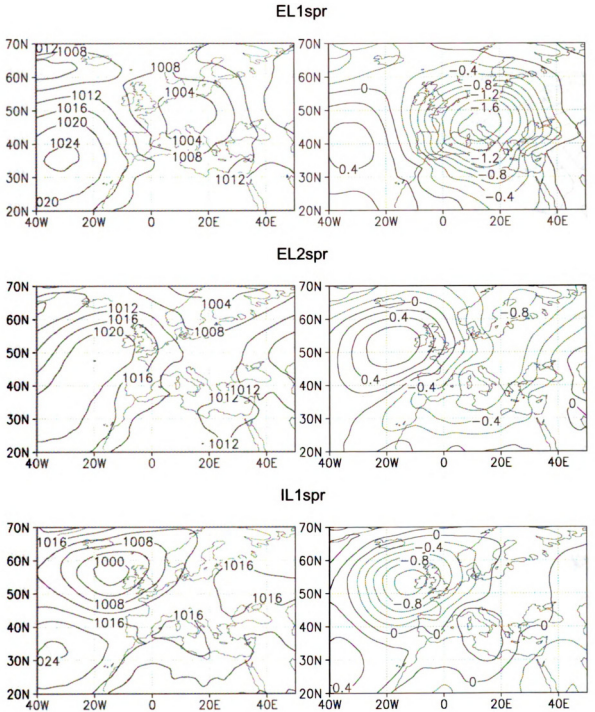

Figure 2-13 continued

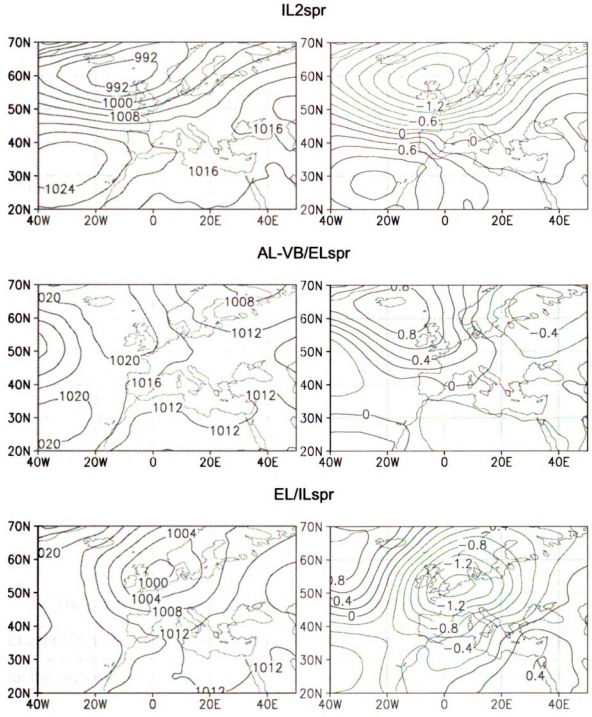

Figure 2-13 continued

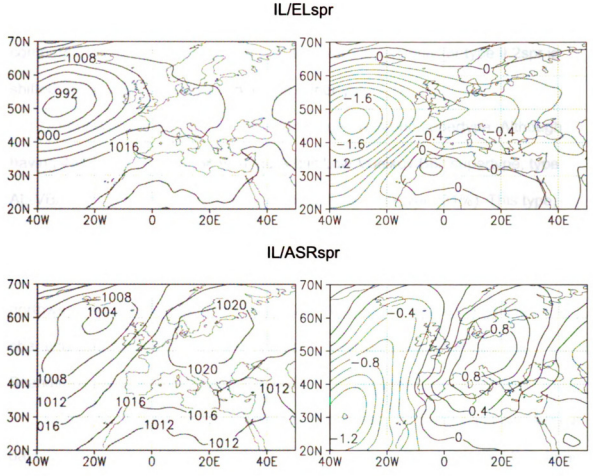

Figure 2-13 continued

The composite maps for type EL1spr (90% days in common) and type EL2spr (85% overlap) are quite similar to the European Low supertype, except for the higher intensity of both anomaly centers for the former and the stronger positive anomaly somewhat displaced to the southwest for the latter.

Types IL1spr (87% days of overlap) and IL2spr (55% overlap) are highly associated with the Icelandic Low supertype. The patterns deviate from the

supertype by the intensity of the anomaly centers, with type IL1spr having a weaker negative anomaly and type IL2spr featuring a stronger negative anomaly, compared to the supertype. In addition, the positive anomaly for type IL2spr is shifted to the west of the location for the supertype.

Four types are mixed, i.e. related to more than one supertype. Although having 48% days in common with the Arctic Low-Voeikov Belt supertype, type AL-VB/ELspr is also related to the European Low supertype (31%). This type, being an intermediate between the above supertypes, features a stronger positive anomaly (compared to both AL-VBspr and ELspr) that is shifted to the northwest over Iceland compared to the AL-VBspr. In addition, the type is characterized by weaker negative anomalies over the Russian Plain / Scandinavia and North Africa, compared to both supertypes.

Type EL/ILspr is an intermediate type between the European Low (49% of days in common) and the Icelandic Low (44% overlap). It is dominated by a large and more intense (compared to both supertypes) negative anomaly centered over Belgium and features a stronger positive anomaly that is displaced southwest of Iceland compared to the location on the composite map of the ELspr supertype.

The composite pattern for type IL/ELspr is related to a greater extent to the Icelandic Low supertype (48% days in common). The type composite features a stronger negative anomaly, displaced to the southwest, compared to both supertypes.

Type IL/ASRspr is divided between the Icelandic Low (43% days in common) and the Azores-Scandinavian Ridge supertypes (32% overlap). It deviates from the Icelandic Low by the intensity (stronger), and position (displaced in tropical Atlantic and extending to Iceland) of the negative anomaly, and from the Azores-Scandinavian Ridge by the position (shifted over central Europe) of the positive anomaly.

4.1.2. c. Frequency of the spring supertypes

In general, the supertypes identified for spring are equally frequent, although the SH-MLspr supertype occurs on slightly more spring days (21.3%) than the other supertypes (Figure 2-14). Least frequent is the Icelandic Low supertype (18.6%). The frequency of the rest of the supertypes is approximately 20% (19.5% for ASRspr, 20.0% for ELspr, and 20.7% for AL-VBspr).

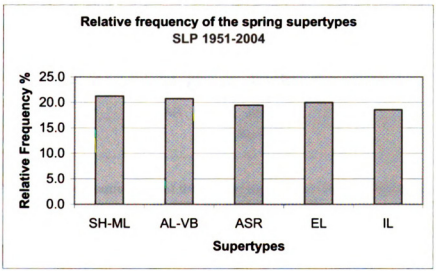

Figure 2-14 Relative frequency of the spring supertypes compared to the total number of spring days in the period (%)

Regarding intra-seasonal variations, March is dominated by a supertype characterized by a strong positive anomaly over most of the continent. The AL-VBspr is most frequent in March, with frequency of 26.3% (Figure 2-15). Least recurrent in March is the SH-MLspr configuration with 13.9% occurrence. April is characterized by an increased frequency (23.4%) of the ELspr supertype. The rest of the supertypes exhibit similar occurrence rates in April, varying between only 18.8% and 19.9%. May is dominated by the SH-MLspr supertype, which at 30.8% is more frequent in May than in any other spring month. Conversely, the other supertypes are least frequent in May.

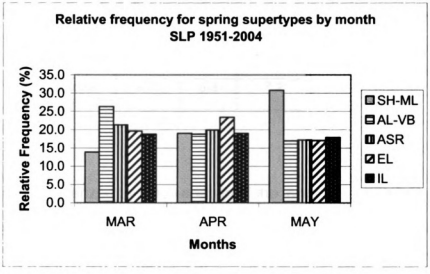

Figure 2-15 Relative frequencies of the spring supertypes compared to the period number of days for each month (%)

4.1.2. d. Seasonal and monthly distribution of the spring types

Although the seasonal frequencies of the supertypes are quite similar (Figure 2-14), the seasonal distribution of the circulation types is more variable.

The AL-VB/ELspr mixed type exhibits the highest frequency (9.1%) for spring (Table 2-14). Second most frequent is the IL1spr with 7.5% of all the spring days. Several types display low recurrence rates for the season. Types AL-VB4spr (3.4%) and AL-VB1spr (2.3%) are least frequent.

Table 2-14 Relative frequency of the spring types compared to the total number of spring days in the period (%)

Type	IL/EL	SH-ML2	IL1	EL/IL	AL-VB/EL	AL-VB2	EL2
Seasonal frequency	4.6	7.0	7.5	4.9	9.1	5.9	5.1

Type	Al-VB4	SH-ML1	ASR3	AL-VB1	EL1	SH-ML3	AL-VB3
Seasonal frequency	3.4	6.3	6.6	2.3	4.3	7.2	4.9

Type	IL2	IL/ASR	ASR1	ASR2
Seasonal frequency	4.0	3.9	7.2	5.8

March is characterized by little variation of the incidence rates for the different types. Except for AL-VB3spr (8.9%) and ASR2spr (9.0%), all the other types occur on 3.5% to 6.9% of the days in March (Table 2-15).

During April, the combined high rate of occurrence of the mixed AL-VB/ELspr (10.0%), EL1spr (5.6%) and EL2spr (6.8%) types, results in the overall greatest recurrence for the associated supertype, ELspr (23.4%, Figure 2-15). Least recurrent is the AL-VB1spr with 0.7%, reflecting the AL-VBspr supertype minimum of 18.8% for April (Figure 2-15).

Table 2-15 Relative frequencies of the spring types compared to the period number of days for each month (%)

Type	IL/EL	SH-ML2	IL1	EL/IL	AL-VB/EL	AL-VB2	EL2
MAR	6.9	4.2	3.5	5.7	5.1	4.1	4.4
APR	5.1	5.0	7.0	5.5	10.0	7.0	6.8
MAY	2.0	11.8	11.9	3.6	12.3	6.7	4.3

Type	AI-VB4	SH-ML1	ASR3	AL-VB1	EL1	SH-ML3	AL-VB3
MAR	6.2	3.6	6.6	5.8	4.4	4.3	8.9
APR	3.0	5.6	7.3	0.7	5.6	7.9	3.4
MAY	0.8	9.6	5.9	0.2	3.0	9.3	2.4

Type	IL2	IL/ASR	ASR1	ASR2
MAR	6.9	4.7	5.8	9.0
APR	3.5	4.0	8.2	4.4
MAY	1.5	2.9	7.8	3.9

May displays even larger differences between the occurrence rates for the different types. While the AL-VB/ELspr type occurs on 12.3% of all days, the AL-VB1spr and AL-VB4spr types occur on less than 1% of May days.

4.1.2. e. Spring Z500 composites characteristics

The Z500 composite for the SH-MLspr supertype displays a split flow with a high amplitude trough/ridge wave over the northern portion of the region corresponding to the Icelandic Low and the Scandinavian high pressure center on the SLP composite map. Within the southern air stream a much less

pronounced ridging over the southern Atlantic (related to the SLP Azores High) is accompanied by weak troughing over the Mediterranean (Figure 2-16). The Z500 composite for the AL-VBspr supertype also shows a split flow pattern. The northern ridge, however, is displaced westward over the Atlantic, compared to the Z500 configuration for the SH-ML supertype, and northern and eastern Europe are influenced by troughs. The Z500 composite for the ASRspr supertype shows a high amplitude ridge-trough pattern. Ridging is affecting the eastern Atlantic and Western Europe resulting in the extended SLP ridge at the surface. Troughing characterizes the areas to the west of Iceland and Eastern Europe. The same configuration, although displaced to the west and featuring a more intense height gradient, is evident on the Z500 composite for the spring ELspr supertype. The Z500 map for the ILspr supertype is characterized by a split flow with a trough over northern Atlantic (corresponding to the large area Icelandic Low) in the northern air stream. Slight ridging over the Mediterranean and troughing over the Black and the Red seas is evident in the southern air stream.

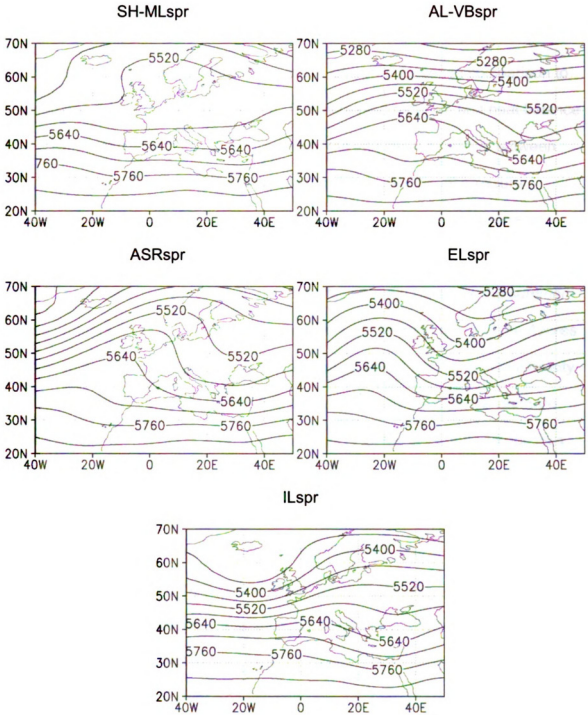

Figure 2-16 Z500 supertypes composites, Spring

4.1.3. Summertime circulation

4.1.3. a. Summer supertype patterns

Summer circulation patterns are much less pronounced in comparison to the patterns during the rest of the year. The increased radiative and heat balance of the Northern Hemisphere, the decrease of the latitudinal contrasts between the polar and the tropical regions lead to much lower meridional pressure gradients and as a consequence less vigorous, more stagnant atmospheric circulation during this season.

Three supertypes were suggested by the synoptic typing for the summer season (Figure 2-17). All of the supertypes indicate the importance of the Azores High in summer, depicting its augmented areal coverage and increased intensity. The circulation centers of action shift to the north in summer, and the northern displacement of the Azores High is well evident in all the supertype composites. In addition to the Azores High, a thermal cyclone over the Arabian Peninsula and the Persian Gulf is apparent for all the summertime supertypes. This thermal low, referred to here as the Persian Gulf Low, reflects the increased heating of the continental areas in summer. Two of the supertypes are also characterized by anomaly centers located over Scandinavia. The **Azores-Scandinavian Ridge** (ASRsum) supertype, similarly to its spring counterpart, features a strong area of higher than normal SLP over Scandinavia. The differences between the spring and summer supertypes, however, reflect the lower circulation intensity in summer. The positive anomaly is smaller in extent and the anomaly gradient over Iceland is much weaker in summer. While most of western and northern Europe

is dominated by anticyclonic conditions, the eastern portions of the continent are affected by northerly-northeasterly low-level airflow. The anomaly center over Scandinavia is of opposite sign, indicating lower than normal SLP, for the **Arctic Low-Persian Gulf Low** (AL-PGLsum) supertype. This supertype is also characterized by a stronger Persian Gulf negative anomaly compared to the ASRsum supertype. While western and northern Europe are affected by a southerly surface flow, most of central and eastern Europe is characterized by weak pressure gradients. The AL-PGLsum supertype does not have a counterpart in the other seasons.

The **Weak Persian Gulf Low** (WPGLsum) supertype also is only present in summer. It is dominated by a single, strong positive anomaly center, located over the Arabian Peninsula and the Persian Gulf. This positive anomaly is reflected in the occurrence of a weaker than in the other supertypes thermal cyclone on the surface SLP composite map. The majority of western Europe is influenced by a westerly/southwesterly airflow, while the eastern and southeastern portions of the continent experience westerly/northwesterly airflow.

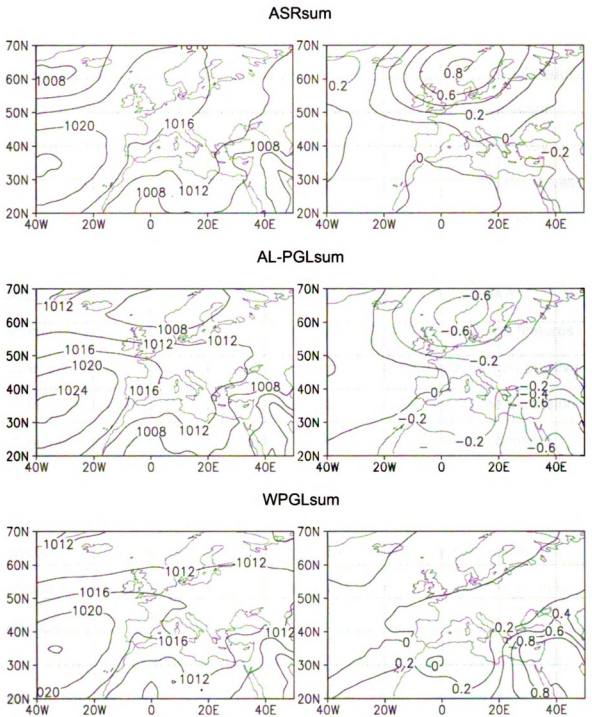

Figure 2-17 Supertypes composites for summer – pressure patterns (left column) and standardized anomaly patterns (right column)

4.1.3. b. Relationships between the supertypes and the types for summer[6]

The types associated with the WPGLsum supertype are WPGL1sum (100% of days in common), WPGL2sum (96%), WPGL3sum (91%), WPGL4sum (90%), WPGL5sum (76%), and WPGL6sum (74%) (Table 2-16). WPGL1sum differs slightly from the supertype in that displays a stronger positive anomaly over the Persian Gulf. Type WPGL2sum configuration features an additional well defined negative anomaly over the northern Atlantic and Scandinavia. The composite for type WPGL3sum differs from the supertype map in terms of an additional negative anomaly over the central Mediterranean and positive anomalies over the mid-Atlantic and Scandinavia. The WPGL4sum type features lower than normal SLP over most of the mid-continent and a well-defined positive anomaly over Iceland. WPGL5sum diverges from the supertype by the extension of the positive anomaly from the Persian Gulf over almost the entire continent and northern Africa. Negative anomalies are seen in the northern portions of the study domain. The last type (WPGL6sum) displays a more intense and extensive positive anomaly from the Persian Gulf area to the western Mediterranean compared to the supertype. A weak negative anomaly over the Russian Plain is also seen.

The six types associated with the ASR supertype and the percentage of days in common are: ASR1sum (93%), ASR2sum (86%), ASR3sum (84%), ASR4sum (72%), ASR5sum (59%), and ASR6sum (55%). The types can be divided into two groups depending on their differences from the supertype. The

[6] The types composite maps are arranged according to the sequence in which they are addressed in the text.

first group includes ASR1sum, ASR3sum, ASR4sum and ASR5sum. All four types display either a similar or stronger positive anomalies in the northern portions of the map domain. For ASR3sum, the location of the positive anomaly is similar, whereas for ASR4sum the largest positive deviations are located somewhat further north over the North Atlantic. For ASR1sum, the area of positive anomalies extends farther south into Mediterranean and North Africa, while the positive anomalies extend eastward for ASR5sum. The other two types exhibit either a weaker positive anomaly with a more intense Persian Gulf anomalous area (ASR2sum), or without Persian Gulf anomaly evident (ASR6sum). All of these types also feature additional strong negative anomalies in the northern corners of the domain or over the mid-latitude Atlantic.

Table 2-16 Classification of the atmospheric circulation over Europe - Summer types
Association between the types and supertypes
*** Mixed types have less than 50% days overlap with any one supertype.**

Type abbreviation	Associated supertype	Overlap with supertype(s) %
WPGL1sum	Weak Persian Gulf Low (WPGLsum)	100%
WPGL2sum		96%
WPGL3sum		91%
WPGL4sum		90%
WPGL5sum		76%
WPGL6sum		74%
ASR1sum	Azores-Scandinavian Ridge (ASRsum)	93%
ASR2sum		86%
ASR3sum		84%
ASR4sum		72%
ASR5sum		59%
ASR6sum		55%
AL-PGL1sum	Arctic Low-Persian Gulf Low (AL-PGLsum)	100%
AL-PGL2sum		96%
AL-PGL3sum		84%
AL-PGL4sum		70%
AL-PGL5sum		68%
AL-PGL6sum		66%
AL-PGL/ASR/ WPGLsum	*Mixed between AL-PGLsum, ASRsum and WPGLsum	37%/36%/28%

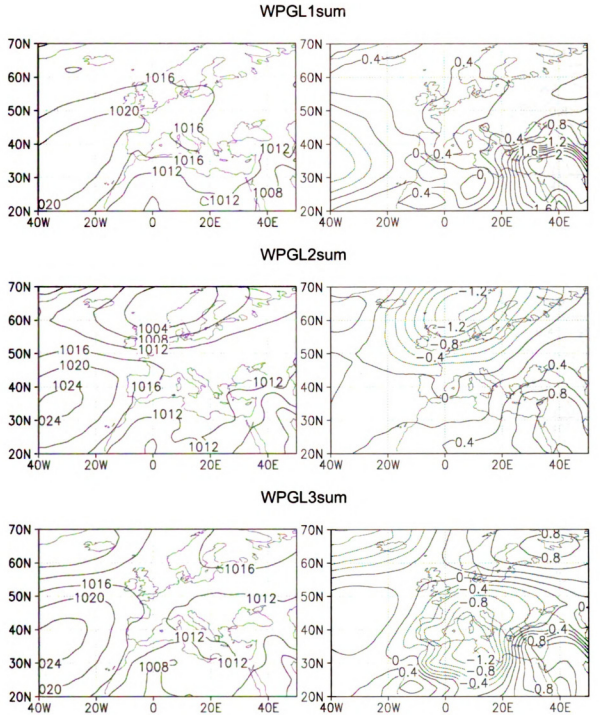

Figure 2-18 Summer types composites – pressure patterns and standardized anomalies The left column presents the SLP patterns, while the right column displays the standardized anomaly patterns

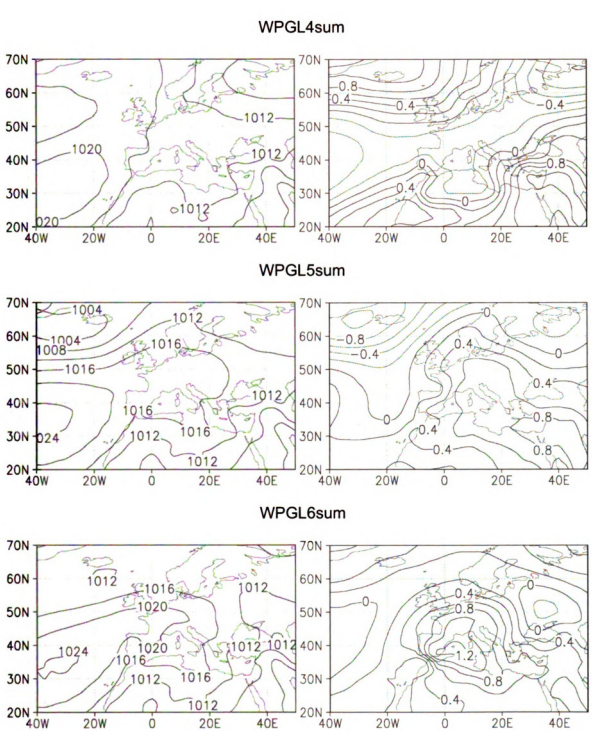

Figure 2-18 continued

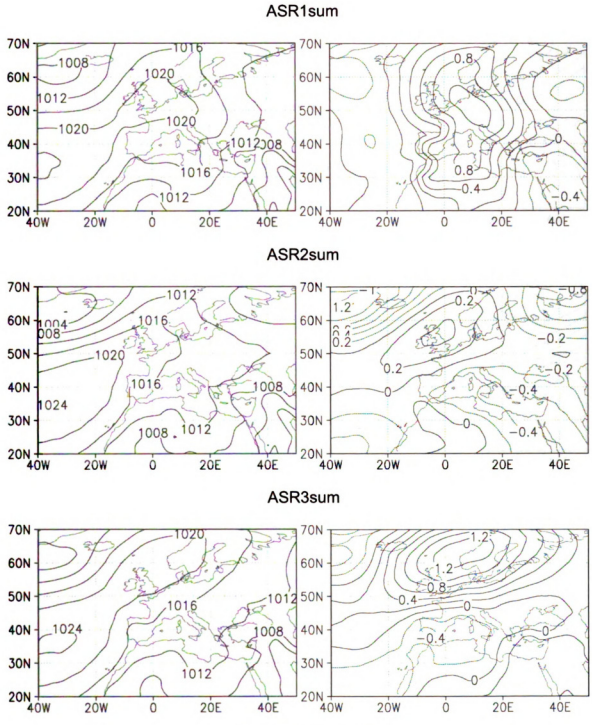

Figure 2-18 continued

ASR4sum

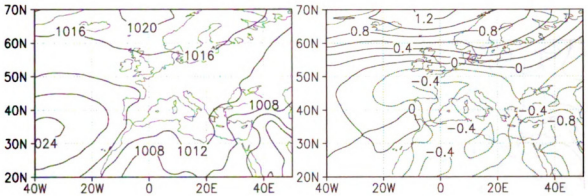

ASR5sum

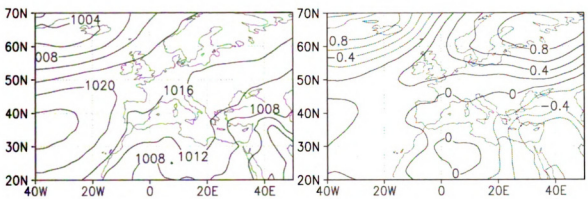

ASR6sum

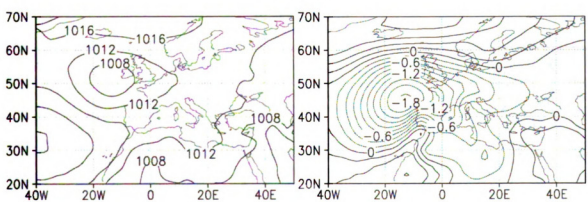

Figure 2-18 continued

70N
60N
50N
40N
30N
20N
4

70N
60N
50N
40N
30N
20N
4

70N
60N
50N
40N
30N
20N
4

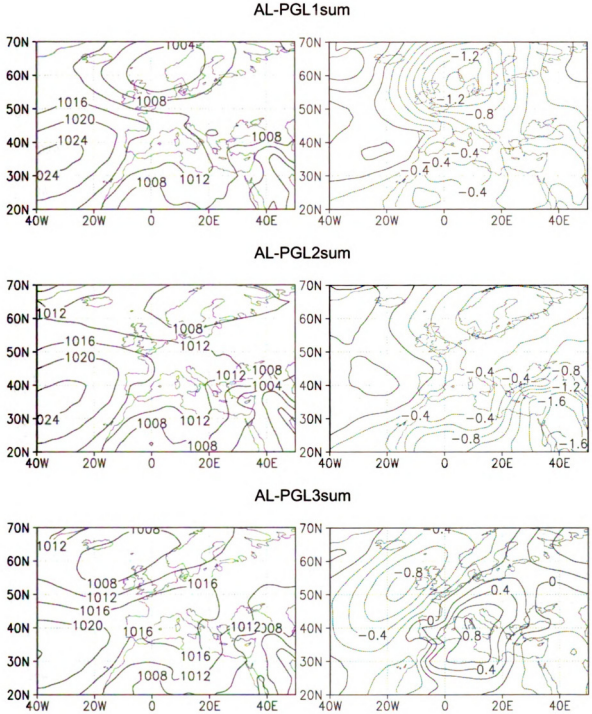

Figure 2-18 continued

AL-PGL4sum

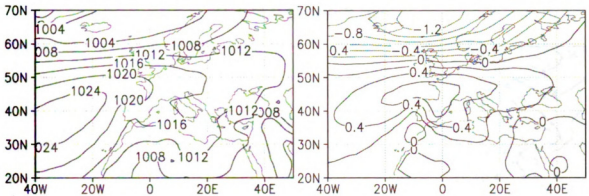

AL-PGL5sum

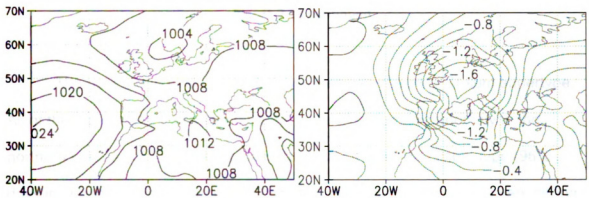

AL-PGL6sum

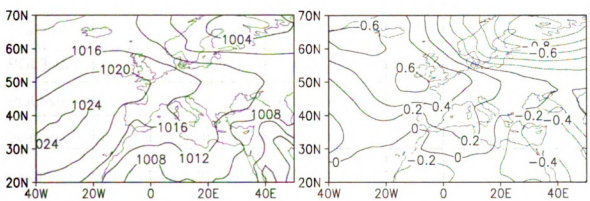

Figure 2-18 continued

AL-PGL/ASR/WPGLsum

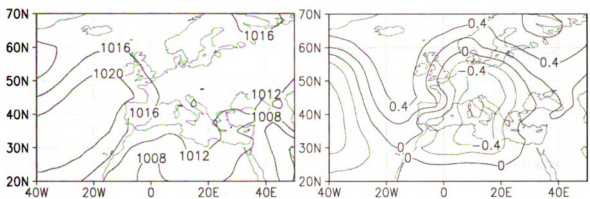

Figure 2-18 continued

The next group of six types is associated with the AL-PGLsum supertype. All of the types feature stronger than the supertype negative anomaly in the northern portions of the study domain except for the AL-PGL2sum type (96% days in common with the supertype) which is characterized also by a very strong Persian Gulf negative anomaly. Three of the types display a shift of the Arctic negative anomaly. This anomaly is: a) displaced to the southwest for AL-PGL3sum (84%); b) shifted to the south over the European continent for AL-PGL5sum (68% overlap); or c) displaced to the east for AL-PGL6sum (66% overlap). In combination with the displacement of the negative Arctic anomaly, the above types feature a weak Persian Gulf anomaly (AL-PGL3sum, AL-PGL5sum, AL-PGL6sum) or a lack of such an anomaly (AL-PGL4sum). Three types display additional positive anomalies located either over the continent (AL-PGL3sum and AL-PGL4sum) or extending from Iceland to the southwest of Europe (AL-PGL6sum).

In summer, one type is mixed, i.e., related to more than one supertype. Despite having 37% days in common with the Arctic Low-Persian Gulf Low supertype, type AL-PGL/ASR/WPGLsum is also associated with the Azores-Scandinavian Ridge (36%), and the Weak Persian Gulf Low (28%) supertypes. The similarities between this mixed type and the three supertypes are: a) a strong negative anomaly located over Italy and affecting central and southern Europe, somewhat similar to AL-PGLsum; b) positive anomalies over northern Europe, the Russian Plain and the eastern Atlantic, similar to the ASRsum supertype; and c) a positive Persian Gulf anomaly, as in the WPGLsum pattern.

4.1.3. c. Frequency of the summer supertypes

The supertypes are approximately equally frequent in summer. The seasonal frequency varies between 31.7% for the WPGLsum supertype and 35.1% for the AL-PGLsum supertype (Figure 2-19).

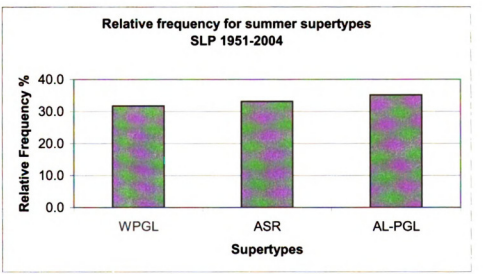

Figure 2-19 Relative frequency of the summer supertypes compared to the total number of summer days in the period (%)

2-2

ref

and

cor

Gu

(AS

fre

day

am

dee

and

cor

ap

June is strongly dominated by the WPGLsum supertype (56.2%, Figure 2-20), which occurs twice as frequently as the other two supertypes. This finding reflects the evolution of the thermal conditions in the beginning of the summer, and in particular the gradual warming of the continents, in this case the Asian continent, which subsequently leads to the development of the strong Persian Gulf thermal low. The other supertypes occur on 19.4% (AL-PGL) and 24.3% (ASRsum) of the June days for the period. In the middle of summer the most frequent supertype is the AL-PGLsum supertype, occurring on 50.0% of the July days for the period. With the continents having accumulated already vast amounts of heat during the summer months, the Persian Gulf thermal low deepens, and the Weak Persian Gulf supertype, characterized by a positive anomaly over the Arabic Peninsula, is considerably less frequent in July compared to June (12.8% of the July days for the period). The supertypes are approximately equally frequent in August.

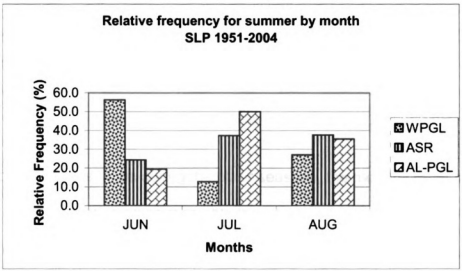

Figure 2-20 Relative frequencies of the summer supertypes compared to the period number of days for each month (%)

4.1.3. d. Seasonal and monthly distribution of the summer types

The types are approximately equally frequent in summer (Table 2-17). Most often, excluding the AL-PGL5 supertype, highest frequency (between 5.0% and 6.6%) exhibit the types associated with the most frequent summer supertype, i.e. AL-PGLsum. Some of the types, related to the least frequent supertype in summer (WPGLsum), exhibit the lowest frequency (WPGL1sum, WPGL3sum and WPGL4sum).

Table 2-17 Relative frequency of the summer types compared to the total number of summer days in the period (%)

Type	AL-PGL1	AL-PGL/ ASR/WPGL	ASR2	ASR4	WPGL4	WPGL6	ASR6
Seasonal frequency	5.7	5.8	5.6	5.3	4.6	5.7	4.2

Type	Al-PGL2	AL-PGL5	AL-PGL3	ASR5	WPGL3	ASR1	AL-PGL6
Seasonal frequency	5.0	3.8	6.0	6.0	3.9	5.9	6.1

Type	WPGL5	ASR3	WPGL2	WPGL1	AL-PGL4
Seasonal frequency	5.7	6.1	5.6	2.7	6.6

In most of the cases, as during the other seasons, the monthly rates of occurrence of the circulation types resemble the intra-seasonal distribution of the supertypes (Table 2-18). In June, highest rate of occurrence exhibit the types associated with the WPGLsum supertype. In July, in addition to the highly recurrent types related to the AL-PGLsum supertype, some types associated with

the ASRsum supertype (ASR1sum, ASR4sum and ASR5sum) are also quite frequent. In August, the types related to the WPGLsum supertype are generally less frequent.

Table 2-18 Relative frequencies of the summer types compared to the period number of days for each month (%)

Type	AL-PGL1	AL-PGL/ ASR/WPGL	ASR2	ASR4	WPGL4	WPGL6	ASR6
JUN	2.1	5.4	2.7	2.5	8.9	8.4	7.2
JUL	8.2	4.9	5.6	7.8	1.1	5.1	2.4
AUG	6.6	7.0	8.5	5.6	3.8	3.6	3.2

Type	Al-PGL2	AL-PGL5	AL-PGL3	ASR5	WPGL3	ASR1	AL-PGL6
JUN	1.2	3.0	3.5	2.5	8.7	3.9	4.2
JUL	9.6	3.2	8.2	9.7	0.6	8.4	8.1
AUG	4.0	5.1	6.3	5.7	2.6	5.3	5.9

Type	WPGL5	ASR3	WPGL2	WPGL1	AL-PGL4
JUN	8.7	5.6	8.7	7.6	5.4
JUL	2.4	4.8	2.4	0.1	7.4
AUG	5.9	7.8	5.7	0.5	7.0

4.1.3. e. Summer Z500 composites characteristics

As expected, given the small differences in the summertime supertypes, the Z500 composite patterns are quite similar to one another. All display a slight ridge over the tropical Atlantic, a prominent closed blocking high over Africa and an inconspicuous trough over the Black Sea (Figure 2-21). The Z500 composites corresponding to the ASRsum and AL-PGLsum supertypes display a split flow with a ridge over northern Europe for the former and a trough between Iceland

and Scandinavia for the latter. The airflow is mostly zonal over western Europe on the Z500 composite for the WPGLsum supertype.

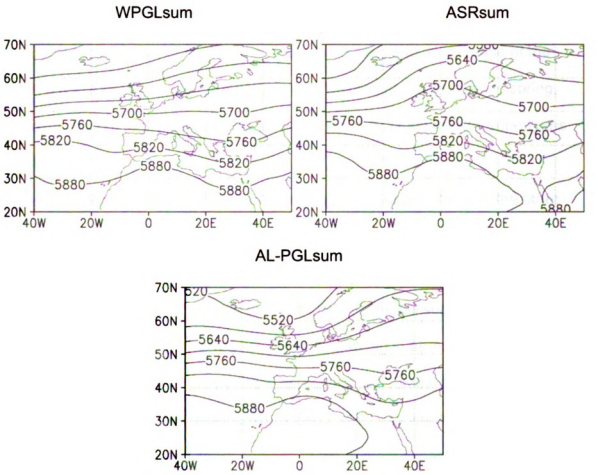

Figure 2-21 Z500 supertypes composites, Summer

4.1.4. Falltime circulation

4.1.4. a. Fall supertype patterns

The fall season is a period of transition between the weaker summer circulation and the robust winter state of the atmospheric circulation. Although the changes in fall are in the opposite direction (towards a decrease of the heat accumulation, especially north of the tropical latitudes, and an increase of the north-south thermal, and subsequently pressure gradient) compared to spring, the other transitional season, some similarities in their characteristic supertypes exist.

Three of the supertypes for fall correspond to supertypes from the other seasons. Two of these supertypes are characterized by two anomaly centers. The **Arctic Low/Voeikov Belt** (AL-VBfal) supertype is somewhat similar to the winter and spring supertypes with the same name. The fall supertype, however, differs from the AL-VB supertypes in winter and spring in terms of a less intense negative anomaly area in the northern portions of the domain that is more limited in extent compared to the other seasons and shifted eastward. In addition, the positive anomaly in the southern portions of the domain expands over most of Europe and features two closed centers of higher than normal SLP, one over France and a larger and more intense anomaly over Egypt. The surface gradient is strongest over Scandinavia and the Russian Plain. This supertype induces mostly zonal flow over northern Europe, while the rest of the continent is dominated by anticyclonic conditions.

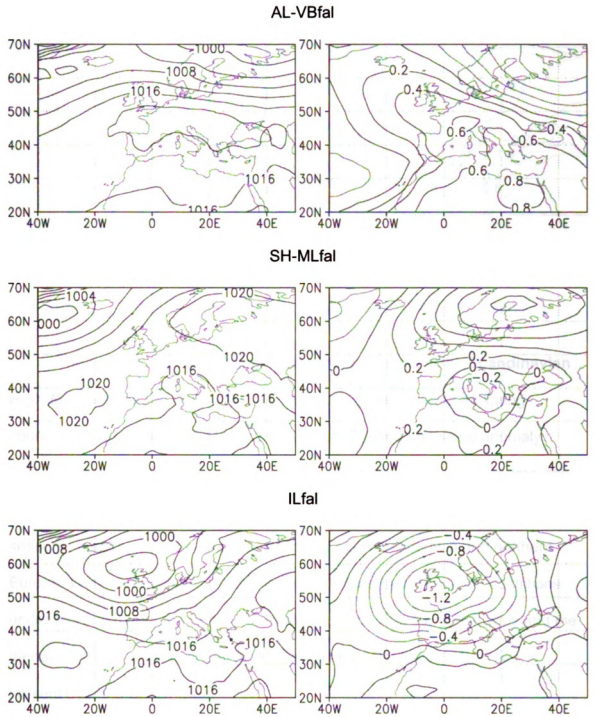

Figure 2-22 Supertypes composites for fall – pressure patterns (left column) and standardized anomaly patterns (right column)

PGLfal

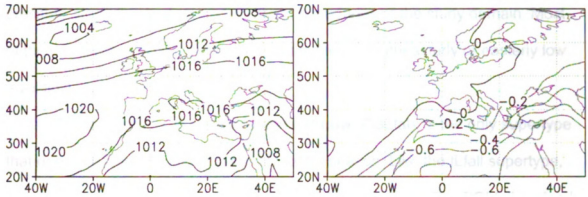

Figure 2-22 continued

The second supertype featuring two anomaly areas is the **Scandinavian High-Mediterranean Low** (SH-MLfal). Although quite similar to its spring counterpart, this supertype has a stronger, better defined negative anomaly centered over Italy. Compared to the winter supertype with the same name, the SH-MLfal supertype features less intense negative anomaly. As in the other seasons, a strong positive anomaly is located over Scandinavia and northern Europe. While northeastern Europe is characterized by anticyclonic conditions under this supertype, the rest of the continent, excluding the British Isles and the Iberian Peninsula, is influenced by easterly airflow. Southwesterly airflow is present over the British Isles.

Another fall season supertype that is also seen in other seasons is the **Icelandic Low** (ILfal). This supertype is dominated by a single large area of lower than normal SLP centered over the northern portions of the British Isles, similar to the IL supertypes for winter and spring. The fall IL supertype differs

from its spring counterpart by the more limited area of higher than normal pressure along the eastern and southern boundaries of the study domain. Most of the continent in fall is influenced by a southerly, southeasterly or easterly low level flow.

The last supertype, the **Persian Gulf Low** (PGLfal), is the only supertype that does not have a counterpart in any other season. Like the ILfall supertype, only one anomaly area is evident for the PGLfall supertype. The PGLfall is clearly a transitional circulation between the summer and the fall months as it is dominated by the strong negative anomaly located over the Arabian Peninsula and the Persian Gulf, which is characteristic of the summer season. The transport of air over most of the continent is from the west.

4.1.4. b. Relationships between the supertypes and types for fall[7]

Several types have overlap days with the Persian Gulf Low fall supertype (Table 2-19). Despite the variety of the types associated with the PGLfal supertype, all of them have in common the intense area of lower than normal sea-level pressure over the Persian Gulf/Arabian Peninsula. The pattern closest to the supertype is PGL1fal (100% overlap) featuring a more intense negative anomaly over the Persian Gulf/Arabian Peninsula (Figure 2-23). PGL2fal (82%) also displays a stronger Persian Gulf/Arabian Peninsula anomaly. In addition, it features a positive anomaly over Scandinavia, not present on the supertype composite. The rest of the types associated with the PGLfall supertype exhibit

[7] The types composite maps are arranged according to the sequence in which they are addressed in the text.

less intense negative anomalies over the Persian Gulf/Arabian Peninsula compared to the supertype. These types also deviate from the supertype by: a) the existence of a strong positive anomaly over Central and Western Europe and negative anomaly over the northern portion of the map domain (PGL3fal and PGL6fal); b) a strong negative center over the British Isles (PGL4fal); or c) a large positive anomaly over the British Isles and a negative anomaly over Scandinavia (PGL5fal).

The AL-VBfal supertype is related to types AL-VB1fal (97% in common), AL-VB2fal (72% days in common), and AL-VB3fal (51%). Although type AL-VB1fal is closest to the supertype, it displays more intense negative and positive anomaly areas compared to the supertype. AL-VB3fal also features a more intense positive anomaly centered between the British Isles and Scandinavia. In addition, this type displays a positive anomaly over the tropical Atlantic. Type AL-VB2fal differs from the supertype by the existence of two positive anomaly areas (over the Persian Gulf and west of Ireland) and of a well defined area of lower than normal pressure over Italy.

The SH-MLfal supertype is very well depicted by type SH-ML1fal (100% days in common). The only deviation of the type from the supertype is the higher intensity of the anomaly areas over Scandinavia and the Mediterranean. The composite for type SH-ML2fal (71% in common with the supertype) is characterized by a displacement of the Scandinavian positive anomaly to the southwest and a westward shift of the negative anomaly over the Mediterranean compared to the composite for the supertype. Type SH-ML3fal (with only 56%

overlap days with the supertype) features a very strong negative anomaly over Italy, surrounded by weak positive anomalies to the west, north and east.

Table 2-19 Classification of the atmospheric circulation over Europe – Fall Types Association between the types and supertypes
*** Mixed types have less than 50% days overlap with any one supertype.**

Type abbreviation	Associated supertype	Overlap with supertype(s) %
PGL1fal	Persian Gulf Low (PGLfal)	100%
PGL2fal		82%
PGL3fal		78%
PGL4fal		59%
PGL5fal		58%
PGL6fal		55%
AL-VB1fal	Arctic Low-Voeikov Belt (AL-VBfal)	97%
AL-VB2fal		72%
AL-VB3fal		51%
SH-ML1fal	Scandinavian High-Mediterranean Low (SH-MLfal)	100%
SH-ML2fal		71%
SH-ML3fal		56%
IL1fal	Icelandic Low (ILfal)	91%
IL2fal		67%
IL3fal		51%
SH-ML/ILfal	*Mixed between SH-ML and IL	49%/48%
AL-VB/ILfal	Mixed between AL-VB and IL	46%/39%

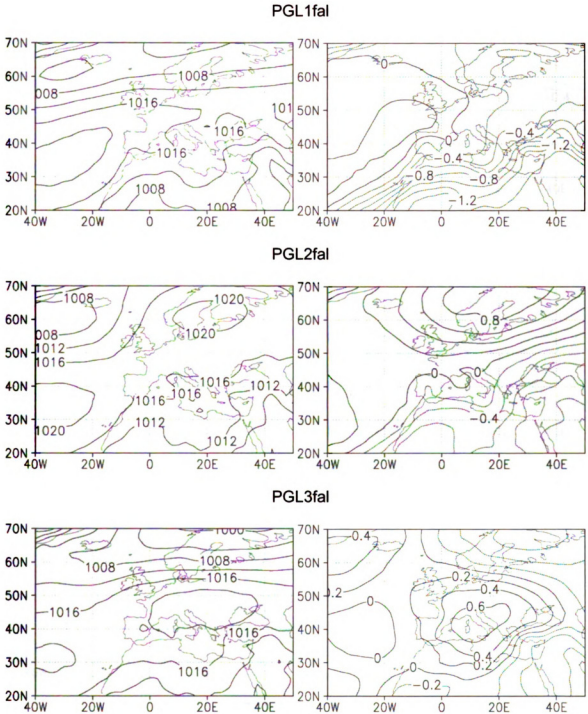

Figure 2-23 Fall types composites – pressure patterns and standardized anomalies

PGL4fal

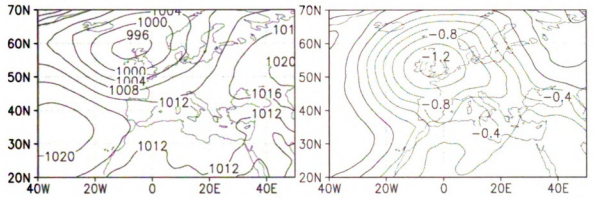

PGL5fal

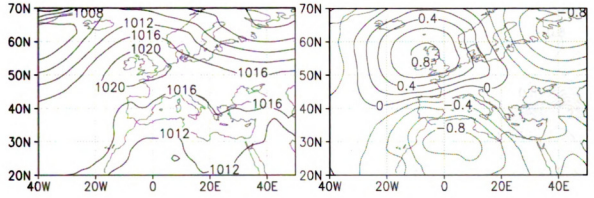

PGL6fal

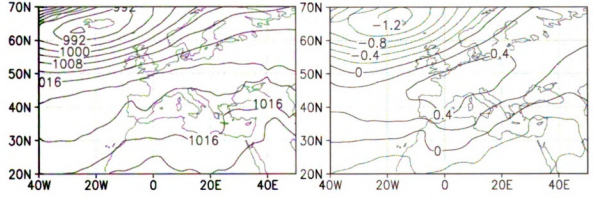

Figure 2-23 continued

AL-VB1fal

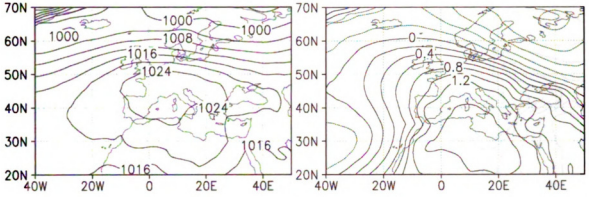

AL-VB2fal

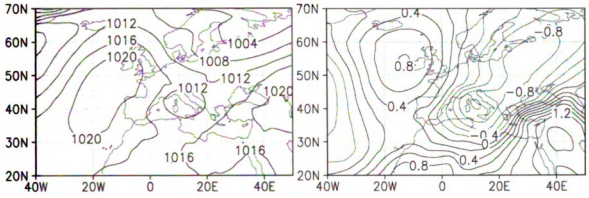

AL-VB3fal

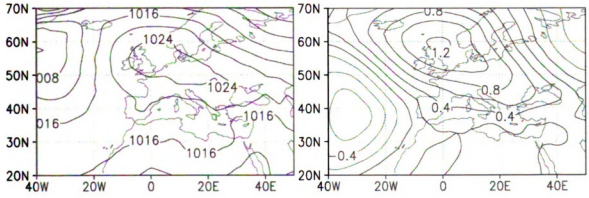

Figure 2-23 continued

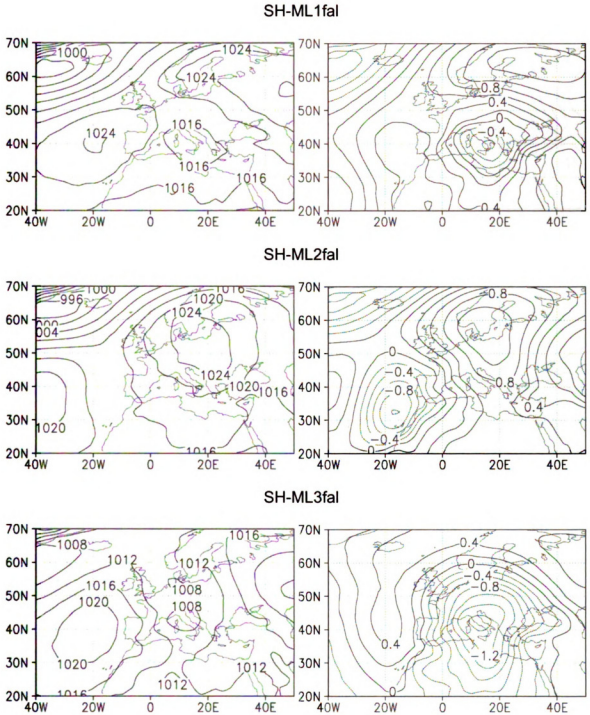

Figure 2-23 continued

IL1fal

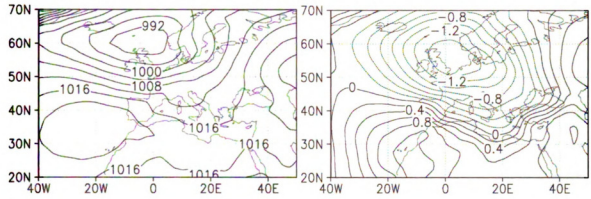

IL2fal

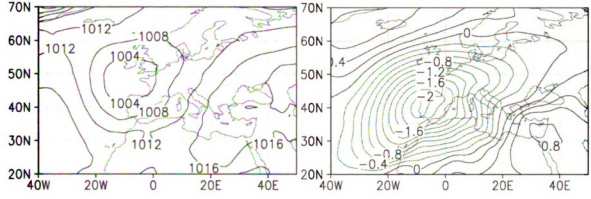

IL3fal

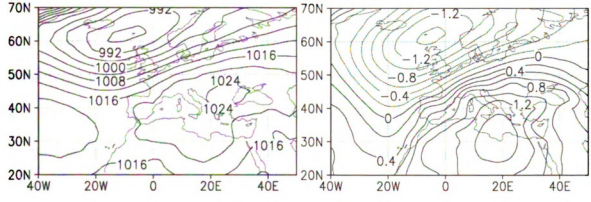

Figure 2-23 continued

SH-ML/ILfal

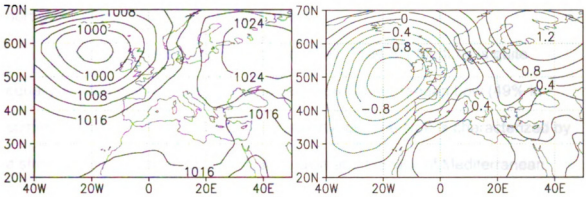

AL-VB/ILfal

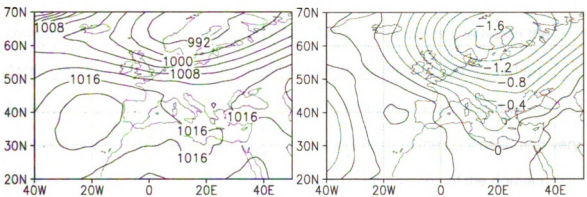

Figure 2-23 continued

Three circulation types are associated with the Icelandic Low fall supertype. IL1fal, with 91% days in common, is the most closely related to the supertype, although the negative anomaly over the northern portion of the map domain is more intense. For IL2fal (67%) the negative anomaly is also stronger than that for the supertype, but in addition the anomaly is shifted southward over western Spain. The composite map for IL3fal is also characterized by a strong negative anomaly in the northwest of the map domain. However, this type also is influenced by a strong positive anomaly over North Africa. The other two types

are also characterized by positive anomaly areas over the Persian Gulf and over northwest Africa (IL1fal), or Iceland (IL2fal).

Two mixed types were determined in fall. Type SH-ML/ILfal is quite equally divided between the Scandinavian High-Mediterranean Low (49% in common) and the Icelandic Low (48%) supertypes. The type is characterized by a stronger positive anomaly over Scandinavia and the lack of Mediterranean negative anomaly, compared to SH-MLfal supertype. This mixed type also features a less intense negative anomaly which is shifted to the west of Ireland, compared to the ILfal supertype. Type AL-VB/ILfal is transitional between the Arctic Low-Voeikov Belt (46% overlap) and the Icelandic Low (39% overlap) supertypes. Compared to both supertypes, it features a stronger negative anomaly located over Scandinavia that influences most of the continent, and very weak positive anomalies in the southern and western portions of the domain, compared to the AL-VBfal supertype.

4.1.4. c. Frequency of the fall supertypes

The supertypes are almost equally frequent during the fall season. An exception is the PGLfal supertype (36.2%) which occurs on about 15% more fall days than each of the other supertypes (22.4% for AL-VBfal, 21.3% for SH-MLfal and 20.1% for ILfal) (Figure 2-24). The beginning of the fall season is greatly dominated by the intermediary PGLfall pattern, occurring on 82% of all September days (Figure 2-25). October is characterized by similar rates of incidence for all the four supertypes, varying between 23.7% and 25.9%. The Persian Gulf Low supertype is very infrequent in November with only a 0.7%

recurrence. The other supertypes are more frequent in November compared to September and October. The AL-VBfal supertype (37.2%) shows a slight prevalence over the SH-MLfal (31.1%) and the ILfal (29.8%) supertypes.

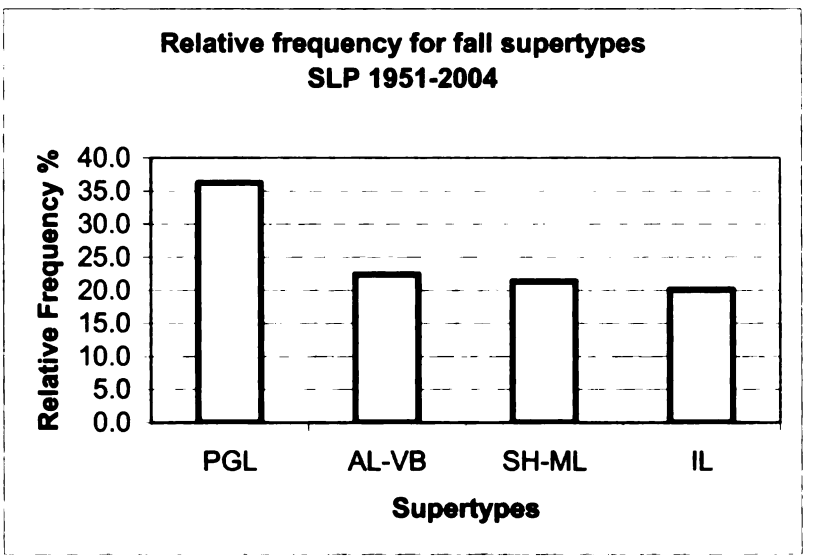

Figure 2-24 Relative frequency of the fall supertypes compared to the total number of fall days in the period (%)

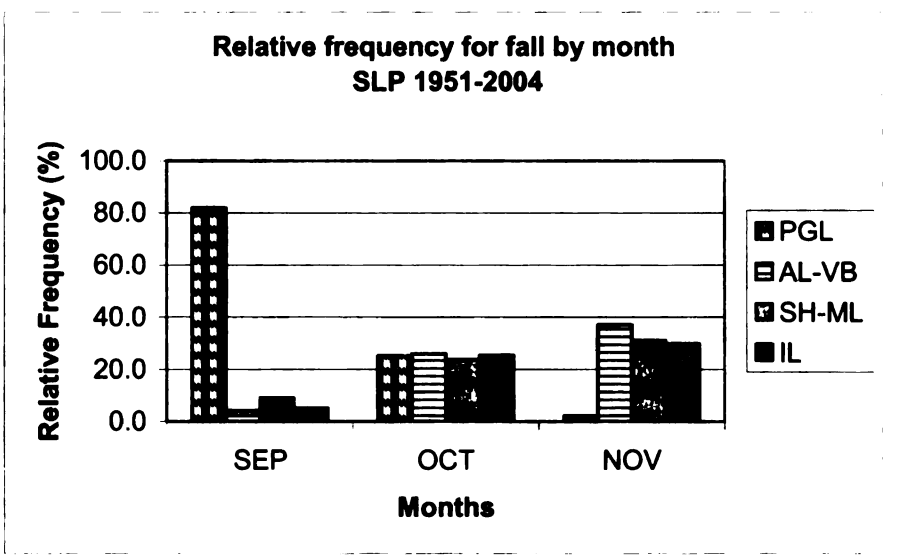

Figure 2-25 Relative frequencies of the fall supertypes compared to the period number of days for each month (%)

4.1.4. d. Seasonal and monthly distribution of the fall types

The seasonal frequency of the circulation types is similar that of the respective supertypes (Table 2-20). The types related to the PGLfal supertype are the most frequent, occurring on 5.9% to 10.4% of fall days. The other types occur on 4.0% to 6.7% of fall days.

Table 2-20 Relative frequency of the fall types compared to the total number of fall days in the period (%)

Type	PGL3	IL2	PGL6	AL-VB2	SH-ML/IL	AL-VB1	IL3
Seasonal frequency	7.4	4.8	6.7	4.1	5.0	5.6	4.2

Type	AL-VB/IL	PGL2	IL1	SH-ML2	SH-ML1	AL-VB3	SH-ML3
Seasonal frequency	5.5	10.4	4.9	4.0	4.9	6.7	5.8

Type	PGL1	PGL4	PGL5
Seasonal frequency	7.7	6.5	5.9

As in the other seasons, the monthly frequency of the types corresponds to the monthly occurrence of the supertypes (Table 2-21). September is dominated by types related to the PGLfal supertype. In October, in accordance with the almost equal frequency of the supertypes, all the types feature similar incidences. In November, the recurrence of the types associated with the PGLfal supertype is lowest, varying between 0.0% and 2.7%.

Table 2-21 Relative frequencies of the fall types compared to the period number of days for each month (%)

Type	PGL3	IL2	PGL6	AL-VB2	SH-ML/IL	AL-VB1	IL3
SEP	14.8	0.4	6.2	0.0	1.2	0.1	0.1
OCT	6.8	5.7	10.9	1.6	7.0	4.9	4.7
NOV	0.7	8.3	2.7	10.7	6.9	11.9	7.6

Type	AL-VB/IL	PGL2	IL1	SH-ML2	SH-ML1	AL-VB3	SH-ML3
SEP	1.9	26.7	0.0	0.8	0.1	3.0	3.7
OCT	8.3	4.3	3.3	5.2	2.6	10.8	8.5
NOV	6.3	0.3	11.4	6.1	11.9	6.0	5.2

Type	PGL1	PGL4	PGL5
SEP	21.7	12.1	7.2
OCT	1.4	5.9	8.1
NOV	0.0	1.5	2.3

4.1.4. e. Fall Z500 composites characteristics

The Z500 composite map for the PGLfal supertype displays split flow (Figure 2-26). An inconspicuous trough over the north Atlantic and an almost zonal flow over Europe characterize the northern air flow. A ridge over the tropical Atlantic and troughs southwest of Spain and over the eastern Mediterranean are evident in the southern air flow. The Z500 map for the AL-VBfal SLP supertype also shows split flow. The southern areas of the analysis domain are characterized by the same features as for the previous supertype, i.e., a ridge over the tropical Atlantic and troughs southwest of Spain and over the eastern Mediterranean. To the north, intense ridging over the Atlantic and

troughing over northeastern Europe correlate well with the SLP configuration. A stronger north-south gradient is also evident compared to the Z500 map for the previous supertype. The Z500 composite map for the SH-MLfal SLP supertype is dominated by even more distinct split flow. It is characterized also by well-developed ridges over the mid-Atlantic and Scandinavia, and troughing areas west of Iceland and over central Europe. The composite Z500 map is well related to the SLP ILfal supertype, showing a pronounced trough, with an axis extending over the eastern Atlantic, and ridging over the Russian Plain.

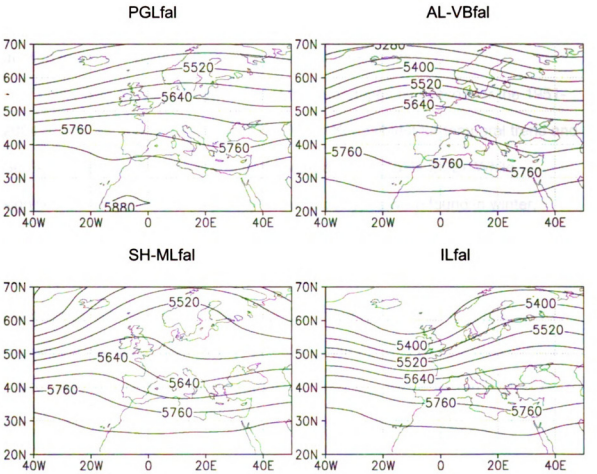

Figure 2-26 Z500 supertypes composites, Fall

4.2. Interannual variations of the frequency of the circulation supertypes

In order to investigate the interannual variations in the frequency of the circulation patterns, plots of the seasonal relative frequencies (in percent) of the supertypes against time were created (Figure 2-27 to Figure 2-30). Visual inspection of the plots revealed interesting year-to-year variations. Tests for trends were employed in order to investigate the statistical significance of the visually identified interannual changes in the frequencies of the supertypes. The trends for the 1951-2004 period were assessed for every supertype. Subsequently, the time series for every supertype were examined for break points which are indicators of a change in the series. Tests for trend were then applied to the sub-periods determined by the break points.

The time series of frequencies of the supertypes by season for the 1951-2004 period were tested for trends. The Mann Kendall test for temporal trend and Sen's nonparametric estimator of trend were applied (Table 2-22). While significant changes in the frequency of the supertypes were found in winter, summer and fall, no significant trends were evident for spring. Most of the supertypes dominated (spatially) by anticyclonic features or positive anomalies, more specifically AL-VBwin, EHwin, WPGLsum, and AL-VBfal, exhibit positive (increasing with time) trends for 1951-2004 (Figure 2-27, Figure 2-29 and Figure 2-30). Several supertypes dominated by cyclonic features, ILwin, AL-PGLsum and PGLfal, display significant negative trends (Figure 2-27, Figure 2-29 and Figure 2-30). It is interesting to compare the trends of SH-MLfal and SH-MLwin because these counterpart supertypes are characterized by opposite in sign

trends. While the fall supertype displays significant positive trend in frequency, the winter supertype displays a negative trend. Both supertypes, SH-MLfal and SH-MLwin, are characterized by two SLP anomalies, a positive anomaly to the north and negative anomaly to the south. For the SH-MLfal supertype, however, the negative anomaly over the Mediterranean has very limited spatial extent and the supertype is dominated by the positive anomaly over Scandinavia. Hence, the trend in fall probably reflects the dominance for this supertype of the Scandinavian high. For the SH-MLwin supertype both anomalies are large in extent and almost of equal size. Mediterranean cyclones are more frequent in winter than in fall (Trigo et al., 1999), hence the negative trend of the SH-MLwin supertype possibly reflects a decrease in the frequency of Mediterranean cyclones.

The Pettit and SNH tests for break points in the 1951-2004 time series of supertype frequency agree for almost all of the supertype/season combinations (Table 2-23). Only for a few occasions do the tests suggest different years for the breakpoints or only one test shows a break point. These discrepancies can be attributed to the fact that the Pettit test is more sensitive to breaks in the middle of the period, while the SNHT is more sensitive to breaks in the beginning and end of the series.

Table 2-22 Summary of the results from the Mann-Kendall test for trend of the frequency of the supertypes and the Sen's nonparametric estimator of trend (days change/decade), 1951-2004

Season	Supertype	Existence of Trend at α=0.05	Existence of Trend at α=0.01	Direction of Trend	Magnitude of Trend
Winter	AL-VB	Yes	Yes	Positive	2.7/decade
	ML-NAH	No	No		
	EH	Yes	Yes	Positive	2.5/decade
	SH-ML	Yes	Yes	Negative	-2.5/decade
	IL	Yes	No	Negative	-1.5/decade
Spring	SH-ML	No	No		
	AL-VB	No	No		
	ASR	No	No		
	EL	No	No		
	IL	No	No		
Summer	WPGL	Yes	Yes	Positive	3.3/decade
	ASR	No	No		
	AL-PGL	Yes	Yes	Negative	-3.5/decade
Fall	PGL	Yes	Yes	Negative	-3.7/decade
	AL-VB	Yes	Yes	Positive	2.3/decade
	SH-ML	Yes	No	Positive	1.4/decade
	IL	No	No		

The tests indicate breaks for all of the supertypes in winter (Figure 2-27). One break point was determined for all supertypes, except for ILwin for which two breakpoints were identified, 1966 and 1979. For the other supertypes, the tests determined as breakpoints 1972 for AL-BNwin, 1976 for ML-NAHwin, 1981 for EHwin and 1985 for SH-MLwin. In contrast, no break points were found in spring for four of the five supertypes (Figure 2-28). Only the ILspr supertype is

characterized by a break point in 1966. In summer, the frequency time series of the ASRsum supertype does not show discontinuity, while two break points were determined for WPGLsum, 1966 and 1975, and one break point for AL-PGLsum, 1966-1967 (Figure 2-29). In fall, all the supertypes except for ILfal have break points in their frequency of occurrence. The tests indicated two break points for PGLfal, 1966 and 1975, and only one break point for AL-VBfal, 1968, and SH-MLfal, 1971. The reason why most of the break points occur in the 1960s and 1970s might be related to the increased amount of satellite information incorporated in the NCEP/NCAR reanalysis data since then. This hypothesis, however, was not tested and the mechanisms that might be involved are not clear.

Table 2-23 Summary of the results of the Pettit test and the SNHT for break points, 1951-2004*

*Critical values for the Pettit test for n=54 are 293 at α=0.01 and 235 at α=0.05

Critical values for the SNHT for n=54 are 11.38 at α=0.01 and 8.45 at α=0.05

(values in bold represent significant breaks)

Season	Supertype	Pettit Test (Xe)	Year of discontinuity	SNHT (To)	Year of discontinuity
Winter	AL-VB	**426**	1972	**15.3**	1972
	ML-NAH	**364**	1976	7.6	
	EH	**381**	1981	**15.5**	1981
	SH-ML	**452**	1986	**12.2**	1986
	IL	**357**	1979	**8.9**	1966
Spring	SH-ML	172		3.3	
	AL-VB	142		2.5	
	ASR	140		2.8	
	EL	211		3.1	
	IL	**386**	1966	**10.8**	1966
Summer	WPGL	**447**	1975	**17.6**	1966
	ASR	177		3.3	
	AL-PGL	**543**	1967	**26.9**	1966
Fall	PGL	**653**	1975	**32.3**	1966
	AL-VB	**368**	1968	**12.6**	1968
	SH-ML	**239**	1971	5.5	
	IL	163		2.9	

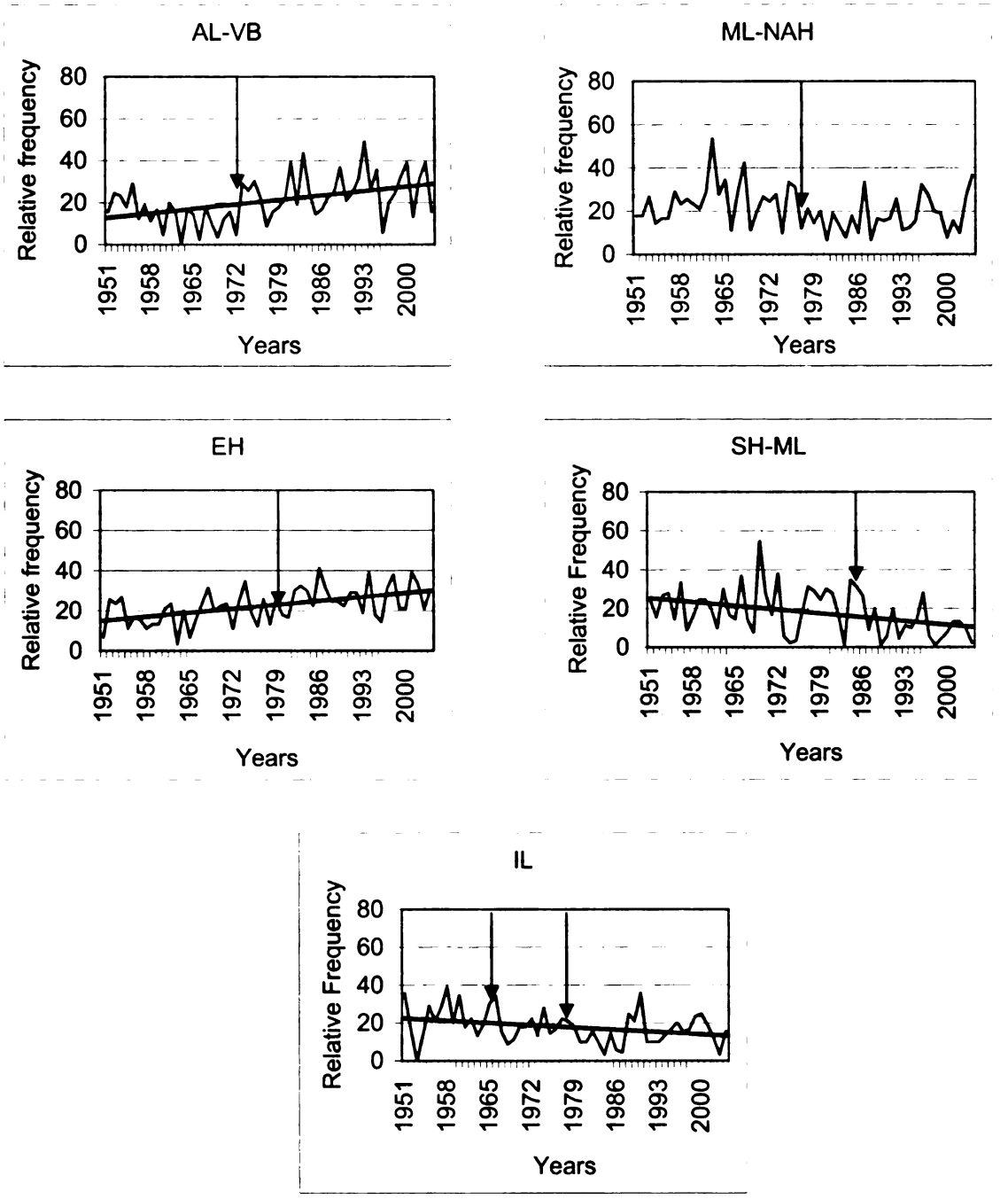

Figure 2-27 Break points in the series and overall trends in relative frequency of the winter supertypes

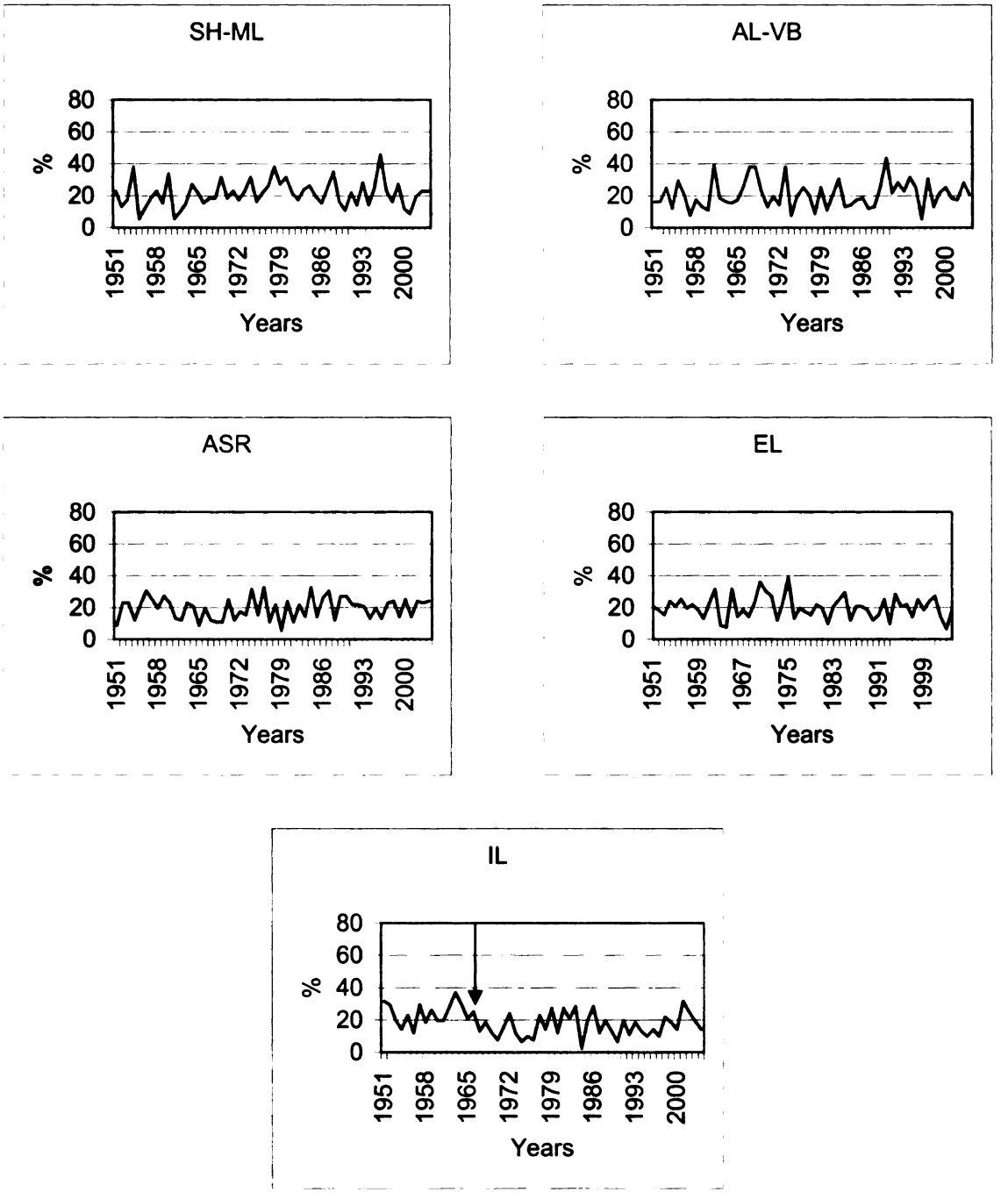

Figure 2-28 Break points in the series and overall trends in relative frequency of the spring supertypes

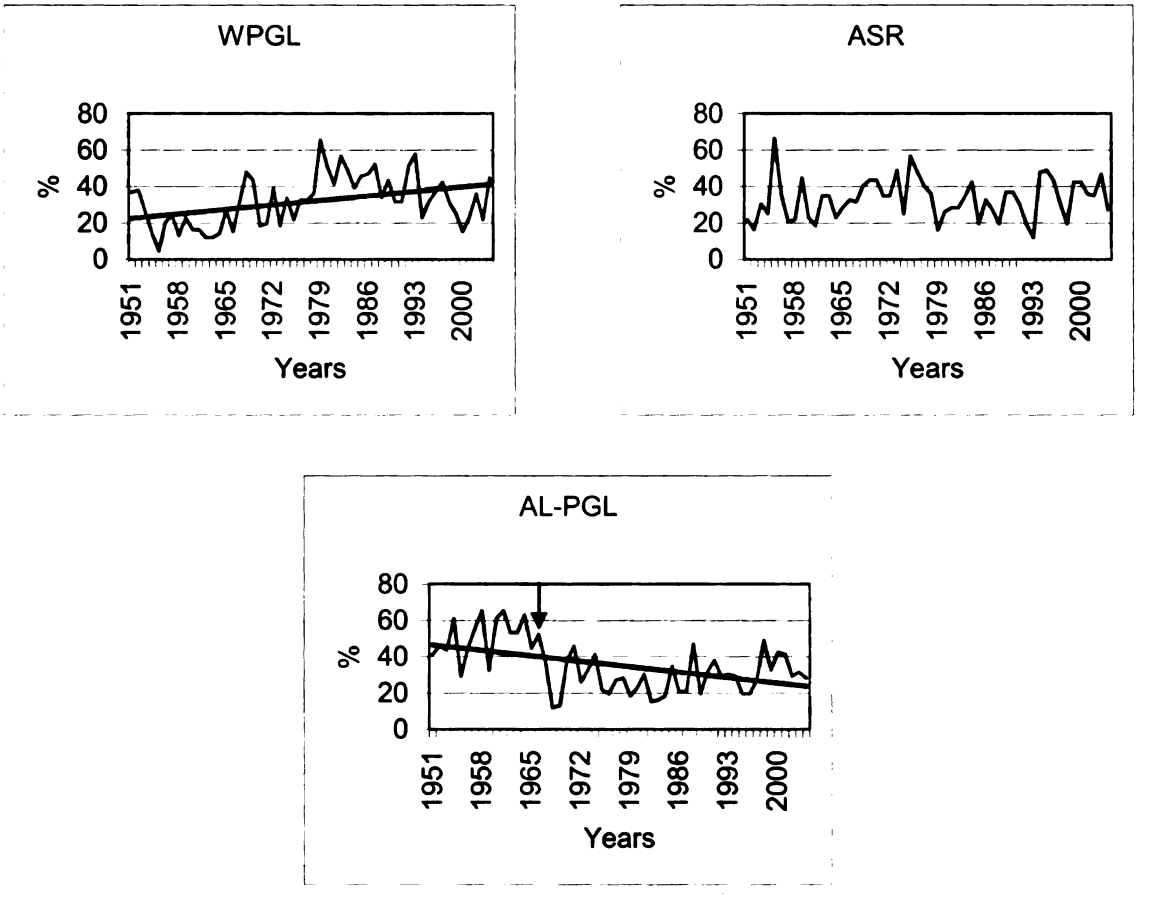

Figure 2-29 Break points in the series and overall trends in relative frequency of the summer supertypes

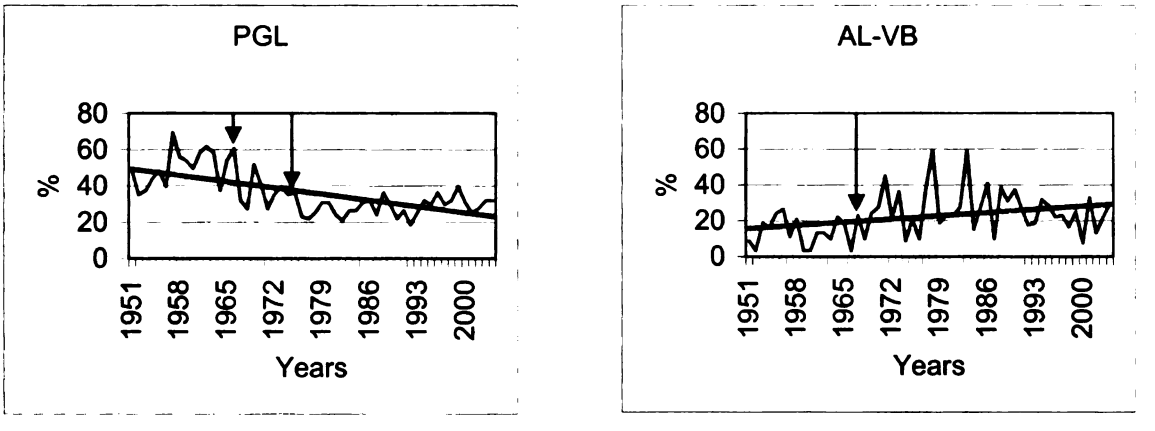

Figure 2-30 Break points in the series and overall trends in relative frequency of the fall supertypes

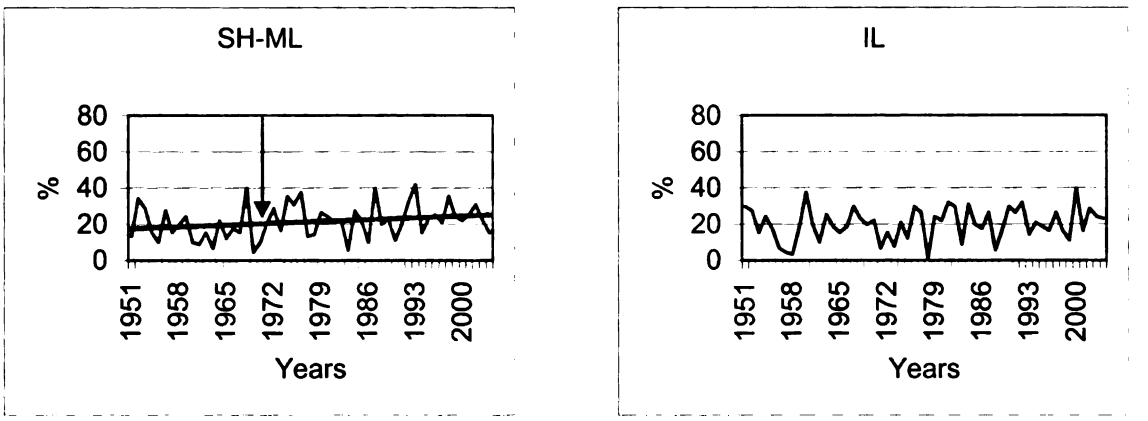

Figure 2-30 continued.

The sub-periods determined by the break points were investigated in turn using the same tests. The testing was performed only if the sub-periods were at least 20 years in length, similar to the threshold used by Kysely and Domonkos (2006, p.464). The tests indicate that for most of the sub-periods no additional breaks are evident. Exceptions are the AL-VBwin, WPGLsum and PGLfal supertypes (Table 2-24). The results for the PGLfal supertype confirmed the same break points as those obtained by testing of the overall period. The sub-period discontinuities for AL-VBwin and WPGLsum will not be considered further, since either only one of the two tests suggested a breakpoint or the timing of the breakpoints differed between the two tests.

Table 2-24 Additional break points for the supertypes

for n=20 Xe=71 at 1%, Xe=57 at 5%, for n=30 Xe=133 at 1%, Xe=107 at 5%

for n=20 To=9.56 at 1%, To= 6.95 at 5%, for n=40 To=11.01 at 1%, To=8.1 at 5%

Season	Supertype	Pettit Test (Xe)	Year of discontinuity	SNHT (To)	Year of discontinuity
Winter	AL-VB	**82 for n=22**	1962	**7.5 for n=22**	1955
	ML-NAH				
	EH				
	SH-ML				
	IL				
Spring	SH-ML				
	AL-VB				
	ASR				
	EL				
	IL				
Summer	WPGL	**148 for n=29**	1993		
	ASR				
	AL-PGL				
Fall	PGL	**120 for n=25**	1966	**10.1 for n=38**	1975
	AL-VB				
	SH-ML				
	IL				

Three supertypes exhibit significant trends during sub-periods (Table 2-25). Although displaying an overall positive trend of 2.7 days/decade, the winter AL-VB supertype demonstrates a negative trend during the 1951-1972 sub-period with a rate of change of -5.7 days per decade. Within the overall positive trend of 3.3 days/decade, the WPGLsum supertype shows a significant negative trend during 1976-2004 with a rate of 6.7 days/decade. More complicated are the temporal variations of the PGLfal supertype. Although the overall trend for the 1951-2004 period is negative (-3.7 days/decade), this supertype displays positive trends during the 1951-1966 (10 days/decade) and 1976-2004 sub-periods (2.2 days/decade).

Table 2-25 Summary of the results from the Mann-Kendall test for existence of trend and the Sen's nonparametric estimator of trend (days change/decade) in supertypes frequency for the sub-periods

Season	Supertype	Sub period	Existence of trend	Direction of trend	Magnitude of trend
Winter	AL-VB	1951-**1972**	Yes	Negative	-5.7/decade
		1973-2004	No		
	ML-NAH	1951-**1976**	No		
		1977-2004	No		
	EH	1951-**1981**	No		
		1982-2004	No		
	SH-ML	1951-**1986**	No		
		1987-2004	No		
	IL	1951-**1966**	No		
		1967-2004	No		
		1951-**1979**	No		
		1980-2004	No		
Spring	SH-ML				
	AL-VB				
	ASR				
	EL				
	IL	1951-**1966**	No		
		1967-2004	No		
Summer	WPGL	1951-**1966**	No		
		1967-2004	No		
		1951-**1975**	No		
		1976-2004	Yes	Negative	-6.7/decade
	ASR				
	AL-PGL	1951-**1966**	No		
		1967-2004	No		
Fall	PGL	1951-**1966**	Yes	Positive	10/decade
		1967-2004	No		
		1951-**1975**	No		
		1976-2004	Yes	Positive	2.2/decade
	AL-VB	1951-**1968**	No		
		1969-2004	No		
	SH-ML	1951-**1970**	No		
		1971-2004	No		
	IL				

4.3. Persistence of the circulation patterns

4.3.1. Total persistence

As mentioned in the Methods section, the number of consecutive days during which a given supertype dominates the study domain characterizes the 'persistence' of this supertype. The persistence characteristics summarized over the entire period are termed 'total' persistence in this study. Following Huth (1997), three main parameters were used to characterize the total persistence of each supertype: a) the number of 1-day events, or transitional events; b) the percentage of days included in events lasting 4 days or longer; and c) the average event length in days, based on all events. In addition, the percentage of days included in events lasting 2 and 3 days, was also calculated per season and supertype. An 'event' was considered to be the uninterrupted sequence of days classified with the same supertype.

The total persistence does not indicate clear relationship between higher or lower persistence and the prevalence of positive or negative anomalies for the respective supertypes. In winter, two supertypes, SH-MLwin and ILwin, typically occur within events lasting 4 days or more, 63% and 61%, respectively (Table 2-26). These supertypes are also characterized by longer average event length, compared to the rest of the wintertime supertypes. In spring, SH-MLspr appears more often than the other supertypes of this season in longer events lasting 4 days or more (67%). The remaining supertypes in spring show almost equal frequency within longer events, and also have similar average event lengths. Two of the supertypes, ELspr and ILspr, occurred more often in one day, transitional events, than the rest of the supertypes in spring. In summer, all of the

types are characterized by a similar percentage of occurrence within transitional events, and also within longer events. The average event length of the supertypes is almost the same also, varying between 3.4 and 3.9 days. In fall, the PGLfal supertype is characterized by highest average event length and occurs most often within events lasting 4 days or more compared not only to the remaining fall supertypes, but to the supertypes from the other seasons as well.

Table 2-26 Total persistence of the supertypes by season

Season	Super type	Total number of days with a given supertype per season	% of transition (1 day) events (from total number of days with a supertype)	% of days in events lasting 2-3 days (from total number of days with a supertype)	% of days in events ≥ 4 days (from total number of days with a supertype)	Average event length in days – (includes all events)
Winter	AL-VB	1011	12	36	52	2.7
	ML-NAH	1021	13	30	57	2.8
	EH	1092	14	34	52	2.6
	SH-ML	868	8	29	63	3.4
	IL	868	10	29	61	3.3
Spring	SH-ML	1056	9	24	67	3.3
	AL-VB	1030	12	42	46	2.6
	ASR	967	12	40	48	2.6
	EL	993	16	40	44	2.4
	IL	922	14	38	48	2.6
Summer	WPGL	1577	8	25	67	3.6
	ASR	1646	8	26	66	3.4
	AL-PGL	1745	7	25	68	3.9
Fall	PGL	1781	3	11	86	7.1
	AL-VB	1100	6	21	73	4.0
	SH-ML	1047	7	27	66	3.6
	IL	986	6	27	67	3.7

4.3.2. Trends in the persistence characteristics of the supertypes

Several persistence characteristics were tested for the existence of a trend: the average event length, the number of transitional events, the frequency of events lasting 2 to 4 days, the frequency of events lasting more than 4 days, their average length and the total number of days in events lasting more than 4 days. For some characteristics the pentadal values (five year averages or five year sums) were used instead of the annual values for the trend analysis, because events of a given length were not recorded every year. For example, in some years there were no events lasting 4 days or longer for some supertypes.

The average event length decreases for three supertypes. The SH-MLwin, the AL-PGLsum and the PGLfall supertypes exhibit significant negative trends of -0.39, -0.45 and -0.71 days/decade (Table 2-27). These supertypes are dominated either by a combination of a positive anomaly to the north and a negative anomaly over the southern portions of the domain (SH-MLwin) or only by negative anomalies (AL-PGLsum and PGLfal).

The number of transitional events exhibits opposite changes for some supertypes. The frequency of one-day events declines for the ELspr supertype by -0.13 days/pentad, while it increases for the ILfal supertype by 0.07 days/pentad. No significant changes are evident in the frequency of the events lasting 2 to 4 days except for the EHwin supertype. This supertype is characterized by a significant positive trend of 0.2 days/pentad.

Table 2-27 Trend analysis for persistence characteristics of supertypes, 1951-2004 (change per decade, except where the analyses were performed by pentads, change per pentad)

WINTER

Persistence Parameter/ Supertype	AL-VB	ML-NAH	EH	SH-ML	IL
Average length of all events per supertype				Yes/No* Negative (-0.39)	
Number of 1 day (transitional) events BY PENTADS					
Frequency of events lasting 2 to 4 days BY PENTADS			Yes/No Positive (0.2)		
Frequency of events lasting > 4 days BY PENTADS	Positive 0.17	Yes/No Negative (-0.1)			Yes/No Negative (-0.06)
Average length of events > 4 days BY PENTADS	Positive 0.1		Yes/No Positive 0.08	Negative (-0.1)	
Total number of days in events > 4 days BY PENTADS	Positive 1.1	Yes/No Negative (-0.53)	Yes/No Positive 0.68	Yes/No Negative (-0.73)	Yes/No Negative (-0.6)

* Yes/No means that the trends are significant only at 0.05 level of significance, but not at 0.01.

Table 2-27 continued

SPRING

Persistence Parameter/Supertype	SH-ML	AL-VB	ASR	EL	IL
Average length of all events per supertype					
Number of 1 day (transitional) events BY PENTADS				Yes/No Negative (-0.13)	
Frequency of events lasting 2 to 4 days BY PENTADS					
Frequency of events lasting > 4 days BY PENTADS					
Average length of events > 4 days BY PENTADS					
Total number of days in events > 4 days BY PENTADS					

SUMMER

Persistence Parameter/Supertype	WPGL	ASR	AL-PGL
Average length of all events per supertype			Negative (-0.45)
Number of 1 day (transitional) events BY PENTADS			
Frequency of events lasting 2 to 4 days BY PENTADS			
Frequency of events lasting > 4 days BY PENTADS			
Average length of events > 4 days BY PENTADS	Yes/No Positive 0.08		
Total number of days in events > 4 days BY PENTADS			

Table 2-27 continued

FALL

Persistence Parameter/Supertype	PGL	AL-VB	SH-ML	IL
Average length of all events per supertype	Yes/No Negative (-0.71)			
Number of 1 day (transitional) events BY PENTADS				Yes/No Positive 0.07
Frequency of events lasting 2 to 4 days BY PENTADS				
Frequency of events lasting > 4 days BY PENTADS				Yes/No Positive 0.1
Average length of events > 4 days BY PENTADS	Yes/No Negative (-0.18)	Yes/No Positive 0.06	Positive 0.06	
Total number of days in events > 4 days BY PENTADS	Yes/No Negative (-2.08)			

The last three measures consider events lasting more than 4 days. In winter, all the supertypes dominated by anticyclonic features over central Europe (AL-VBwin and EHwin) exhibit increasing trend in these measures. The supertypes dominated by cyclonic features (ML-NAHwin and ILwin) or by a combination of a strong negative and a positive anomaly (SH-MLwin) show a decrease in persistence as evaluated by the frequency of events longer than 4 days. No changes in the persistence of the long duration events were evident for spring for any of the supertypes. The summer and fall seasons feature significant trends for some of the parameters and supertypes. The average length of events longer than 4 days increases for the WPGLsum, AL-VBfal and SH-MLfal supertypes. All of these supertypes are dominated by strong positive anomalies.

The PGLfal supertype, which is characterized by an intense negative anomaly over the Persian Gulf displays a decrease in the average length of the longer events and in the total number of days per event lasting more than 4 days.

5. Discussion

5.1. Comparison to previous circulation classifications

As was summarized earlier, several subjective and computer-assisted atmospheric circulation classifications for Europe exist. Most of them have limited areal extent since they cover only central Europe (Hess-Brezowsky, 1969), the British Isles (Lamb, 1972; Jones et al., 1993), the European Alpine region (Schüepp, 1979), or western Europe (Plaut and Simonnet, 2001; Esteban et al., 2006). For other classifications, the patterns were distinguished according to the positioning of the main circulation features with respect to specific countries: Hungary (Péczely, 1957), Greece (Maheras et al., 2000; Kassomenos et al., 2003). In addition, some of the classifications combine location-specific surface air mass characteristics and synoptic conditions. For example, Kassomenos et al. (2003) subjected to cluster analysis the scores of surface meteorological elements from Athens together with the scores of the SLP fields over the continent which resulted in the derivation of patterns that are not easily distinguishable.

The classification in the current study is quite unique compared to all the existing classifications. In terms of areal extent, the classification does not focus on atmospheric circulation over a limited area, but rather the supertypes and

types are applicable to the entire European continent and a large portion of the northern Atlantic.

In addition, in contrast to some other classifications for which the circulation types are subsequently subjectively agglomerated into larger groups for further analyses (e.g., Kysely [2002a], grouped the circulation types from the Hess-Brezowsky classification into Cyclonic and Anticylconic types), the classification presented here features two distinctive solutions obtained using objective statistical methodology. The coarse solution, consisting of the supertypes, highlights the main characteristics of the large-scale atmospheric circulation over Europe and is applicable for baseline analyses of the interannual changes in the circulation configurations. The fine solution is a detailed classification consisting of numerous circulation types per season, and is applicable for the investigation of specific research questions about the relations between large-scale circulation characteristics and local climates.

Breaking with the traditional naming convention based mostly on the direction of the airflow or the curvature of the circulation entities, the supertypes and types of the classification presented here are named after the physical entities (i.e., European High, Icelandic Low, etc.) which dominate the specific patterns. The distinctiveness of this classification is also evident in that the circulation patterns were derived by season, rather than annually, thus revealing the particular circulation characteristics of the separate seasons.

Since the classification was produced using computer-assisted methods, the methodology is easily transferable to any other region on any other continent.

The chosen approach also permitted all days to be classified, thus specifically allowing for transitional patterns.

The classification captures the main centers of action that influence the weather and climate of the European continent and the north Atlantic. The prevalent zonal westerly flow (more intense during the cooler half of the year) is well depicted in the AL-VBwin, AL-VBspr and AL-VBfal supertypes. The importance and strength of the Icelandic Low during the cooler season is reflected in the ILwin, ILspr and ILfal supertypes, all of which are dominated by a large and intense negative anomaly located in the vicinity of Iceland. The Azores High, although present on the average SLP maps throughout the year, increases in areal extent and becomes more intense in the summer season. The larger spatial extent and higher intensity are evident in all of the supertypes for summer. The cool season center of cyclogenesis over the Gulf of Genoa is well represented in the ML-NAHwin, SH-MLwin, SH-MLspr and SH-MLfal supertypes. The extensions of the Siberian High in winter, as evident in the high pressure features found over the Russian Plain, and of the Asian thermal cyclone in summer, as represented by the Persian Gulf Low within the map domain, are also captured by the different supertypes. The high pressure features over the continent are also well depicted in the EHwin, ASRspr and ASRsum supertypes.

An initial crude visual comparison of the earlier circulation classification catalogues to the supertype patterns presented here was performed (Appendix Table 1). Only the most popular and frequently used catalogues are discussed here. For all seasons, the Lamb air flow types relate well to the supertypes from

this classification for all seasons. Only Lamb's 'Northerly' and 'Northwesterly' types in winter and fall, 'Northerly' type in summer, and 'Southerly' type in spring and summer do not have clear counterparts in the supertypes. Compared to the Hess Brezowsky classification, the supertypes from this study also match up to most of the subjectively identified types. Exceptions are some of the subjective types belonging to the 'Northerly' class in spring, to the 'Southerly', 'Northerly', and 'Westerly' classes in summer, and to the 'Northerly', 'Southerly', 'Anticyclonic' and 'Cyclonic' classes in fall. The Hess-Brezowsky catalogue includes only types persisting for at least 3 days.

5.2. Frequency of occurrence of circulation patterns

The results of the current study are in general agreement with most of the analyses to date regarding changes with time in atmospheric circulation. A specific one-to-one comparison of the patterns derived in this study to configurations from other studies is hampered to an extent by differences in the classification methods.

An important characteristic of the atmospheric circulation in the 20th century have been the observed changes in the number of days with 'Westerly' (zonal) flow. Briffa, Jones and Kelly (1990), using the Lamb airflow types, confirmed Lamb's (1972) observation of a decline in the frequency of the 'Westerly' weather types since the 1950s. In addition, they found that the decrease was evident through the 1980s and is observed in all seasons, although the decline is not as pronounced in fall. Jones, Hulme and Briffa (1993)

also agreed with Lamb (1972) that the frequency of 'Westerly' days was at historically low levels during the late 1960s, 1970s, and early 1980s. Stefanicki et al. (1998), using Scüepp's classification, found a decrease in the occurrence of the 'Westerly' airflow during 1945-1994. Later, Werner et al. (2000), who investigated the frequency and persistence of the Hess-Brezowsky 'Westerly' (zonal) type, found that although the frequency was low during the 1950s and 1960s, an abrupt increase in frequency was evident near the beginning of the 1970s. In addition, Kysely and Huth (2006), using the Hess-Brezowsky classification along with an objective classification of Z500 patterns, identified an increase in the frequency of the 'Westerly' (zonal) type in winter from the 1960s to the early 1990s.

The results posted here agree, in general, with these previous studies, although some differences exist due to the different areal extent. The analyses presented here suggest a decrease in zonal airflow until the early 1970s, but they do not show a decrease in the 1980s. The AL-VBwin pattern, which represents zonal situations over the British Isles and the mid-continent and is comparable to the Lamb 'Westerly' type, is infrequent during the 1960s and early 1970s. In fall, the AL-VBfal pattern also displays low frequency in the 1950s and 1960s. Similar low frequency was not evident for the spring supertype AL-VBspr, and a zonal supertype is not present in summer. Good correspondence exists between the results of Werner et al. (2000), and to an extent the results of Kysely and Huth (2006), and the trends in occurrence of the AL-VBwin pattern in this study. This supertype has a significant negative trend for 1951-1972, but the subsequent

increase in AL-VBwin frequency after 1972 is so distinct that the overall trend for 1951-2004 is positive.

Another important characteristic of the historical frequency of the circulation patterns over Europe is that in the second half of the 20th century, anticyclonic types have displayed positive trends, whereas cyclonic types have had negative trends. Briffa, Jones and Kelly (1990) established that the decrease in the zonal flow in the 1980s was compensated by an increase in the anticyclonic and cyclonic circulation. Stefanicki et al. (1998) and Maheras et al. (2000) found that the frequency of anticyclonic circulation increased by 9.1 days/decade after 1945, as determined by the former authors, and by 9.9 days/decade after 1958, as determined by the latter authors. Maheras et al. (2000) also observed a downward trend for cyclonic circulation during 1958-1997 with a slope of -15.1days/decade. Kassomenos et al. (2003) observed an increase in anticyclonic activity after the mid 1970s, and a significant negative trend in the wintertime frequency of cyclonic circulation. Huth (2001) determined that anticyclonic types have become more frequent at the expense of cyclonic types in summer and winter. Kysely and Huth (2006) described a rise in the frequency of anticyclonic patterns in winter up to the early 1990s with a subsequent decrease. For the cyclonic patterns they determined a decline. Esteban et al. (2006) found that some circulation patterns exhibit significant trends during 1960-2001. For example, type 'Azores Anticyclone 1' displays a negative trend, and type 'Central Europe High' shows a positive trend.

All of these conclusions are in accord with the findings in this study. The anticyclonic supertypes increase in frequency, while the cyclonic supertypes decrease in frequency. Only the magnitude of the changes differs from some previous studies. For the supertypes dominated by anticyclonic features, the slope of the trend line varies between 1.4 days/decade for the SH-MLfal supertype and 2.7 days/decade for the AL-VBwin supertype, which is less than the values reported by Stefanicki et al. (1998) and Maheras et al. (2000). For the cyclonic supertypes, the trend varies between -1.5 days/decade for the ILwin supertype and -3.7 days/decade for the PGLfal supertype, which is also lower than the values in previous studies. The AL-PGLsum supertype, which is similar to the 'Azores Anticyclone 1' circulation pattern derived by Esteban et al. (2006), has a negative trend of -3.5 days/decade, which is higher compared to the decrease of -1.9 days/decade of the 'Azores Anticyclone I'. On the other hand, the EHwin supertype in winter and the similar 'Central Europe High' circulation type from Esteban et al. (2006), both have positive trends in the order of 2.5 days/decade.

Several researchers have found a decrease in the historical frequency of the 'Northerly' airflow types over Europe. Briffa, Jones and Kelly (1990) showed that the increase in cyclonic and/or anticyclonic types since 1980s has occurred at the expense of the 'Northerly' and/or 'Northwesterly' types. Stefanicki et al. (1998) found a decrease of the occurrence of the 'Northerlies' during the 1945-1994 period. Kysely and Huth (2006) also determined a decrease in the 'Northerly' types in winter up to the mid-1970s. In addition, Kysely and Huth

found an increase until the mid-1980s and a subsequent decrease of the frequency of the 'Northerly' types in summer. Esteban et al. (2006) found significant negative trends for the 'Central Europe Low-northerly advection' type (which is typical for spring and summer), and for 'North Atlantic Anticyclone' type (which induces northerly flow over western Europe and is most frequent in summer) for the period 1960-2001. They concluded that surface meridional flows have become less important in terms of frequency in summer. The correspondence of the results in this study to previous research is evident in: a) the decrease in the frequency of some of the supertypes comparable to Lamb's 'Northwesterly' type (for example, the AL-PGLsum) in 1951-2004, compared to the findings of Briffa et al (1990); and b) the significant negative trend of the WPGLsum (similar to Hess-Brezowsky 'Northerly' type in summer) during the 1976-2004 sub period, compared to the findings of Kysely and Huth (2006).

5.3. Persistence of circulation patterns

The comparison of the persistence characteristics of the circulation patterns in this study to the results from the existing research is difficult since the majority of the studies to date have utilized the Hess Brezowsky classification in their analyses or objective classifications based on 500 hPa geopotential height. The Hess-Brezowsky classification is subjective and the circulation types have a typical duration of at least 3 days. Also many authors have agglomerated circulation patterns into groups due to the low rate of occurrence of the circulation configurations in some or all seasons (for example, Kysely and Huth, 2006, and Kysely and Domonkos, 2006) or due to the nature of the classification

they derived (Stefanicki et al., 1998 combine as convective types the high and the low pressure situations).

Bardossy and Caspary (1990), who investigated the frequency and persistence of Hess Brezowsky circulation types, found that there were no significant changes for 1881-1989 in the duration of periods with the same circulation type. Later research, however, indicated periods of increased persistence of many circulation patterns. Stefanicki et al. (1998), using Schüepp's classification, determined that an increase of the average length of 'Convective' types (which include types with 'high, flat and low 500 hPa pressure distribution', Stefanicki et al, 1998) and a decrease of the 'Advective' ones (which include the directional air flow types) has occurred during 1970-1994 compared to the 1945-1969 period. Werner et al. (2000) investigated the occurrence of the 'Westerly' (zonal) type from the Hess-Brezowsky classification and the 'Westerly' types from Lamb's airflow types for the winter season. The authors documented an abrupt increase in the persistence of the zonal state in winter near the beginning of the 1970s. They identified the decade 1981-1990 to be an outlier because of longer residence times (persistence) of the 'Westerly' patterns.

This study also found that the persistence of the zonal supertypes increased. More specifically, the total number of days within events longer than 4 days (for AL-VBwin), the average event length of these events (for AL-VBwin and AL-VBfal) and the frequency of the longer than 4 days events (for Al-VBwin) have exhibited significant positive trends. Both supertypes display a strong zonal flow over the British Isles, and the mid-continent, or over northern Europe.

Kysely and Domonkos (2006), using the Hess Brezowsky classification, investigated the persistence of groups of circulation types in all seasons during 1881-2000. While the 1960s and 1970s were characterized by low persistence, a general sharp increase in persistence from the 1970s to the late 1980s and 1990s was observed for all seasons and for many circulation groups. Statistically significant positive trends in persistence in 1881-2000 were determined for several circulation groups, in particular the 'Westerly' type in winter and spring; 'Southerly' type in spring, and fall; 'Northerly' type in spring and summer; 'Easterly' type in winter, and 'Northwesterly' type in fall. The period 1986-2000 was reported to be an outlier, i.e., characterized by higher persistence, and the most pronounced change point in the time series was in the mid-1980s.

Regarding the total persistence of the circulation types, Kassomenos et al. (2003) established that during the cold period (from mid-October to mid-March) types similar to EHwin and ILwin supertypes in this classification were more persistent, which was confirmed in this study for the ILwin supertype. The warm period indicated, according to Kassomenos et al. (2003), that a type comparable to WPGLsum supertype in this classification is the most persistent which was not found in this study.

6. Conclusions

A comprehensive two-tier circulation classification was derived for the European/North Atlantic domain using principal components analysis and cluster analysis. The classification is comprised of two solutions. One solution consists

of 'supertype' circulation patterns for every season and is more general and appropriate for a general analysis of the frequency and persistence of atmospheric circulation. The other, detailed, solution consists of numerous circulation 'types' per season, applicable for the investigation of specific research questions about the relationships between large-scale circulation characteristics and local climates. The classification is based on a large area encompassing the entire European continent and major portions of the northern Atlantic. It is applicable to different research agendas for any region within the continent and covers a long time period extending from 1951 to 2004. Since the classification was produced using computer-assisted methods, the methodology is easily transferable to any other region on any other continent. The frequency and persistence of the atmospheric circulation were investigated using the circulation 'supertype' patterns. In the last chapter the circulation 'types' will be used to better understand relationships between large-scale circulation and extreme temperature events.

The results from the investigation of the large-scale atmospheric circulation characteristics of the European/North Atlantic domain are as follows:

- Five circulation patterns are identified for winter. These supertypes are: Arctic Low-Voeikov Belt, Mediterranean Low-North Atlantic High, Scandinavian High-Mediterranean Low, European High and the Icelandic Low.
    - The typical supertypes for December are the Arctic Low-Voeikov Belt, the European High and the Mediterranean Low-North Atlantic High.

- In January the European High and the Arctic Low-Voeikov Belt supertypes are most frequent.
- February is dominated by the Mediterranean Low-North Atlantic High and the Scandinavian High-Mediterranean Low supertypes.

- The Arctic Low-Voeikov Belt, the Scandinavian High-Mediterranean Low and the Icelandic Low supertypes are still evident in spring. Two additional patterns, the Azores-Scandinavian Ridge and the European Low, are identified. The European High and Mediterranean Low-North Atlantic High supertypes are not present in spring.
  - The Arctic Low-Voeikov Belt supertype is most frequent in March.
  - The European Low occurs more often in April, compared to the remaining supertypes.
  - May is clearly dominated by the Scandinavian High-Mediterranean Low supertype.
- In summer, the variety and intensity of the circulation are reduced, and only three supertype patterns are derived. They are the Weak Persian Gulf Low, the Azores-Scandinavian Ridge and the Arctic Low-Persian Gulf Low.
  - June is strongly dominated by the Weak Persian Gulf Low supertype.
  - In July, the Arctic Low-Persian Gulf Low supertype is most frequent and the Weak Persian Gulf supertype is least frequent.
  - In August, the Azores-Scandinavian Ridge is more frequent than the other supertypes.

- Four supertypes, the Persian Gulf Low, Arctic Low-Voeikov Belt, Scandinavian High-Mediterranean Low, and Icelandic Low, are derived for fall. The AL-VBfal, SH-MLfal and ILfal supertypes have counterparts in other seasons.
    - The supertypes exhibit almost equal seasonal frequency except for the Persian Gulf Low supertype which occurs on 36.2% of fall days.
    - September is greatly dominated by the Persian Gulf Low supertype, occurring on 82% of all September days.
    - In October, all of the supertypes are equally frequent.
    - In November, the supertypes display similar rate of incidence except for the Persian Gulf Low supertype, which has a distinct minimum with 0.7% recurrence.
- The trend tests for 1951-2004 indicated that:
    - All the supertypes dominated by anticyclonic features or positive SLP anomalies feature positive overall trends. These supertypes include: Arctic Low-Voeikov Belt and European High in winter, Weak Persian Gulf Low in summer, Arctic Low-Voeikov Belt and Scandinavian High-Mediterranean Low in fall.
    - The supertypes dominated by cyclonic features all display significant negative trends: Scandinavian High-Mediterranean Low and Icelandic Low in winter, Arctic Low-Persian Gulf Low in summer and Persian Gulf Low in fall.

- Trends in the supertypes' frequency were evident in all seasons, except for spring.
- The results from the tests for break points in 1951-2004 time series of supertype frequency suggest that for most supertypes breakpoints occurred in the 1960s and 1970s.
- Several supertypes exhibit significant trends during sub periods that differ from the overall trend for 1951-2004. The frequency of the Arctic Low-Voeikov Belt winter supertype decreases in 1951-1972, while the frequency of the Weak Persian Gulf Low summer supertype decreases in1976-2004. The frequency of the Persian Gulf Low fall supertype displays positive trends during 1951-1966 and 1976-2004 sub-periods.

- Regarding the interannual changes in persistence characteristics, the results indicate that:
  - The average event length for the Scandinavian High-Mediterranean Low in winter, the Arctic Low-Persian Gulf Low in summer and the Persian Gulf Low in fall, has decreased.
  - The number of transitional (or 1-day) events is decreasing for the European Low supertype in spring and increasing for the Icelandic Low supertype in fall.
  - The frequency of circulation events lasting 2 to 4 days does not change with time, except for the European High supertype in winter which has a significant positive trend.

- Regarding the changes in frequency, length and total number of days in events lasting more than 4 days:
    - In winter, all the supertypes dominated by anticyclonic features (Arctic Low-Voeikov Belt and European High in winter) exhibit increasing trends of these parameters. The supertypes dominated by cyclonic features, Mediterranean Low-North Atlantic High, Icelandic Low and Scandinavian High-Mediterranean Low in winter) show a decrease.
    - In spring, no trends were evident in the events longer than 4 days.
    - In summer, only the Weak Persian Gulf Low supertype has a positive trend (similar to the winter supertypes dominated by positive anomalies) in the average length of the longer events.
    - In fall, the Persian Gulf Low supertype is characterized by a decrease in the average length of the longer events and in the number of days included in these events, similar to the winter supertypes dominated by negative anomalies. The rest of the fall supertypes feature positive trends for some of the characteristics.

The next chapter will focus on the historical changes in temperature extreme events in Bulgaria.

Chapter 3 Historical characteristics of the temperature extreme events in Bulgaria

1. Introduction

The rate of global warming appears to be increasing. The 100-year linear trend, reported by Working Group I of the Intergovernmental Panel for Climate Change (IPCC), for the period 1906 through 2005 is 0.74°C (IPCC FAR, 2007), compared to only 0.6°C for the period 1901-2000, reported by the IPCC Third Assessment report (IPCC TAR, 2001). Since the occurrence of temperature extremes is related in a non-linear manner to the mean temperatures (Mearns et al., 1984), the changing average temperatures can affect greatly the frequency of the extremes.

In recent years, interest in extreme weather and climate events has increased dramatically because many disastrous events since the 1980s have caused large economic losses (Karl and Easterling, 1999) and considerable loss of life. In light of the potential future climate changes, many researchers (Hennessy and Pittock, 1995; DeGaetano, 1996; Brazdil et al., 1996; Karl and Knight, 1997; Heino et al., 1999; Easterling et al., 2000; Horton et al., 2001; Salinger and Griffiths, 2001; Frich et al., 2002; Klein Tank and Können, 2003; Luterbacher et al., 2004; Moberg and Jones, 2005, to name a few) focused their attention on whether changes in climate extremes have already occurred on global or regional scales. Research, except for one study (Koleva, 1987), concerning the changes in climate and weather extremes in Bulgaria, however, is lacking as is discussed in more detail later in this chapter.

Significant changes in the frequency of occurrence of the anticyclonic and the cyclonic circulation supertypes were established in the previous chapter. The supertypes dominated by anticyclones have risen, and the supertypes dominated by cyclonic features have declined in frequency, during the 1951-2004. In addition, significant increasing or decreasing trends were found for several supertypes for sub-periods within the study period, for example the AL-VBwin supertype demonstrated a negative trend during 1951-1972. Since atmospheric circulation is one of the leading factors influencing the climate of an area, and more specifically the occurrence and intensity of climate and weather extremes, the overall goal of this portion of the study is to investigate how frequency and intensity of extreme temperature events have changed in Bulgaria during the second half of the 20th century. The issue about the temperature extremes changes in Bulgaria will be addressed using two methods: trend and extreme value analysis of the time series of temperature extremes.

1.1. What are temperature extreme events?

If we consider the empirical distribution of the air temperature at a location, extremes are the high and low values in the tails of the distribution that occur infrequently or in other words are "far from the mean or median of the distribution" (Meehl, et al. 2000). In climatological research, when analyzing the temperature characteristics of a location, in addition to the highest and the lowest temperatures (or the absolute extremes), other temperature extreme events are employed as well, depending on the study objectives, for example frost days, heat waves, and cold spells. Domonkos and Piotrowicz (1998) compiled a

detailed list of previous definitions of temperature extreme events. These definitions of temperature extreme events can be categorized in three broad groups. The first group includes definitions that consider a single value equal to or exceeding a chosen threshold (also called a 'day event' by Mearns et al., 1984). The second group includes definitions regarding the most extreme value of a period (Tabony, 1983). The third group consists of definitions related to periods of several consecutive or non-consecutive days with temperatures equal to or exceeding a chosen threshold (also called 'run events' by Mearns et al., 1984, and Colombo et al., 1999). The thresholds can be absolute or based on percentiles of the empirical temperature distributions. According to Domonkos and Piotrowicz (1998), the reason why many different definitions exist is that the description of the temperature extremes is strongly dependent on the specific application.

In an attempt to improve consistency in terminology and methodology, the World Meteorological Organization (WMO), the Global Climate Observing System (GCOS) and the Climate Variability and Predictability program (CLIVAR) organized a Workshop on Indices and Indicators for Climate Extremes that was held on 3-6 June, 1997, in Ashville, North Carolina. Other foci of the workshop were to promote the development of global data sets and to determine whether extreme weather and climate events were becoming more extreme or variable (Karl et al., 1999). The participants in the workshop published guidelines regarding the indices of climate extremes to be used in studies of changes of these extremes on a global and regional scale, and the data required to improve

the monitoring of climate extremes. In addition, reports about the observed changes in climate and weather extremes on global and regional scales were prepared.

1.2. Rationale for the choice of extreme events indices in this study

The recommendations of the Workshop on Indices and Indicators of Climate Extremes (Folland et al., 1999) influenced the choice of indices that are the focus of this part of the analysis. Traditional extremes indicators of the temperature regime of a place (absolute highest or lowest temperatures for a given period) as well as temperature extreme events that can affect society directly or can be detrimental to sectors of the economy were chosen. Nine indices of temperature extreme events were employed: 1) absolute annual and seasonal daily maximum and minimum temperatures; 2) daily temperature range; 3) inter-period differences (differences between mean temperature anomalies for non-overlapping periods of different length) of maximum and minimum temperatures; 4) heat waves; 5) cold spells; 6) frost period severity; 7) frost period duration; 8) cooling degree days; and 9) heating degree days.

Diurnal temperature range (DTR) and the inter-period temperature differences were included as they represent the temperature variability of a given location. From a statistical point of view, the inter-period differences (IPDs) are the first differences of a series. An advantage of using the IPDs, as pointed out by Karl et al., (1995), is that the first differences are much less affected by high and low frequency variability compared to standard deviations. Changes in inter-

period variability could have large practical implications. For example, decreased variability could lead to longer spells of extreme conditions.

The frequency, length and intensity of heat waves and cold spells, signify the immediate impact of temperature extremes on society and sectors of the economy. Prolonged periods of high or low temperatures affect mortality rates (Changnon et al., 1996), cattle production (Thatcher, 1974) and plant productivity, and can interfere with the tourism industry through changes in vacation destinations (IPCC, TAR 2001). In addition, long periods of high temperatures can aggravate drought conditions and increase the chance of wild fires (Salinger and Griffiths, 2001).

The frost period duration and severity indices supply information about the cold season. The frost period duration is inversely related to the length of the growing season. Any changes in the frost period length will reflect in turn opposite changes in the length of the growing season. The frost period severity indicates the amount of frost days (days with minimum temperature below 0°C) within each month during the frost period.

Cooling (CDD) and heating degree-days (HDD) accumulations reflect the impact of thermal conditions on the energy sector. More specifically, these indices represent the demands to cool or heat buildings to reach the human comfort level of 65° F or 18.3°C (http://www.weather2000.com/dd_glossary.html). The changes of these indices are usually incorporated in the planning measures of the energy sector (Soulé and Suckling, 1995). Specific details of the derivation of the indices and the analyses applied to each index are presented in section 6.

1.3. Historical trends in temperature extreme events

Several European and international agencies have focused their attention over the last decade on climate changes and their impacts in Europe (e.g., the European Environmental Agency (EEA), the Jackson Environmental Institute at the University of East Anglia, Norwich, United Kingdom, and the IPCC). All the reports published by these agencies agree that the annual temperature in Europe has increased during the 20th century and the latest estimate of this change is 0.95ºC (EEA, 2004). Several trends were pointed out regarding temperature extreme events in the last report of the EEA. Historically, the number of cold and frost days has diminished, while the occurrence of hot summer days (days with temperature above 25°C) and heat waves has increased for the continent as a whole (EEA, 2004).

Differences in the observed changes of temperature extremes for the entire continent were found by some authors when sub-periods were considered. Klein Tank et al. (2003) studied changes in daily temperature extremes in 1946-1999 using 86 stations in Europe. The indices of temperature extremes utilized in their analysis were based on absolute thresholds, for example, frost days (based on 0ºC minimum temperature threshold), summer days (based on 25ºC maximum temperature threshold), or on percentile thresholds. Examples of indices based on percentile thresholds are: the number of cold nights with minimum temperature (TMIN) below the 10th percentile of the daily temperature distribution for the respective day in the baseline 1961-1990 period and the number of warm nights, determined similarly but using the 90th percentile of the daily minimum temperature distribution. Similar indices, e.g., number of cold days

and warm days, based on the 10th and 90th percentiles of the maximum temperature (TMAX) distributions, were also applied. The frost days and the indices based on the 10th percentile values for TMAX and TMIN were termed 'cold extremes', while the summer days and the indices based on the 90th percentiles for TMAX and TMIN, where called 'warm extremes' in their study. Klein Tank et al. (2003) found that in the 1946-1975 sub-period, the annual number of warm extremes decreased but the annual count of the cold extremes did not change, implying a decrease in temperature variability. During the 1976-1999 period, the annual number of warm extremes increased at a faster rate than the rate of decline of the cold extremes, which indicated an increase in temperature variability in Europe (Klein Tank et al., 2003).

Regional changes in temperature extremes in Europe have also been detected during the 20th century. A parallel rise in: the daily maximum and minimum temperatures was observed in northern and central Europe in 1901-1995 (Heino et al.,1999); the warm and cold tails of TMAX and TMIN in central and western Europe in 1901-1999 (Moberg and Jones, 2005). Heino et al. used a total of 20 stations and the following indices: mean daily maximum and minimum temperatures, diurnal temperature range (DTR), and number of frost days. Furthermore, since the daily minimum temperatures increased at a higher rate, the daily temperature range decreased in northern and central Europe, found Heino et al. (1999). In addition, a decrease in the number of frost days also occurred. Moberg and Jones (2005) studied the winter and summer changes in the 10th and 90th percentiles of the maximum and the minimum temperature

distributions. They found that, comparing the first half of the 1901-1999 period to the second half, the winter temperatures increased in the second half with the cold tail of the minimum temperatures demonstrating the largest changes. Less evidence was found to a widespread warming in summer for the second half of the 20th century.

Other regional changes include, for example, a decrease in the length of the cold season in central Europe, as estimated from one station in Poland and two in Hungary (Domonkos and Piotrovicz, 1998). The authors studied winter temperature characteristics for central Europe in 1901-1993. Several indices were used to characterize the winter season: daily mean and 5-day average temperatures and anomalies; length, starting and ending dates of the cold season; and extreme cold events defined using absolute (-5°C and -10°C), and percentile based thresholds. Domonkos and Piotrovicz found that most of the characteristics of the cold season showed a slight decrease in severity in Central European winters. Only the trends for the mean seasonal temperature, the annual minimum temperature (both displaying an increase), the length of the cold season and the number of low anomalies (both showing a decrease), however, were significant at α=0.05 in some stations.

At a finer spatial scale, the daily maximum and minimum extreme temperatures, and the heat waves duration have generally increased, while the number of frost days has declined, at the majority of stations in western Germany during 1958-2001 (Hundecha and Bardossy, 2005). The indices of temperature extremes used in their analysis were: the 90th percentile daily maximum

temperature, the 10th percentile daily minimum temperature, the number of frost days and the heat wave duration. Similar findings were reported for three stations in Hungary by Domonkos (1998), who determined that the number of days within periods with extreme low daily mean temperatures and the length of the periods with extreme low temperatures have decreased since the 1940s.

One previous study, by Koleva (1987), utilized a limited set of indices to investigate temporal variations by month in temperature extremes in Bulgaria. Although the overall period was 1896-1980, shorter periods were used for some stations depending on their starting date of operation. The analysis was based on 10-year running means plots for 25 stations. The extremes, chosen to characterize the winter months (December, January and February) included the frequency of mean daily temperatures below 0°C, minimum daily temperatures below -5°C and maximum daily temperatures above 10°C. The extremes utilized for the summer months (June, July and August) were the daily mean temperatures above 20°C and daily minimum temperatures above 15°C. According to Koleva (1987), cooler wintertime periods, based on the higher frequency of the studied temperature extremes in December and January, were evident in 1938-1947 and 1960-1969. A warmer period, based on the lower frequency of the considered extremes in December and January, was observed in 1948-1957. The temperature extremes in February did not show large variations throughout the 1896-1980 period, except for 1926-1935, when a cooler period was identified, based on the increased number of days with mean

temperature below 0°C. For the summer season, no consistent variations were evident among the stations.

1.4. Past studies using extreme value analysis of extreme events

All of the studies, addressed above, have used mostly trend analysis to assess the changes in temperature extreme events during the second half of the 20th century. Another approach that can be applied to evaluate the differences in temperature extremes in separate periods within the 20th century, however, is to use extreme value analysis and to evaluate the changes in return levels[8] of temperature extremes, based on different periods of interest.

Past research, in which extreme value analysis was applied to study climate change and extreme events, mostly focused on methodological or Global Circulation Model (GCM) validation questions. The comparison of return levels between different time periods has been limited to assessment of changes between future and current climate. For example, Zwiers and Kharin (1998) explored changes in annual absolute temperature extremes between the climate simulated by the Canadian Center for Climate Modeling (CCCma) GCM2 under CO_2 doubling, and the observed climate on a global and regional scale. They modeled annual absolute temperature extremes with the Generalized Extreme Value distribution (GEV). Another example is the study by Kysely and Huth (2001), who investigated whether global climate models were able to reproduce

[8] Return levels are the *(1-p)th* quantiles of the GEV or GP distribution, where *p* is the probability of occurrence of an extreme event in any given year (Katz et al., 2002). Return levels are "thresholds that will be exceeded on average once every return period" (Zwiers and von Storch, 1999), where return periods (equal to *1/p*) could be 10, 20, 50, 100 or any other number of years.

annual absolute temperature extremes and heat/cold waves in central Europe. The authors also modeled the annual absolute TMAX and TMIN extremes using the GEV. Extreme value theory has also been applied to evaluate observed climate extremes. Kysely (2002b) compared probability estimates of temperature extreme events (annual temperature maxima and heat waves) in the Czech Republic, using a stochastic modeling approach and extreme value distributions. He recommended modelling the annual absolute temperature extremes with the GEV distribution.

Comparisons of return levels of temperature extremes for different historical time periods to my knowledge do not exist. Extreme value analysis was used in this study to compare changes in return levels in different sub-periods during the second half of the 20th century.

1.5. Research question and objectives

Given that the only study to date, concerning extreme temperature events in Bulgaria, was quite limited in scope (Koleva, 1987), the research question in this part of the study is: What are the changes in extreme temperature events in Bulgaria between 1951-1979 (referred to as the 'early period') and 1973-1999, referred to as the 'late period'? (The periods were dictated by the data as discussed below.) This question will be addressed by: 1) trend analysis of different indices of temperature extremes for the two periods, and 2) exploring the changes in return levels for temperature extremes between the early and late periods.

Additional objectives in this analysis are to examine, where possible, the spatial consistency between the trends, extreme value distribution models and return levels. In addition, the changes in perception of extremes by using single absolute extremes and extremes, based on threshold exceedances, will be explored.

2. Sources of temperature data and preprocessing

The application of trend and extreme value analysis, and the interpretation of the results from these analyses, are hindered if the available data are not homogeneous. Hence, it is of utmost importance to identify stations with homogeneous records.

2.1. Data availability

The Bulgarian Meteorological Yearbooks, published since the 1890s until 1980, contain primarily monthly data from hundreds of meteorological stations in the country. For a limited number of stations, daily observations are also available in the Yearbooks from 1951 and ending in either 1979 or 1980. Daily data were required for this study, which limited the analysis to five stations: Sofia, Obraztsov Chiflick, Plovdiv, Pleven and Varna. Daily maximum (TMAX) and minimum (TMIN) temperature data for these five stations were extracted by hand from the Yearbooks for the period 1951-1979, except for the data for 1960 for Pleven, which were missing. Although other sources of Bulgarian data exist, the cost for acquiring these data was well beyond the budget of this research project. It was not possible to acquire additional data from Bulgaria at a reasonable cost.

In addition, to the data obtained from the Yearbooks, temperature observations were acquired from the Global Summary of the Day dataset archived at the National Climatic Data Center (NCDC). The Global Summary of the Day is an electronic dataset containing daily mean values of temperature, dew point, SLP, and wind speed, along with maximum and minimum temperature, precipitation amount and some other surface variables for approximately 8000 stations around the globe (Winkler, 2004). The majority of the observations are available from 1982 onward, while less complete data are also available since 1973, and for some stations even back to 1930. Only gross error checking for random errors has been performed on these data (Winkler, 2004). Daily TMAX and TMIN data for four stations which had the same names as those already acquired from the Yearbooks (i.e., Sofia, Plovdiv, Pleven and Varna) were extracted from NCDC for the period 1973-2004. For Pleven, data were available only up to 1999. In addition, data for Obraztsov Chiflick were not available from the Global Summary of the Day data base, however this station was still considered for completeness of the early period analysis. A limitation of the Global Summary of the Day dataset was that observations for 1996 were missing for all stations.

2.2. Gross error checks and preprocessing

Unrealistic, or also called gross errors, are the values which are too high or too low for a given period. The gross error check on the data obtained from the Global Summary of the Day had been already performed at NCDC. The daily maximum and minimum series from the Bulgarian Yearbooks were examined for

unrealistic values by calculating the daily temperature range (DTR) for each station. The DTR was computed by subtracting the daily TMIN from the daily TMAX. The reasoning, for using DTR, is that this variable combines the maximum and minimum series and allows for a detection of unrealistic values and obvious problems in both data series, including: negative DTR values caused by maximum temperatures lower than the minimum values for a day; very large DTR values (greater than 25°C) due to very high maximum temperature values or unseasonably low daily minimum temperatures. The threshold value of 25°C was chosen as it represents an unrealistically large DTR. Time series plots of DTR for each station were created (see Figure 3-1 for an example).

If problems in the data were detected, the TMAX and TMIN for the respective day were compared to temperature observations at 7am, 2 pm and 9 pm for the same day. The TMAX and TMIN values for the preceding and following day were also compared to the unrealistic values. The problematic TMAX or TMIN data values were adjusted using the monthly mean TMAX or TMIN values, following the steps below (based on a personal communication with Dr. Fred Nurnberger):

a) The monthly average TMAX or TMIN, available from the Meteorological Yearbooks, was multiplied by the number of days in the month and the value, Total1, was obtained;

b) The daily temperatures for all the days, except the day with problematic data, were summed to obtain Total2;

c) The suspect temperature value was replaced by the difference of Total2 and Total1.

In rare cases, daily data values were missing and the monthly means were calculated using all the days in the month but the days with the missing value. In these cases, the means of the TMAX or TMIN from the days before and after the day with a missing value were used instead. A summary of the number of corrected data is given in Table 3-1.

Since the data were transferred from a hard copy into electronic form, many typos existed in the time series. For example, in Figure 3-1, several unrealistic DTR values are evident. All the unrealistic values, resulting from the transfer of the data into electronic form, were compared with the actual printed data and corrected using the real data values from the hard copies.

Figure 3-1 Example of a daily temperature range plot for Pleven, 1951-1959, Yearbook data

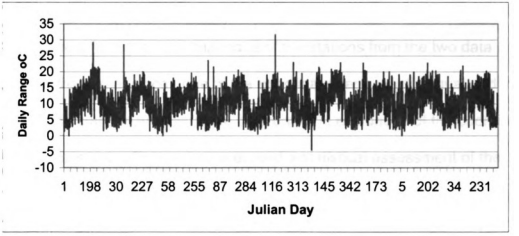

Table 3-1 Summary table of the number of corrected data for the stations obtained from the Meteorological Yearbooks using the above mentioned steps, (absolute count and %)

Station	Obraztsov Chiflcik	Varna	Plovdiv	Pleven	Sofia
Total number of data	10585	10585	10585	10220	10585
Number (percentage) of corrected data values	5 (0.047%)	2 (0.019%)	2 (0.019%)	3 (0.029%)	6 (0.057%)

3. Comparison of the stations in the two datasets

In many of the large cities in Bulgaria, several reporting meteorological stations at different locations exist under the management of different institutions. Thus, it is possible that the stations that were obtained from the two data sets, the Bulgarian Yearbooks and the Global Summary of the Day from NCDC, might not be the same. The equivalence of the stations was evaluated initially by comparing their geographical coordinates and altitude above sea level (Table 3-2). It is evident from the table that none of the stations from the two data sources are the same, since none of the coordinates are exactly equal and the altitudes of the stations are also quite different. The evaluation of the coordinates of the stations is not sufficient, however, and a statistical assessment of the temperature differences between the stations was performed.

Table 3-2 Geographical coordinates and altitude above se level for the stations from the Bulgarian Yearbooks and the stations obtained from NCDC

Station	Latitude Yearbook	Latitude NCDC	Longitude Yearbook	Longitude NCDC	Altitude Yearbook	Altitude NCDC
Sofia	42° 42'	42° 65'	23° 20'	23° 38'	552 m	591 m
Plovdiv	42° 09'	42° 13'	24° 42'	24° 75'	160 m	185 m
Pleven	43° 25'	43° 41'	24° 35'	24° 60'	123 m	71 m
Varna	43° 12'	43° 20'	27° 55'	27° 91'	3 m	43 m
Obraztsov Chiflick	43° 48'	n/a	26° 02'	n/a	152 m	n/a

The daily temperatures for every year of the overlap period (1973-1979) for the two data sets were differenced separately for TMAX and TMIN. For example, the daily values for TMAX for station Sofia extracted from the Yearbooks were subtracted from the respective daily values for TMAX obtained from the Global Summary of the Day. The results were plotted and an example of the plots for Pleven is shown in Figure 3-2. A comparison of the plots indicates that the differences are not equal to zero. To assess whether the differences are statistically significant, the paired comparisons *t*-test was performed by year and for the 1973-1979 period as a whole.

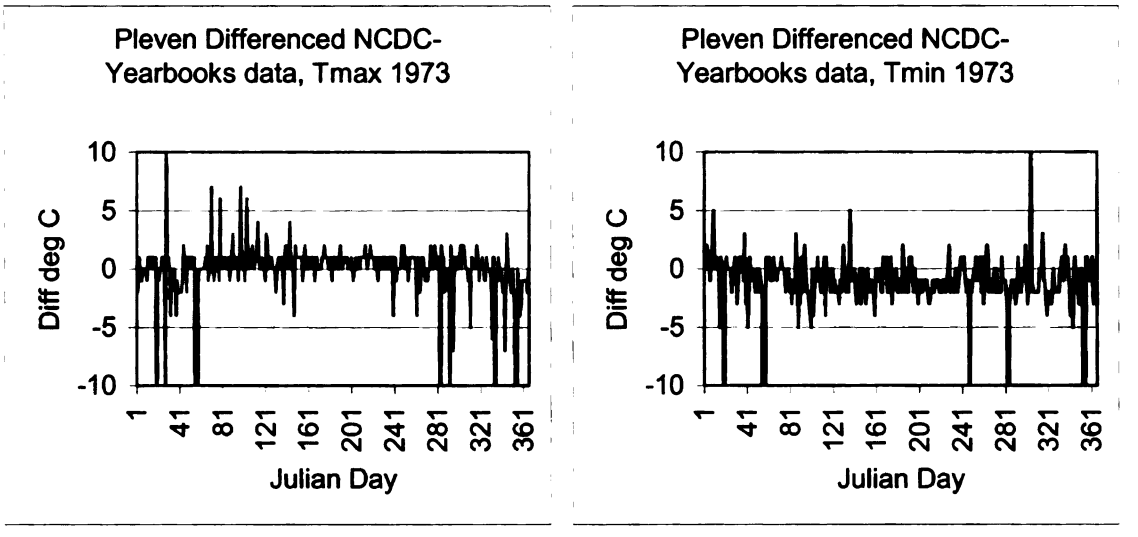

Figure 3-2 Plots of the differences between the NCDC and the Yearbooks data for TMAX and TMIN, 1973, station Pleven

The calculation steps for the test are as follows (Earickson and Harlin, 1994):

1) Determine the mean of the differences series for TMAX or TMIN for a given station.

$$\overline{d} = \frac{\sum_{i=1}^{n} d_i}{n}$$

where d_i is each daily difference, n is the number of differences in the series, and $\overline{d}$ is the mean of the differences.

2) Calculate the variance for the differences, s_d^2,

$$s_d^2 = \frac{n\sum_{i=1}^{n} d_i^2 - \left(\sum_{i=1}^{n} d_i\right)^2}{n(n-1)}$$

3) Calculate the standard error of the mean of the differences, $\sigma_{\bar{d}}$,

$$\sigma_{\bar{d}} = \frac{s_d}{\sqrt{n}}$$

4) Calculate the *t* statistic

$$t = \frac{\bar{d} - 0}{\sigma_{\bar{d}}}$$

At a level of significance α=0.05, the critical value for $|t|$ is 1.96. The null hypothesis, that the mean (for TMAX and TMIN separately) of the calculated differences between the paired Yearbook and NCDC values is equal to zero, is accepted if the calculated $|t| \leq 1.96$. The results of the *t-test* are presented in Table 3-3. The null hypothesis is accepted for only a few years of the annual comparison. For the entire overlap period, the null hypothesis is accepted for TMAX at Pleven and TMIN at Sofia. The results from the statistical testing confirm the outcome from the visual inspection, i.e., that the stations are different. As a consequence, the comparisons of the changes in temperature extremes will be based on two different stations at each city, which limits the interpretation. This approach however is still acceptable since the stations are not located too far apart.

Table 3-3 Paired comparisons T-test of the differences in Tmax and Tmin for 1973-1979 between the Yearbooks and NCDC data (Critical value at α=0.05 is |t| = 1.96) The underlined values in the table represent the cases when Ho was accepted

Number of days	N=365	N=365	N=365	N=365	N=365	N=365	N=365	N=2555
Year	1973	1974	1975	1976	1977	1978	1979	1973-1979
Station/ Statistic	|t|	|t|	|t|	|t|	|t|	|t|	|t|	|t|
Pleven								
Tmax	2.02	1.11	8.80	0.19	3.93	2.33	1.62	1.01
Tmin	10.17	11.37	6.13	3.52	8.86	13.05	7.11	22.42
Plovdiv								
Tmax	5.73	2.43	4.83	5.74	6.75	2.10	2.25	10.24
Tmin	7.32	5.50	7.89	4.62	0.14	2.56	1.99	10.91
Sofia								
Tmax	1.86	0.64	2.83	2.92	5.53	1.88	1.23	6.33
Tmin	1.83	1.01	1.34	0.40	2.93	1.07	0.06	0.20
Varna								
Tmax	1.88	0.69	10.79	9.51	9.38	8.23	6.06	16.36
Tmin	6.99	8.38	10.44	1.14	4.76	5.08	6.87	2.94

4. Homogeneity testing

Since an objective of this study is to investigate the historical changes of temperature extreme events in Bulgaria, the homogeneity of the temperature series must be evaluated. Homogeneous climate data reflects only the variations in weather and climate (Conrad and Pollak, 1950, as summarized by Peterson, et al., 1998). The inhomogeneities in the data may distort or even hide the climate signal (Tuomenvirta, 2001) resulting in erroneous analyses (Peterson et al., 1998). Data homogeneity can be affected by changes in station location, instrumentation, observation practices, and data processing methods. Different methods exist for homogeneity testing of monthly and annual data (an exhaustive list is presented in Peterson et al., 1998). The two major approaches to

homogeneity testing are the direct methods, for example, use of metadata, side by side comparisons of instruments and statistical studies of instrumental changes, and the indirect methods. The indirect methods can be applied to a single station or can use a reference series, and also include subjective assessments and objective tests (for example, the Standard normal homogeneity test of Alexandersson, 1986; the Craddock test, 1979). Despite the long list of homogeneity tests available for annual and monthly data, well-established tests for daily data do not exist (Wijngaard et al., 2003). Instead, Wijngaard et al. (2003) introduced a 'hybrid approach' for homogeneity testing of daily data. The 'hybrid' approach is based on the development of annual resolution set of variables from daily data. Subsequently, traditional homogeneity tests for annual data are applied to the developed set of variables. The results from the homogeneity tests are used to classify the data series in terms of data quality. In this study, the 'hybrid' approach of Wijngaard et al. (2003) was used.

4.1. Testing variables

The two variables used in the homogeneity testing are the annual mean diurnal temperature range (DTR) and the annual mean of the absolute day-to-day differences of the DTR (Wijngaard et al., 2003). Annual mean DTR was computed by summing all the daily DTR values for a given year and dividing by the number of days in the year (the leap year days were not used in the analysis). The annual mean of the absolute day-to-day differences of the DTR was calculated as follows:

a) the DTR for day 1 was subtracted from the DTR for day 2, the DTR for day 2 was subtracted from the DTR for day 3, and so on;

b) the absolute values of the DTR differences were summed by year;

c) the annual mean of the DTR day-to-day differences was obtained by dividing the sum by the number of days in the year.

These two variables were chosen for the homogeneity testing by Wijngaard et al. (2003) because they were more sensitive to the homogeneity tests than the annual means of TMAX and TMIN, or the annual daily mean temperature series. A break that is evident in the DTR series may be more difficult to detect in the TMAX and TMIN series, and may not appear at all in the annual mean temperature series. An additional reason for using the annual mean absolute day-to-day differences of the DTR as a homogeneity testing variable is that inhomogeneities may be more apparent and easier to find in a higher order statistical moment than in the means (Wijngaard et al., 2003). Standard deviations, which are another higher order statistical moment, were not chosen as a testing variable because they are more influenced by high and low-frequency variability compared to the absolute day-to-day differences of the DTR (Wijngaard et al., 2003; Karl et al., 1995). In addition, Moberg et al. (2000) found that the day-to-day temperature differences were quite sensitive to inhomogeneities. In summary, the advantage of using DTR variables for the homogeneity testing is their sensitivity to inhomogeneities in the data series which are supported by metadata and their ability to distinguish between climate variations and artificial breaks, as found by Wijngaard et al. (2003).

4.2. Homogeneity tests

The four tests used in the homogeneity testing are the Alexandersson Standard Normal Homogeneity test (SNHT) for a single break (Alexandersson. 1986), the Buishand range test (Busihand, 1982), the Pettit test (Pettitt, 1979) and the Von Neumann ratio test (Von Neumann, 1941). Unlike many homogeneity tests, these tests do not compare a series to that of a nearby station. Rather, they are absolute tests, relying only on the information from only the station of interest. All four tests assume that the annual values of the testing variables are independent and identically distributed. The null hypothesis is that the testing series is homogenous, while the alternative hypothesis states that a step-like shift is present, or in the case of the Von Neumann ratio, the tested series is not randomly distributed (Wijngaard et al., 2003). While the SNHT, Pettit and Buishand tests provide the year of the detected break, the Von Neumann provides only an indication that inhomogeneity exists within the series. The SNHT and the Buishand range test assume that the values of the series of interest are normally distributed, while the Pettit test does not make this assumption. The Pettit test is less sensitive to outliers compared to the other tests since it is based on the ranks and not on the actual values of the testing variables. The Buishand and the Pettit tests can identify breaks in the middle of the tested period, while the SNHT is more sensitive to breaks in the beginning and end of the series. The computational details of the homogeneity tests are presented in the following subsections.

4.2. a. Buishand range test

This test is based on the assumption that the series is normally distributed. The 'adjusted partial sums', S_k^*, are calculated by:

$$S_k^* = \sum_{i=1}^{k} (Y_i - \overline{Y}) \text{ , for } k = 1, 2, \ldots, n, \text{ and } i = 1,\ldots,k.$$

In this formula Y_i is an annual value of the testing variable, $\overline{Y}$ is the mean of testing variable for the period of record, *k* and *i* are sequence numbers of the values, and *n* is the total number of years in the period of record.

The series is homogeneous if the adjusted partial sums, S_k^*, vary around zero, as this indicates that no systematic change in the values of Y_i compared to the long-term mean, $\overline{Y}$, exists (Wijngaard et al., 2003). If a break in the series is present, S_k^* has a maximum or a minimum near the year of the break. A plot against time of the parameter

$$(S_k^* / s) / \sqrt{n} \text{ ,}$$

calculated for every year, where *s* is the sample standard deviation of the testing variable and *n* is the number of values, is very informative. The significance of the break can be found using the 'rescaled adjusted range, *R*'.

$$R' = (\max_{0 \le k \le n} S_k^* - \min_{0 \le n \le k} S_k^*) / s,$$

where S_k^* are the adjusted partial sums, *k* is the sequence number of the years, *n* is the total number of years, and *s* is the standard deviation of the series of the testing variable. Critical values for *R/SQRT(n)* are given in Buishand (1982) and

Wijngaard et al. (2003, p.691). If the *R/SQRT(n)* value is smaller than the critical value at a given level of significance, the null hypothesis that the series is homogeneous is accepted.

4.2. b. Standard normal homogeneity test

The *T*(*k*) statistic compares the mean for the first *k* years of the period to the mean for the *n-k* years of the period.

$$T(k) = k\bar{z}_1^2 + (n-k)\bar{z}_2^2,$$

where $k = 1,\ldots, n$, and n is the total number of years in the period,

$$\bar{z}_1 = \frac{1}{k}\sum_{i=1}^{k}(Y_i - \bar{Y})/s \quad \text{and} \quad \bar{z}_2 = \frac{1}{n-k}\sum_{i=k+1}^{n}(Y_i - \bar{Y})/s,$$

for which Y_i is an annual value of the testing variable, $\bar{Y}$ is the mean of the testing variable for the entire period, and s is the standard deviation of the testing variable for the entire period. If a break exists, the maximum value of *T(k)* indicates the year of the break. The test statistic is T_0, defined as

$$T_0 = \max_{1 \le k < n} T(k)$$

The null hypothesis is rejected if T_0 is above the critical value at a chosen level of significance (see Table III, Wijngaard et al., 2003).

4.2. c. Pettit test

If $Y_1, Y_2, \ldots, Y_n$ is the series of the testing variable, and $r_1, r_2, \ldots, r_n$ are the ranks of the values, a statistic can be calculated using:

$$X_k = 2\sum_{i=1}^{k} r_i - k(n+1) \quad ,$$

where $k = 1, \ldots, n$, and n is the total number of years in the period. X_k is plotted against years. The maximum or minimum value of X_k values signifies a break in the testing variable series if the critical value is exceeded at a chosen level of significance.

$$X_{BREAK} = \max_{1 \le k \le n} |X_k|$$

The critical values for given levels of significance are given in Pettit (1979).

4.2. d. Von Neumann Ratio test

The Von Neumann ratio (N) is the ratio of the mean squared year to year differences of the testing variable to the variance of the testing variable (Von Neumann, 1941; Wijngaard et al., 2003).

$$N = \sum_{i=1}^{n-1} (Y_i - Y_{i+1})^2 \Big/ \sum_{i=1}^{n} (Y_i - \overline{Y})^2 \quad ,$$

where Y_i is the annual value of the testing variable for a particular year, $\overline{Y}$ is the mean of the testing variable for the period of years, i is the successive number of the years, and n is the total number of years. If the series is homogeneous, the expected value of N is 2. If the series is not homogeneous, the value of N is lower than the expected value (Buishand, 1981; Wijngaard et al., 2003). Critical values for N can be found in Table VI (p.691) in Wijngaard et al. (2003).

4.3. Classification of the stations based on homogeneity testing results

Wijngaard et al. (2003) developed a classification of the applicability of the tested series to trend and variability analysis, based on the results of the homogeneity testing. According to the authors, the time series for a particular station is:

a) "useful" if one or no tests reject the null hypothesis at the 1% significance level. No clear signal of an inhomogeneity in the series is apparent. The series is sufficiently homogeneous for trend analysis and variability analysis (Wijngaard et al., 2003)
b) "doubtful" if two tests reject the null hypothesis at the 1% level. The results of trend and variability analysis should be interpreted critically (Wijngaard et al., 2003).
c) "suspect" if three or four tests reject the null hypothesis at the 1% level. "Suspect" series should not be used in trend and variability analyses

Since the tests are applied to both testing variables, two classifications per station are available. If the results of the homogeneity testing differed for the two testing variables, the station was assigned the poorer of the two classifications. Only series classified as "useful", or homogeneous portions of series classified as "doubtful", were considered for further analysis.

4.4. Results of the homogeneity analysis

4.4.1. Homogeneity analysis of the Meteorological Yearbooks data

For stations Obraztsov Chiflick, Plovdiv, Varna and Pleven, the Buishand and the Pettit tests do not indicate the existence of breaks in the temperature series (Table 3-4). None of the test statistics exceed the critical values. For Sofia, however, both tests indicate a possible break based on the annual mean absolute differences of the DTR (testing variable 1). On the other hand, Von Neumann Ratio and the SNH tests suggest that all stations except for Plovdiv have inhomogeneities. For Obraztsov Chiflick and Sofia both tests suggest significant break points, whereas for Varna only the SNHTest statistic for testing variable 1 exceeded the critical value. For Pleven the Von Neumann test exceeded the critical value only for testing variable 2.

The results from the four homogeneity tests are:

- Plovdiv was classified as 'useful',
- Varna was classified as 'useful',
- Pleven was classified as 'useful',
- Obraztsov Chiflick was classified as "doubtful"
- Sofia was classified as "suspect".

Table 3-4 Summary of the homogeneity testing of the stations from the Bulgarian Meteororlogical Yearbooks, 1951-1979
(critical values for α=0.01 are given in bold; cases with rejection of the null are underlined)

Test	Buishand Range test		Pettit test	
Station	Abs Difference in Annual Mean DTR (Testing variable 1)	Annual Mean DTR (Testing variable 2)	Abs Difference in Annual Mean DTR (Testing variable 1)	Annual Mean DTR (Testing variable 2)
Obraztsov Chiflick	1.3 < **1.7**	1.3 < **1.7**	118 < **133**	78 < **133**
Plovdiv	0.9 < **1.7**	1.4 < **1.7**	68 < **133**	122 < **133**
Sofia	<u>1.8 > **1.7**</u>	1.1 < **1.7**	<u>175 > **133**</u>	86 < **133**
Varna	1.1 < **1.7**	1 < **1.7**	116 < **133**	84 < **133**
Pleven*	1.5 < **1.7**	1.67 < **1.7**	71 < **133**	126 < **133**
Test	Von Neumann Ratio Test		SNHT	
Station	Testing Variable 1	Testing Variable 2	Testing Variable 1	Testing Variable 2
Obraztsov Chiflick	1.22 > **1.2**	<u>1 < **1.2**</u>	8.7 < **10.45**	<u>17.2 > **10.45**</u>
Plovdiv	1.4 > **1.2**	1.6 > **1.2**	4 < **10.45**	7.5 < **10.45**
Sofia	<u>1 < **1.2**</u>	1.7 > **1.2**	<u>14.3 > **10.45**</u>	3.9 < **10.45**
Varna	1.4 > **1.2**	1.7 > **1.2**	<u>12 > **10.45**</u>	5.4 < **10.45**
Pleven*	1.3 > **1.2**	<u>1 < **1.2**</u>	3.4 < **10.45**	9.5 < **10.45**

*** 1960 is missing for Pleven. The year was not included in the analysis.**

Although the test statistics for each test and station combination were plotted, only the plots displaying breaks, confirmed by at least two tests, are

shown below. Inspection of the plots for Sofia helped pinpoint the year of the break in the series (Figure 3-3). The break point, as confirmed by all three location specific tests, is 1969. Given these results Sofia will not be considered further in the study, since the overall period is split into two quite short periods of 19 and 10 years length (Table 3-5). For Obraztsov Chiflick, only the SNHTest plot for the annual mean DTR reveals the year of the break, since the Von Neumann Ratio test is not location specific. The year of the inhomogeneity is 1953 (Figure 3-4). Since the year of the break is in the very beginning of the available period of data for Obraztsov Chiflick, the period 1953-1979 will be used in the subsequent analysis. The homogeneity of the period 1953-1979 was not tested in this study, however, the results from the homogeneity testing performed for the European Climate Assessment, available online at (http://eca.knmi.nl/dailydata/datadictionaryhomogeneity.php), showed that the period after 1953 is homogeneous for Obraztsov Chiflick. In conclusion, four of the stations (Varna, Plovdiv, Obraztsov Chiflick and Pleven) contain homogeneous data and will be used in the subsequent analyses of the extreme temperature events (Table 3-5).

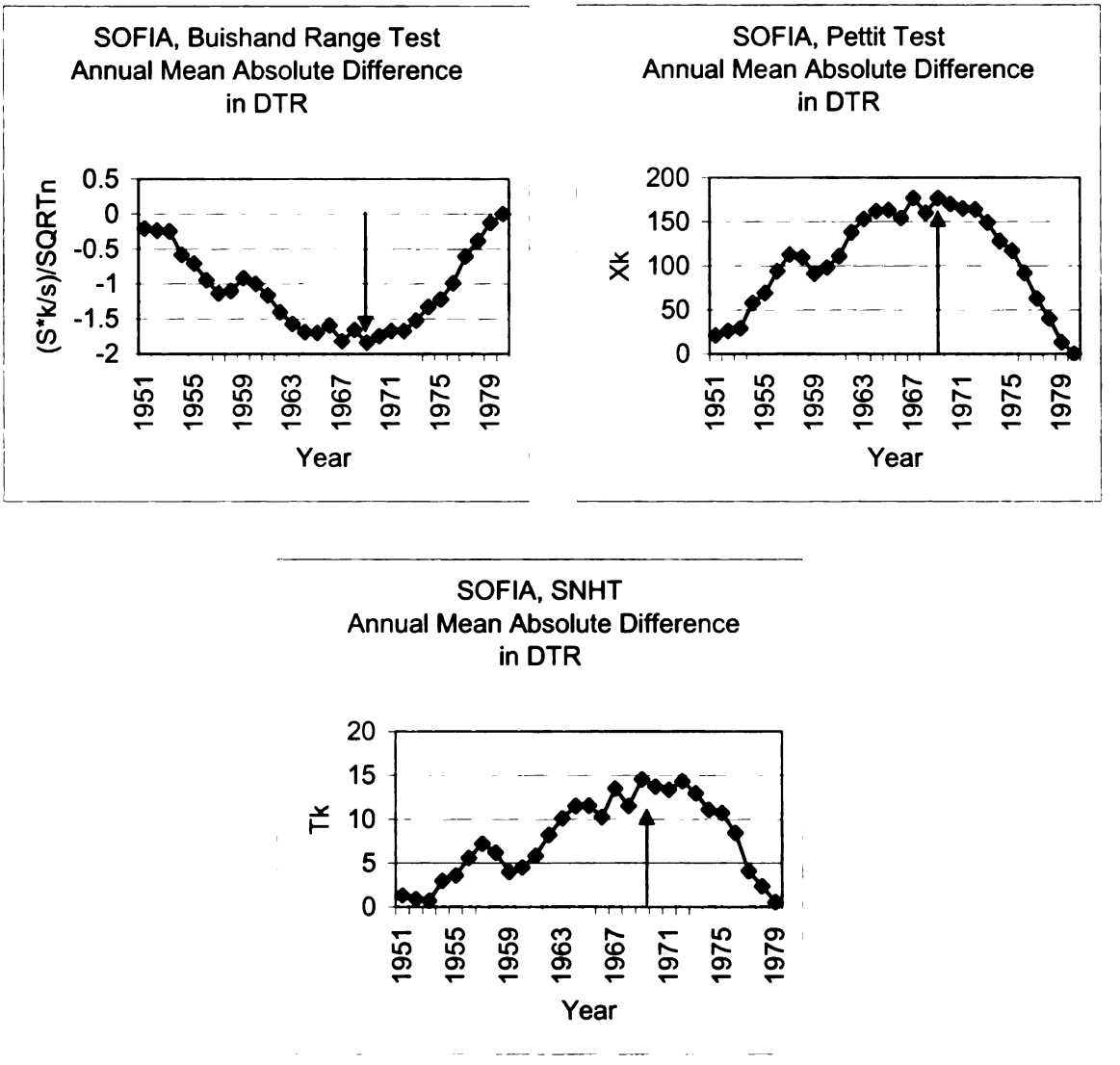

Figure 3-3 Plots of the test statistics for the Buishand Range test, the Pettit test, and the SNHT for Varna (A "Break" is possible when the calculated statistic reaches maximum/minimum that exceeds the critical value of the test)

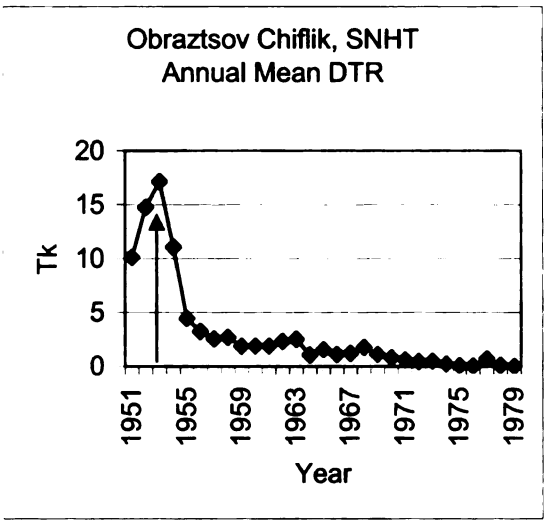

Figure 3-4 Plot of the test statistic for the SNHTest for Obraztsov Chiflick

Table 3-5 Summary table of the available homogeneous periods for the stations from the Meteorological Yearbooks

Station	Break	Homogeneous period	Number of years	% missing data
Varna	No	1951-1979	29	0
Plovdiv	No	1951-1979	29	0
Obraztsov Chiflick	1953	1953-1979	27	0
Sofia	1969	1951-1969	19	0.02%, 2 of 10585
		1970-1979	10	
Pleven	No	1951-1979	28	3.48%, 3+365 of 10585

4.4.2. Homogeneity analysis of the NCDC data

The tests were applied to the Global Summary of the Day data for 1973-2004 (1973-1999 for Pleven). The year 1996 was not considered in the analyses since data for this year was missing for all stations. Only for Pleven, all the tests indicated that the temperature series are homogeneous (Table 3-6). The null

hypothesis was rejected for the other stations for both testing variables. Based on the outcomes from the homogeneity testing Pleven was classified as being "useful" for further trend analysis, because none of the tests rejected the null hypothesis at 1% significance level. Stations Plovdiv, Varna and Sofia were categorized as being "suspect" because all four of the applied tests indicated that breaks in the temperature series exist.

Table 3-6 Summary of the homogeneity testing of the stations from NCDC, 1973-2004 (Critical values for α=0.01 are given in bold; cases with rejection of the null are underlined) Year 1996 is missing for all the stations and was not considered in the analyses.

Test	Buishand Range test		Pettit test	
Station	Abs Difference in Annual Mean DTR (Testing Variable 1)	Annual Mean DTR (Testing Variable 2)	Abs Difference in Annual Mean DTR (Testing Variable 1)	Annual Mean DTR (Testing Variable 2)
Plovdiv	1.6 < **1.7**	1.9 > **1.7**	154 > **133**	156 > **133**
Sofia	1.65 < **1.7**	2.4 > **1.7**	178 > **133**	238 > **133**
Varna	2.2 > **1.7**	2.6 > **1.7**	218 > **133**	240 > **133**
Pleven*	1.66 < **1.7**	1.6 < **1.7**	121 < **133**	95 < **133**
Test	Von Neumann Ratio Test		SNHT	
Station	Testing Variable 1	Testing Variable 2	Testing Variable 1	Testing Variable 2
Plovdiv	1 < **1.2**	1 < **1.2**	11.3 > **10.45**	10.1 < **10.45**
Sofia	1.3 > **1.2**	0.4 < **1.2**	13.3 > **10.45**	23.5 > **10.45**
Varna	0.7 < **1.2**	0.1 < **1.2**	18.2 > **10.45**	27.5 > **10.45**
Pleven*	1.5 > **1.2**	1.7 > **1.2**	6.1 < **10.45**	7.4 < **10.45**

*** The available data for Pleven covers the period 1973-1999. Year 1996 is missing and was not included in the analysis.**

Inspection of the plots of the test statistics for the "suspect" stations revealed two breaks in each data series. For Sofia, the plots of the annual mean DTR display 1989 as a break point, while the plots of the annual mean of the absolute differences of DTR point to 1981 as a break point (Figure 3-5). Both years are accepted as break points, since they have been indicated by different tests and also the years are not close enough to be considered as representing the same break. The overall period for Sofia is considered to be composed of three separate homogeneous periods of data, 1973-1981, 1982-1989, and 1990-2004, (Table 3-7), all of which were considered to be too short for the trend and extreme value analysis.

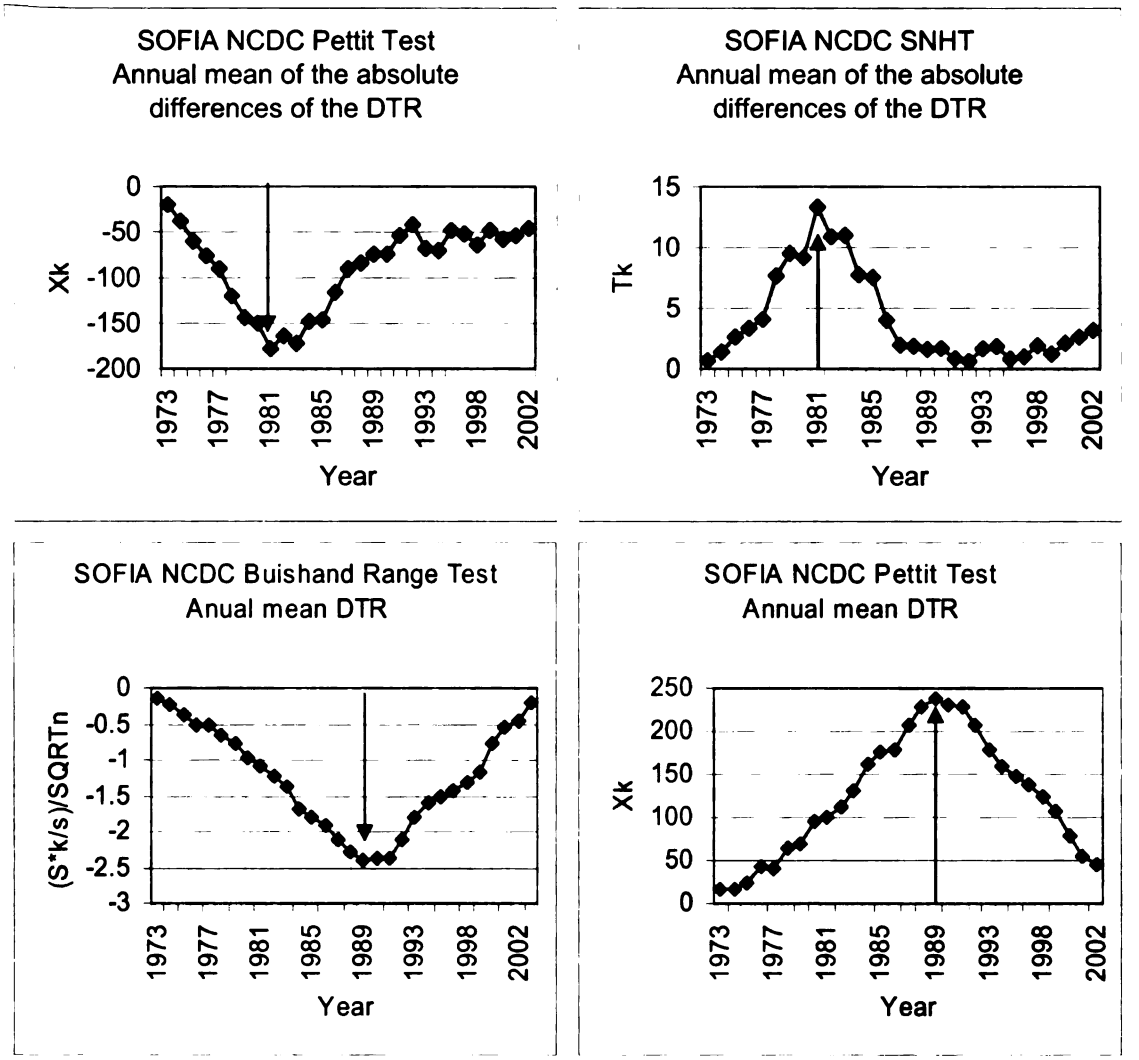

Figure 3-5 Plots of the test statistics for the different homogeneity tests, station Sofia, NCDC data

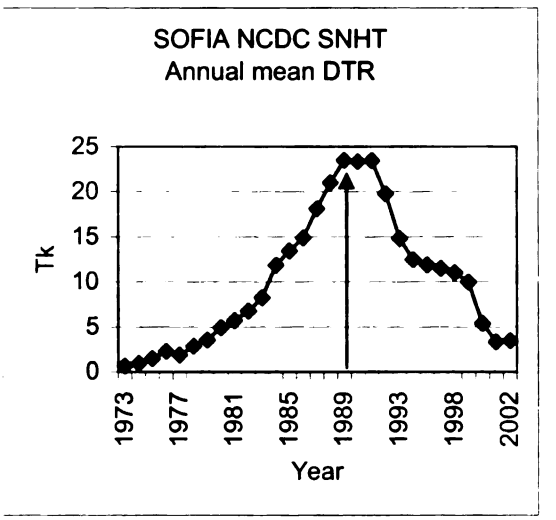

Figure 3-5 Continued

For Plovdiv, the plots of the test statistics for the annual mean absolute differences in DTR suggest a breakpoint at 1994, while plots for the test statistics calculated from annual mean DTR suggest 1988 as a break point (Figure 3-6). As for station Sofia, both years are accepted as break points. Thus, the Plovdiv record consists of three separate, relatively short sub-periods of homogeneous data (1973-1988, 1989-1994 and 1995-2004), (Table 3-7).

Varna is also characterized by two break points in the data series. The test statistics calculated from the annual means of the absolute differences in the DTR indicate a breakpoint in 1987 (Figure 3-7), whereas, the test statistics based on the annual mean DTR suggest breakpoints in 1987 and 1988 (Pettit test), 1987 and 1989-1990 (Buishand test), 1987 and 1990 (SNHTest). Given these somewhat diverging results, 1987 and 1990 were considered to be break points, and two separate homogeneous periods were determined, 1973-1987 and 1990-2004, (Table 3-7).

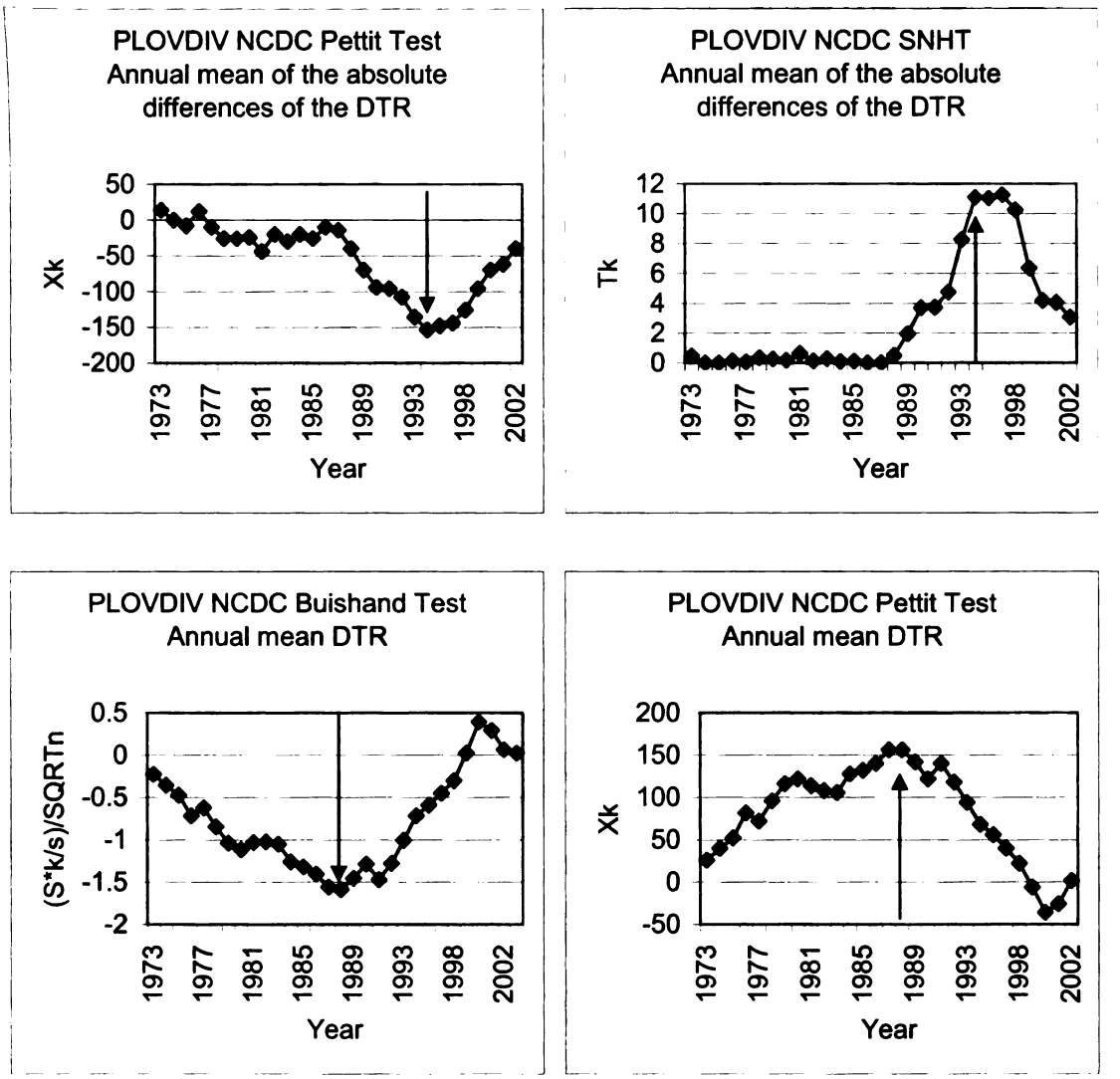

Figure 3-6 Plots of the test statistics for the different homogeneity tests, station Plovdiv, NCDC data

In conclusion, only Pleven has a somewhat long (greater than 20 years) homogeneous period of 26 years (Table 3-7). The data series for Varna, Plovdiv and Sofia are divided into quite short (less than 20 years long) homogeneous periods varying in length between 6 and 16 years.

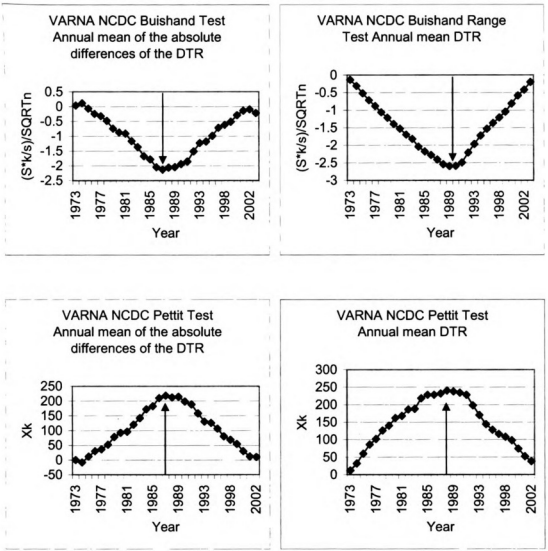

Figure 3-7 Plots of the test statistics for the different homogeneity tests, station Varna, NCDC data

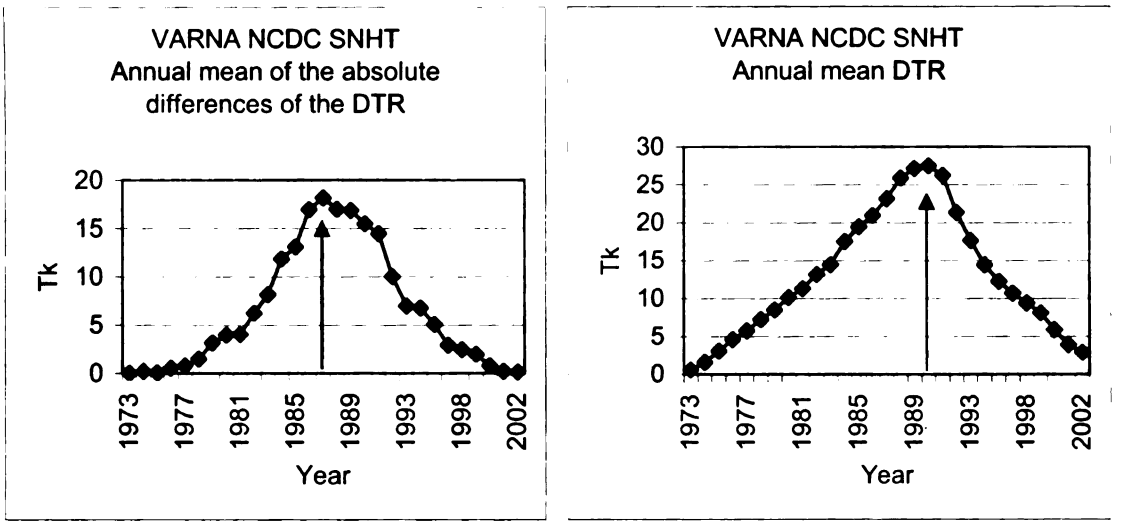

Figure 3-7 – Continued.

Table 3-7 Summary table of the available homogeneous periods for the stations from NCDC

Station	Break	Homogeneous period	Number of years	% missing data
Varna	1987, 1990	1973-1987	15	3.28%
		1990-2004	14	383 of 11680
Plovdiv	1988, 1994	1973-1988	16	3.59%
		1989-1994	6	419 of 11680
		1997-2004	8	
Sofia	1981, 1989	1973-1981	9	3.24%
		1982-1989	8	378 of 11680
		1990-2004	14	
Pleven	No	1973-1999	26	6.36% 627 of 9855

5. Spatial distribution of the stations used in the analysis

The main research question of this part of the study concerns the changes in the temperature extreme events in Bulgaria during the second half of the 20th century. The results from the homogeneity analysis indicated that four out of the five stations from the Meteorological Yearbooks, Obraztsov Chiflick, Pleven, Varna and Plovdiv, categorized as being "useful", can be used in this study. Sofia, which was classified as being "suspect", was not considered in the subsequent analyses. Due to the homogeneity issues with the obtained NCDC series, only one station, Pleven, was used for the assessment of the changes in temperature extreme events in the late period. The other three stations, Varna, Sofia and Plovdiv, obtained from the Global Summary of the Day data set, were not considered further in the analysis of the NCDC data. In summary, the set of four stations from the Yearbooks with data for 1951-1979, and Pleven from the NCDC data set with data for 1973-1999, were employed to investigate the changes in the temperature extremes in Bulgaria. The chosen periods were dictated by the data limitations, more specifically the accessibility of data and the homogeneity of the obtained temperature series. In addition, the missing observations for 1960 for Pleven and 1996 for Pleven NCDC were ignored in all the further analyses, following Katz et al. (2002). Station Pleven, obtained from the NCDC data set, is called in the subsequent analyses Pleven NCDC to distinguish it from the early period station Pleven, with data obtained from the Yearbooks.

The stations from the Meteorological Yearbooks – Obraztsov Chiflick, Varna, Plovdiv, and Pleven, are located in different areas of the country: three

are in northern Bulgaria (Pleven, Varna and Obraztsov Chiflick), one of which (Varna) is on the Black sea coast, and one (Plovdiv) is in the middle of southern Bulgaria (Figure 3-8). The spatial distribution of the meteorological stations will allow the exploration of the question whether geographical variations exist in the changes in the temperature extremes, as reflected in the observed trends and the return levels for the early period.

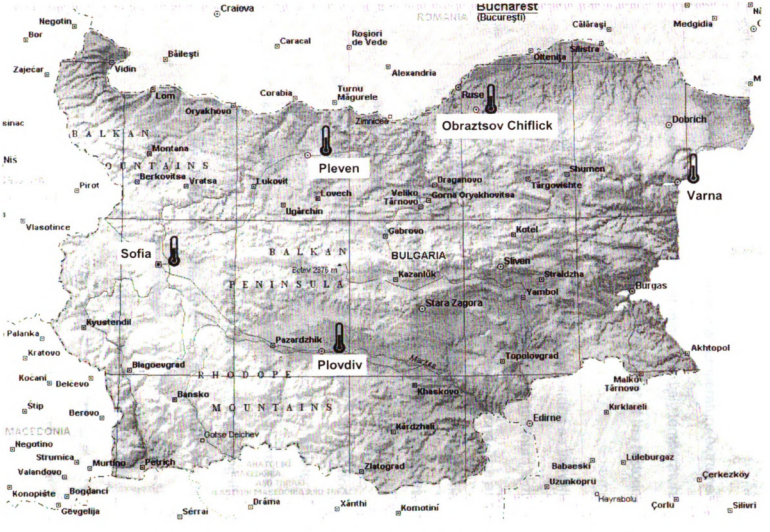

Figure 3-8 Map of the used stations, indicated with the thermometer symbol. (from http://www.bulgariancastles.com/index_pictures/bulgaria_map-01.jpg)

6. Calculation of the indices of temperature extremes

The indices of temperature extremes used in this study were defined/ calculated as follows:

a) The absolute annual and seasonal temperature extremes are the highest maximum and lowest minimum daily temperatures on annual and seasonal scales for every year of the historical period of interest at each station.

b) The diurnal temperature range was calculated as the difference between the daily values of maximum and minimum temperature for the overall historical period for all the stations. The annual and seasonal values of the DTR were analyzed, as recommended by the Workshop for Indices and Indicators of Climate Extremes (Folland et al., 1999).

c) The 5- and 10-day inter-period differences in TMAX and TMIN (centered on day 3 and day 5, respectively) were determined by subtracting from TMAX or TMIN for each day the respective long-term daily mean to obtain a daily anomaly, averaging the anomalies for non-overlapping consecutive 5- or 10-day periods using a moving window of one day; and finding the absolute values of the differences of the 5- or 10-day mean anomalies, again using a moving window of one day (similar to Folland et al., 1999). The inter-period differences were averaged by year and by season as recommended by the Workshop in Ashville (Folland et al., 1999).

d) The frost period severity was determined as the percentage of time by month for each year when daily TMIN ≤ 0°C. Although the term 'severity' is used here, following Folland et al. (1999), it does not refer to the intensity of a single frost event, but rather characterizes the overall frost period by indicating how many frost days (with TMIN ≤ 0°C) occurred per month.

e) The frost period duration was defined as the length of the period between the first and the last frost days of the year, where the year starts on August 1st and ends on July 31st.

f) The Cooling Degree Days (CDDs) are defined as follows: CDD = (Tmean – Threshold), where Tmean is the daily mean temperature calculated as the average of TMAX and TMIN, and the Threshold is widely accepted to be 18.3°C (65°F). The CDDs are accumulated per calendar year.

g) The Heating Degree Days (HDDs) are determined as follows: HDD = (Threshold – Tmean). The Tmean is again the daily mean temperature calculated as the average of TMAX and TMIN, and the Threshold is 18.3°C (65°F). The HDDs are accumulated for the year starting in July 1st, as defined by the Climate Prediction Center, http://www.cpc.ncep.noaa.gov/products/analysis_monitoring/cdus/degree_days/ddayexp.shtml).

h) The heat waves in summer were defined as periods with daily TMAX above a threshold, lasting a minimum of three days. The threshold of 30°C was used and interruptions in these periods were allowed, similar to Huth et al. (2000). More details about the acceptable interruptions within the heat waves are given in subsection 8.1.3. The duration (length in days of a heat wave), the maximum excess (highest temperature of any heat wave per year), and the number of heat waves per season were the indices used in trend analysis.

i) The cold spells in winter were defined as periods with daily TMIN below -5°C, lasting a minimum of three days. The threshold of -5°C was determined using extreme values analysis techniques for identification of thresholds, in combination with practical considerations, as explained in subsection 8.2.3.a. Interruptions were also allowed in the cold spells, as explained in subsection 8.1.4. As for the heat waves, the duration, the maximum excess (lowest temperature of any cold spell per year), and the number of cold spells were studied using trend analysis.

Several hypotheses were formulated regarding changes in the above specified indices during the early and the late periods. The absolute highest maximum temperatures on annual and seasonal scales are expected not to change or to decrease during the early period and to increase during the late

period, since the early period was regarded as being a cooler sub-period during the second half of the 20th century (Klein Tank et al., 2003), and the late period coincides to a great extent with the the warmer sub-period at the end of the century, as determined by the same authors. The absolute lowest minimum temperatures on annual and seasonal scales are anticipated to increase during the early and late periods, based on observed historical changes of these indices in Europe. The hypothesized changes in the daily maximum and minimum temperatures during the early and late periods (e.g., the expected decrease or lack of change in the daily TMAX and the increase in TMIN during 1951-1979, and the increase in both TMAX and TMIN in 1973-1999) possibly might result in a decrease in the daily temperature range (DTR) during the early period and in an increase in the DTR in the late period. The inter-period differences (IPDs) are expected to decrease, similar to the changes observed in different regions around the world (Karl et al., 1995), and also in accordance with the increase in persistence in some circulation supertypes determined in this study. In agreement with the expected changes in the daily minimum temperatures, the frost period duration is hypothesized not change or to decrease in the early period, and to decrease during the late period. Regarding the frost period severity, the expectation is that it will decrease or not change in 1951-1979 and decrease in 1973-1999. The hypotheses for the coolling and heating degree days are opposite, more specifically: in 1951-1979 the cooling degree days (CDDs) are expected to decrease and the heating degree days (HDDs) are hypothesized to increase. In 1973-1999, the CDDs are expected to increase, while the HDDs

should decrease. The frequency and duration of the heat waves are anticipated to decrease in 1951-1979 and increase during 1973-1999. In contrast, the frequency and duration of the cold spells are hypothesized to increase in the early and decrease in the late period.

7. Methods for comparison of the temperature extreme events for the early and late periods

7.1. Trend analysis

The trends of the indices of temperature extremes were evaluated based on the homogeneous data from the four stations from the early period (1951-1979) and Pleven NCDC from the late period (1973-1999). The multiple stations representing the early period allowed the examination of the spatial differentiation of the observed trends.

Some extreme temperature events were not observed every year, for example minimum temperatures below 0°C are infrequent in October at Obraztsov Chiflick, Plovdiv and Pleven. Consequently, the frost period severity for October was calculated only for these years when temperatures ≤ 0°C were recorded. The trend analysis for the frost severity in October and for some other indices was preformed using pentadal values instead of the annual values of the indices, following Changnon and Changnon (1992). The pentadal values are based on five-year consecutive non-overlapping periods. Depending on the index either pentadal averages or pentadal sums were used.

To assess the observed trends, the Mann Kendall nonparametric test for the existence of trend and Sen's nonparametric estimator of slope were applied.

As mentioned in Chapter 2, the Mann Kendall nonparametric trend test allows for missing data in the series and does not assume that the observations have a specific distribution (Gilbert, 1987). The testing procedure varies depending on the length of the series, more specifically, depending on whether the examined series comprises 40 values or less, or is longer than 40 values (Gilbert, 1987). In the latter case the normal approximation test (Gilbert, 1987, p.211) needs to be applied. Sen's (1968) method for calculation of the slope builds on a test by Theil (1950). Sen's test is not affected by the existence of missing values, outliers or gross data errors (Gilbert, 1987). The details of the Mann-Kendall test for existence of trend and of the Sen's nonparametric estimator of trend were presented in Chapter 2.

7.2. Extreme Value Analysis

In addition to the application of trend analysis, the return levels of some of the indices of temperature extremes were employed to investigate the changes in temperature extremes in Bulgaria in the early and late periods.

Two of the main approaches to extreme value (EV) analysis are the classical and the peaks-over-thresholds (POT) methods (Smith, 2003). The classical method, or also called "block maxima approach", examines the maxima of equal length blocks of data (for example, annual maxima of TMAX) (Coles, 2001; Gilleland and Katz, 2005). In contrast, the POT method focuses on exceedances over, or deficiencies below, a given threshold value (Coles, 2001;

Smith, 2003). An additional approach which combines the classical and the POT methods is the point process approach (Gilleland and Katz, 2005).

7.2.1. Classical Extreme Value analysis approach to modeling of extremes

An important assumption of the classical EV theory is that the original data are independent and identically distributed (i.e. belong to a single population) random variables (Tabony, 1983), or, stated alternatively, that the extremes are derived from samples taken from stationary stochastic processes (Zwiers and Ross, 1991). The classical EV theory explains how "for sufficiently long sequences of independent and identically distributed random variables the maxima of samples of size *n*, for large *n*, can be fitted to one of three basic families" (Palutikof et al, 1998). The three families (Gumbel, Fréchet and Weibull) were combined into one distribution by Von Mises (1936) and this single distribution is known as the Generalized Extreme Value (GEV) distribution (Palutikof et al., 1998).

The cumulative distribution function of the GEV is as follows:

$$F(x) = \begin{cases} \exp\left\{-\left[1-ky\right]^{1/k}\right\}, k \neq 0 \\ \exp\{-\exp[-(y)]\}, k = 0 \end{cases}$$

where *k* is the shape parameter which regulates the type of the EV distribution (Palutikof et al., 1998). The standardized, or also called 'reduced variate', *y*, is:

$$y = \frac{x-\beta}{\alpha}, \text{ where}$$

β is the location parameter, α is the scale parameter of the GEV distribution, and x is each value from the series of interest (Palutikof et al., 1998). The location parameter specifies where the distribution is "centered" and the scale parameter characterizes its "spread" (Katz et al., 2005). When $k > 0$, the GEV distribution is *heavy tailed* and referred to as the Fréchet distribution. In this case, the probability density function decreases at a slow rate in the upper tail (Katz et al., 2002). When $k < 0$, then the distribution has a bounded upper tail and is called a Weibull distribution. When $k = 0$ the distribution is called the Gumbel distribution, and it has an unbounded, thin tail (Katz et al., 2002) which decreases at a relatively rapid (i.e., exponential) rate (Katz et al., 2005).

The classical method can be applied not only to period maxima (e.g., annual or seasonal), but also to period minima. In order to apply the same distributions to the period minima, the data are transformed by multiplying the original series by -1.

7.2.2. Peaks-over-Threshold approach to modeling of extremes

A disadvantage of the classical method is that it relies on only one extreme value per period (e.g. year), hence the information contained in the second, third, etc. maxima for the period is lost. This inefficient use of the information (Smith, 2003) can be remedied by the application of the peaks-over-thresholds (POT) approach. The threshold methods are more flexible than the block maxima approach, because they use the data more efficiently and they can be extended to describe how the extremes of a variable depend on other

variables (Smith, 2003).The POT method, in its simplest form, models the "occurrence of peaks by a Poisson process and the magnitude by exponential random variables" (Zwiers and Ross, 1991). A more recent approach is to use the Generalized Pareto distribution to model the magnitudes of the peaks over a threshold. The GP distribution "is the analog for threshold exceedances of the GEV distribution for annual maxima" (Smith, 2003). One of the foci of this part of the analysis is the behavior of the exceedances over, or deficiencies below, a given threshold (i.e. the magnitudes of the peaks) of the daily TMAX or TMIN. Thus, the magnitudes of the peaks were modeled using the Generalized Pareto (GP) distribution in this study.

If one considers the intensity of an extreme event, or the "excess", Y, over a threshold u, $Y = X - u$, where X is the value of the extreme event, the distribution of the excess should have an approximate Generalized Pareto (GP) distribution for a sufficiently high threshold (Katz et al., 2005, Pickands, 1975). The GP has a cumulative distribution function $F(x)$ as follows:

$$F(x) = 1 - [1 - \frac{k}{\alpha}(x - \xi)]^{1/k},$$

where k is the shape parameter, α is the scale parameter, x are the values of the random variable being modeled, ξ is the chosen threshold. As for the GEV distribution, the scale parameter is representative of the spread of the distribution. The shape parameter determines three types of GP distributions. When $\xi = 0$, the distribution is light-tailed, and is called exponential distribution; when $\xi > 0$, the distribution is heavy-tailed, and is called Pareto distribution; and when $\xi < 0$, the distribution is bounded, and is called beta distribution.

Caution needs to be exercised when determining the thresholds for the GP distribution. If the threshold is too low the parameter estimates will be biased because data outside of the tails of the parent distribution will be included. However, a threshold that is too high will result in high variance of the parameter estimates (Gilleland and Katz, 2005). In other words, a trade-off exists between choosing a threshold high enough to ensure that the GP approximation is valid, but not so high that the number of exceedances will be too small for accurate estimation of the parameters (Katz, et al., 2005). In this study two graphical approaches for the choice of an appropriate threshold were used:

a. a Mean Residual Life plot (Figure 3-9), also called Mean Excess Function or Conditional Mean Exceedances graph (Palutikof et al., 1998), which depicts the mean excess values (averages of all the excesses per threshold) of the variable for numerous thresholds (Gilleland and Katz, 2005);
b. a plot of the estimated parameters of the GP distribution (GPD) fitted over multiple thresholds (Figure 3-10). This second approach allows the stability of the parameter estimates of the GPD to be assessed for different thresholds.

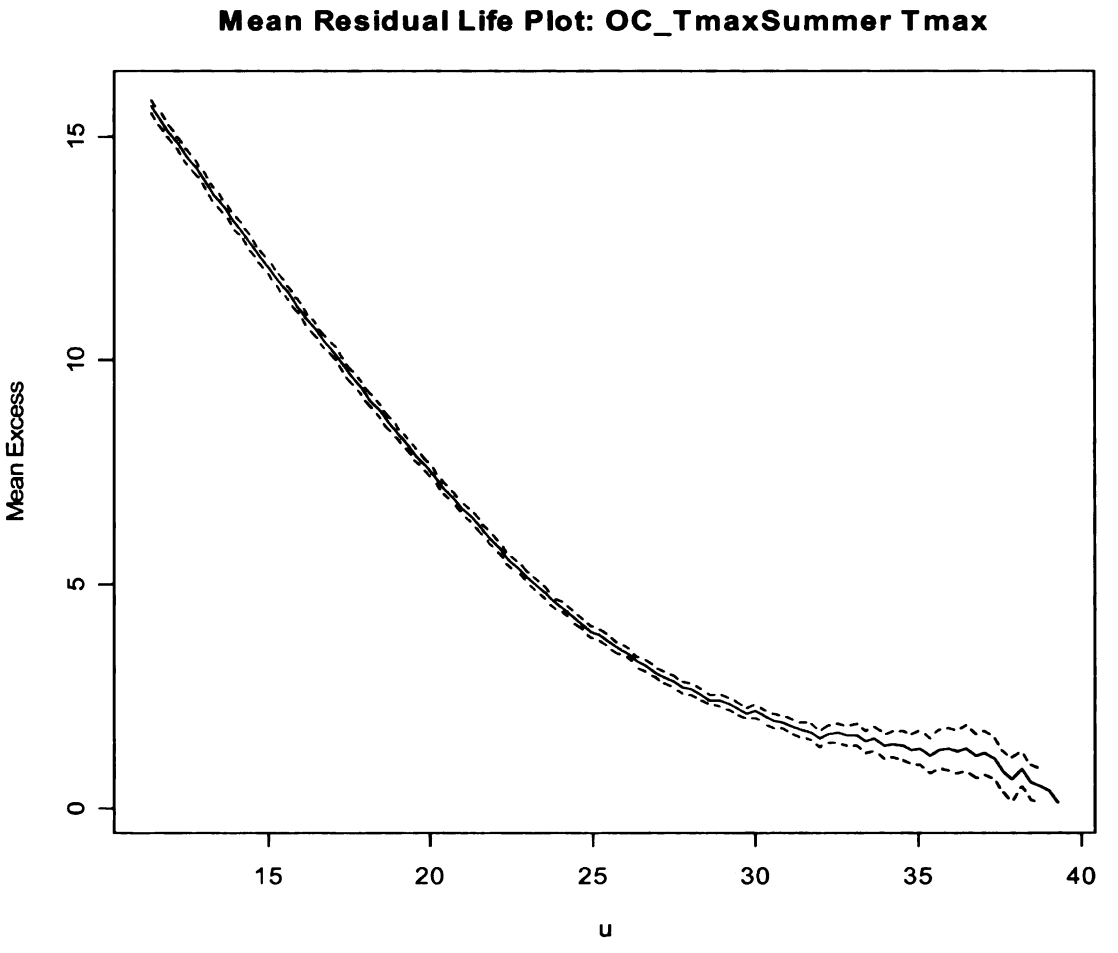

Figure 3-9 Mean Residual Life Plot for Obraztsov Chiflick, Summer TMAX 1953-1979. (Thresholds (u) are plotted versus mean temperature excess (°C) over these thresholds; the dashed lines represent the 95% confidence interval)

When using the Mean Residual Life Plot, one needs to determine the lowest point on the curve, below which the curve becomes more horizontal and the confidence interval starts to broaden (Palutikof et al., 1998, Gilleland and Katz, 2005), or in other words, one needs to find the flex point after which the curve almost levels off. The threshold corresponding to the respective flex point is used in the subsequent extreme value analysis of the exceedances over the determined threshold or of deficiencies below the determined threshold. In this

example (Figure 3-9) for summer maximum temperatures at Obraztsov Chiflick, a threshold (u) of 32°C seems appropriate because it corresponds to the flex point on the mean residual life curve where the curve becomes flatter. In addition, the confidence interval widens at higher temperature thresholds.

The example (Figure 3-10) of the second type of plot used to determine an appropriate threshold displays the shape and modified scale parameters plotted against 50 thresholds varying between 25°C and 35°C for Obraztsov Chiflick. The goal is to find a threshold corresponding to a point after which the parameters just vary around a certain level. In the case of Obraztsov Chiflick, 32°C again seems as a good threshold, because the parameter values do not change much after 32°C, but simply fluctuate around that level. Moreover, the uncertainty of the estimated parameters, as represented by the 95% confidence interval bars, is less at 32 °C and increases rapidly at larger thresholds.

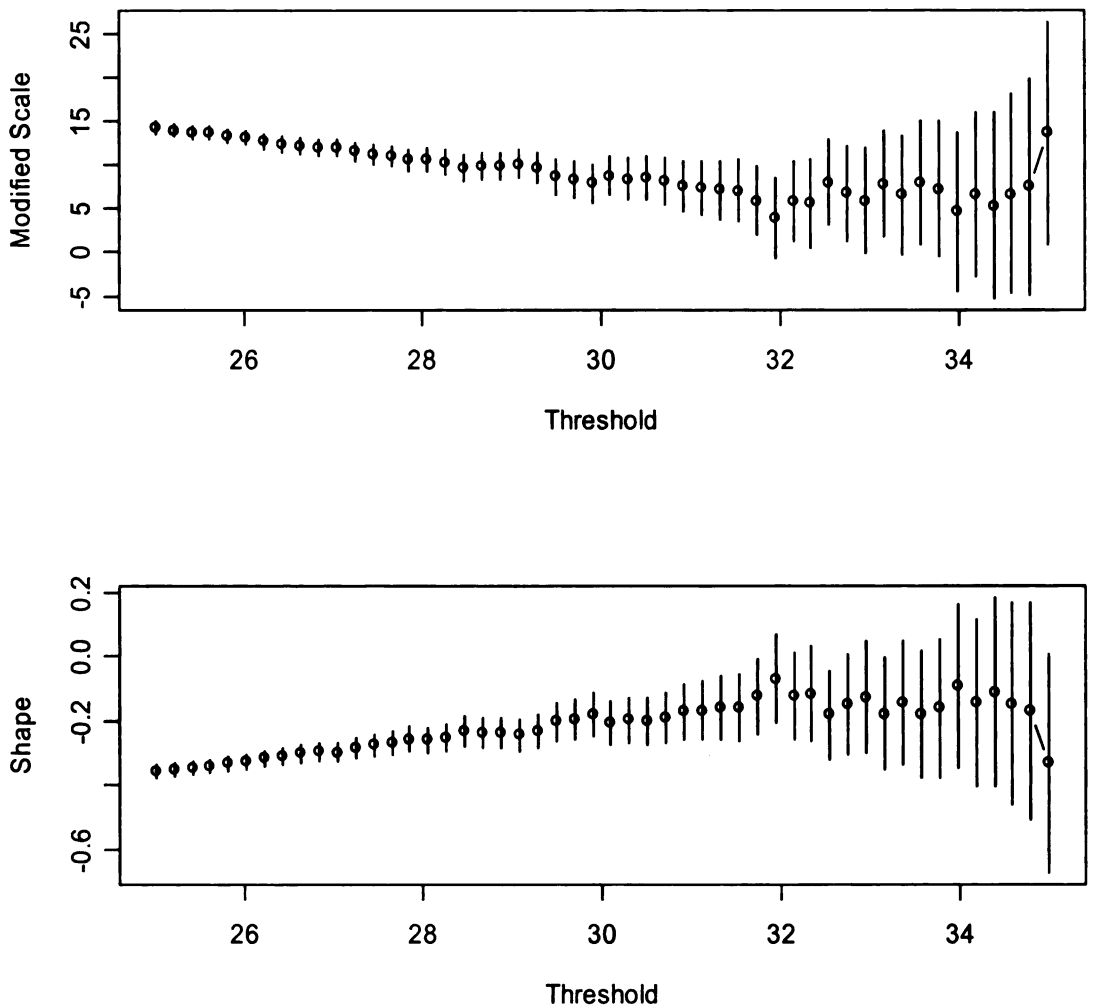

Figure 3-10 GPD fits for a range of 50 thresholds from 25°C to 35°C for Obraztsov Chiflick summer TMAX (the bars represent the 95% confidence interval)

7.2.3. Methods for parameter estimation

Several methods exist for estimating the parameters of a given statistical distribution including the method of moments, the maximum likelihood (ML) method, and the probability weighted moments (PWM, also called the L-moments). The ML method is considered to be the most powerful for parameter

estimation, especially for large samples (Smith, 2003). As Palutikof et al. (1998) state, "inefficiencies in determining model parameters and arbitrary choice of statistical model" can give rise to uncertainty in the model parameters and return levels estimation. In relation to this statement, an additional important advantage of the ML method is that standard errors of the parameters of the distribution and the return levels can be easily produced, allowing for the assessment of the uncertainty of the model fit and of the return level estimates (Katz et al., 2002). Some authors (for example, Hosking, 1990) have argued that the L-moments method is superior to ML estimates for small samples. A disadvantage of the L-moments, however, is that, the L-moments parameter estimation is not always feasible (Chen and Balakrishnan, 1995; Dupuis, 1996).

The temperature series used in this analysis are longer than 25 years, which is the cutoff value according to Katz et al. (2002) below which the performance of the ML method can be very erratic. Thus, ML estimation of the model parameters was performed in this study, which also allowed the estimation of the uncertainty of the modeling.

7.2.4. Assessment of goodness-of-fit of the model to the empirical distribution

The goodness of fit of a model to the empirical distribution usually can be inferred by applying formal statistical testing or by evaluating the plots of the modeled and empirical probability and quantile distributions. Since the GEV and the GP distributions are described by a shape parameter in addition to the scale parameter, it is not appropriate to use standard goodness-of-fit tests, such as the Kolmogorov-Smirnov test (Gilleland, 2007, personal communication). Davison

and Smith (1990), because of the lack of tests for goodness-of-fit for the GP distribution, used the renormalized Kolmogorov-Smirnov and Anderson-Darling statistics to test only the exponentiality of the empirical data. However, the authors added that it was "suspect" to use 5% critical points for the exponential distribution in order to compare the calculated test statistics, since the exponential distribution is only a sub-model of the GP distribution, and the "true critical points are smaller" (Davison and Smith, 1990). Choulakian and Stephens (2001) presented goodness-of-fit tests for the generalized Pareto distribution based on the Cramér-von Mises W^2 and the Anderson-Darling A^2 statistics. These tests, however, are appropriate only if the threshold is high enough that only about two cases per year exceed it (Choulakian, 2007, personal communication).

Given the limitations of the tests available for the assessment of the goodness-of-fit of GEV and GP distributions, the goodness-of-fit of the models to the empirical distributions was assessed graphically from probability and quantile plots (Figure 3-11). If a sample of ordered independent observations, X_i, from a population with estimated distribution function, $\hat{F}$, is given:

$$X_{(1)} \leq X_{(2)} \leq \ldots \leq X_{(n)},$$

where n is the total number of observations, the *probability plot*, is based on all points

$$\left\{\left(\hat{F}(x_{(i)}), \frac{i}{n+1}\right) : i = 1, \ldots, n\right\}.$$

If $\hat{F}$ is a reasonable model for the population distribution, the points will lie close to the unit diagonal (Coles, 2001).

The *quantile plot,* consist of all the points

$$\{(\hat{F}^{-1}(\frac{i}{n+1}), x_{(i)}) : i = 1,..., n\}$$

Again the points will lie along the unit diagonal, if $\hat{F}$ is a reasonable estimate of the population distribution (Coles, 2001). The probability and quantile plots represent basically the same information but on different scales (Coles, 2001), which allows for a better judgment of the goodness-of-fit. Large deviations from the straight line are indicative of a departure from the theoretical distribution. The plots, obtained for the GEV and GP model fit to the series in this analysis, were compared to the example plots in the textbook by Coles (2001), in order to create a framework for the goodness of fit assessment. Based on the evaluation criteria employed by Coles, the model fit was classified as: 'good', 'acceptable' and 'poor'. In the example of the probability and quantile plots for the annual highest daily TMAX for Plovdiv (Figure 3-11), both plots suggest a 'good' fit of the empirical data by the GEV distribution because the data points follow very well the unit diagonal.

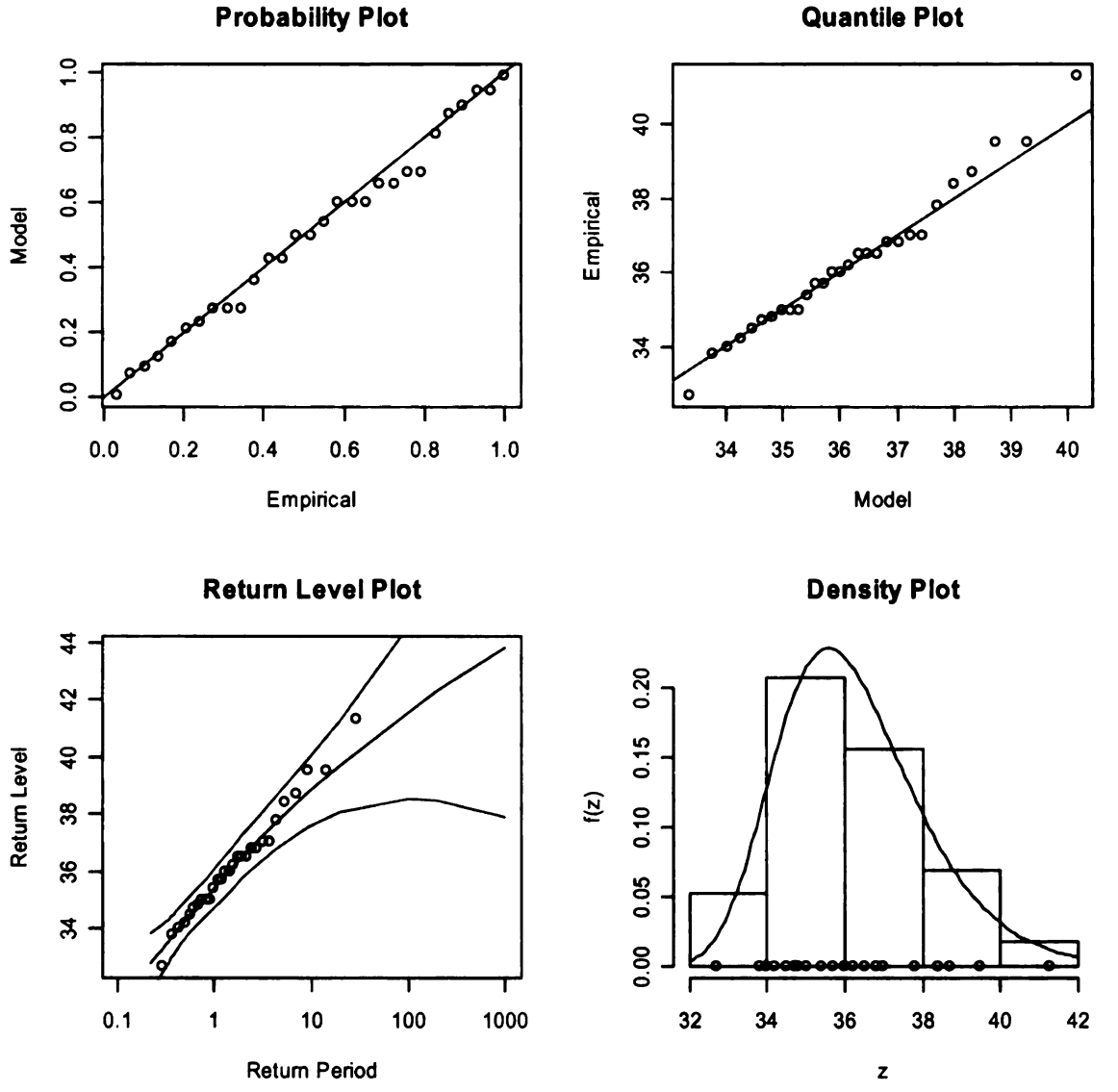

Figure 3-11 Plots for the GEV fit of the annual highest daily TMAX for Plovdiv, 1951-1979

In the next plot for Varna (Figure 3-12), there are some areas of underestimation or overestimation of the empirical data by the model, however, a reasonable linearity is still evident and the return level points all lie within the confidence interval limits. This example was classified as being 'acceptable'.

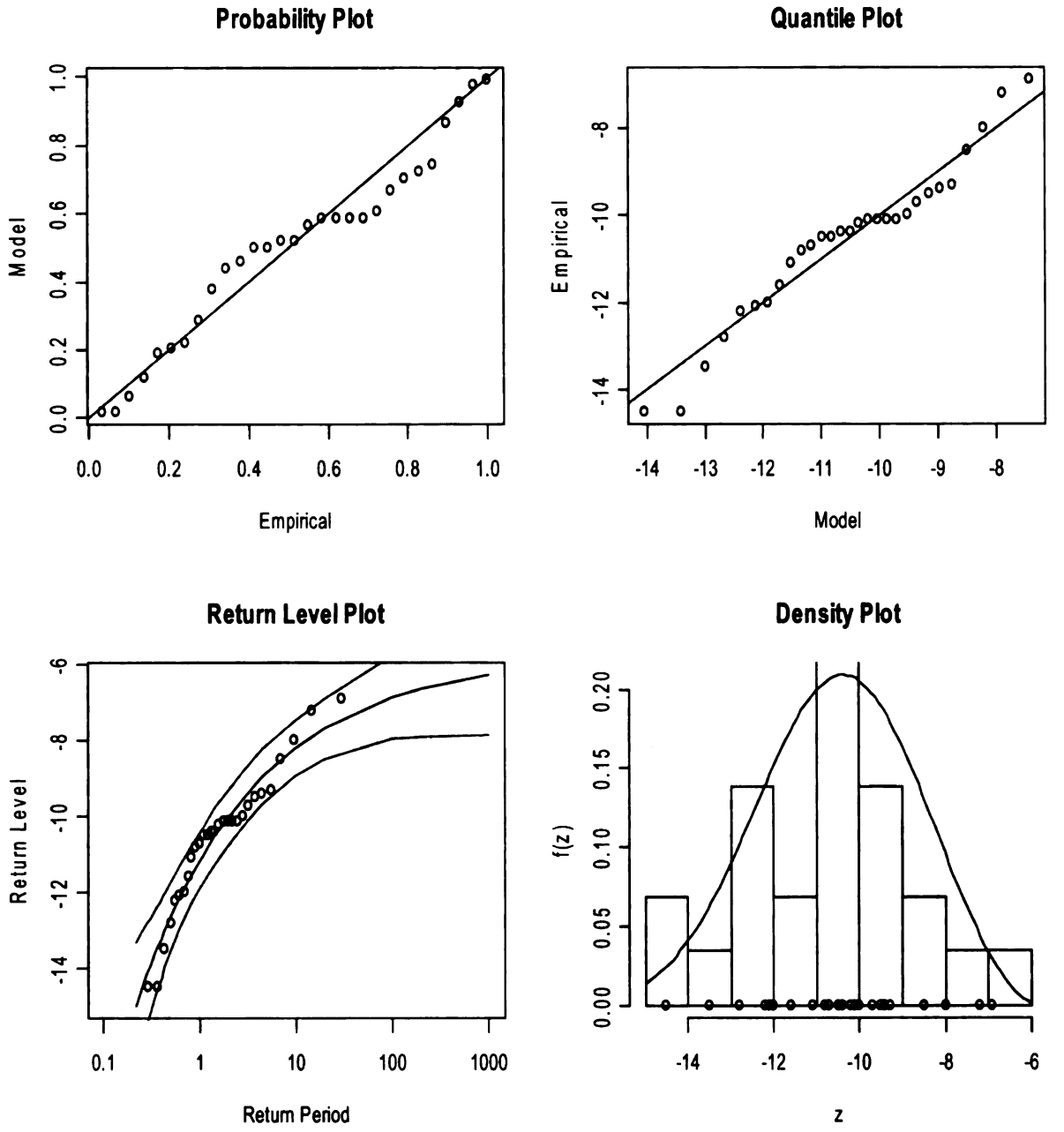

Figure 3-12 Plots of the GEV fit of the summer lowest daily TMIN temperature for Varna, 1951-1979.

The last set of plots (Figure 3-13) illustrates a 'poor' fit of the model to the empirical data. The example is for winter lowest minimum daily temperatures at Pleven NCDC. The probability and quantile plots reveal a deviation in the middle of the data range from the optimal line of correspondence between the

theoretical and the empirical distribution. Also, the estimate of the probability density distribution does not fit well the histogram of the data, as presented in the density plot.

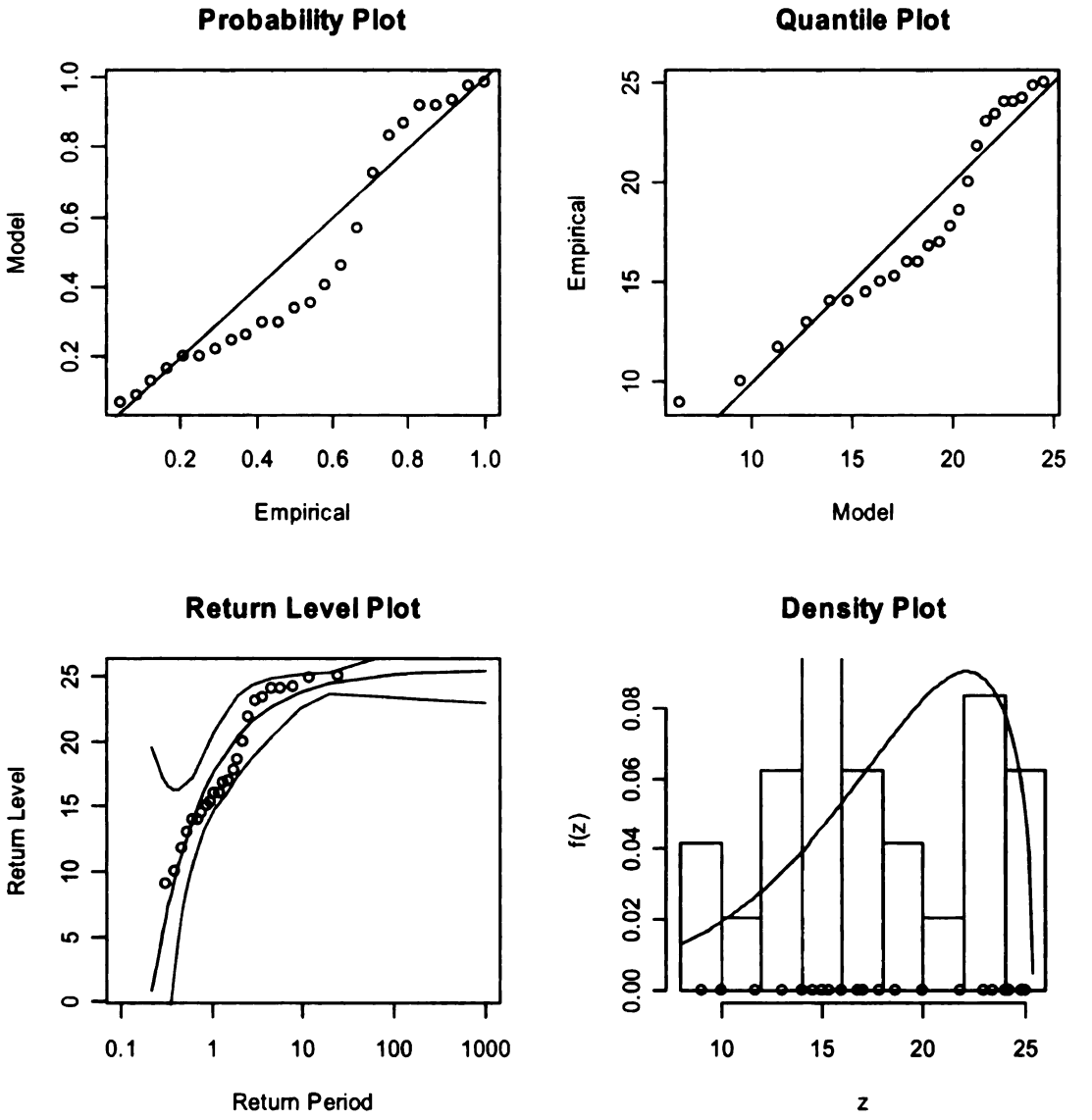

Figure 3-13 Plots of the GEV fit of the winter lowest daily TMIN for Pleven NCDC, 1973-1999.

7.2.5. Other considerations in EV analysis

7.2.5. a. Seasonality

Seasonality or cyclo-stationarity[9] interferes with the assumptions of the EV analysis (Palutikof et al., 1998). It is often the case that a climate variable has a considerable annual cycle, and that consequently, the annual maximums will be observed at about the same time each year. Thus, the annual maximums are actually drawn from smaller sub samples of only two or three months, rather than from the 365 daily values of the year. Hence, it is argued that the observed variability in the annual extremes reflects the variability only in these months (Zwiers and Ross, 1991). One option, as recommended by Palutikof et al. (1998), is to perform the EV analysis on the extreme events by season, rather than on annual extremes. Thus, this study considered both, annual and seasonal temperature extremes.

7.2.5 .b. Non-stationarity

Potential non-stationarity[10] of the temperature series (i.e. an existing trend in the series or error that causes non-homogeneities) will also affect the appropriateness of EV theory. To avoid the influence of potential non-stationarity in the series, Palutikof et al. (1998) recommend the use of only the homogeneous portions of a time series. Another potential solution is to filter the series using a high-pass filter to remove any trend (Zwiers and Ross, 1991).

---

[9] Cyclo-stationary processes have mean, variance and covariance that are cyclic with period one year (Zwiers and Kharin, 1998; Huang and North, 1996). "Most climate parameters that are sampled more frequently than one per year are non-stationary but cyclo-stationary, because of the seasonal forcing of the climate system" (Zwiers and von Storch, 1999).

[10] Stationary process is a stochastic process with properties that do not change over time or space (AMS Glossary). Non-stationarity refers "to interannual fluctuations due either to natural causes (for example, a trend towards higher temperatures caused by climate change) or to human intervention or error (change in instrument type, faulty instrumentation or poor exposure)" (Palutikof et al., 1998).

Some violations of the assumptions of EV, however, are allowable without negatively impacting the analysis. Leadbetter et al. (1983), as summarized in Zwiers and von Storch (1999), showed "that the independence assumption can be substantially relaxed" and that "the same asymptotic results obtained in the classical setting are obtainable when extremes are those of samples taken from a weakly stationary, ergodic[11] time series". In this study, periods of homogeneous data were determined for each station (described earlier) and extreme value analysis was applied only to those periods. Trends were not removed given that weak trends do not appear to have large influence on the analysis.

In summary, the GEV distribution was employed to model the absolute highest TMAX and lowest TMIN on an annual and seasonal scale. In addition, the POT approach was used to model the excesses over or below pre-determined thresholds in order to obtain return levels for several temperature indices at four stations in Bulgaria. The return levels from two consecutive periods (1951-1979 and 1973-1999) were compared to assess the changes in the indices of temperature extremes.

7.2.6. Details of the practical application of the EV analysis in this study

The software utilized in this study was the interactive toolkit extRemes (Gilleland and Katz, 2005), which operates within the R statistical programming language. This interactive program allows one to fit GEV, GP distribution, Poisson process or Point Process to a given time series. The program supplies

[11] Ergodic – A system in which the time mean of every measurable function of the system equals its space mean. (AMS Glossary)

maximum-likelihood estimates of the parameters of the distributions. To assess the uncertainty of the model fit, standard errors of the parameters are obtained also using the program. The toolkit provides a set of four plots: a probability plot, a quantile plot, a return level versus return period plot and a probability density plot (as shown in Figure 3-11), which are used to assess the goodness-of-fit of the model to the empirical distribution.

The extreme upper quantiles of the GEV and GP distributions, or the return levels, are estimated by the program. Given the limited length (only about 30 values) of the time series in this study, only return levels for 10, 20 and 50 year return periods were considered. The toolkit allows the assessment of the (1 – α) % confidence intervals of the return levels. The confidence intervals width represents the uncertainty of the estimated parameters, in this case the return levels. A very wide interval might indicate that more data are needed for a more accurate assessment of the return levels (Easton and McColl, 1997). In order to evaluate whether the estimated confidence intervals are 'correctly' determined (categorization given by Gilleland and Katz, 2005), the extRemes toolkit supplies profile likelihood plots. An example of a profile likelihood plot is given in Figure 3-14. According to Gilleland and Katz (2005), the confidence limits are 'correct' if the dashed vertical lines (representing the lower and upper confidence limits), the profile likelihood line (the curved line) and the lower horizontal line on the profile-likelihood plots, all intersect exactly at the same points. In this study, the 95% confidence limits of the return levels were estimated using the profile likelihood plots.

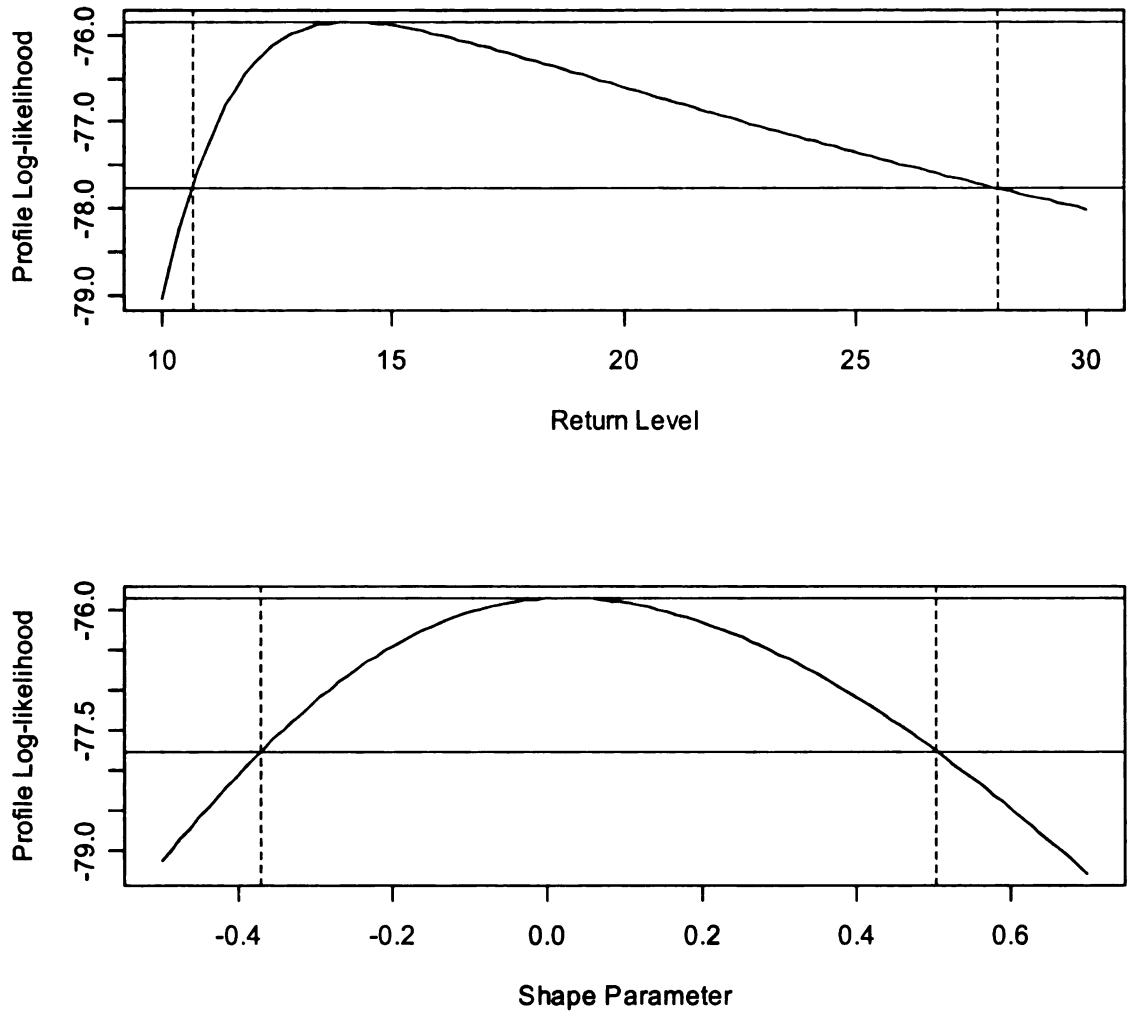

Figure 3-14 Profile likelihood plots for the 20-year return level (in °C) and shape parameter (ξ) of the GEV distribution fit for FALL lowest daily TMIN for Obaztsov Chiflick, 1953-1979

8. Comparison of the changes in temperature extreme events between the early and late periods

8.1. Trend Analysis results by index

8.1.1. Changes in the annual and seasonal highest maximum and lowest minimum temperatures and the daily temperature range

During the early period (1951-1979), the highest daily maximum temperature either does not change or decreases. The series of highest annual and seasonal maximum daily temperatures at Varna and Obraztsov Chiflick do not display significant trends (Table 3-8). Except for the fall season, the two interior stations (Pleven and Plovdiv) also do not feature trends in the highest maximum temperatures for the year and for the seasons (Figure 3-15). A significant decrease in the highest daily temperatures, of -1.2°C/decade at Pleven and -1.4°C/decade at Plovdiv, is seen for fall.

On a seasonal scale, changes during 1951-1979 in the lowest daily minimum temperatures are evident only for spring when all stations have positive trends (Figure 3-16) varying between 2.2°C/decade at Obraztsov Chiflick and 1.4°C/decade at Varna and Pleven. At two of the stations, Obraztsov Chiflick and Plovdiv, the annual lowest minimum temperatures also warm up significantly in 1951-1979 (Figure 3-17, Table 3-8). The disparity in the observed trends at the different stations could be due to local site factors or undetected inhomogeneities.

Table 3-8 Summary table for the existence and magnitude of trends (°C/decade) (*Yes/No* means that trend is significant at α=0.05, and not at α=0.01; *Yes* means that trend is significant at both levels of significance; *No* means that there is no significant trend)

Index/Station Period	**Obraztsov Chiflick** 1953-1979	**Plovdiv** 1951-1979	**Varna** 1951-1979	**Pleven*** 1951-1979	**Pleven NCDC**** 1973-1999
Highest Tmax (°C) Annual	No	No	No	No	No
Winter	No	No	No	No	**Yes/No** 1.4
Spring	No	No	No	No	**Yes/No** 1.1
Summer	No	No	No	No	No
Fall	No	**Yes** -1.4	No	**Yes/No** -1.2	No
Lowest Tmin (°C) Annual	**Yes** 1.5	**Yes/No** 2.3	No	No	No
Winter	No	No	No	No	No
Spring	**Yes/No** 2.2	**Yes/No** 1.6	**Yes/No** 1.4	**Yes/No** 1.4	No
Summer	No	No	No	No	No
Fall	No	No	No	No	No
DTR (°C) Annual	No	**Yes** -0.3	No	**Yes/No** -0.3	**Yes/No** 0.6
Winter	No	No	No	No	**Yes/No** 0.9
Spring	No	No	**Yes/No** 0.3	No	No
Summer	No	**Yes** -1	No	**Yes** -0.8	**Yes** 0.8
Fall	No	No	No	No	No

*** 1960 is missing, ** 1996 is missing**

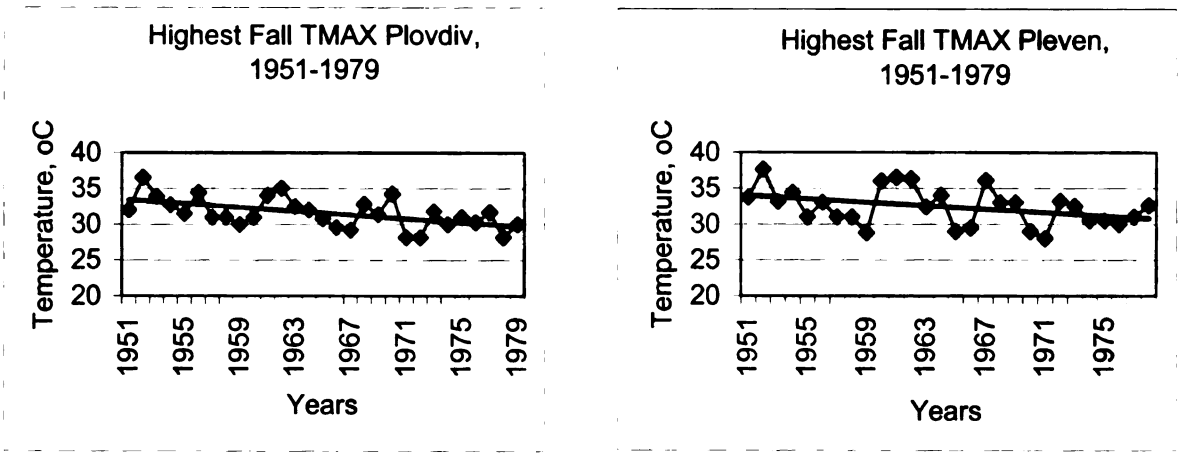

Figure 3-15 Changes in fall highest daily maximum temperatures (°C) for stations Plovdiv and Pleven, 1951-1979

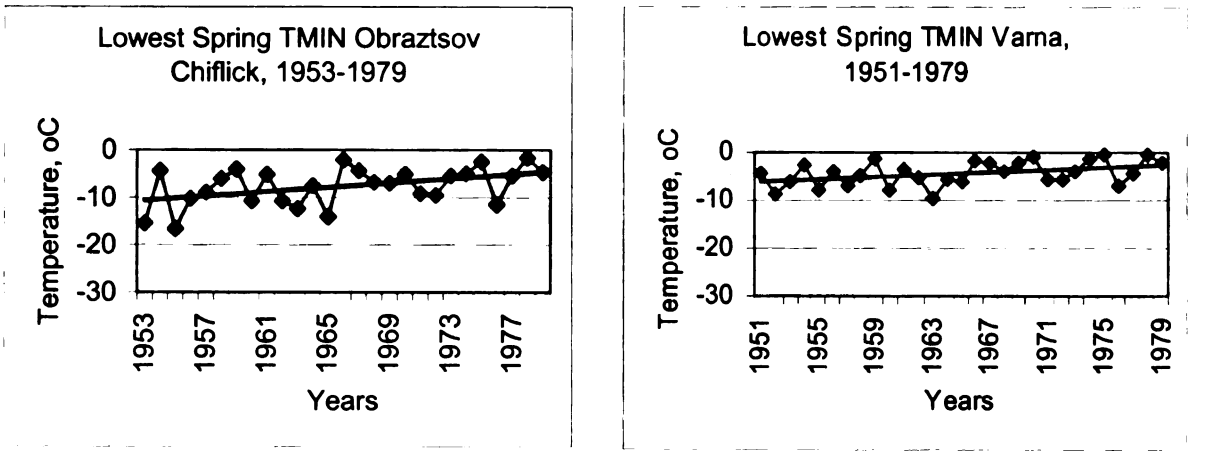

Figure 3-16 Changes in spring lowest daily minimum temperatures (°C) for all stations, 1951-1979

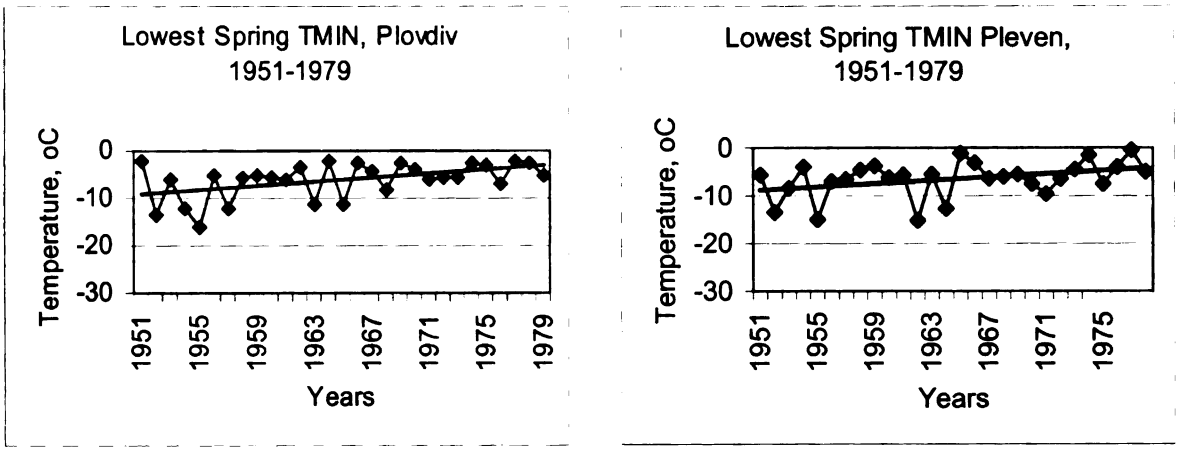

Figure 3-16 Continued.

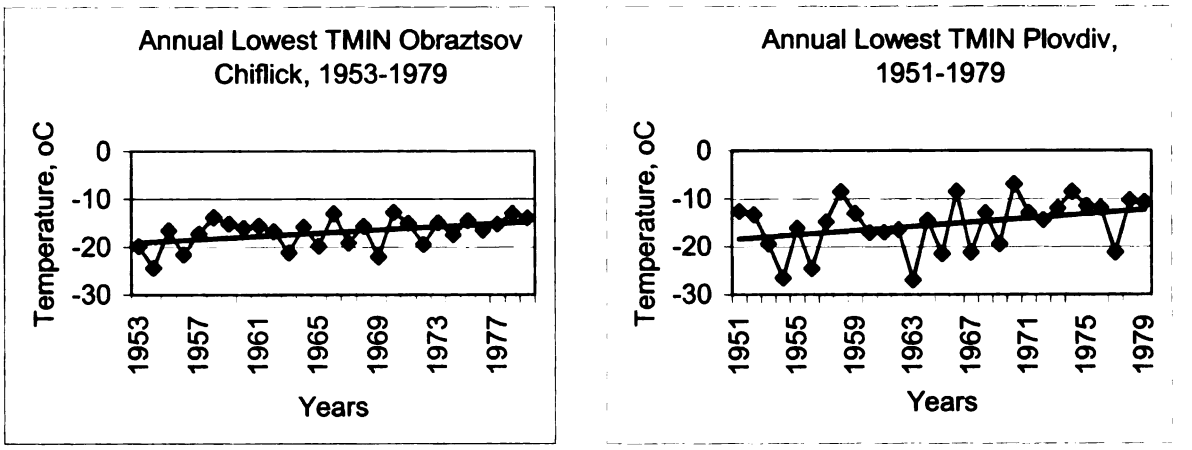

Figure 3-17 Changes in annual lowest daily minimum temperatures (°C) for Obraztsov Chiflick and Plovdiv, 1951-1979

Compared to Pleven, the results for Pleven NCDC indicate an increase in the winter (1.4°C/decade) and spring (1.1°C/decade) highest daily maximum temperatures during 1973-1999 (Figure 3-18). The lowest minimum daily temperature does not display any trends on annual or seasonal scales. The trend results for Pleven NCDC need to be considered with caution since a large percentage of the data was missing (6.36%, 627 days of 9855).

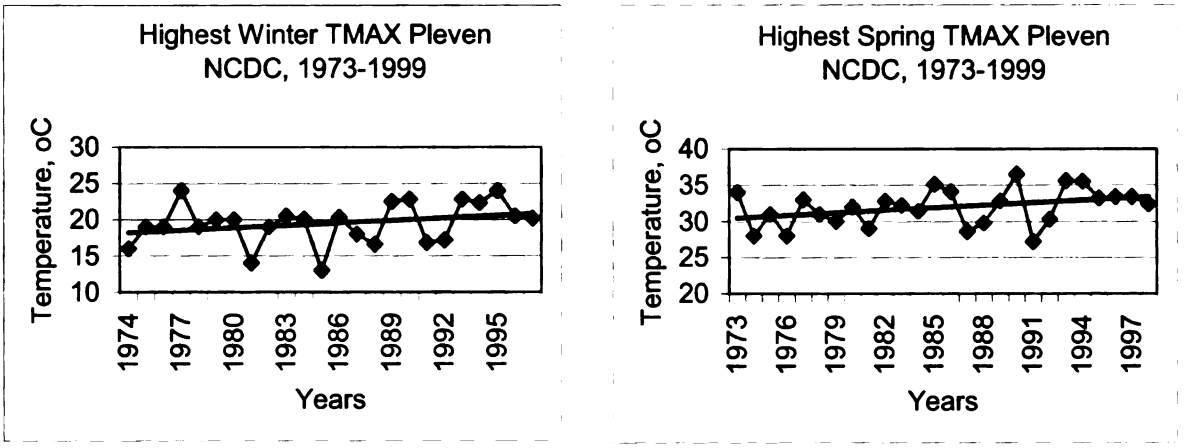

Figure 3-18 Changes in winter and spring highest daily maximum temperatures (°C) for Pleven NCDC, 1973-1999

All stations from the early period, except for Obraztsov Chiflick, are characterized by changes in the mean annual or seasonal DTR. Varna, located on the Black sea coast, displays an increasing trend of 0.3°C/decade during spring (Figure 3-19), and the two interior stations exhibit a decreasing annual (-0.3°C/decade for Plovdiv and Pleven) and summer (-1°C/decade for Plovdiv and -0.8°C/decade for Pleven) DTR (Table 3-8).

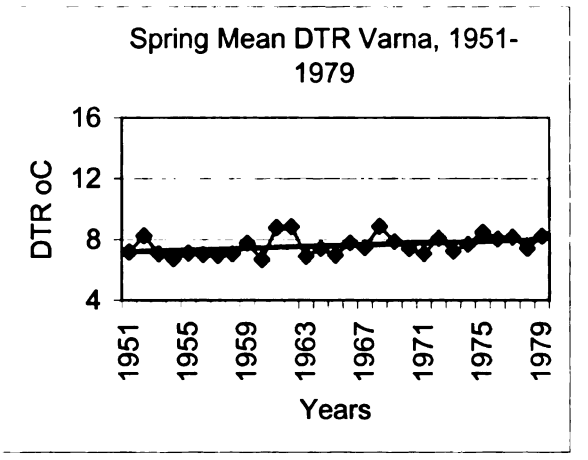

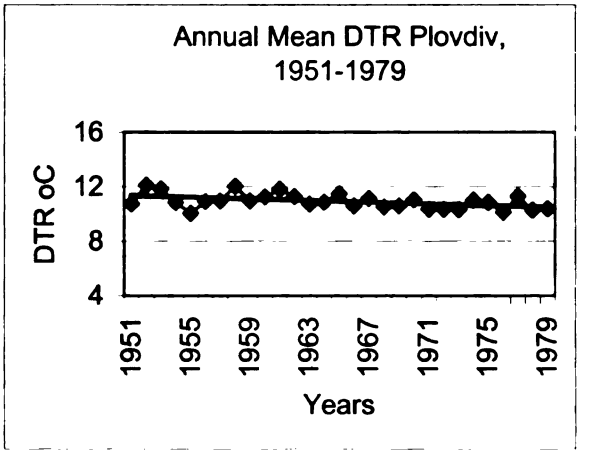

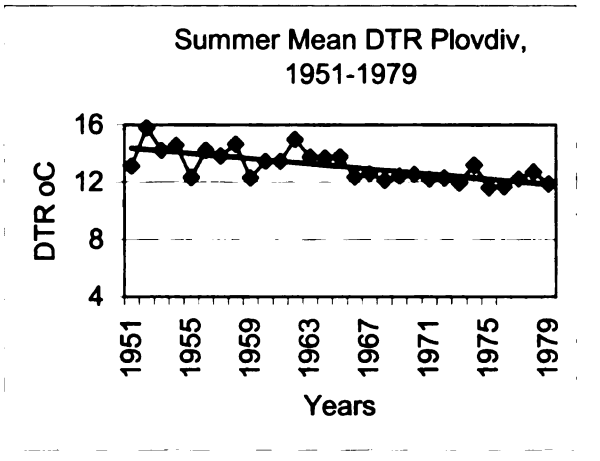

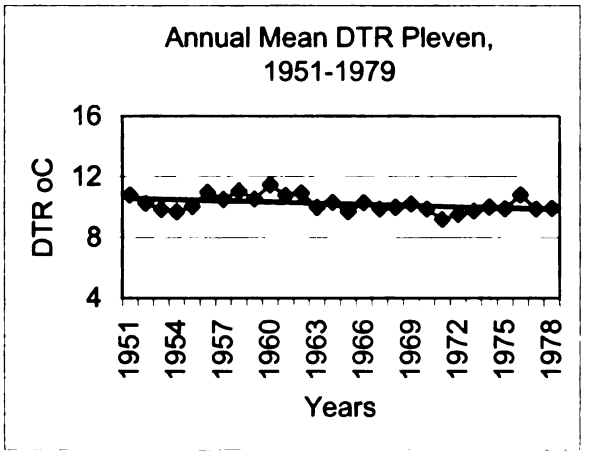

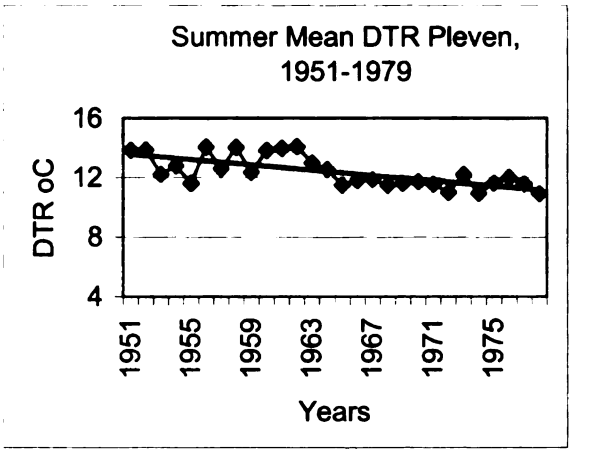

Figure 3-19 Changes in annual or seasonal DTR for Varna, Plovdiv and Pleven , 1951-1979

In contrast to the results for Pleven, Pleven NCDC is characterized by significant increasing trends of the mean annual and summer (0.6°C/decade and 0.8°C/decade respectively) DTR (Figure 3-20, Table 3-8). In addition, a significant positive trend for Pleven NCDC is evident also for the winter season (0.9°C/decade).

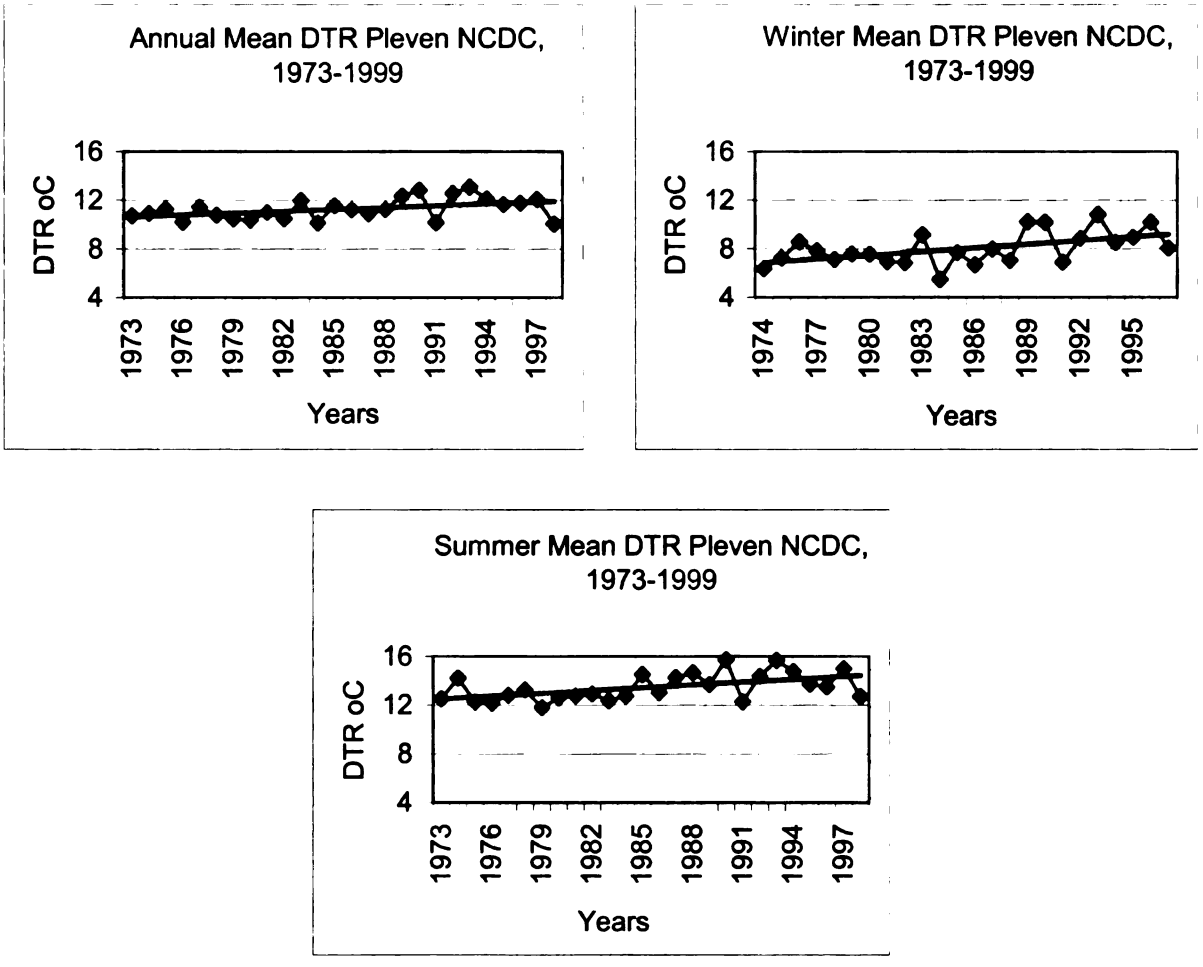

Figure 3-20 Changes in the annual, winter and summer DTR for Pleven NCDC, 1973-1999

8.1.2. Changes in the annual and seasonal 5- and 10-day inter-period differences (IPD) for TMAX and TMIN

In addition to the DTR, the inter-period differences (IPDs) of TMAX and TMIN represent the variability of the temperature series. Higher differences indicate larger variability, and lower differences suggest less variability and more stagnant thermal conditions at a location. The results from this analysis are presented only in tabular form.

There is no consistency in the trend results for any index/season combination across the stations. The 1951-1979 period is characterized, in general, by the lack of significant trends for the TMAX and TMIN IPDs (Table 3-9). A decrease in variability of the maximum and/or minimum temperature, based on some of the IPD indices, is evident on an annual basis at Plovdiv and Obraztsov Chiflick, and also on a seasonal basis for the winter and spring seasons at Obraztsov Chiflick, Plovdiv and Varna. The summer season, in general, does not display any trends. Fall is also characterized by no trends in maximum or minimum temperature variability.

While station Pleven does not exhibit any changes in the inter-period differences, Pleven NCDC indicates an increase in TMIN variability during the late period in winter and spring, based on some of the indices (Table 3-9). The results are to be regarded cautiously, however, due to the large amount of missing data at Pleven NCDC.

Table 3-9 Summary table for the existence and magnitude of trends in TMAX and TMIN inter-period differences (°C/decade)
(Yes/No means that trend is significant at α=0.05, and not at α=0.01; Yes means that trend is significant at both levels of significance)
*** 1960 is missing, ** 1996 is missing**

Index/Station Period	**Obraztsov Chiflick** 1953-1979	**Plovdiv** 1951-1979	**Varna** 1951-1979	**Pleven*** 1951-1979	**Pleven NCDC**** 1973-1999
5-day IPD TMAX (°C) Annual	No	No	No	No	No
Winter	**Yes/No** -0.4	No	No	No	No
Spring	No	No	**Yes/No** -0.2	No	No
Summer	No	No	No	No	No
Fall	No	No	No	No	No
5-day IPD TMIN (°C) Annual	No	**Yes/No** -0.1	No	No	No
Winter	No	No	No	No	No
Spring	**Yes/No** -0.3	**Yes/No** -0.1	No	No	**Yes/No** 0.2
Summer	No	No	No	No	No
Fall	No	No	No	No	No
10-day IPD TMAX (°C) Annual	**Yes/No** -0.2	No	No	No	No
Winter	**Yes** -0.6	No	No	No	No
Spring	No	No	No	No	No
Summer	No	No	No	No	No
Fall	No	No	No	No	No
10-day IPD TMIN (°C) Annual	**Yes/No** -0.1	**Yes/No** -0.1	No	No	No
Winter	**Yes/No** -0.4	**Yes/No** -0.4	**Yes/No** -0.3	No	**Yes/No** 0.5
Spring	**Yes/No** -0.3	**Yes/No** -0.1	No	No	**Yes/No** 0.2
Summer	**Yes/No** 0.1	No	No	No	No
Fall	No	No	No	No	No

8.1.3. Changes in the heat waves in summer

The 30°C threshold was chosen similarly to Huth et al. (2000). As mentioned earlier in Section 6, the heat waves include interruptions. This means that temperatures equal to the threshold and temperatures lower than the threshold, are also included within some heat waves. Despite the interruption in the heat waves, however, the mean temperature of the heat wave still has to be above the chosen threshold, similarly to Huth et al. (2000). Additional condition was imposed that there should be at least three days with temperatures higher than the threshold before or after the one day with a drop in thermal conditions, since the emphasis in using this index is on extreme conditions that can affect the human well being due to longer persistence. For example, a period with higher than the threshold temperature on the first day, a drop below the threshold on the next day, followed by two more days with higher temperatures above the threshold is not considered a heat wave, as it is too short a period of high temperatures to impose considerable heat stress on humans. Another additional condition is that the drop should not be larger than 1°C, so that the overall mean maximum temperature for the heat wave still stays above the chosen threshold. The restrictive 1°C drop was adopted to minimize any alleviation of the oppressiveness of the warm conditions. It should be kept in mind, however, that such a small drop is similar to the range of measurement errors that might occur due to faulty instrument or an observer mistake. In the summary table, 'maximum excess' is defined as the highest heat wave intensity per year. 'Intensity', is the difference between the temperatures within a heat wave and the respective threshold.

The early period (1951-1979) is characterized by a significant decrease in the frequency of heat waves and their average length for the three stations located in the interior (Table 3-10, Figure 3-21). An interesting finding is that although the heat waves became less frequent and shorter during 1951-1979, the highest intensity per year (the maximum excess) remained unchanged. Varna is characterized by smaller number of heat wave occurrences, in general, compared to the interior stations. In 1951-1979 Varna did not display any trends in the heat wave frequency, length or maximum excess.

The late period, represented by Pleven NCDC, is characterized by a significant increase in the frequency (0.8 counts/decade) and length (1.5 days/decade) of heat waves (Table 3-10, Figure 3-22). As for the early period, the highest temperatures per year recorded within a heat wave do not show any trends during 1973-1999.

Table 3-10 Summary table for the existence and magnitude of trends in heat waves and cold spells (per decade, except where specified per pentad)
(Yes/No means that trend is significant at α=0.05, and not at α=0.01; Yes means that trend is significant at both levels of significance)

Index/Station Period	**Obrazstov Chiflick** 1953-1979	**Plovdiv** 1951-1979	**Varna** 1951-1979	**Pleven*** 1951-1979	**Pleven NCDC**** 1973-1999
Heat Waves Number per Year **(count)**	**Yes** -1.2	**Yes/No** -0.5	By pentads No	**Yes/No** -0.7	**Yes/No** 0.8
Ave Length per Year **(days)**	**Yes/No** -0.8	**Yes** -1	By Pentads No	**Yes** -1.1	**Yes** 1.5
Maximum Excess per Year (°C)	No	No	By Pentads No	No	No
Cold Spells Number per Year **(count)**	No	No	By Pentads No	No	No
Ave Length per Year **(days)**	**Yes** -1.3	No	By Pentads No	No	**Yes/No** 0.9
Maximum Excess per Year (°C)	No	No	By Pentads No	No	No

*** 1960 is missing**

**** 1996 is missing; 1991 was ignored for the heat waves and 1991/92 was ignored for the cold spells due to the large percentage of missing data.**

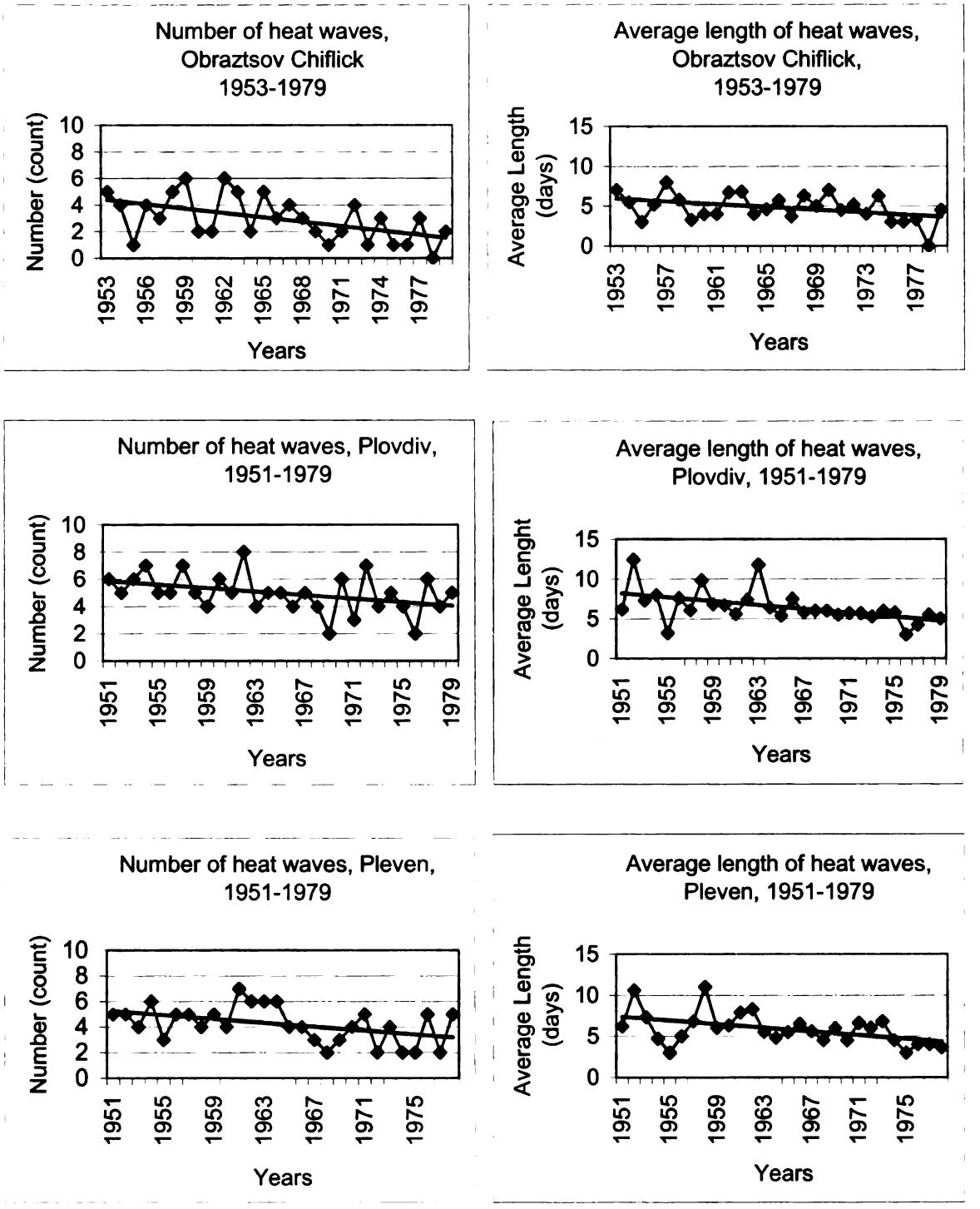

Figure 3-21 Changes in the number and average length of heat waves for Obraztsov Chiflick, Plovdiv and Pleven, 1951-1979

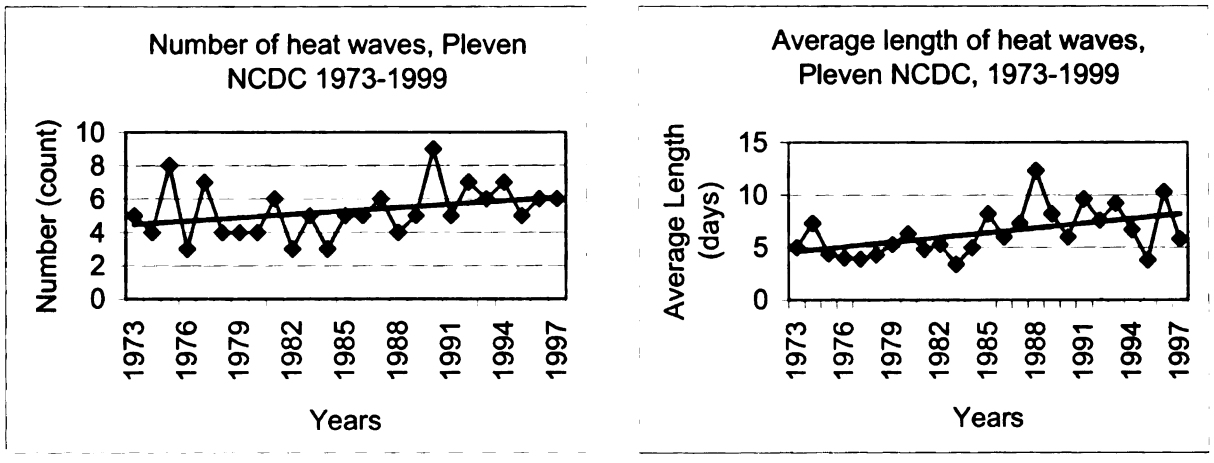

Figure 3-22 Changes in the number and average length of heat waves for Pleven NCDC, 1973-1999

8.1.4. Changes in the cold spells in winter

The threshold of -5°C was utilized to determine the cold spells (more details about the choice of the threshold are given in subsection 8.2.3.a). As with the heat waves, interruptions, meaning days with temperatures higher or equal to the chosen threshold, are allowed within the cold spells. The rise in minimum temperature cannot be larger than 1°C, similar to the restriction imposed on the heat waves, so that the overall mean minimum temperature for the cold spell is still below the chosen threshold. The day with a rise in temperature, similar to the heat waves, should be preceded or succeeded by at least three days with temperatures lower than the threshold. The restrictive 1°C drop was adopted to minimize any alleviation of the severity of a cold spells. Similar to the heat waves indices, 'maximum excess' is the lowest cold spell intensity per year.

The cold spells do not indicate any changes in frequency, maximum excess or average length for the early period for any station, except for Obraztsov Chiflick (Table 3-10, Figure 3-23). At this station the average length of

the cold spells decreased by -1.3 days/decade in 1953-1979. While Pleven did not display any trends in the cold spells characteristics in 1951-1979, the average length of the cold spells increased by 0.9 days/decade in 1973-1999 at Pleven NCDC (Table 3-10, Figure 3-23).

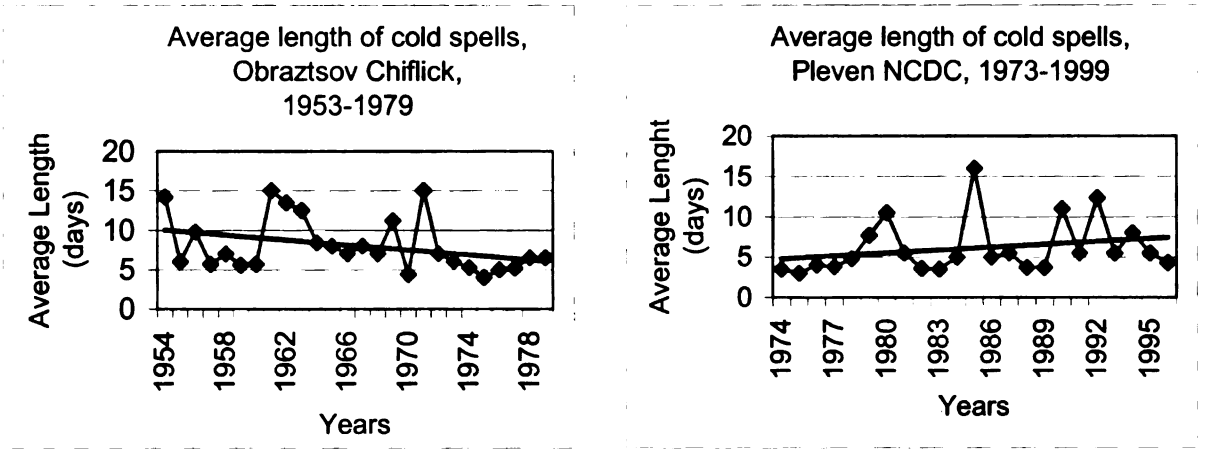

Figure 3-23 Changes in average length of cold spells for Obraztsov Chiflick (1951-1979) and Pleven NCDC (1973-1999)

8.1.5. Changes in frost period severity and duration, cooling degree days and heating degree days

The frost period duration does not show any trends for the early period 1951-1979 at any of the stations (Table 3-11). The frost period severity[12] (defined as the percentage of days within a month with minimum temperatures below 0°C) also does not change significantly for any of the stations during November, December, January and February. In October, the frost period severity increases

[12] For most of the stations in October, April and for Varna also in November, frost days (with minimum temperature below 0°C) did not occur every year. This is why the frost period severity for these months was calculated using pentadal periods, i.e. the average frost period severity per non-overlapping pentads was subjected to trend analysis.

at Obraztsov Chiflick and Pleven, by 0.19%/pentad and 0.22%/pentad, respectively (Figure 3-24). In March, the frost severity displays significant decreasing trends for all the stations during 1951-1979, varying between -8.5%/decade at Plovdiv and -16.1%/decade at Pleven (Figure 3-25). In April, only Obraztsov Chiflick displays a significant negative trend of -0.25/pentad (Figure 3-26).

In contrast to Pleven, for which no changes in the frost period duration were evident, the results for Pleven NCDC indicate a significant negative trend of -13.2 days/decade (Table 3-11, Figure 3-27). While at Pleven the frequency of frost days increased in October and decreased in March during 1951-1979, no significant changes in the frost period severity were observed at Pleven NCDC in 1973-1999.

Table 3-11 Summary table for the existence and magnitude of trends in frost period severity and duration, HDDs and CDDs (per decade except where specified per pentad) (Yes/No means that trend is significant at α=0.05, and not at α=0.01; Yes means that trend is significant at both levels of significance)

Index/ Station Period	**Obraztsov Chiflick** 1953-1979	**Plovdiv** 1951-1979	**Varna** 1951-1979	**Pleven*** 1951-1979	**Pleven NCDC**** 1973-1999
Frost Period Severity (%) October	By Pentads **Yes/No** 0.19/pentad	By Pentads No	---------	By Pentads **Yes/No** 0.22/pentad	By Pentads No
November	No	No	By Pentads No	No	No
December	No	No	No	No	No
January	No	No	No	No	No
February	No	No	No	No	No
March	**Yes** -11	**Yes/No** -8.5	**Yes/No** -8.9	**Yes** -16.1	No
April	By Pentads **Yes/No** -0.25/pentad	By Pentads No	---------	By Pentads No	By Pentads No
Frost Period Duration (days) Annual	No	No	No	No	**Yes/No** -13.2
Cooling degree days Annual	**Yes/No** -35.8	No	No	**Yes/No** -42.7	**Yes** 90.8
Heating degree days Annual	No	No	No	No	**Yes/No** -160.9

*** 1960 is missing, ** 1996 is missing**

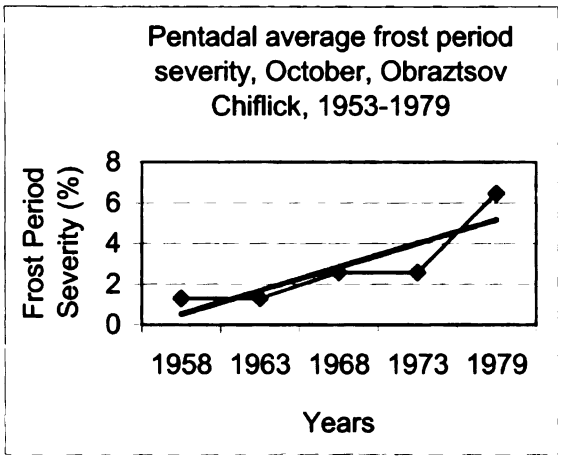

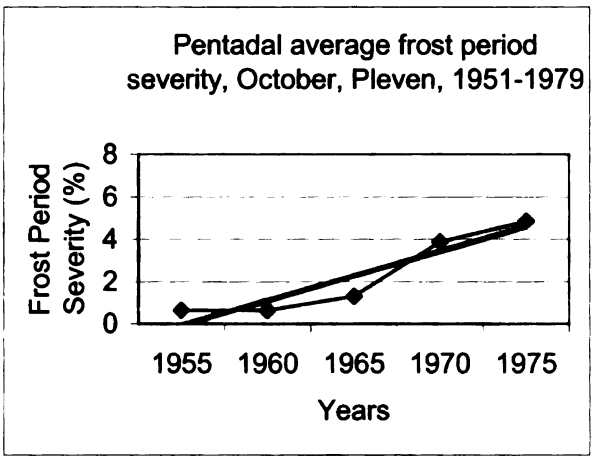

Figure 3-24 Changes in frost period severity (%) in October for Obraztsov Chiflick (1953-1979) and Pleven (1951-1979), based on average pentadal values

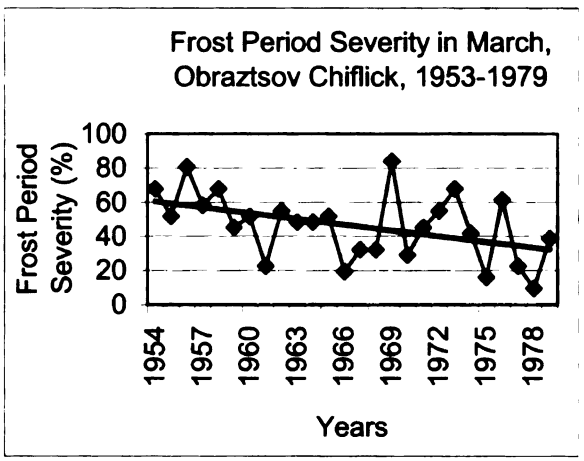

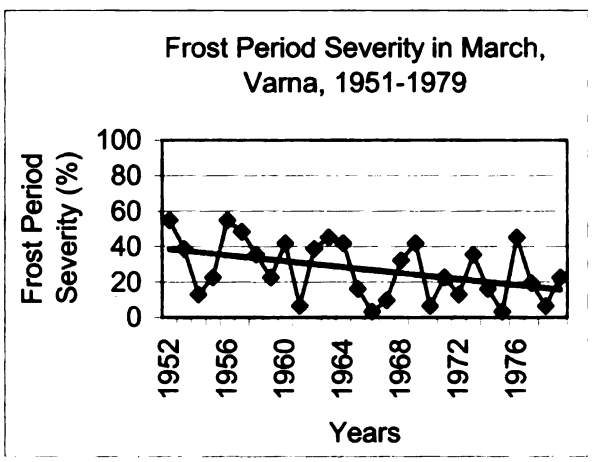

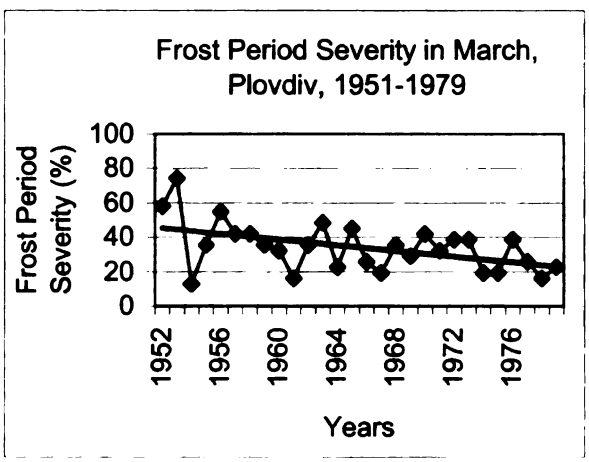

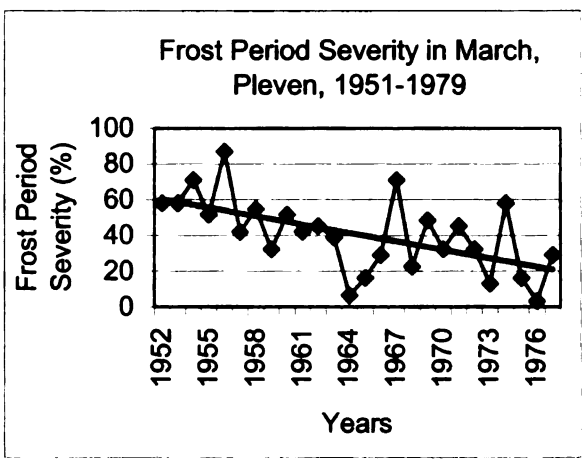

Figure 3-25 Changes in frost period severity (%) in March for all stations, 1951-1979

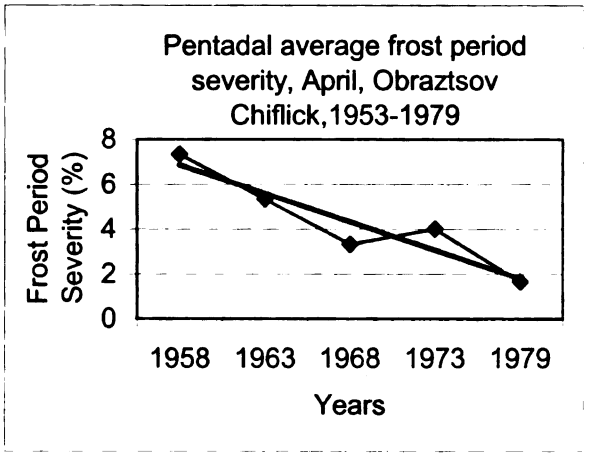

Figure 3-26 Changes in frost period severity (%) in April in Obraztsov Chiflick, 1953-1979, based on average pentadal values

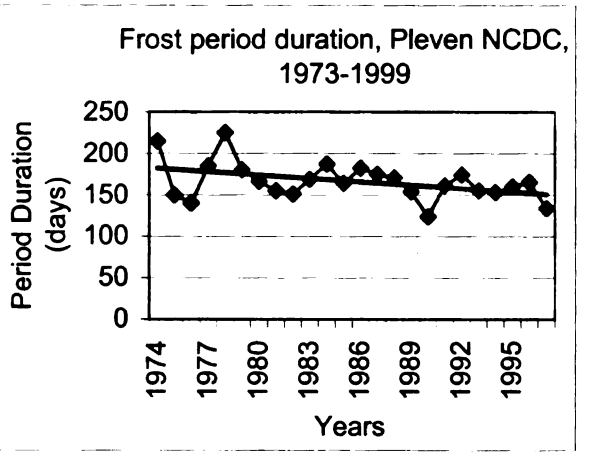

Figure 3-27 Changes in the frost period duration (days) for Pleven NCDC, 1973-1999

The trends in heating degree days are not significant at all stations for the early period (1951-1979). These results relate well with the outcomes from the analysis of the changes in the number, average length and maximum excess of the cold spells in winter for most stations (except for Obraztsov Chiflick), as well as with the results regarding the frost period severity. The late period, as represented by Pleven NCDC, displays a significant negative trend (-160.9

HDDs/decade), which indicates warming during the cooler part of the year (Table 3-11, Figure 3-29).

The cooling degree days index is characterized by opposite trends during the early period (negative changes) and the late period (positive changes) (Table 3-11). Obraztsov Chiflick and Pleven display a decrease of -35.8 CDDs/decade and -42.7 CDDs/decade (Figure 3-28), respectively, reflecting a decreased need for air conditioning during the warmer half of the year in 1951-1979 (1953-1979 for Obraztsov Chiflick). In contrast to Pleven from the early period, a significant increasing trend (90.8 HDDs/decade) is evident in the cooling degree days at Pleven NCDC (Figure 3-29), indicating a rise in the temperatures during the warmer half of the year.

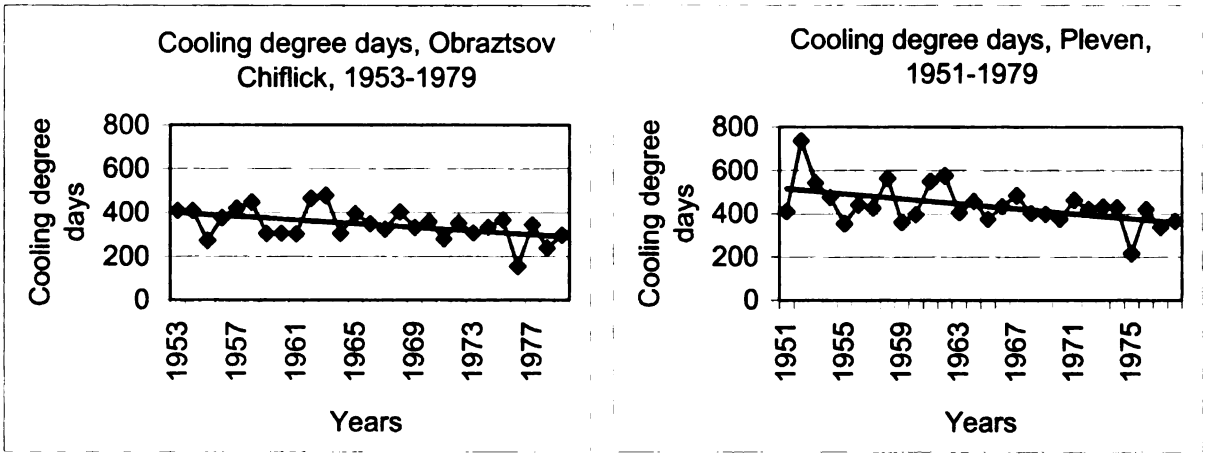

Figure 3-28 Changes in cooling degree days for Obraztsov Chiflick (1953-1979) and Pleven (1951-1979)

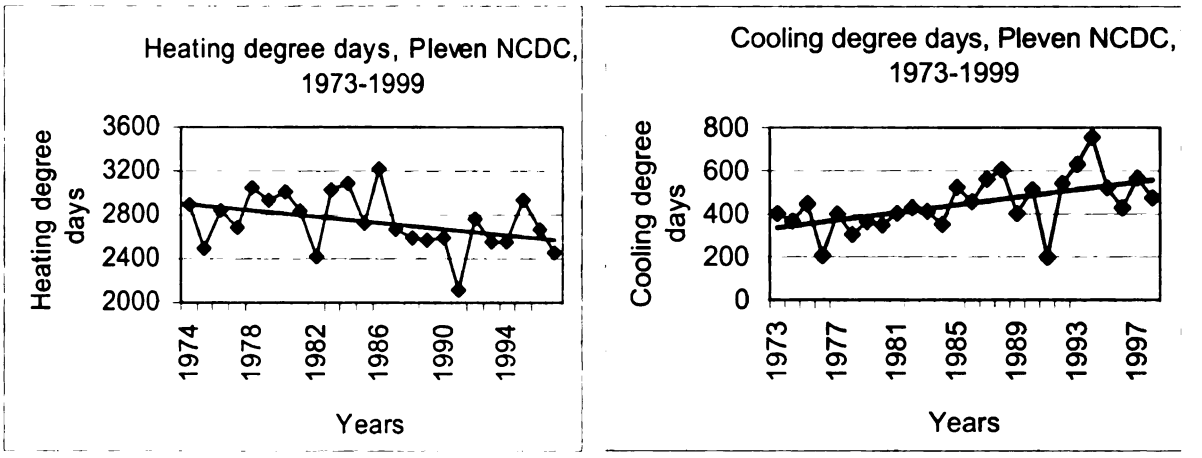

Figure 3-29 Changes in heating and cooling degree days for Pleven NCDC, 1973-1999

8.2. Extreme value analysis of temperature extreme events

The series of annual and seasonal highest daily TMAX and lowest daily TMIN for the available homogeneous periods for each of the four stations from the Yearbooks, and for Pleven NCDC, were modeled using the Generalized Extreme Value distribution. All the exceedances over a chosen threshold in summer and below a chosen threshold in winter were modeled using the GP distribution. The choice of the employed thresholds was based on graphical techniques, as explained in detail in subsection 8.2.3.a. The aim of the application of the extreme value analysis was to obtain return levels for different return periods for 1951-1979 and 1973-1999, in order to assess changes in return levels between the early and late period. All of the plots for the model fit to the temperature data at each station, together with the detailed tables listing the model parameters and standard errors, are located in the Appendix to Chapter 3.

8.2.1. Generalized Extreme Value distribution results – Annual and seasonal highest maximum temperature

For the highest annual and seasonal TMAX, the fit of the model to the empirical data was judged to be 'good' for most of the stations, based on visual inspection of the probability, the quantile and the probability density plots (Table 3-12). Exceptions are the highest annual and summer TMAX series for Varna, for which the correspondence between the model and the temperature data was 'poor'; and the highest TMAX for Obraztsov Chiflick in spring and for Varna in fall, for which the fit was 'acceptable'. An explanation of the 'poor' fit at Varna could be that a few quite large values greatly affect the distribution of the data (Appendix Figure 4, Appendix Figure 16). These large values were suspicious, because they deviated greatly from the data for the remaining years, however, due to the lack of metadata the values were kept within the temperature series. The fit for the summer and the annual highest TMAX is almost exactly the same for all stations since the annual highest temperatures are mostly drawn from the highest summer temperatures. Minor deviations occur when the highest annual series include values recorded in seasons other than summer (e.g., spring or fall).

	Period	Stations	Fit category	Type of model	10 year return period		20 year return period		50 year return period	
					Return level (°C)	95% conf. limits	Return level (°C)	95% conf. limits	Return level (°C)	95% conf. limits
Annual	Early	Obraztsov Chiflick	Good	GEV-3,Weibull	38.2°	37.5°, 39.5°	38.8°	38.1°, 40.6°	39.3°	38.6°, 41.9°
		Varna	**Poor**	GEV-2, Fréchet	35.4°	34.6°, 37.1°	36.3°	35.3°, 38.9°	37.5°	36.0°, 41.9°
		Plovdiv	Good	GEV-3,Weibull	38.7°	37.8°, 40.7°	39.7°	38.5°, 42.7°	40.8°	39.3°, 45.8°
		Pleven	Good	GEV-3,Weibull	39.8°	38.9°, 41.4°	40.5°	39.6°, 43.0°	41.2°	40.2°, 45.3°
	Late	Pleven NCDC	Good	GEV-3,Weibull	41.1°	40.1°, 43.1°	41.9°	40.8°, 45.0°	42.7°	41.5°, 47.8°
Winter	Early	Obraztsov Chiflick	Good	GEV-3,Weibull	20.1°	19.4°, 20.6°	20.4°	19.9°, 21.2°	20.5°	20.3°, 21.7°
		Varna	Good	GEV-3,Weibull	20.3°	19.6°, 21.5°	20.8°	20.2°, 22.5°	21.4°	20.7°, 23.9°
		Plovdiv	Good	GEV-3,Weibull	21.2°	20.1°, 23.8°	22.2°	20.9°, 26.8°	23.6°	21.7°, 32.2°
		Pleven	Good	GEV-3,Weibull	21.7°	20.4°, 23.9°	22.7°	21.3°, 25.9°	23.8°	22.3°, 28.7°
	Late	Pleven NCDC	**Accept.**	GEV-3,Weibull	22.9°	22.0°, 24.3°	23.5°	22.7°, 25.5°	24.0°	23.3°, 26.8°
Spring	Early	Obraztsov Chiflick	**Accept.**	GEV-3,Weibull	33.0°	31.7°, 37.4°	34.3°	32.6°, 43.1°	35.8°	33.5°, 40°
		Varna	Good	GEV-2, Fréchet	30.4°	28.7°, 34.6°	32.1°	29.9°, 40.2°	34.5°	31.3°, 51.6°
		Plovdiv	Good	GEV-3,Weibull	33.2°	32.2°, 35.2°	34.1°	33.0°, 37.3°	35.0°	33.8°, 40.4°
		Pleven	Good	GEV-3,Weibull	33.7°	32.8°, 35.4°	34.5°	33.5°, 37.1°	35.2°	34.2°, 39.4°
	Late	Pleven NCDC	Good	GEV-3,Weibull	35.0°	34.1°, 36.6°	35.7°	34.8°, 38.0°	36.3°	35.5°, 39.8°

Table 3-12 Summary of the GEV modeling of highest TMAX for all stations form 1951-1979 and Pleven NCDC from 1973-1999 period

	Period	Stations	Fit category	Type of model	10 year return period		20 year return period		50 year return period	
					Return level (°C)	95% conf. limits	Return level (°C)	95% conf. limits	Return level (°C)	95% conf. limits
Summer	Early	Obraztsov Chiflick	Good	GEV-3,Weibull	38.2°	37.5°, 39.5°	38.8°	38.1°, 40.6°	39.3°	38.6°, 42.1°
		Varna	**Poor**	GEV-2, Fréchet	35.3°	34.5°, 36.8°	36.2°	35.2°, 38.5°	37.3°	35.9°, 41.0°
		Plovdiv	Good	GEV-3,Weibull	38.7°	37.8°, 40.7°	39.7°	38.5°, 42.7°	40.8°	39.3°, 45.8°
		Pleven	Good	GEV-3,Weibull	39.8°	38.9°, 41.4°	40.5°	39.6°, 43.0°	41.2°	40.2°, 45.3°
	Late	Pleven NCDC	Good	GEV-3,Weibull	41.1°	40.1°, 43.2°	41.9°	40.8°, 45.2°	42.7°	41.5°, 48.2°
Fall	Early	Obraztsov Chiflick	Good	GEV-3,Weibull	34.2°	33.2°, 36.1°	35.0	33.9°, 37.9°	35.8°	34.7°, 40.4°
		Varna	**Accept.**	GEV-3,Weibull	31.8°	30.9°, 33.4°	32.7°	31.7°, 34.9°	33.7°	32.5°, 37.0°
		Plovdiv	Good	GEV-3,Weibull	34.2°	33.3°, 36.1°	35.1°	34.0°, 38.1°	36.1°	34.8°, 41.0°
		Pleven	Good	GEV-3,Weibull	35.7°	34.5°, 38.2°	36.7°	35.4°, 40.9°	37.8°	36.2°, 45.1°
	Late	Pleven NCDC	Good	GEV-3,Weibull	36.9°	35.3°, 40.9°	38.4°	36.4°, 45.5°	40.3°	37.6°, 53.7°

Table 3-12 Continued (Accept. means 'acceptable' fit)

Apart from the annual, spring and summer highest TMAX for Varna, which were fitted using the GEV-2 Fréchet model, all the highest TMAX data series were modeled using the GEV-3, Weibull distribution. The reasons for the different GEV model for Varna in some seasons are not clear. It is possible that the suspiciously high values, mentioned earlier, affect the empirical distributions during the warmer half of the year, or the coastal location of Varna is reflected in the different model used for the fit. From the calculated standard errors it is evident that the uncertainty of the estimated model parameters is small for most stations, regardless of the time scale (annual or seasonal). The standard errors are large, between 0.47 and 1.2, only for wintertime highest TMAX at Obraztsov Chiflick.

The estimated return levels display spatial variation. The three interior stations, Obraztsov Chiflick, Pleven and Plovdiv, feature higher projected annual and seasonal maximum temperatures, compared to Varna, for any return period. The return level projections are highest for Pleven, followed by Plovdiv in most cases.

Similar to Pleven, the annual and seasonal highest TMAX for Pleven NCDC are modeled using the GEV-3 Weibull distribution (Table 3-12) and the uncertainty of the estimated model parameters is small. The fit between the model and the highest TMAX was judged as 'good' for the year and for all seasons, except for winter. In winter, the fit of the model to the empirical data was evaluated as 'acceptable', because the empirical data deviated from the model in the middle of the distribution (Appendix Figure 10). For the year and for

all the seasons Pleven NCDC displays higher estimates for the different return levels for the late period, compared to Pleven from the early period. The width of the 95% confidence intervals for each return level for Pleven NCDC has also increased, compared to Pleven, for the annual, summer and fall highest TMAX. The increased confidence interval width reflects the higher estimates for the upper confidence limits, especially for 50-year return levels. In addition, the wider confidence intervals indicate larger uncertainty in the estimated return levels compared to the early period estimates.

8.2.2. Generalized Extreme Value distribution results – Annual and seasonal lowest minimum temperature

The annual and seasonal series of lowest TMIN for most of the stations for the early period were modeled well by the GEV distribution (Table 3-13). For several stations some underestimation or overestimation of parts of the data series existed. However, a reasonable linearity of the model-empirical data line was still evident on the probability and quantile plots. For these stations and seasons (Pleven, and Plovdiv in spring, and Varna in summer), the fit was categorized as 'acceptable'. The lowest daily TMIN were fit by the GEV-3 Weibull distribution for most of the station-season combinations. Exceptions are the annual, summer and fall series at Obraztsov Chiflick and the spring series at Plovdiv, which were modeled using the GEV-2 Fréchet distribution with a positive shape parameter. The plots for the GEV modeling of the annual lowest daily TMIN are almost exactly replicated by the plots of the model fit for the winter

season, since in most cases the lowest temperatures per year are actually drawn from the winter season.

At all stations, the standard errors suggest a somewhat larger uncertainty of the model parameters for the annual lowest TMIN, compared to the annual highest TMAX. On a seasonal scale the uncertainty in the model parameters for the lowest TMIN is generally low, especially in summer.

Spatial variation in projections of the return levels is evident. Varna displays highest return levels for all the return periods on an annual and seasonal scale. Plovdiv is characterized by lowest estimated return levels for most return periods on annual scale, in winter and spring. In summer and fall, however, Obraztsov Chiflick features the lowest return levels for any return period. The condifedence intervals are somewhat wider for Obraztsov Chiflick and Plovdiv for the year, in winter, and spring, compared to the rest of the stations, indicating larger uncertainty in the estimated return levels. In all seasons and for all stations the confidence intervals are assymetrical to the estitamed return levels, usually displaying close to the return level upper limit and quite low lower limit.

For Pleven NCDC, the GEV model did not fit well the annual and the winter data. The probability and quantile plots for the GEV fit for station Pleven NCDC indicate that the model fit is influenced by several very low extreme temperature values (Appendix Figure 26, and Appendix Figure 27). Furthermore, the empirical density plot shows that the distribution might be bimodal in both cases rather than a unimodal one. Based on these discrepancies, the GEV model fit for Pleven NCDC lowest TMIN in winter was categorized as 'poor

'(Table 3-13). The fit of the model was assessed as 'acceptable' for spring and summer, and 'good' for fall. The annual, summer and fall lowest TMIN for Pleven NCDC were modeled using the GEV-2 Fréchet distribution, while winter and spring were modeled by the GEV-3 Weibull distribution.

The projected 10-, 20- and 50-year return levels at Pleven NCDC were lower than those at Pleven for the annual, winter, summer and fall lowest TMIN, and the uncertainty of the estimates, as indicated by the width of the 95% confidence intervals, was always larger. In spring, the estimated return levels for Pleven NCDC were higher than the projections for Pleven for any return period. On an annual scale and for fall, the lower limits of the 95% confidence intervals for the 50-year return level were not estimated successfully. In the summary table, an asterisk was placed instead of a value for the lower limit of the 95% confidence interval for the 50-year return level (Table 3-13).

8.2.3. Generalized Pareto Distribution modeling of the exceedances above chosen thresholds

8.2.3.a. Choice of thresholds

The Mean Residual Life plots and the plots of the GP distribution fit over a range of thresholds for every station for winter and summer were used to determine the appropriate thresholds (the plots are presented in the Appendix to Chapter 3, Appendix Figure 43 to Appendix Figure 49). Following the directions for evaluation of the plots, discussed in more detail in sub-section 7.2.2., the 32°C was determined as being an appropriate threshold for exceedances in summer for almost all of the stations. Only for the data from Varna was this threshold too high, since the climate of this city is moderated by the sea and

occurrences of extreme high temperatures above 32°C are rare. However, since the 32°C threshold was appropriate for the rest of the stations and to perform an inter-station and inter-period (early versus late period) comparison of the return levels, the same threshold was used for all the locations.

	Period	Stations	Fit category	Type of model	10 year return period		20 year return period		50 year return period	
					Return level (°C)	95% conf. limits	Return level (°C)	95% conf. limits	Return level (°C)	95% conf. limits
Annual	Early	Obraztsov Chiflick	Good	GEV-2, Fréchet	-20.9°	-19.0°, -26.1°	-22.8°	-20.3°, -32.5°	-25.4°	-21.7°, -45.2°
		Varna	Good	GEV-3,Weibull	-14.8°	-13.3°, -18.0°	-16.2°	-14.4°, -21.3°	-17.7°	-15.6°, -26.4°
		Plovdiv	Good	GEV-3,Weibull	-22.4°	-19.4°, -29.3°	-25.2°	-21.6°, -37.3°	-28.9°	-23.9°, -51.5°
		Pleven	Good	GEV-3,Weibull	-20.8°	-18.9°, -24.5°	-22.5°	-20.3°, -28.2°	-24.4°	-21.8°, -33.7°
	Late	Pleven NCDC	**Poor**	GEV-2, Fréchet	-23.5°	-20.6°, -32.2°	-26.6°	-22.5°, -43.4°	-30.9°	-24.4°, *
Winter	Early	Obraztsov Chiflick	Good	GEV-2, Fréchet	-20.8°	-18.8°, -26.0°	-22.7°	-20.1°, -32.1°	-25.3°	-21.6°, -43.6°
		Varna	Good	GEV-3,Weibull	-14.9°	-13.3°, -18.7°	-16.3°	-14.5°, -22.8°	-18.0°	-15.7°, -29.5°
		Plovdiv	Good	GEV-3,Weibull	-22.3°	-19.2°, -29.1°	-25.2°	-21.5°, -36.5°	-28.5°	-23.8°, -48.6°
		Pleven	Good	GEV-3,Weibull	-21.0°	-18.9°, -25.0°	-22.7°	-20.4°, -28.9°	-24.5°	-21.9°, -34.6°
	Late	Pleven NCDC	**Poor**	GEV-3,Weibull	-23.8°	-22.0°, -27.0°	-24.4°	-23.3°, -30.1°	-24.9°	-24.2°, -34.4°
Spring	Early	Obraztsov Chiflick	Good	GEV-3,Weibull	-12.9°	-10.6°, -18.7°	-15.1°	-12.2°, -25.4°	-17.8	-13.9°, -37.6°
		Varna	Good	GEV-3,Weibull	-7.5°	-6.4°, -10.0°	-8.5°	-7.3°, -12.7°	-9.5°	-8.1°, -17.0°
		Plovdiv	Accept.	GEV-2, Fréchet	-11.5°	-8.4°, -23.8°	-15.2°	-10.4°, -45.5°	-21.6°	-12.7°, *
		Pleven	Accept.	GEV-3,Weibull	-11.4°	-9.3°, -15.7°	-13.4°	-10.8°, -20.4°	-15.9°	-12.5°, -28.2°
	Late	Pleven NCDC	Accept.	GEV-3,Weibull	-10.0°	-8.2°, -14.0°	-11.7°	-9.5°, -18.4°	-13.9°	-10.9°, -26.0°

Table 3-13 Summary of the GEV modeling of lowest TMIN for all stations form 1951-1979 and Pleven NCDC from 1973-1999 period

	Period	Stations	Fit category	Type of model	10 year return period		20 year return period		50 year return period	
					Return level (°C)	95% conf. limits	Return level (°C)	95% conf. limits	Return level (°C)	95% conf. limits
Summer	Early	Obraztsov Chiflick	Good	GEV-2, Fréchet	6.4°	7.5°, 3.7°	5.4°	6.8°, 0.4°	4.0°	6.0°, -6.0°
		Varna	Accept.	GEV-3,Weibull	8.2°	8.9°, 7.2°	7.7°	8.4°, 6.3°	7.2°	7.8°, 5.2°
		Plovdiv	Good	GEV-3,Weibull	7.9°	8.5°, 6.8°	7.4°	8.0°, 5.7°	6.8°	7.5°, 4.2°
		Pleven	Good	GEV-3,Weibull	7.8°	8.5°, 6.5°	7.2°	8.0°, 5.2°	6.4°	7.4°, 3.2°
	Late	Pleven NCDC	Accept.	GEV-2, Fréchet	4.4°	6.0°, 0.2°	2.9°	5.0°, -5.2°	0.6°	3.8°, -16.0°
Fall	Early	Obraztsov Chiflick	Good	GEV-2, Fréchet	-11.5°	-8.9°, -18.9°	-14.1°	-10.7°, -28.1°	-17.5°	-12.5°, -46.2°
		Varna	Good	GEV-3,Weibull	-5.5°	-4.4°, -7.5°	-6.5°	-5.3°, -9.4°	-7.5°	-6.2°, -12.1°
		Plovdiv	Good	GEV-3,Weibull	-7.2°	-6.0°, -9.8°	-8.2°	-6.9°, -12.7°	-9.4°	-7.7°, -17.7°
		Pleven	Good	GEV-3,Weibull	-8.5°	-6.8°, -12.5°	-10.1°	-8.1°, -17.2°	-12.1°	-9.4°, -25.8°
	Late	Pleven NCDC	Good	GEV-2, Fréchet	-13.0°	-9.2°, -26.3°	-18.0°	-11.5°, -49.6°	-27.7°	-14.7°, *

Table 3-13 Continued

Based again on the Mean Residual Life plots and the plots for the GP distribution fit to multiple thresholds for the winter season, 0°C and -5°C were potential choices for thresholds at all of the stations (Appendix Figure 50 to Appendix Figure 59). Using the 0°C value, however, resulted in a large number of exceedances over the threshold (in winter the original series are multiplied by -1), i.e., almost the entire winter season was included in the analysis for each station. Hence, data not actually pertaining to the lower tail of the minimum temperature distribution was considered when this threshold was used. Moreover, in this study focus of attention are exceedances that potentially can affect negatively the human well being, hence, the threshold needs to be lower than 0°C. Given these considerations, the -5°C was chosen as more suitable for the objectives of the study and more appropriate for the achievement of non-biased estimators of the parameters of the GP distribution. Furthermore, a threshold of -5°C has been used by some authors in their research of extreme temperature events during the colder half of the year in Bulgaria (Koleva, 1987), in south central Europe (Domonkos et al., 2003) and in central Europe (Domonkos et al., 1998).

8.2.3.b. GPD modeling of summer TMAX exceedances over 32°C

The fit of the GP model to the empirical data for all stations, except for Varna, was assessed as 'good' (Appendix Figure 60 to Appendix Figure 62). For Varna the fit was evaluated as 'poor' since a significant underestimation by the model is evident in the upper quantiles, due to the influence of several quite large temperature values on the overall distribution (Appendix Figure 63).

The data for all the stations from the early period were modeled using the GPD-3 beta distribution with negative shape parameter, except for the data at Varna. The Varna summer TMAX exceedances were fitted using the GPD-2 Pareto distribution with a positive shape parameter. The standard errors are quite low indicating that the uncertainty in the estimated parameters is not high (Appendix Table 12). The return levels for the exceedances over the 32°C threshold are highest at Pleven (Table 3-14) and second highest at Plovdiv. All the 95% confidence intervals of the return levels for the stations with 'good' fit of the GPD model to the data are quite narrow indicating lesser uncertainty in the estimates.

The exceedances of the summer TMAX over the 32°C threshold at Pleven NCDC were modeled also using the GPD-3, beta distribution and the standard errors of the model parameters were not high (Appendix Table 12). At Pleven NCDC, the return level estimates are higher, compared to the return levels at Pleven from the early period (Table 3-14).

Comparing the projected return levels at each station based on the GEV fit of the extreme high summer TMAX, to the estimated return levels at the same station from the GPD fit, no consistency of the results is evident. At Pleven the GPD projections are warmer for all return periods; at Obraztsov Chiflick the GPD model projections are the same as the estimates for the GEV modeling for the 10 and 20 year return periods, but are higher for the 50 year return period; at Plovdiv the GPD model estimated higher return levels for 10 and 20 year return periods, and lower for the 50 year return period; at Pleven NCDC the 10 year

estimates are warmer based on the GPD fit, but the 20 and 50 year return levels are lower, and at Varna the estimates are the same regardless of return period.

Table 3-14 Summer TMAX exceedances over a 32°C threshold – GPD fit
Return levels for different return periods
(Ret. Level means Return level)

Station	Obraztsov Chiflick		Varna		Plovdiv		Pleven		Pleven NCDC	
Return Period	Ret. Level	95% Conf. Interv.	Ret. Level	95% Conf. Interv.	Ret. Level	95% Conf. Interv.	Ret. Level	95% Conf. Interv.	Ret. Level	95% Conf. Interv.
10 years	38.2°	37.6° 39.4°	35.3°	34.6° 36.8°	39.3°	38.7° 40.3°	40.2°	39.5° 41.2°	41.2°	40.8° 41.8°
20 years	38.8°	38.1° 40.3°	36.2°	35.2° 38.5°	39.9°	39.2° 41.2°	40.8°	40.0° 42.1°	41.6°	41.1° 42.4°
50 years	39.5°	38.6° 41.5°	37.3°	35.9° 41.3°	40.7°	39.8° 42.3°	41.4°	40.5° 43.1°	42.0°	41.5° 43.0°

8.2.3.c. GPD modeling of winter TMIN deficiencies below -5°C

The fit of the GP distribution to the deficiencies below -5°C was assessed as 'good' for all the stations in the early period (Appendix Figure 65 through Appendix Figure 69). Some slight underestimation is evident in the upper quantiles at Pleven (since the data were multiplied by -1 on the plots the lowest values are represented by the upper quantiles) and in the middle of the distribution at Plovdiv. For all of the stations, the winter TMIN deficiencies were fitted using the GPD-3 beta distribution, with negative shape parameters (Appendix Table 13). The uncertainty in the estimated parameters is low given the small values of the standard errors, varying between 0.02 and 0.4.

For the early period, Plovdiv features the lowest return levels for any return period (Table 3-15). Even the 10-year projection is lower than the 50-year projections for the other stations. In addition, the estimated return levels for Plovdiv are characterized by the greatest uncertainty, as indicated by the widest 95% confidence intervals. Varna displays highest return levels (i.e., "warmest" low temperatures) due to its proximity to the Black Sea.

For the late period, the winter TMIN deficiencies below -5°C at Pleven NCDC were also modeled using the GPD-3, beta distribution. The parameter estimates have small standard errors indicating lower uncertainty in the model. The projected return levels are lower compared to Pleven from the early period (Table 3-15). The 95% confidence intervals are wider, indicating greater uncertainty in the estimated return levels, compared to Pleven from the early period.

Table 3-15 Winter TMIN deficiencies below a -5°C threshold, GPD fit Return levels for different return periods
(Ret. Level means Return Level)

Station	Obraztsov Chiflick		Varna		Plovdiv	
Return Period	Ret. Level	95% Conf. Interv.	Ret. Level	95% Conf. Interv.	Ret. Level	95% Conf. Interv.
10 years	-22.5°	-21.5° -24.1°	-15.7°	-15.1° -16.9°	-25.5°	-22.8° -30.2°
20 years	-23.4°	-22.2° -25.3°	-16.4°	-15.7° -17.8°	-28.1°	-24.6° -34.4°
50 years	-24.3°	-23.0° -26.6°	-17.1°	-16.3° -18.8°	-31.5°	-26.7° -40.3°

Table 3-15 continued

Station	Pleven		Pleven NCDC	
Return Period	Ret. Level	95% Conf. Interv.	Ret. Level	95% Conf. Interv.
10 years	-22.1°	-21.0° -23.9°	-24.3°	-22.6° -27.0°
20 years	-23.1°	-21.8° -25.2°	-25.7°	-23.7° -29.1°
50 years	-24.2°	-22.7° -26.8°	-27.3°	-24.9° -31.6°

When comparing by station the return level estimates from the GEV fit to the absolute lowest TMIN in winter, to the projected return levels based on the GPD model fit to the exceedances below the -5°C threshold, some consistency is evident. For all the stations, the estimated 10 and 20 year return levels obtained from the GPD fit are colder than those projected using the GEV fit. In addition, the 50 year return levels are also lower at Plovdiv and Pleven NCDC, compared to the results from the GEV projections for these stations. Only at Obraztsov Chiflick, Varna, and Pleven the 50 year projected return levels are warmer than the respective 50 year projections based on the GEV fit for these stations.

9. Discussion

Not only has the global surface temperature risen during the last 100 years but other thermal characteristics of the climate for different regions and worldwide have changed considerably as well. Both the daily maximum and minimum extreme temperatures have increased over the second half of the 20th

century, although at dissimilar rates (Easterling et al. 1997, 2000a). Karl et al. (1991) found that the absolute annual and monthly extremes of TMAX and TMIN in the USA and the Former Soviet Union (FSU) show little or no trend for TMAX, but generally show a strong rise in TMIN from 1951-1989. This asymmetry in the extreme maximum and minimum temperature changes on an annual basis was observed also by Easterling et al. (1997) on a global scale, Brazdil et al. (1996) for Central Europe, Heino et al. (1999) for Northern and Central Europe, Jones et al. (1999) for the Central England Temperature record, and Hundecha and Bardossy (2005) for Western Germany.

Earlier in this study several hypotheses were formulated regarding changes in the specified indices during the early and the late periods. For Bulgaria, the absolute highest maximum temperatures were hypothesized not to change or to decrease while the lowest minimum temperatures on annual and seasonal scales were expected to increase during the early period. In contrast, the hypothesis regarding the changes in absolute highest and lowest temperatures during the late period was for an increase in both indices. The results of this study are in agreement with the initial speculation and the findings of previous studies for the highest annual maximum temperatures, which do not change for any of the stations in Bulgaria. Additionally, in agreement with other studies and the hypothesized changes the absolute annual minimum temperatures increase significantly at Obraztsov Chiflick and Plovdiv during 1951-1979. The reasons why these trends are not observed at the rest of the stations during the early period might be related to unidentified inhomogeneities.

From a seasonal perspective, in winter and spring, during the late period, in accordance with the stated hypothesis, the absolute highest maximum temperature was found to increase at Pleven NCDC. Furthermore, in agreement with the overall rise in the minimum temperature extremes in spring, as reported by Karl et al. (1991) for other regions around the globe, and in accordance with the initial hypothesis, the results from this study indicate significant positive trends of the lowest spring minimum temperatures for all stations during the early 1951-1979 period. In summer, Frich et al. (2002) established that during 1946-1999 the warm summer nights (with minimum temperature above the 90th percentile) have increased in frequency on a global scale, especially in the mid-latitudes and the subtropics. Moberg and Jones (2005) confirmed that the warm tail of daily TMIN displayed significant positive trends during the past century in western and central Europe. In contrast, no significant trends of the extreme summer maximum or minimum temperatures were observed in Bulgaria during the second half of the 20th century.

In fall, Hundecha and Bardossy (2005) found that the 90th percentile TMAX and 10th percentile TMIN indices were decreasing in Western Germany for the 1958-2001 period, although these trends were significant for only a few stations. Similar results were attained in this study. A significant decrease was found in the highest maximum temperatures in fall for Pleven and Plovdiv during 1951-1979, but not for the rest of the stations. This finding is also in accord with the conclusions of Koleva (1987), who determined, based on monthly

temperature data, that the fall season in 1971-1984 was characterized by cooling in Bulgaria.

Many authors have reported a decreasing trend of the daily temperature range (DTR) during the past century. Brazdil et al. (1996) found a small decline of about -0.08°C in DTR for Central Europe during 1951-1990. Heino et al. (1999) also identified a decrease in the DTR in Northern and Central Europe in 1901-1995. Klein-Tank et al. (2003) observed a negative trend of -0.04°C/decade in Europe during the 1946-1999. The latest document of the IPCC, the Summary for Policymakers (IPCC, FAR 2007), reports that due to the simultaneous rise at similar rates of day-time and night-time temperatures the DTR has not changed globally during 1979-2004. The researchers from Working Group I also stated that the observed trends in DTR varied widely from region to region. The initial hypothesis in this study consisted of the expectation of a decrease in the daily temperature range (DTR) during the early period and in an increase in the DTR in the late period due to the expected much faster rise in the daily maximum than in the daily minimum temperatures. The changes in DTR established in this study were not consistent between the stations. The annual mean and the summer mean DTR decreased at Plovdiv and Pleven for 1951-1979, in agreement with the hypothesized expectations and most of previous research. While, contrary to previous studies the spring mean DTR for Varna increased which might be related to either maximum temperatures increasing faster than the minimum temperatures, or lower minimum temperatures due to longer lasting ice cover of the sea waters. These hypotheses have not been tested. Also in contrast to past

studies, the annual, winter and summer mean DTR increased at Pleven NCDC in 1973-1999, which agreed with the expected direction of change in the DTR.

Other measures of temperature variability have changed during the 20th century as well. Karl et al. (1995) reported a decrease in intraseasonal variability in the Northern Hemisphere based on a study of the 1-, 2-, 5-, 10-day and 30-day inter-period temperature differences. The authors found a significant decrease in the day-to-day variability for the US in 1911-1989 resulting mostly from spring and summer changes. Similar reduction in the intraseasonal variability of the DTR was identified in China during 1952-1989 and the FSU during 1935-1989, also stemming from the spring and summer changes (Karl et al., 1995). In this research the inter-period differences (IPDs) were expected to decrease, similar to the changes observed in the different regions around the world, and also in accordance with the increase in persistence in some circulation supertypes determined in this study. In agreement with the results of Karl et al. (1995), in 1951-1979, a decrease was evident for three stations for the annual, winter and spring 5- and 10-day inter-period differences (IPDs) for TMAX and TMIN. A single case of a significant positive trend was observed at Obraztsov Chiflick for the 10-day TMIN summer IPDs in the early period. An increase in the spring and winter intraseasonal variability was found during 1973-1999 in Bulgaria, based on the results for Pleven NCDC. However, these results might be influenced by the amount of missing data at Pleven NCDC or by other factors.

In parallel to the established rise in the extreme daily TMIN, the number of days with TMIN below 0°C (frost days) has decreased in many regions around

the world. Heino et al. (1999) observed this trend of the frost days in Northern and Central Europe during 1905-1995. Plummer et al. (1999), as summarized by Easterling et al. (2000a), also reported a decline in the number of frost days in Australia and New Zealand. Easterling et al. (2000b) determined a decreasing trend in the days with daily TMIN below 0°C in the US during 1910-1998. Frich et al. (2002) established the existence of a decreasing trend on a larger spatial scale, i.e. in the extra-tropics in the Northern Hemisphere during 1946-1999. Klein-Tank et al. (2003) confirmed the decline in the number of frost days for the entire European continent during the second half of the 20th century. Regarding the frost period severity, which represents the number of frost days per month, the expectation in this study was that the frost period severity would decrease or not change in 1951-1979, and would decrease in 1973-1999. In Bulgaria, the number of frost days has decreased significantly in spring during 1951-1979 as reflected in the decline in frost period severity in March for all stations and in April for Obraztsov Chiflick. Only in fall, an increase in the percentage of days in a month with TMIN below 0°C was observed at Obraztsov Chiflick and Pleven during the early period, in accordance with the stated hypothesis. The number of frost days did not change significantly during 1973-1999, based on the results from station Pleven NCDC, which is in disagreement with previous research and the hypothesized expectations of change.

The decrease in the number of frost days is closely related to the reduction in cold season length, and lengthening of the frost-free period. Cooter and LeDuc (1995) determined that the frost-free period started earlier in the

1990s than in the 1950s in the northeastern US, thus decreasing the cold season length. Domonkos et al. (1998) established that the cold period in Hungary and Poland started later and ended earlier during 1901-1993 resulting in a reduction of its length. In agreement with the expected changes in the daily minimum temperatures, the frost period duration was hypothesized not to change or to decrease in the early period, and to decrease during the late period. This research found that in Bulgaria, although the duration of the frost period did not change in the early period, it decreased by -13.2 days/decade in 1973-1999, in accordance with the stated hypothesis.

Other indices of temperature extremes have also changed during the past century in different regions of the world. Kysely (2002a) studied in depth heat waves characteristics at Prague-Klementum, one of the oldest meteorological stations in the Czech Republic. He reported that heat wave severity increased from 1910-1940 and from the late 1970s through the early 1990s. The author established also that heat waves were infrequent at the beginning of the 20th century and around 1980, while the frequency of heat waves was large in the 1940s to early 1950s and again in the 1990s. Domonkos et al. (2003) determined similar timing of periods of high and low frequency of extreme warm events in Central and Southern Europe during the 20th century. Hundecha and Bardossy (2005) found that in Western Germany heat wave duration increased for all seasons in 1958-2001. The frequency and duration of the heat waves were hypothesized in this study to decrease in 1951-1979 and increase during 1973-1999. This research found that in Bulgaria only the frequency and average

length of the heat waves have changed in the second half of the 20th century while the severity remained unchanged. During 1951-1979, in agreement with the findings of Kysely (2002a) and with the previously stated hypothesis, the frequency and average length of heat waves decreased for the interior stations. No changes were evident for the coastal station. The late period, 1973-1999, was characterized by a significant positive trend in occurrence and duration of the heat waves at Pleven NCDC, similar to the results reported by Kysely (2002a) and Hundecha and Bardossy (2005), and in accordance with the hypothesized expectations.

Regarding the characteristics of extreme cold events, Domonkos (1998) found a decrease in the length of extreme cold periods in 1901-1993 for Hungary. Later, Domonkos et al. (2003) reported that the highest frequency of extreme cold events was observed in the early 1940s and in the early 1960s in Central and Southern Europe. While the frequency and duration of the cold spells were hypothesized to increase in the early and decrease in the late period in this study, it was determined that in Bulgaria, the frequency and intensity of cold spells did not display any trends in the early or late periods at any station. The length of cold spells declined significantly only at Obraztsov Chiflick in 1951-1979 and increased at Pleven NCDC in 1973-1999, contrary to the stated hypothesis.

The hypotheses for the coolling and heating degree days stated earlier in this chapter were opposite, more specifically: in 1951-1979 the cooling degree days (CDDs) were expected to decrease and the heating degree days (HDDs) were hypothesized to increase. In 1973-1999, the CDDs were expected to

increase, while the HDDs should decrease. The earlier period, 1951-1979, was characterized by a significant decrease in the CDDs for Obraztsov Chiflick and Pleven, which also parallels the decline in frequency and length of the heat waves in summer at these stations. In accordance with the observed temperature trends in Bulgaria during 1973-1999 and in agreement with the stated hypotheses, the heating degree days exhibited a decrease while the cooling degree days displayed an increase.

10. Conclusions

Temperature extremes in Bulgaria were studied based on data for four stations from 1951-1979 and one station from 1973-1999, that were judged to have relatively homogeneous temperature time series. To investigate the changes in the temperature extremes, trend and extreme value analysis were performed on the series of indices of temperature extremes for the early and late periods. Due to the large amount of missing data at Pleven NCDC, the analyses outcomes for the late period are to be regarded with caution. The results from the trend and extreme value analyses are summarized below:

- The highest maximum temperatures do not change at all stations, or decrease in fall season at some of the stations (Pleven and Plovdiv) during 1951-1979. In contrast, the lowest annual minimum temperatures at some stations (Obraztsov Chiflick and Plovdiv), and the lowest spring minimum temperatures at all stations increase significantly during the same period. While no changes are

evident in the late period for the lowest minimum temperatures, the winter and spring highest maximum temperatures increased at Pleven NCDC.

- The daily temperature range (DTR) decreased in 1951-1979 for the year as a whole and in summer at two stations (Plovdiv and Pleven), and increased for one station (Varna) in spring. No changes were observed in the DTR in winter and fall. Significant increasing trends in annual, winter and summer DTR for the late period are evident based on Pleven NCDC.
- No change or negative trends for the 5- and 10-day inter-period differences (IPD) of TMAX and TMIN were evident on an annual basis and in winter and spring during 1951-1979. A positive trend was observed only at Obraztsov Chiflick for the summer 10-day TMIN IPD. No significant trends were identified in fall for any of the IPD indices. The late period (1973-1999) was characterized by significant positive trends in spring and winter intraseasonal variability.
- While the frequency and average length of heat waves decreased for the interior stations during 1951-1979, their intensity did not change. No trends were evident for the coastal station. In contrast, during 1973-1999, significant increasing trend was observed in the heat wave frequency and duration.

- The number and intensity of cold spells did not change during the early or late periods. The average length, however, decreased at Obraztsov Chiflick in the early period and increased at Pleven NCDC during the late period.
- Although the length of the frost period did not change during the early period, the frost period severity increased at the stations in northern Bulgaria (Obraztsov Chiflick and Pleven) in October. In addition, decreasing trends were evident in frost period severity at all stations in March and at Obraztsov Chiflick in April. In contrast, the 1973-1999 period was characterized by a significant decreasing trend in frost period duration which was not accompanied by any changes in frost period severity.
- During 1951-1979, the number of cooling degree days (CDDs) decreased at two stations (Obraztsov Chiflick and Pleven). An opposite trend was evident in 1973-1999, when the number of CDDs increased at Pleven NCDC.
- Changes in heating degree days (HDDs) were evident only during the late period. The significant negative trend indicates warming during the cooler part of the year.
- Most of the one-day TMAX and TMIN extremes series were fitted by the GEV-3, Weibull distribution, and in some cases the GEV-2, Fréchet distribution provided a better fit. No connection, however,

was found between the type of fitted distribution and the spatial distribution of the stations.

- The interior stations displayed highest return levels regardless of return period for the one-day TMAX extremes, and lowest estimated return levels for any return period for the TMIN extremes. Lowest estimated return levels for the TMAX extremes and highest for the TMIN extremes were evident for the coastal station Varna. The return levels at Pleven NCDC for 1973-1999 were found to be always higher than those at Pleven for the TMAX extremes on any time scale and lower than Pleven for the TMIN for the year, and all seasons, except for spring.
- The exceedances above or the deficiencies below a threshold were modeled in most cases using the GPD 3 beta distribution.
- The return levels for the exceedances above the 32°C threshold in summer were highest at Pleven for the early period. Compared to the early period the projected return levels were higher at Pleven NCDC.
- The return levels of the deficiencies below the -5°C were lowest at Plovdiv among the early period stations. Pleven NCDC featured lower estimated return levels regardless of return period compared to Pleven, corroborating the results obtained from the GEV fitting to the one-day extremes for TMIN.

- When comparing the results obtained from the GEV fit, to the results from the GPD fit for the summer and winter seasons, consistency by station was evident only in winter. The projected 10 and 20 year return levels were lower at all stations based on the GPD modeling.

Significant changes in some temperature extreme events have occurred in two sub-periods of the second half of the 20th century in Bulgaria. Many of these changes correspond to observed trends in these extremes on a larger spatial scale, i.e., regional or global. Higher consistency in the results across stations was observed for the heat waves and cold spells, than for the one-day temperature extremes. The heat waves and cold spells appear not to be as affected by changes in site characteristics or undetected inhomogeneities as the absolute highest or lowest temperature extremes, based on the statistic analyses performed.

CHANGES IN ATMOSPHERIC CIRCULATION OVER EUROPE AND THE RELATIONSHIP TO TEMPERATURE EXTREMES IN BULGARIA

Volume II

By

Galina Stefanova Guentchev

A DISSERTATION

Submitted to
Michigan State University
in partial fulfillment of the requirements
for the degree of

DOCTOR OF PHILOSOPHY

Department of Geography

2007

Chapter 4 Relationships between atmospheric circulation and temperature extreme events

1. Introduction

The temporal and spatial characteristics of extreme temperature events affect many sectors of the economy (e.g., agriculture, forestry, tourism, and the energy sector), the natural environment, and human well being. Uncovering the underlying relationships influencing the behavior of temperature extremes is of great interest for the planning of coping and mitigation measures during or in advance of disastrous temperature events. In recent years, many authors have studied extreme temperature events at different spatial scales (Changnon, 1993; Rohli and Keim, 1994; Hennessy and Pittock, 1995; DeGaetano, 1996; Salinger and Griffiths, 2001, for example). A number of researchers have sought to relate the characteristics of the atmospheric circulation to the occurrence and intensity of temperature extremes. More specifically, such studies for Europe have focused on Hungary (Domonkos, 1998), the Czech Republic (Huth, 2001; Kysely, 2002a), south central Europe (Domonkos et al., 2003), and Greece (Katsoulis et al., 2005).

1.1. Research to date

Several researchers have utilized existing atmospheric circulation catalogues or circulation indices to investigate the relationships between circulation and the occurrence and intensity of temperature extremes. For example, the Hess-Brezowsky catalogue has been used to relate circulation to temperature extreme events in central (Kysely, 2002a) and south central Europe

(Domonkos et al., 2003), and the Péczely macrocirculation types were related to extreme temperature anomalies in Hungary (Domonkos, 1998). In addition, Kysely (2002a) correlated the North Atlantic Oscillation Index with heat waves in the Czech Republic. Other researchers have simply visually compared daily surface and upper-level weather maps during spells of consecutive hot days with temperatures above 30°C in order to identify the atmospheric circulation associated with these events (Katsoulis et al., 2005)

Most authors agree that significant relationships exist between atmospheric circulation and the occurrence and intensity of temperature extreme events. Domonkos et al. (2003) found strong statistical relationships between the frequency of extreme temperature events, especially extreme cold events, in south central Europe and the occurrence of circulation patterns as defined by the Hess-Brezowsky catalogue. In an earlier study, Domonkos (1998) established that the frequent recurrence of certain Péczely macrocirculation types was more typical than the persistence of these types during periods of extreme temperature anomalies in Hungary. Kysely (2002a) determined that a significant positive relationship existed between the North Atlantic Oscillation Index in spring and the severity of heat waves in Prague-Klementinum in the following summer. The percentage of explained variation, however, was low. The specific circulation patterns favoring the occurrence of temperature extremes in these referenced studies are presented in detail in the next paragraph.

All researchers determined that temperature extremes occur preferably under specific circulation types. For the most part, these studies utilized

temperature extremes that exceed specified thresholds. One limitation of the previous studies is that they were based on a relatively small number of stations ranging from 3 stations used Domonkos (1998) to 16 stations used by Katsoulis et al. (2005). The results of these studies indicate certain similarities in the relationships between circulation and extreme temperature across central and eastern Europe. In Hungary, periods with wintertime extreme high temperatures occurred under the Hess Brezowsky "Southerly" and "Westerly" circulation types, while periods with extreme low temperatures were favored under anticyclonic conditions (Domonkos, 1998). Extreme low temperatures in south central Europe were observed also under anticyclonic patterns, along with the Hess Brezowsky "Northerlies", "Easterlies", and "Meridional" types (Domonkos et al., 2003). In summer, anticyclones over central or eastern Europe create favorable conditions for the occurrence of warm periods of extreme anomalies in Hungary (Domonkos, 1998). Anticyclones, as well as airflow from the south, contributed to the occurrence of heat waves in the Czech Republic (Kysely, 2002a) and in south central Europe (Domonkos et al., 2003). For Greece, the probability of a hot spell (42%) was highest when the Azores High was located over North Africa and extended towards the east-northeast, creating a westerly-northwesterly airflow over the region. In addition, heat waves in Greece were observed when: a) an Azores anticyclone extended towards western and central Europe and a secondary high pressure system was present in the central and eastern Mediterranean and over the Balkans; or b) when a weak upper-level ridge was situated over the Eastern Mediterranean; or c) when an anticyclone or a ridge

was located over the Mediterranean and a weak thermal low was evident over the Balkans (Katsoulis et al., 2005). Periods with low temperatures in summer occurred in Hungary under the influence of northerly airflow (Domonkos, 1998).

Although Velev (1996) pointed out that changes in the atmospheric circulation could possibly explain some of the observed changes in mean climatic conditions during the 20th century in Bulgaria, the relationships between the large-scale circulation patterns and temperature extremes have not been explored.

1.2. Review of methods applied in previous studies

Diverse methods have been used to relate the temporal and spatial characteristics of the large-scale circulation to temperature extreme events in the above studies. Some authors used conditional frequencies. For example, Domonkos (1998) determined the conditional frequencies of Péczely macrocirculation types (Péczely, 1957) during periods of extreme high or low temperatures. These conditional frequencies were compared to the unconditional (climatological) frequencies of the circulation types by applying a χ^2 test. The circulation types used in the analysis were agglomerated according to the prevailing airflow and the cyclonic/anticyclonic character of the circulation configuration. Kysely (2002a) grouped the circulation types from the Hess-Brezowsky catalogue into cyclonic and anticyclonic configurations over central Europe and into types with a generally increased or decreased heat wave frequency in his study of the heat waves in Prague-Klementinum. Subsequently, the author calculated frequencies of the agglomerated circulation types during

warm and cold decades. The warm and cold decades were identified according to heat wave severity at the Prague-Klementinum station. The conditional frequencies were compared to the climatological mean frequency of the circulation types for the period 1901-1997. To investigate the changes in the relationships between temperature extremes and the Hess-Brezowsky circulation types in their study focusing on south central Europe, Domonkos et al. (2003) computed conditional frequencies of temperature extremes under given circulation patterns and subjected the frequencies to trend analysis.

Correlation analysis has also been employed in the referenced studies of the relationships between temperature extremes and circulation patterns. Kysely (2002a), as mentioned above, correlated heat wave characteristics at Prague-Klementinum with the North-American Oscillation index. Domonkos et al. (2003) correlated the frequency of extreme temperature events and circulation patterns by season and for overlapping decades.

Another approach to assess the association between circulation configurations and temperature extremes, used in the cited studies, was to visually compare weather maps during extreme events. Katsoulis et al. (2005) examined daily surface and upper level weather charts in order to subjectively classify the synoptic situations conducive to the occurrence of hot spells in Greece.

In addition, authors have employed coefficients of relative frequency to investigate the relationships between the large-scale atmospheric circulation and temperature extremes. Huth et al. (2000) related circulation types obtained from

500 hPa geopotential fields to heat waves and dry spells based on observed and model simulated data. The authors calculated coefficients of the relative contribution of a circulation type to an extreme event. According to Huth et al. (2000), when the value of the coefficient is larger (smaller) than one, then the extreme events occur more (less) frequently under the respective circulation type in comparison to the case when no relation to the circulation exists.

1.3. Objectives

Given the lack of studies considering the relationships between atmospheric circulation and temperature extremes in Bulgaria, and to assess the performance of the circulation classification derived in Chapter 2, the aim of this portion of the research is twofold:

a) to explore the relationships between observed temperature extreme events in Bulgaria and the large-scale atmospheric circulation, and

b) to investigate the usefulness of the atmospheric circulation classification presented in Chapter 2, by addressing the question whether temperature extremes are more likely with different circulation types.

2. Method

The coefficient of relative frequency proposed by Huth et al. (2000) is used in this study. The choice of this method was based on the consideration

that, as pointed out by Huth et al. (2000), this coefficient, which will be referred to below as the 'contribution coefficient', allows for the assessment of the contribution of each circulation type to the occurrence of a given extreme event. As was pointed out in subsection 1.2., previous analyses often agglomerated circulation types into larger groups with higher rates of occurrence in order to obtain meaningful results. Given that the relative frequency of the circulation types varies between regions and seasons, Huth et al. (2000) proposed to include the relative frequency of the circulation patterns within the contribution coefficient. By considering the relative frequencies of the circulation types the method ensures that circulation types with low relative frequencies are given the same weight as the types with high relative frequency. This approach eliminates the need to agglomerate the circulation types as was done in past studies.

2.1. Calculation of the contribution coefficient

The contribution coefficient was calculated as follows:

a) for a given temperature index, the ratio between the number of extreme event days classified with a given circulation type and the total number of extreme event days is calculated. Using summer heat waves at Plovdiv as an example, the total number of days within heat waves for the period 1951-1979 is 943. The number of days within heat waves that had circulation type AL-PGL1sum is 106. The ratio of heat wave days with the AL-PGL1sum circulation type to the total number of heat wave days is (106/943)*100 or 11.2%.

b) the ratio between the event days (event days are the days when an extreme event was observed) with given circulation type and the total number of event days is subsequently divided by the relative frequency of the circulation type in order to permit comparisons across circulation types. The relative frequency is determined by dividing the number of days with a given circulation type by the total number of days for the period. Continuing with the example for Plovdiv, the ratio (11.2%) for type AL-PGL1sum was divided by the relative frequency of this circulation type during 1951-1979. Since the relative frequency of the AL-PGL1sum type is 7.3% (the number of days classified with AL-PGL1sum compared to the total number of summer days in 1951-1979), the contribution coefficient was found to be 11.2%/7.3% = 1.5. The coefficient is higher than one which, according to Huth et al. (2000), means that heat wave events occur more frequently under AL-PGL1sum type than if there were no relationship with the atmospheric circulation.

2.2. Indices of temperature extremes used in the analysis

Many diverse indices were employed in this study to investigate the historical temporal and spatial characteristics of the temperature extremes based on maximum (TMAX) and minimum (TMIN) daily temperatures in Bulgaria. As mentioned in subsection 1.1., past studies related circulation to only threshold indices of temperature extremes that were based either on absolute values or on

percentiles (for example, the 10^{th} and the 90^{th} percentiles of the TMAX or TMIN empirical distributions). In this study, the contribution coefficient was used to assess the importance of atmospheric circulation types occurring on days within heat waves in summer and cold spells in winter (i.e., threshold extremes), and also on days when the seasonal highest maximum and lowest minimum temperatures were observed (i.e., absolute or one-day extremes). The choice of only these indices was based on the supposition that the relationships between the extremes from the tails of the TMAX and TMIN distributions (as represented by the threshold and absolute extremes) and the circulation types would be sufficiently strong to be reflected well by the contribution coefficient.

Several groups of indices from Chapter 3 were not used in this analysis due either to the complicated nature of the calculation of some indices, their accumulation over their entire year, or the use of both TMAX and TMIN to calculate the index. For example, cooling and heating degree day indices are accumulated over the entire year and are based on daily mean (rather than TMAX or TMIN) temperature deviations from the human comfort level temperature of 65°F (18.3°C). The 5- and 10-day inter-period differences in maximum and minimum temperatures are calculated by subtracting 5- and 10-day means of maximum and minimum temperature anomaly values using overlapping periods with a one-day time step. The daily temperature range combines the daily maximum and minimum temperatures, and the circulation types affect TMAX and the TMIN differently. The frost period length and severity are also difficult to relate to the circulation types.

The relative frequencies of the circulation types used in the calculations of the contribution coefficients were not based on the overall 1951-2004 period, but rather on the length of the data periods for the different stations, i.e. 1951-1979 for Varna and Plovdiv, 1953-1979 for Obraztsov Chiflick, 1951-1979 excluding 1960 for Pleven and 1973-1999 excluding 1996 for Pleven NCDC. The time periods ending in 1979 are referred below to as the "early period", and the 1973-1999 period for Pleven NCDC is referred to as the "late period", similar to the nomenclature in Chapter 3.

3. Results

In this section, the emphasis is on the circulation types from the classification presented in Chapter 2 rather than on the supertypes, because the finer detail that is represented in the circulation types will allow for a better understanding of the complexity and nuances of the relationships between atmospheric circulation and temperature extremes. The contribution coefficients of the circulation types associated with temperature extreme events are discussed. The text is primarily focused on the circulation types that are identified as important to the occurrence of temperature extremes at all stations during the early period, since the consistency of the results allows for greater confidence in the identified relationships. In addition, changes in the contribution coefficients between the early and late periods at Pleven and Pleven NCDC are discussed. The results listed in the following tables are sorted depending on the number of

stations for which the circulation types contribute to the occurrence of temperature extremes during the early period.

3.1. Threshold temperature extremes

3.1.1. Summer heat waves

Most of the circulation types associated with the AL-PGLsum supertype, with the exception of the AL-PGLsum3 type contributed to the occurrence of heat waves in Bulgaria during the early period (Table 4-1). The similarities between these types include a large cyclonic area over Scandinavia (referred to here as the Arctic Low), an intense Azores High that extends over continental Europe, and a thermal cyclone over the Persian Gulf (Figure 2-18). Bulgaria is situated in an unorganized zone of higher pressure between the two cyclonic features and near the eastern edge of the Azores High. Weak pressure gradients are evident over the country resulting in weak winds.

Three other circulation types, ASR4sum, ASR5sum and AL-PGL/ASR/WPGLsum, were also found to be important for the occurrence of summertime heat waves at all the stations. The ASR5sum type features an extension of the Persian Gulf thermal low over the country, while the ASR4sum and the mixed AL-PGL/ASR/WPGLsum types display lower pressure, perhaps a thermal low, over central and western Europe. The latter thermal low feature is located within a broader area of surface ridge extending from the southwestern portion of the analysis domain to the northeast over Scandinavia and the Russian Plain. The main circulation types contributing to the occurrence of heat waves at

Pleven for the early period are also important at Pleven NCDC during the late period.

In contrast, all of the WPGLsum types were not conducive for the occurrence of heat waves. Most of the WPGL types, due to the configuration of pressure features, are associated with northerly low-level airflow over Bulgaria. Under some types (i.e., WPGL2sum and WPGL4sum), the pressure gradient and the airflow are quite weak. In addition, heat waves were not observed under the ASR3sum type, which also is characterized by northerly or northeasterly airflow over Bulgaria.

Table 4-1 Contribution coefficients (CCs) for circulation types during summertime heat waves.
Values in bold are CCs > 1 at all stations during 1951-1979; underlined values are CCs > 1 at any station. The values on the second line of each cell of the table are the absolute frequency (days), and, in parentheses, the ratio (expressed as a percent) of the absolute frequency of a particular circulation type during a summertime heat wave to the total number of summertime heat wave days for the station.

Station	Obraztsov Chiflick (OC)	Varna (VN)	Plovdiv (PD)	Pleven (PL)	Pleven NCDC (PL NCDC)
AL-PGL1sum	**2.0**	**1.4**	**1.5**	**1.8**	1.6
	61 (14.5%)	18 (10.4%)	106 (11.2%)	89 (12.4%)	51 (6.0%)
AL-PGL2sum	**1.3**	**1.1**	**1.3**	**1.3**	1.5
	44 (10.5%)	14 (8.1%)	90 (9.5%)	68 (9.5%)	21 (2.5%)
AL-PGL4sum	**1.1**	**1.0**	**1.1**	**1.0**	1.1
	26 (6.2%)	10 (5.8%)	63 (6.7%)	44 (6.1%)	65 (7.6%)
AL-PGL5sum	**2.1**	**1.3**	**1.5**	**1.8**	1.6
	39 (9.3%)	10 (5.8%)	65 (6.9%)	60 (8.4%)	44 (5.2%)
AL-PGL6sum	**1.9**	**1.3**	**1.4**	**1.8**	1.3
	54 (12.8%)	15 (8.7%)	87 (9.2%)	89 (12.4%)	56 (6.6%)

Table 4-1 Continued

Station	Obraztsov Chiflick (OC)	Varna (VN)	Plovdiv (PD)	Pleven (PL)	Pleven NCDC (PL NCDC)
ASR4sum	**1.5**	**1.6**	**1.3**	**1.1**	1.1
	43 (10.2%)	19 (11.0%)	83 (8.8%)	5.3 (7.4%)	32 (3.8%)
ASR5sum	**1.2**	**2.2**	**1.2**	**1.1**	1.5
	28 (6.7%)	21 (12.1%)	62 (6.6%)	42 (5.8%)	65 (7.6%)
AL-PGL/ ASR/WPGLsum	**1.1**	**1.3**	**1.2**	**1.0**	1.2
	23 (5.5%)	12 (6.9%)	59 (6.3%)	40 (5.6%)	62 (7.3%)
AL-PGL3sum	0.9	1.1	1.0	0.8	1.0
	20 (4.8%)	10 (5.8%)	50 (5.3%)	30 (4.2%)	59 (6.9%)
ASR1sum	0.3	1.1	0.7	0.5	1.0
	9 (2.1%)	11 (6.4%)	39 (4.1%)	23 (3.2%)	47 (5.5%)

Table 4-1 Continued

Station	Obraztsov Chiflick (OC)	Varna (VN)	Plovdiv (PD)	Pleven (PL)	Pleven NCDC (PL NCDC)
ASR2sum	0.6	1.3	0.9	0.9	1.1
	13 (3.1%)	12 (6.9%)	48 (5.1%)	37 (5.2%)	56 (6.6%)
ASR6sum	0.7	0.7	0.9	1.0	1.0
	12 (2.9%)	5 (2.9%)	32 (3.4%)	28 (3.9%)	39 (4.6%)
ASR3sum	0.3	0.4	0.6	0.6	0.9
	9 (2.1%)	5 (2.9%)	35 (3.7%)	29 (4.0%)	50 (5.9%)
WPGL1sum	0.0	0.0	0.1	0.1	0.1
	0 (0.0%)	0 (0.0%)	2 (0.2%)	2 (0.3%)	3 (0.4%)
WPGL2sum	0.5	0.5	0.9	0.7	1.2
	8 (1.9%)	4 (2.3%)	38 (4.0%)	23 (3.2%)	73 (8.6%)

Table 4-1 Continued

Station	Obraztsov Chiflick (OC)	Varna (VN)	Plovdiv (PD)	Pleven (PL)	Pleven NCDC (PL NCDC)
WPGL3sum	0.6	0.0	0.4	0.4	0.5
	11 (2.6%)	0 (0.0%)	16 (1.7%)	14 (1.9%)	17 (2.0%)
WPGL4sum	0.7	0.0	0.7	0.8	0.8
	10 (2.4%)	0 (0.0%)	22 (2.3%)	18 (2.5%)	41 (4.8%)
WPGL5sum	0.6	0.5	0.6	0.6	0.7
	11 (2.6%)	4 (2.3%)	26 (2.8%)	20 (2.8%)	38 (4.5%)
WPGL6sum	0.3	0.4	0.5	0.3	0.6
	5 (1.2%)	3 (1.7%)	20 (2.1%)	9 (1.3%)	34 (4.0%)

3.1.2. Winter cold spells

Four circulation types (SH-ML1win, SH-ML2win, ML-NAH/SH-MLwin and ML-NAH/EHwin) contributed to the occurrence of cold spells at all stations (Table 4-2, Figure 2-8). Under types SH-ML1win and ML-NAH/EHwin, Bulgaria is influenced by strong anticyclones centered over Scandinavia and the Russian Plain for the former, or located over western and central Europe for the latter. The anticyclonic conditions create optimal setting for intense radiational cooling of the surface air during the night and the persistence of low minimum temperatures. Also, surface airflow over Bulgaria is likely easterly or northeasterly, which would contribute to cold air transfer from the interior of the Asian continent or from northern Europe and the Arctic. The SH-ML2win and ML-NAH/SH-MLwin types are both characterized by a strong anticyclone over

Scandinavia and Russia and a cyclone over the Mediterranean, Iberian Peninsula, and North Africa. Bulgaria appears to be dominated by the easterly airflow associated with the cold anticyclone, whereas the warmer southerly airflow associated with the Mediterranean cyclone is confined to southwestern Europe. Almost all of the circulation types under which cold spells occurred at Pleven in the early period were also found to be important for the occurrence of cold spells at Pleven NCDC during the late period. An exception is type ML-NAH/SH-MLwin which did not contribute to occurrence of cold spells during the late period, but was important for the early period.

Cold spells did not occur with circulation types AL-VB3win and IL1win. Under the former type, Bulgaria is influenced by a modified marine westerly airflow around the northern edge of a strong Azores High, extending from the tropical Atlantic over southwestern Europe and north Africa. Under the latter type, a southerly flow influences the country. Interestingly, circulation type SH-ML3win was associated with cold spells only at the three northern stations (Obraztsov Chiflick, Pleven and Varna). The type is characterized by a large but not very intense depression over the British Isles and a high pressure center over Russia extending over North Africa. Plovdiv, in southern Bulgaria, appears to be primarily influenced by a foehn effect from the easterly-southeasterly airflow due to the existence of a high mountainous area to the south of the city, whereas northern Bulgaria experiences directly the easterly airflow from the cold interior of the Asian continent.

Table 4-2 Contribution coefficients (CCs) for circulation types during wintertime cold spells.
Values in bold are CCs > 1 at all stations during 1951-1979; underlined values are CCs > 1 at any station. The values on the second line of each cell of the table are the absolute frequency (days), and, in parentheses, the ratio (expressed as a percent) of the absolute frequency of a particular circulation type during a wintertime cold spell to the total number of wintertime cold spell days for the station.

Station	Obraztsov Chiflick (OC)	Varna (VN)	Plovdiv (PD)	Pleven (PL)	Pleven NCDC (PL NCDC)
SH-ML1win	**1.4**	**2.0**	**1.6**	**1.3**	1.9
	89 (13.2%)	50 (17.7%)	53 (14.4%)	66 (11.3%)	68 (15.7%)
SH-ML2win	**1.3**	**1.1**	**1.2**	**1.3**	1.6
	54 (8.0%)	19 (6.7%)	28 (7.6%)	47 (8.0%)	24 (5.5%)
ML-NAH/ SH-MLwin	**1.1**	**1.1**	**1.0**	**1.2**	0.7
	61 (9.0%)	26 (9.2%)	29 (7.9%)	56 (9.6%)	16 (3.7%)
ML-NAH/EHwin	**1.5**	**2.0**	**1.5**	**1.6**	1.7
	89 (13.2%)	48 (17.0%)	46 (12.5%)	78 (13.3%)	68 (15.7%)
SH-ML3win	1.2	1.4	0.8	1.3	0.8
	53 (7.9%)	25 (8.9%)	18 (4.9%)	51 (8.7%)	13 (3.0%)
AL-VB1win	0.9	1.1	0.8	1.0	1.0
	25 (3.7%)	13 (4.6%)	12 (3.3%)	24 (4.1%)	45 (10.4%)
EH1win	1.0	1.3	0.9	0.9	0.9
	39 (5.8%)	20 (7.1%)	18 (4.9%)	29 (5.0%)	42 (9.7%)
ML-NAH1win	1.0	0.5	0.9	1.1	1.2
	44 (6.5%)	10 (3.5%)	22 (6.0%)	43 (7.4%)	26 (6.0%)
IL2win	1.0	0.6	1.2	0.9	0.6
	45 (6.7%)	11 (3.9%)	30 (8.2%)	33 (5.6%)	23 (5.3%)
ML-NAH2win	0.9	0.7	1.0	0.9	1.2
	45 (6.7%)	15 (5.3%)	29 (7.9%)	43 (7.4%)	33 (7.6%)

Table 4-2 Continued

Station	Obraztsov Chiflick (OC)	Varna (VN)	Plovdiv (PD)	Pleven (PL)	Pleven NCDC (PL NCDC)
AL-VB2win	0.8	0.4	1.0	0.7	0.6
	31 (4.6%)	7 (2.5%)	22 (6.0%)	26 (4.4%)	17 (3.9%)
EH2win	0.8	1.0	0.6	0.8	0.9
	45 (6.7%)	24 (8.5%)	17 (4.6%)	41 (7.0%)	23 (5.3%)
AL-VB3win	0.4	0.4	0.7	0.5	0.4
	17 (2.5%)	7 (2.5%)	15 (4.1%)	17 (2.9%)	16 (3.7%)
IL1win	0.6	0.3	0.8	0.6	0.8
	38 (5.6%)	7 (2.5%)	28 (7.6%)	31 (5.3%)	20 (4.6%)

3.2. Absolute temperature extremes

The yearly absolute extremes of maximum and minimum temperature for each season can also be related to the circulation types. A limitation of this part of the analysis is that, as there is only one value per year for any season and the study periods are relatively short, the contribution coefficients are based on only a small number of values. Thus, the results of this portion of the analysis need to be considered with caution. Only the circulation types which favor or do not favor the occurrence of absolute extremes at all stations during the early period are discussed. The comparison between the early and late periods for Pleven and Pleven NCDC is limited to only the general correspondence between the circulation types.

3.2.1. Extreme maximum temperatures

For any season and at all stations, the highest values of TMAX during 1951-1979 occurred predominantly under the influence of southerly or southwesterly airflow over Bulgaria. Circulation types associated with the extreme warm temperatures that are characterized by distinct surface low pressure systems include IL1win, SH-ML1spr, SH-ML3spr, AL-VB/ELspr, and PGL4fal (Table 4-3). The composites for IL1win, SH-ML1spr and PGL4fal all feature a strong Icelandic Low centered over the British Isles. Bulgaria is located to the southeast of the Icelandic Low, and the surface airflow around the cyclonic feature is directed from the south-southwest over the country. A distinct low pressure center is also evident for circulation type SH-ML3spr, although the low is located over central and south central Europe. Under this type, Bulgaria appears to be located within the warm sector of the low pressure system and experiences southerly surface airflow. Under the AL-VB/ELspr type Bulgaria is located within a trough of lower pressure extending from Scandinavia to North Africa. One interpretation is that the high temperatures are associated with southerly airflow ahead (east) of the trough axis.

A circulation type that appears to be responsible for wintertime warm absolute extremes is AL-VB2win. In this case, the surface anticyclone in the western portion of the Voeikov Belt is weaker than normal, and the Arctic Low, although intense, is confined to extreme Scandinavia and northern Europe. Bulgaria experiences either weak or modified marine westerly airflow around the northern edge of the surface anticyclone located over western Mediterranean and north Africa. The only summertime pattern with contribution coefficients >1 at

all four stations is ASR2sum. Bulgaria is located within a trough of lower pressure extending northwestward from the thermal low over the Persian Gulf and Arabian Peninsula. The PGL1fal type, which contributes to the occurrence of extreme high temperatures in fall, is similar to the ASR2sum type, and features negative pressure anomalies extending northwestward over Bulgaria from the Arabian Peninsula.

A number of circulation types are infrequently associated with seasonal extremes of TMAX. Two wintertime circulation types with contribution coefficients <1 at all stations are AL-VB1win and EH2win (Table 4-3). For both types, a strong anticyclone is centered over the Iberian Peninsula and western Europe, and northerly surface airflow is evident over Bulgaria. Another circulation type rarely associated with wintertime extreme warm temperatures is SH-ML1win. Under this circulation type, Bulgaria is influenced by a strong anticyclone over Scandinavia and northern Russia, and the surface airflow is predominately northeasterly and easterly. Type EH1win, which also is infrequently associated with warm extreme temperatures in winter, is characterized by a weak low pressure system over the eastern Mediterranean. Bulgaria lies to the north of the surface low and experiences easterly and northeasterly airflow from the Russian Plain and western Asia.

Four of the springtime circulation types are rarely associated with extreme warm temperatures. For both AL-VB1spr and AL-VB3spr, surface anticyclones either over eastern Atlantic and extreme western Europe (for AL-VB1spr) or over western and central Europe (for AL-VB3spr) dominate the composite pressure

patterns. Northerly surface airflow over Bulgaria is characteristic for both circulation types. It is more difficult to explain why the ASR3spr and IL2spr circulation types are rarely associated with extreme warm temperatures, as Bulgaria on both composite maps lies within an area of weak airflow. Under IL2spr, however, the country is situated in a col between two high pressure systems. Around the southern edge of the high pressure system located to the east of Bulgaria, the airflow is easterly and likely affects the country. In summer, extreme warm temperatures are infrequently reported when the Persian Gulf low is weaker than normal as seen in the WPG1sum, WPGL2sum, ASR3sum, and ASR6sum circulation types. For all these types, surface airflow over Bulgaria is weak.

Type SH-ML1fal, like the similar wintertime pattern (i.e., SH-ML1win), rarely is associated with extreme warm temperatures in fall. Other fall patterns that are not conducive for warm extreme temperatures are AL-VB1fal, IL/AL-VBfal, and SH-ML2fal, all of which have northerly surface airflow over Bulgaria. For the AL-VB1fal circulation type, a strong anticyclone is located over western and central Europe. An anticyclone is also evident for SH-ML2fal type, although it is displaced eastward over eastern Europe. Under the AL-VB/ILfal type, Bulgaria located on the western side of surface trough extending from Scandinavia to the Mediterranean Sea. In addition in fall, extreme high temperatures are not observed under AL-VB2fal, IL1fal, IL2fal and SH-ML/ILfal. All of these types indicate easterly surface airflow from Asia over the country.

When the contribution coefficients for the early period at Pleven are compared to the late period at Pleven NCDC, the circulation types both favoring and not favoring extreme warm temperatures correspond well.

Table 4-3 Contribution coefficients for the circulation types favoring/not favoring the occurrence of highest daily maximum temperatures in each season
Values in bold are CCs > 1 at all stations during 1951-1979; underlined values are CCs > 1 at any station. The values on the second line of each cell of the table are the absolute frequency (days), and, in parentheses, the ratio (expressed as a percent) of the absolute frequency of a particular circulation type during an extreme temperature event to the total number of extreme temperature event days for the station.

WINTER					
Station	Obraztsov Chiflick (OC)	Varna (VN)	Plovdiv (PD)	Pleven (PL)	Pleven NCDC (PL NCDC)
IL1win	**3.4**	**3.0**	**1.8**	**2.8**	2.8
	9 (33.3%)	10 (29.4%)	5 (17.9%)	7 (26.9%)	5 (17.2%)
AL-VB2win	**1.3**	**2.8**	**1.7**	**2.4**	1.7
	2 (7.4%)	6 (17.6%)	3 (10.7%)	4 (15.4%)	3 (10.3%)
ML-NAH1win	1.1	1.8	1.6	0.6	0.7
	2 (7.4%)	4 (11.8%)	3 (10.7%)	1 (3.8%)	1 (3.4%)
ML-NAH2win	1.9	1.2	0.9	1.9	0.6
	4 (14.8%)	3 (8.8%)	2 (7.1%)	4 (15.4%)	1 (3.4%)
ML-NAH/ SH-MLwin	1.4	1.5	2.2	0.5	0.7
	3 (11.1%)	4 (11.8%)	5 (17.9%)	1 (3.8%)	1 (3.4%)
IL2win	0.0	0.9	1.6	1.2	1.1
	0 (0.0%)	2 (5.9%)	3 (10.7%)	2 (7.7%)	3 (10.3%)

Table 4-3 Continued

WINTER					
Station	Obraztsov Chiflick (OC)	Varna (VN)	Plovdiv (PD)	Pleven (PL)	Pleven NCDC (PL NCDC)
SH-ML2win	1.2	0.5	0.6	1.9	1.9
	2 (7.4%)	1 (2.9%)	1 (3.6%)	3 (11.5%)	2 (6.9%)
SH-ML3win	1.1	0.0	0.5	1.2	2.8
	2 (7.4%)	0.(0.0%)	1 (3.6%)	2 (7.7%)	3 (10.3%)
ML-NAH/EHwin	0.0	0.3	1.3	0.0	0.0
	0 (0.0%)	1 (2.9%)	3 (10.7%)	0 (0.0%)	0 (0.0%)
AL-VB1win	0.0	0.7	0.0	0.0	1.0
	0 (0.0%)	1 (2.9%)	0 (0.0%)	0 (0.0%)	3 (10.3%)
AL-VB3win	0.6	0.5	0.0	0.6	2.1
	1 (3.7%)	1 (2.9%)	0 (0.0%)	1 (3.8%)	6 (20.7%)
SH-ML1win	0.8	0.0	0.0	0.0	0.4
	2 (7.4%)	0 (0.0%)	0 (0.0%)	0 (0.0%)	1 (3.4%)
EH1win	0.0	0.0	0.0	0.0	0.0
	0 (0.0%)	0 (0.0%)	0 (0.0%)	0 (0.0%)	0 (0.0%)
EH2win	0.0	0.4	0.9	0.4	0.0
	0 (0.0%)	1 (2.9%)	2 (7.1%)	1 (3.8%)	0 (0.0%)

Table 4-3 Continued

SPRING					
Station	Obraztsov Chiflick (OC)	Varna (VN)	Plovdiv (PD)	Pleven (PL)	Pleven NCDC (PL NCDC)
SH-ML1spr	**1.2**	**1.6**	**2.2**	**2.2**	1.0
	2 (7.1%)	3 (10.0%)	4 (13.3%)	4 (12.9%)	2 (6.9%)
SH-ML3spr	**2.2**	**1.7**	**1.3**	**2.5**	1.4
	5 (17.9%)	4 (13.3%)	3 (10.0%)	6 (19.4%)	3 (10.3%)
AL-VB/ELspr	**2.3**	**1.8**	**1.4**	**1.0**	1.9
	6 (21.4%)	5 (16.7%)	4 (13.3%)	3 (9.7%)	5 (17.2%)
IL1spr	1.5	0.9	1.4	1.8	2.0
	3 (10.7%)	2 (6.7%)	3 (10.0%)	4 (12.9%)	4 (13.8%)
EL2spr	2.5	0.6	2.4	2.3	3.7
	4 (14.3%)	1 (3.3%)	4 (13.3%)	4 (12.9%)	5 (17.2%)
ASR1spr	0.6	1.6	1.1	1.1	1.3
	1 (3.6%)	3 (10.0%)	2 (6.7%)	2 (6.5%)	3 (10.3%)
AL-VB4spr	1.9	0.0	0.0	1.7	1.0
	2 (7.1%)	0 (0.0%)	0 (0.0%)	2 (6.5%)	1 (3.4%)
AL-VB2spr	0.0	1.0	0.0	0.0	0.0
	0 (0.0%)	2 (6.7%)	0 (0.0%)	0 (0.0%)	0 (0.0%)
ASR2spr	0.6	0.6	1.2	0.6	0.0
	1 (3.6%)	1 (3.3%)	2 (6.7%)	1 (3.2%)	0 (0.0%)
IL/ELspr	0.6	0.5	0.0	1.1	0.0
	1 (3.6%)	1 (3.3%)	0 (0.0%)	2 (6.5%)	0 (0.0%)

Table 4-3 Continued

SPRING					
Station	Obraztsov Chiflick (OC)	Varna (VN)	Plovdiv (PD)	Pleven (PL)	Pleven NCDC (PL NCDC)
EL/ILspr	0.0	0.7	1.4	0.7	0.8
	0 (0.0%)	1 (3.3%)	2 (6.7%)	1 (3.2%)	1 (3.4%)
SH-ML2spr	0.0	2.0	0.5	0.0	0.0
	0 (0.0%)	4 (13.3%)	1 (3.3%)	0 (0.0%)	0 (0.0%)
EL1spr	0.9	0.9	1.8	0.9	1.9
	1 (3.6%)	1 (3.3%)	2 (6.7%)	1 (3.2%)	3 (10.3%)
ASR3spr	0.5	0.0	0.5	0.5	0.5
	1 (3.6%)	0 (0.0%)	1 (3.3%)	1 (3.2%)	1 (3.4%)
AL-VB1spr	0.0	0.0	0.0	0.0	0.0
	0 (0.0%)	0 (0.0%)	0 (0.0%)	0 (0.0%)	0 (0.0%)
IL2spr	0.0	0.0	0.8	0.0	0.0
	0 (0.0%)	0 (0.0%)	1 (3.3%)	0 (0.0%)	0 (0.0%)
AL-VB3spr	0.8	0.7	0.7	0.0	0.0
	1 (3.6%)	1 (3.3%)	1 (3.3%)	0 (0.0%)	0 (0.0%)
IL/ASRspr	0.0	0.9	0.0	0.0	1.0
	0 (0.0%)	1 (3.3%)	0 (0.0%)	0 (0.0%)	1 (3.4%)

Table 4-3 Continued

SUMMER					
Station	Obraztsov Chiflick (OC)	Varna (VN)	Plovdiv (PD)	Pleven (PL)	Pleven NCDC (PL NCDC)
ASR2sum	**2.9**	**1.1**	**2.9**	**2.8**	1.5
	5 (16.1%)	2 (6.3%)	5 (15.6%)	5 (15.6%)	3 (9.1%)
AL-PGL1sum	2.2	0.9	3.0	2.3	2.4
	5 (16.5%)	2 (6.3%)	7 (21.9%)	5 (15.6%)	3 (9.1%)
AL-PGL5sum	2.9	0.7	1.4	2.0	3.7
	4 (12.9%)	1 (3.1%)	2 (6.3%)	3 (9.4%)	4 (12.1%)
WPGL5sum	1.4	0.7	1.3	1.3	0.9
	2 (6.5%)	1 (3.1%)	2 (6.3%)	2 (6.3%)	2 (6.1%)
WPGL4sum	2.8	0.9	0.9	1.9	1.0
	3 (9.7%)	1 (3.1%)	1 (3.1%)	2 (6.3%)	2 (6.1%)
ASR4sum	0.5	3.3	1.9	0.5	0.0
	1 (3.2%)	7 (21.9%)	4 (12.5%)	1 (3.1%)	0 (0.0%)
AL-PGL6sum	0.9	1.8	0.5	1.8	1.2
	2 (6.5%)	4 (12.5%)	1 (3.1%)	4 (12.5%)	2 (6.1%)
AL-PGL/ ASR/WPGLsum	1.3	0.6	0.0	1.2	2.9
	2 (6.5%)	1 (3.1%)	0 (0.0%)	2 (6.3%)	6 (18.2%)
ASR1sum	0.0	1.6	0.5	0.5	0.0
	0 (0.0%)	3 (9.4%)	1 (3.1%)	1 (3.1%)	0 (0.0%)
AL-PGL3sum	0.0	1.8	0.6	0.0	0.0
	0 (0.0%)	3 (9.4%)	1 (3.1%)	0 (0.0%)	0 (0.0%)

Table 4-3 Continued

SUMMER					
Station	Obraztsov Chiflick (OC)	Varna (VN)	Plovdiv (PD)	Pleven (PL)	Pleven NCDC (PL NCDC)
AL-PGL4sum	0.6	0.5	1.1	0.5	0.9
	1 (3.2%)	1 (3.1%)	2 (6.3%)	1 (3.1%)	2 (6.1%)
ASR5sum	0.6	1.1	0.6	0.6	1.7
	1 (3.2%)	2 (6.3%)	1 (3.1%)	1 (3.1%)	3 (9.1%)
WPGL3sum	1.5	0.0	0.0	0.7	0.8
	2 (6.5%)	0 (0.0%)	0 (0.0%)	1 (3.1%)	1 (3.0%)
WPGL6sum	0.8	0.7	0.7	1.4	0.0
	1 (3.2%)	1 (3.1%)	1 (3.1%)	2 (6.3%)	0 (0.0%)
WPGL1sum	0.0	0.0	0.0	0.0	0.0
	0 (0.0%)	0 (0.0%)	0 (0.0%)	0 (0.0%)	0 (0.0%)
WPGL2sum	0.8	0.0	0.0	0.7	0.8
	1 (3.2%)	0 (0.0%)	0 (0.0%)	1 (3.1%)	2 (6.1%)
AL-PGL2sum	0.0	0.4	0.8	0.0	1.8
	0 (0.0%)	1 (3.1%)	2 (6.3%)	0 (0.0%)	1 (3.0%)
ASR3sum	0.0	0.9	0.9	0.5	0.4
	0 (0.0%)	2 (6.3%)	2 (6.3%)	1 (3.1%)	1 (3.0%)
ASR6sum	0.8	0.0	0.0	0.0	0.7
	1 (3.2%)	0 (0.0%)	0 (0.0%)	0 (0.0%)	1 (3.0%)

Table 4-3 Continued

FALL					
Station	Obraztsov Chiflick (OC)	Varna (VN)	Plovdiv (PD)	Pleven (PL)	Pleven NCDC (PL NCDC)
PGL1fal	**3.2**	**2.7**	**3.1**	**3.1**	1.4
	12 (38.7%)	11 (33.3%)	12 (38.7%)	12 (37.5%)	1 (3.7%)
PGL4fal	**1.8**	**1.7**	**1.8**	**3.1**	3.7
	4 (12.9%)	4 (12.1%)	4 (12.9%)	7 (21.9%)	6 (22.2%)
PGL2fal	1.3	1.2	1.2	0.9	1.6
	4 (12.9%)	4 (12.1%)	4 (12.9%)	3 (9.4%)	4 (14.8%)
PGL3fal	0.5	2.4	1.5	0.5	0.8
	1 (3.2%)	5 (15.2%)	3 (9.7%)	1 (3.1%)	2 (7.4%)
PGL5fal	1.7	0.8	0.9	1.7	5.2
	4 (12.9%)	2 (6.1%)	2 (6.5%)	4 (12.5%)	6 (22.2%)
SH-ML3fal	1.5	0.9	1.0	0.9	1.4
	3 (9.7%)	2 (6.1%)	2 (6.5%)	2 (6.3%)	2 (7.4%)
AL-VB3fal	0.5	1.0	1.0	0.5	0.5
	1 (3.2%)	2 (6.1%)	2 (6.5%)	1 (3.1%)	1 (3.7%)
PGL6fal	0.9	0.4	0.9	0.9	1.2
	2 (6.5%)	1 (3.0%)	2 (6.5%)	2 (6.3%)	2 (7.4%)
AL-VB/ILfal	0.0	0.6	0.0	0.0	1.9
	0 (0.0%)	1 (3.0%)	0 (0.0%)	0 (0.0%)	3 (11.1%)
IL1fal	0.0	0.0	0.0	0.0	0.0
	0 (0.0%)	0 (0.0%)	0 (0.0%)	0 (0.0%)	0 (0.0%)
IL2fal	0.0	0.7	0.0	0.0	0.0
	0 (0.0%)	1 (3.0%)	0 (0.0%)	0 (0.0%)	0 (0.0%)

Table 4-3 Continued

FALL					
Station	Obraztsov Chiflick (OC)	Varna (VN)	Plovdiv (PD)	Pleven (PL)	Pleven NCDC (PL NCDC)
SH-ML1fal	0.0	0.0	0.0	0.0	0.0
	0 (0.0%)	0 (0.0%)	0 (0.0%)	0 (0.0%)	0 (0.0%)
SH-ML2fal	0.0	0.0	0.0	0.0	0.0
	0 (0.0%)	0 (0.0%)	0 (0.0%)	0 (0.0%)	0 (0.0%)
SH-ML/ILfal	0.0	0.0	0.0	0.0	0.0
	0 (0.0%)	0 (0.0%)	0 (0.0%)	0 (0.0%)	0 (0.0%)
IL/AL-VBfal	0.0	0.0	0.0	0.0	0.0
	0 (0.0%)	0 (0.0%)	0 (0.0%)	0 (0.0%)	0 (0.0%)
AL-VB1fal	0.0	0.0	0.0	0.0	0.0
	0 (0.0%)	0 (0.0%)	0 (0.0%)	0 (0.0%)	0 (0.0%)
AL-VB2fal	0.0	0.0	0.0	0.0	0.0
	0 (0.0%)	0 (0.0%)	0 (0.0%)	0 (0.0%)	0 (0.0%)

3.2.2. Extreme minimum temperatures

Most of the circulation types with contribution coefficients >1 at all stations for the series of lowest minimum temperature by season during 1951-1979 can be combined in four large groups (Table 4-4). The first group includes circulation types with surface anticyclones over central Europe and positive pressure anomalies extending into Bulgaria. Circulation types AL-VB3spr, IL/ASRspr, SH-ML2fal and AL-VB1fal fall within this group. All are characterized by generally northerly airflow over Bulgaria and were identified above as being least favorable for the occurrence of warm extreme temperatures.

For the second group of circulation types responsible for extreme minimum temperatures in Bulgaria, an anticyclone is evident over the Russian Plain or Scandinavia and extends south or southwestward over Bulgaria. The composite pressure gradients are weak for these circulation types suggesting weak winds. The surface airflow is often easterly. Types that fall in this group include EL/ILspr, IL2spr, ASR2spr, and IL1fal.

The third group consists of circulation types with easterly or northeasterly surface airflow over Bulgaria. These circulation types vary considerably in their configuration. A low pressure system is located over the western Mediterranean and an extension of an anticyclone is found over the Black and Caspian seas for ML-NAH1win, which is the only wintertime circulation type with contribution coefficient >1 at all stations during the early period. Bulgaria is likely experiencing easterly airflow north of a warm front. Under SH-ML1fal, Bulgaria also appears to be located in easterly or southeasterly airflow north of a warm front, although for this circulation type the surface low pressure system is located over the central Mediterranean. On the other hand, the northeasterly airflow seen for type ASR1spr is caused by an anticyclone located over the British Isles. For the ASR2sum circulation type, the Azores High extends northeastward over western Europe, and Bulgaria, which is located southeast of the anticyclone center, experiences northeasterly airflow around this anticyclone.

Finally, extreme minimum temperatures in summer occur when the Persian Gulf low is weaker than normal, as seen by the contribution coefficients

>1 for the WPGL1sum, WPGL2sum, and WPGL3sum circulation types. For these types, airflow over Bulgaria is generally weak.

In addition, a single circulation type, not belonging to the discussed four groups, that also contributes to the occurrence of extreme low temperatures is the IL3fal. This type features a surface anticyclone centered over Bulgaria. The anticyclonic conditions typically bring clear skies and lower humidity, thus creating optimal conditions for intense radiative cooling during the night and the occurrence of extreme minimum temperatures.

Circulation type ASR2sum merits some further discussion as the contribution coefficients were >1 for both the occurrence of extreme minimum temperatures and extreme maximum temperatures in summer. The main pressure feature of this type, the large Azores High anticyclone, expands over western Europe. Temperatures in Bulgaria depend on the specific position of the extending anticyclone over Europe. The farther north and west the center of the anticyclone, the more likely that Bulgaria will be located within a broad area of thermal low pressure centered on the Arabian Peninsula and North Africa and experience warm temperatures. However, if the anticyclone is displaced somewhat to the southeast, the airflow over the country will be northeasterly from Scandinavia and northern Russia, and Bulgaria will experience cooler temperatures.

Extreme low minimum temperatures are not observed in any season when the surface airflow is directed from the south over Bulgaria. Examples of circulation types that produce airflow from southerly directions include SH-

ML1spr, SH-ML3spr, IL1spr, EL1spr, and SH-ML3fal. For types SH-ML1spr and IL1spr, a large Icelandic Low is centered to the west of the British Isles. Bulgaria is situated to the southeast of the cyclonic area and is influenced by a southerly airflow. Types EL1spr, SH-ML3spr and SH-ML3fal are dominated by large depression areas over the central portions of the European continent. Bulgaria is located within the warm sectors of these cyclones. To this group of circulation types can be added also types PGL4fal, IL2fal, and AL-VB/ELspr. Both fall types feature a low over the British Isles and a high pressure area located or extending over the Russian Plain, producing a southerly surface airflow over Bulgaria. As previously stated, the AL-VB/ELspr contributes to the observation of extreme high, rather than extreme low temperatures. Under this type, Bulgaria is located within a trough of lower pressure extending from Scandinavia to North Africa, and is again under the influence of southerly airflow ahead (east) of the trough axis. Similar to the last type, under PGL5fal the country is situated to the east of a trough axis extending from Scandinavia to north Africa and is again influenced by southerly flow.

Some circulation types which feature unorganized zones of higher pressure over Bulgaria, as for example, most of the summer AL-PGLsum types and type PGL6fal, also do not contribute to the occurrence of extreme minimum temperatures. In addition, the ASR4 sum and AL-PGL/ASR/WPGLsum types do not favor the occurrence of extreme low temperatures in summer. These types, as mentioned before, feature somewhat lower pressure, perhaps a thermal low over central and western Europe, within a ridge extending to the northeast from

the tropical Atlantic. All of these summer types were identified as favoring the incidence of heat waves in Bulgaria.

When the country is situated under the influence of the Persian Gulf thermal cyclone, as for example during PGL1fal and PGL2fal circulation types, extreme low temperatures are not observed. Under one circulation type, AL-VB3win, which features a large cyclonic area over Scandinavia and an Azores High extending over the Iberian Peninsula and north Africa, low temperature extremes also have occurred infrequently. This type is characterized by a modified marine westerly flow over Bulgaria. It is not clear why some circulation types did not contribute to the observation of extreme low temperatures. These types are: SH-ML2spr, PGL3fal, and ML-NAH/SH-MLwin.

Although some differences are evident when comparing the results for both Pleven stations from the early and the late periods, overall the correspondence is good. Most of the circulation types important during the early period still show up for most seasons as contributing to the occurrence of extreme minimum temperatures during the late period.

Table 4-4 Contribution coefficients for the circulation types favoring/not favoring the occurrence of lowest daily minimum temperatures in each season

Values in bold are CCs > 1 at all stations during 1951-1979; underlined values are CCs > 1 at any station. The values on the second line of each cell of the table are the absolute frequency (days), and, in parentheses, the ratio (expressed as a percent) of the absolute frequency of a particular circulation type during an extreme temperature event to the total number of extreme temperature event days for the station.

WINTER					
Station	Obraztsov Chiflick (OC)	Varna (VN)	Plovdiv (PD)	Pleven (PL)	Pleven NCDC (PL NCDC)
ML-NAH1win	**1.1**	**1.5**	**1.5**	**2.1**	1.5
	2 (7.1%)	3 (10.0%)	3 (10.3%)	4 (14.3%)	2 (7.1%)
ML-NAH2win	1.4	0.9	1.8	1.3	0.6
	3 (10.7%)	2 (6.7%)	4 (13.8%)	3 (10.7%)	1 (3.6%)
SH-ML1win	1.5	3.3	1.5	0.8	0.9
	4(14.3%)	9 (30.0%)	4 (13.8%)	2 (7.1%)	2 (7.1%)
SH-ML2win	0.6	1.1	1.7	1.2	4.0
	1 (3.6%)	2 (6.7%)	3 (10.3%)	2 (7.1%)	4 (14.3%)
ML-NAH/EHwin	1.7	1.2	1.2	0.8	0.8
	4 (14.3%)	3(10.0%)	3 (10.3%)	2 (7.1%)	2 (7.1%)
EH2win	1.3	1.2	0.4	1.6	1.2
	3 (10.7%)	3(10.0%)	1 (3.4%)	4 (14.3%)	2 (7.1%)
EH1win	1.2	1.2	0.0	0.6	1.3
	2 (7.1%)	2 (6.7%)	0 (0.0%)	1 (3.6%)	4 (14.3%)
AL-VB2win	0.0	0.5	2.2	1.1	0.6
	0 (0.0%)	1 (3.3%)	4 (13.8%)	2 (7.1%)	1 (3.6%)
IL2win	2.1	1.0	0.5	0.0	0.7
	4 (14.3%)	2 (6.7%)	1 (3.4%)	0 (0.0%)	2 (7.1%)
SH-ML3win	0.0	1.0	0.5	1.6	1.0
	0 (0.0%)	2 (6.7%)	1 (3.4%)	3 (10.7%)	1 (3.6%)

Table 4-4 Continued

WINTER					
Station	Obraztsov Chiflick (OC)	Varna (VN)	Plovdiv (PD)	Pleven (PL)	Pleven NCDC (PL NCDC)
IL1win	1.4	0.0	0.7	0.0	1.2
	4 (14.3%)	0 (0.0%)	2 (6.9%)	0 (0.0%)	2 (7.1%)
AL-VB1win	0.0	0.0	0.8	1.7	1.3
	0 (0.0%)	0 (0.0%)	1 (3.4%)	2 (7.1%)	4 (14.3%)
AL-VB3win	0	0.5	0.5	0.6	0.4
	(0.0%)	1 (3.3%)	1 (3.4%)	1 (3.6%)	1 (3.6%)
ML-NAH/ SH-MLwin	0.4	0.0	0.4	0.9	0.0
	1 (3.6%)	0 (0.0%)	1 (3.4%)	2 (7.1%)	0 (0.0%)

Table 4-4 Continued

SPRING					
Circulation type/ Station	Obraztsov Chiflick (OC)	Varna (VN)	Plovdiv (PD)	Pleven (PL)	Pleven NCDC (PL NCDC)
AL-VB3spr	**3.2**	**2.2**	**2.2**	**3.4**	2.9
	4 (14.3%)	3 (9.7%)	3 (10.0%)	5 (15.2%)	4 (14.8%)
IL2spr	**3.3**	**2.3**	**3.2**	**2.1**	4.2
	4 (14.3%)	3 (9.7%)	4 (13.3%)	3 (9.1%)	5 (18.5%)
IL/ASRspr	**1.0**	**1.7**	**1.7**	**1.5**	1.0
	1 (3.6%)	2 (6.5%)	2 (6.7%)	2 (6.1%)	1 (3.7%)
ASR1spr	**1.7**	**3.1**	**1.6**	**1.5**	0.5
	3 (10.7%)	6 (19.4%)	3 (10.0%)	3 (9.1%)	1 (3.7%)
ASR2spr	**1.9**	**1.2**	**3.1**	**2.3**	2.7
	3 (10.7%)	2 (6.5%)	5 (16.7%)	4 (12.1%)	5 (18.5%)

Table 4-4 Continued

SPRING					
Circulation type/ Station	Obraztsov Chiflick (OC)	Varna (VN)	Plovdiv (PD)	Pleven (PL)	Pleven NCDC (PL NCDC)
EL/ILspr	**2.6**	**1.4**	**2.8**	**1.2**	0.8
	3 (10.7%)	2 (6.5%)	4 (13.3%)	2 (6.1%)	1 (3.7%)
AL-VB1spr	2.0	0.0	2.0	3.5	2.5
	1 (3.6%)	0 (0.0%)	1 (3.3%)	2 (6.1%)	2 (7.4%)
AL-VB4spr	0.9	0.0	1.8	0.8	0.0
	1 (3.6%)	0 (0.0%)	2 (6.7%)	1 (3.0%)	0 (0.0%)
EL2spr	0.6	0.0	0.0	1.1	0.0
	1 (3.6%)	0 (0.0%)	0 (0.0%)	2 (6.1%)	0 (0.0%)
IL/ELspr	0.6	0.5	0.5	1.0	0.0
	1 (3.6%)	1 (3.2%)	1 (3.3%)	2 (6.1%)	0 (0.0%)
SH-ML1spr	0.6	0.5	0.0	0.5	0.0
	1 (3.6%)	1 (3.2%)	0 (0.0%)	1 (3.0%)	0 (0.0%)
SH-ML2spr	0.5	0.5	0.5	0.5	0
	1 (3.6%)	1 (3.2%)	1 (3.3%)	1 (3.0%)	0 (0.0%)
AL-VB2spr	0.6	2.0	0.5	0.9	1.3
	1 (3.6%)	4 (12.9%)	1 (3.3%)	2 (6.1%)	2 (7.4%)
SH-ML3spr	0.4	0.8	0.4	0.4	0.0
	1 (3.6%)	2 (6.5%)	1 (3.3%)	1 (3.0%)	0 (0.0%)
ASR3spr	0.0	0.9	0.5	0.4	1.8
	0 (0.0%)	2 (6.5%)	1 (3.3%)	1 (3.0%)	3 (11.1%)
IL1spr	0	0	0	0	0.5
	0 (0.0%)	0 (0.0%)	0 (0.0%)	0 (0.0%)	1 (3.7%)

Table 4-4 Continued

SPRING					
Circulation type/ Station	Obraztsov Chiflick (OC)	Varna (VN)	Plovdiv (PD)	Pleven (PL)	Pleven NCDC (PL NCDC)
EL1spr	0.0	0.0	0.0	0.0	0.7
	0 (0.0%)	0 (0.0%)	0 (0.0%)	0 (0.0%)	1 (3.7%)
AL-VB/ELspr	0.8	0.7	0.4	0.3	0.4
	2 (7.1%)	2 (6.5%)	1 (3.3%)	1 (3.0%)	1 (3.7%)

Table 4-4 Continued

SUMMER					
Station	Obraztsov Chiflick (OC)	Varna (VN)	Plovdiv (PD)	Pleven (PL)	Pleven NCDC (PL NCDC)
ASR2sum	**1.3**	**1.2**	**1.7**	**1.0**	0.0
	2 (6.9%)	2 (6.7%)	3 (9.4%)	2 (5.6%)	0 (0.0%)
WPGL1sum	**9.1**	**10.5**	**4.9**	**4.2**	3.8
	5 (17.2%)	6 (20.0%)	3 (9.4%)	3 (8.3%)	5 (13.5%)
WPGL2sum	**2.5**	**1.5**	**2.7**	**1.8**	1.1
	3 (10.3%)	2 (6.7%)	4 (12.5%)	3 (8.3%)	3 (8.1%)
WPGL3sum	**2.4**	**2.3**	**3.6**	**3.7**	2.7
	3 (10.3%)	3 (10.0%)	5 (15.6%)	6 (16.7%)	4 (10.8%)
ASR3sum	2.0	0.5	1.9	2.5	1.2
	4 (13.8%)	1 (3.3%)	4 (12.5%)	6 (16.7%)	3 (8.1%)
ASR6sum	0.9	3.5	1.6	1.4	0.6
	1 (3.4%)	4 (13.3%)	2 (6.3%)	2 (5.6%)	1 (2.7%)
WPGL4sum	1.0	0.0	0.0	1.7	1.8
	1 (3.4%)	0 (0.0%)	0 (0.0%)	2 (5.6%)	4 (10.8%)

Table 4-4 Continued

SUMMER					
Station	Obraztsov Chiflick (OC)	Varna (VN)	Plovdiv (PD)	Pleven (PL)	Pleven NCDC (PL NCDC)
WPGL6sum	0.0	1.5	0.7	1.2	1.5
	0 (0.0%)	2 (6.7%)	1 (3.1%)	2 (5.6%)	4 (10.8%)
AL-PGL3sum	2.0	0.6	0.6	1.1	0.8
	3 (10.3%)	1 (3.3%)	1 (3.1%)	2 (5.6%)	2 (5.4%)
ASR5sum	1.2	1.8	0.6	0.5	0.0
	2 (6.9%)	3 (10.0%)	1 (3.1%)	1 (2.8%)	0 (0.0%)
ASR1sum	0.5	1.7	0.0	0.0	0.0
	1 (3.4%)	3 (10.0%)	0 (0.0%)	0 (0.0%)	0 (0.0%)
WPGL5sum	0.7	0.0	0.7	1.2	2.4
	1 (3.4%)	0 (0.0%)	1 (3.1%)	2 (5.6%)	6 (16.2%)
AL-PGL1sum	0.0	0.0	0.4	0.0	1.4
	0 (0.0%)	0 (0.0%)	1 (3.1%)	0 (0.0%)	2 (5.4%)
AL-PGL2sum	0.4	0.9	0.0	0.8	1.6
	1 (3.4%)	2 (6.7%)	0 (0.0%)	2 (5.6%)	1 (2.7%)
AL-PGL4sum	0.0	0.0	0.5	0.0	0.0
	0 (0.0%)	0 (0.0%)	1 (3.1%)	0 (0.0%)	0 (0.0%)
AL-PGL5sum	0.8	0.0	0.7	0.6	0.0
	1 (3.4%)	0 (0.0%)	1 (3.1%)	1 (2.8%)	0 (0.0%)
AL-PGL6sum	0.0	0.0	0.9	0.0	0.0
	0 (0.0%)	0 (0.0%)	2 (6.3%)	0 (0.0%)	0 (0.0%)
ASR4sum	0.5	0.5	0.0	0.4	0.0
	1 (3.4%)	1 (3.3%)	0 (0.0%)	1 (2.8%)	0 (0.0%)
AL-PGL/ ASR/WPGLsum	0.0	0.0	1.2	0.5	0.9
	0 (0.0%)	0 (0.0%)	2 (6.3%)	1 (2.8%)	2 (5.4%)

Table 4-4 Continued

FALL					
Station	Obraztsov Chiflick (OC)	Varna (VN)	Plovdiv (PD)	Pleven (PL)	Pleven NCDC (PL NCDC)
SH-ML1fal	**3.2**	**3.9**	**4.2**	**3.4**	1.8
	4 (12.5%)	5 (16.1%)	5 (17.2%)	5 (14.7%)	3 (10.3%)
SH-ML2fal	**2.9**	**1.0**	**2.2**	**3.6**	1.3
	3 (9.4%)	1 (3.2%)	2 (6.9%)	4 (11.8%)	2 (6.9%)
AL-VB1fal	**2.9**	**3.7**	**2.7**	**1.6**	3.1
	5 (15.6%)	6 (19.4%)	4 (13.8%)	3 (8.8%)	6 (20.7%)
IL1fal	**3.8**	**2.8**	**1.0**	**3.5**	1.3
	4 (12.5%)	3 (9.7%)	1 (3.4%)	4 (11.8%)	2 (6.9%)
IL3fal	**2.6**	**3.9**	**6.2**	**4.3**	4.0
	3 (9.4%)	4 (12.9%)	6 (20.7%)	5 (14.7%)	6 (20.7%)
AL-VB2fal	1.9	2.1	0.0	2.8	2.6
	2 (6.3%)	2 (6.5%)	0 (0.0%)	3 (8.8%)	4 (13.8%)
SH-ML/ILfal	2.2	2.8	3.0	0.7	0.7
	3 (9 4%)	4 (12.9%)	4 (13.8%)	1 (2.9%)	1 (3.4%)
AL-VB3fal	1.4	1.6	0.6	0.0	0.9
	3 (9.4%)	3 (9.7%)	1 (3.4%)	0 (0.0%)	2 (6.9%)
AL-VB/ILfal	0.6	0.0	0.0	1.1	1.2
	1 (3.1%)	0 (0.0%)	0 (0.0%)	2 (5.9%)	2 (6.9%)
IL2fal	0.0	0.0	2.5	0.8	0.0
	0 (0.0%)	0 (0.0%)	3 (10.3%)	1 (2.9%)	0 (0.0%)

Table 4-3 Continued

FALL					
Station	Obraztsov Chiflick (OC)	Varna (VN)	Plovdiv (PD)	Pleven (PL)	Pleven NCDC (PL NCDC)
SH-ML3fal	0.5	0.0	0.5	0.4	0.7
	1 (3.1%)	0 (0.0%)	1 (3.4%)	1 (2.9%)	1 (3.4%)
PGL1fal	0.0	0.0	0.0	0.0	0.0
	0 (0.0%)	0 (0.0%)	0 (0.0%)	0 (0.0%)	0 (0.0%)
PGL2fal	0.3	0.3	0.3	0.3	0.0
	1 (3.1%)	1 (3.2%)	1 (3.4%)	1 (2.9%)	0 (0.0%)
PGL3fal	0.5	0.5	0.0	0.9	0.0
	1 (3.1%)	1 (3.2%)	0 (0.0%)	2 (5.9%)	0 (0.0%)
PGL4fal	0.0	0.0	0.0	0.0	0.0
	0 (0.0%)	0 (0.0%)	0 (0.0%)	0 (0.0%)	0 (0.0%)
PGL5fal	0.0	0.0	0.5	0.4	0.0
	0 (0.0%)	0 (0.0%)	1 (3.4%)	1 (2.9%)	0 (0.0%)
PGL6fal	0.4	0.5	0.0	0.4	0.0
	1 (3.1%)	1 (3.2%)	0 (0.0%)	1 (2.9%)	0 (0.0%)

3.3. Quantitative comparison of changes in circulation to changes in heat waves, cold spells and absolute one-day extremes

The occurrence of summertime heat waves is favored at all stations mostly by the types associated with the AL-PGLsum and ASRsum supertypes. Of the two, only the AL-PGLsum supertype was characterized by significant trends in frequency of occurrence and persistence during 1951-2004. The decrease in frequency for AL-PGLsum was accompanied by a decrease in

average length of all events with this supertype. No significant changes during sub-periods were identified. The heat waves at all the stations from the early period (1951-1979) decreased in frequency and average length, which is consistent with the observed decline of the circulation supertype. During the late period (1973-1999), however, at Pleven NCDC the frequency and average length of the heat waves increased significantly, which is not in agreement with the results for the AL-PGLsum supertype.

The wintertime cold spells occur at all stations from the early period under types related to the SH-MLwin supertype and also under two mixed types almost equally related to ML-NAHwin, SH-MLwin and EHwin. While no trend in frequency of occurrence was identified for supertype ML-NAHwin, the SH-MLwin supertype decreased significantly, and the EHwin supertype increased significantly during 1951-2004. For none of the supertypes changes were evident during sub-periods. The persistence of the ML-NAHwin and SH-MLwin supertypes declined in 1951-2004, especially in relation to events lasting more than 4 days. In contrast, the persistence of the EHwin supertype increased. Significant changes in cold spells characteristics were evident only at Obraztsov Chiflick in 1951-1979, and at Pleven NCDC in 1973-1999. While the average length of the cold spells at Obtaztsov Chiflick decreased, in accord with the decrease in frequency and persistence in SH-MLwin supertype, during the late period the average length of the cold spells increased, contrary to the changes in the SH-MLwin supertype.

Comparing trends in the singular extremes to the observed trends in atmospheric circulation, the highest maximum temperature has changed significantly just at two stations during the early period, and only in the fall season. The circulation types which favor the occurrence of extreme high temperatures in the fall are related to the PGLfal supertype. This supertype exhibited a negative trend in frequency and persistence during 1951-2004 period. In addition, during the 1951-1966 and 1976-2004 sub-periods, positive trends were identified in the frequency of occurrence of the PGLfal. The decrease in the fall highest temperatures in 1951-1979 at Pleven and Plovdiv is in accord only with the overall negative trend in frequency and persistence of the PGLfal supertype during the entire period 1951-2004.

The seasonal highest temperatures in winter and spring have changed significantly during the late period, however, these results are based on one station only. The circulation types contributing to the occurrence of extreme high temperatures in winter are associated with the ILwin and AL-VBwin supertypes. While the frequency and persistence of the ILwin supertype have decreased in 1951-2004, the AL-VBwin supertype was characterized by an increase in frequency and persistence. In addition, during the 1951-1972 sub-period the frequency of the AL-VBwin supertype declined significantly. The observed increase in winter highest TMAX at Pleven NCDC in 1973-1999 relates well only to the rise in the frequency and persistence of the AL-VBwin supertype. In spring, the highest TMAX temperatures are observed under circulation types associated with the SH-MLspr supertype and under a mixed type associated with the AL-

VBspr and to the ERLspr supertypes. No significant trends were identified for any of the spring supertypes in 1951-2004.

The lowest minimum temperatures have changed significantly only during the spring season in the early period. Since no significant changes in the spring supertypes were observed in 1951-2004, the observed increase in the absolute extreme temperatures in spring is, perhaps, related to other contributing factors.

4. Discussion

4.1. Comparison of the results of the analysis of atmospheric circulation-temperature extremes relationships to existing studies

Previous researchers have found that persistent anticyclonic conditions and generally southerly or easterly airflow contribute to the occurrence of prolonged periods with high maximum temperatures in their study areas within Europe. Using the subjective Hess-Brezowsky classification, Kyselý (2002a) found that almost 75% of all summertime heat waves in Prague occur under three prevailing groups of circulation types: a) a central European High (Hess Brezowsky type "HM"); b) a Fennoscandian or Norwegian sea/Fennoscandian High (major type "E"); and c) circulation with an inflow of warm air from the southwest to southeast (major types "S", "SW" and "SE"). Domonkos et al. (2003) also employed the Hess-Brezowsky classification and concluded that southerly airflow and persistent anticyclones were favorable for the occurrence of extreme high temperature events in south central Europe. Furthermore, for the mid and southern sub-regions of their study domain (south central Europe) they determined that zonal circulation is frequent during extreme high temperature

events. Based on a visual assessment of surface and upper-air charts, Katsoulis et al. (2005, p.239) established that hot spells were most probable (72% occurrence) over Greece when a "persistent Azores anticyclone appears over North Africa and extends a ridge of high pressure towards the northeastern Mediterranean" and also when an anticyclone located over western or central Europe extended southeastward toward their study area.

The expectations in this study were that in some cases during heat waves in Bulgaria somewhat similar atmospheric circulation conditions might be encountered, however, due to the spatial location of the country and its specific geomorphological characteristics differences were anticipated. During heat waves, Bulgaria is mostly under the influence of an unorganized zone of higher pressure between two cyclonic features and near the eastern edge of the Azores High (as represented in most of the AL-PGLsum types). In addition, the ASR4sum and AL-PGL/ASR/WPGLsum types, which also favor the occurrence of heat waves, are characterized by lower pressure, perhaps, a thermal low over central and western Europe, within a broader area of surface ridge, extending from the southwest to northeast over Scandinavia and the Russian Plain. Under the ASR5sum type which is conducive to the occurrence of heat waves the country is under the influence of an extension of the Persian Gulf thermal low. Hence, the configurations contributing to the occurrence of heat waves in Bulgaria are not comparable to the circulation patterns established to be important for heat waves occurrence in central Europe or in Greece in past studies.

When comparing the occurrences of singular absolute extremes, however, to the circulation types, it was evident that the majority of these extreme high temperature events occurred under southerly or southwesterly flow. In these occasions, either a strong Icelandic Low was located over the British Isles, and Bulgaria was situated to the southeast of this cyclone, or a depression area was evident over central or south central Europe, and the country was situated in the warm sector of the cyclone, or Bulgaria was located within a trough of lower pressure and was influenced by the warm airflow east of the trough axis. In addition, absolute highest temperatures were also observed when a trough of lower pressure extended northwestward over Bulgaria from the thermal low over the Persian Gulf and the Arabian Peninsula, and also under the influence of a mild high pressure system located over the western Mediterranean.

For the winter season, Domonkos (1998), using Péczely's classification, found that anticyclones were the most frequent pressure features during periods with extreme low temperatures in Hungary. In a subsequent study, Domonkos et al. (2003), using the Hess-Brezowsky classification, established that "northerlies" and "easterlies", "meridional" and "anticyclonic" airflow favored the occurrence of extreme cold temperature events in south-central Europe. In agreement with these findings, results presented here show that wintertime cold spells in Bulgaria often occur under circulation types inducing northerly, easterly or north-easterly flow over the country. In addition, the occurrence of absolute extreme low temperatures was also favored by northerly, easterly, north-easterly airflow over Bulgaria around an anticyclone or north of a warm front, or when an

anticyclone was centered over the country. In summer, the extreme low temperatures were favored by circulation types featuring weaker than normal Persian Gulf Low.

4.2. Evaluation of the classification performance

Many previous authors, studying the relationships between atmospheric circulation and temperature extremes, have defined temperature extremes as the exceedances of pre-selected threshold values such as in the definition of heat waves (Domonkos, 1998; Huth et al., 2000; Kysely, 2002a; Domonkos et al., 2003; Kastoulis et al., 2005) or by the exceedances of the upper 90^{th} or lower 10^{th} quantiles of the temperature distribution (Domonkos et al., 2003). In addition, in order to avoid low frequency counts, some authors have agglomerated circulation types into cyclonic/anticyclonic groups or groups favoring/not favoring the occurrence of the extremes (Kysely, 2002a; Domonkos, 1998).

In contrast, in this study the circulation types were related to temperature extremes occurring above or below a threshold (heat waves and cold spells) and to single day temperature extremes (the yearly highest maximum and lowest minimum temperatures per season). Although difficulties emerge when attempting to relate singular extremes to circulation types, consistency was evident in the relationships identified at all stations from the early period. Not only the same circulation types were contributing to the occurrence of absolute extremes of the same sign at all the stations, but the opposite in sign extremes were related to well differentiated, separate circulation types. This consistency of the relationships between extreme temperature events occurring at all the

stations in the early period and the circulation types was apparent also when the threshold extremes, the heat waves and cold spells, were studied. In addition, some of the circulation types contributing to the occurrence of threshold extremes were found not to be important for the occurrence of singular absolute extremes of the opposite sign. For example, most of the AL-PGLsum types which favored the occurrence of heat waves at all stations were found not to be important for the occurrence of absolute lowest summer temperatures at all stations. This is another illustration of the good differentiation between the circulation types contributing to the incidence of opposite sign temperature extremes.

In summary, the overall performance of the circulation classification may be evaluated as insightful, based on consistency of the results for all stations in the early period, the good differentiation, in most cases, between the circulation types conducive to the occurrence of opposite in sign temperature extremes, and the correspondence between circulation types found important for the occurrence of singular extremes and for threshold extremes.

5. Conclusions

The relationships between atmospheric circulation types and temperature extreme events were explored for Bulgaria during the historical 1951-1979 and 1973-1999 periods. An important objective of this part of the analysis was also to test the applicability of the classification scheme to a specific research question whether the temperature extremes are favored by certain circulation types. To achieve this objective, threshold extremes, heat waves and cold spells lasting at

least three days, as well as singular (one day) extremes were used. The results from the analysis can be summarized as follows:

a) Heat waves in summer are favored when Bulgaria is situated within an unorganized zone of higher pressure between two cyclonic features and near the edge of the Azores high. In addition, when lower pressure, perhaps a thermal low over central and western Europe, within a broader area of surface ridge extending from the southwest to northeast over Scandinavia and the Russian Plain, is evident on the composite maps, heat waves are observed in Bulgaria. Also, prolonged periods with high maximum temperatures were observed when an extension of the Persian Gulf thermal low appears over the country.

b) Cold spells in winter occur mostly under circulation types producing northerly, northeasterly or easterly airflow over Bulgaria around anticyclones situated either over western and central Europe, or over Scandinavia and the Russina Plain.

c) Contributing to the occurrence of the absolute highest temperature extremes are the circulation types that produce southerly or southwesterly flow over Bulgaria. In addition, the circulation types under which the country is influenced by the thermal low over the Persian Gulf, or the circulation type which produces modified marine westerly flow over Bulgaria also contribute to the occurrence of extreme high temperatures. The existence of a trough of lower pressure extended from Scandinavia to

North Africa, inducing southerly flow over the country, is also favorable to the occurrence of absolute high temperatures.

d) The circulation types which favored the occurrence of the absolute lowest minimum temperatures in any season were those that featured anticyclones over central Europe or the Russian Plain and Scandinavia extending over Bulgaria, and producing northwesterly to northeasterly and easterly airflow at the surface over the country. Some circulation types that featured weaker than normal Persian Gulf Low were also found important in the summer season for the occurrence of extreme low temperatures. In addition, in fall lowest minimum temperatures were registered when a surface anticyclone was situated over the country.

e) In general, the circulation types which were important for the occurrence of temperature extremes in the early period were found also to be important during the late period.

f) Some correspondence between the trends in frequency and persistence of some circulation supertypes related to the types contributing to the occurrence of temperature extremes, and the trends in characteristics of the temperature extremes, was evident based on a qualitative evaluation. Further quantitative assessment, however, is needed.

The comparison of the circulation types to the observed threshold and absolute extremes was insightful. The results for most of the stations showed consistency, the opposite types of extremes were influenced in most cases by

different circulation types, and a good correspondence between the circulation types contributing to the threshold as well as to the singular extremes was found. The inconsistency in some results reflects the limited number of cases when comparing circulation types to singular extremes, and also the importance of additional factors, apart from the atmospheric circulation, for the evaluation of the temporal and spatial characteristics of these extremes.

Chapter 5 Conclusions and future work

1. Summary of major findings

Large-scale atmospheric circulation patterns over Europe and their relationships to extreme temperature events in Bulgaria were investigated. The major goals of this research were to: 1) develop a classification scheme of sea-level pressure circulation patterns, 2) identify changes in temperature extremes in Bulgaria during the second half of the 20th century, and 3) determine the circulation patterns associated with the occurrence of these temperature extremes.

1.1. Atmospheric circulation classification for Europe

To explore the changes in the atmospheric circulation in the European/North Atlantic domain a comprehensive two-tier circulation classification was derived using the methods of principal components analysis and cluster analysis. The variety of existing classifications hampers greatly the comparison of research outcomes between studies. This issue is recognized by the European Science Foundation which oversees a current project regarding the "Harmonization and applications of weather type classifications for European regions". The main purpose of this project is "to achieve a general numerical method for assessing, comparing and classifying typical weather situations in European regions" (COST action 733, http://www.cost733.org/). The two-tier atmospheric circulation catalogue developed in this study represents a unified framework, one solution to the important need for consistency and

standardization of the research approaches to classifying the climate of any region in Europe or the entire European continent.

In contrast to other classifications for which the circulation types are subsequently subjectively agglomerated into larger groups for further analyses (e.g., Kysely [2002a], grouped the circulation types from the Hess-Brezowsky classification into Cyclonic and Anticyclonic types), the classification presented here features two distinctive solutions obtained using an objective statistical methodology. One tier of the classification comprises 'supertype' patterns that highlight the main characteristics of the large-scale atmospheric circulation over Europe and are applicable for baseline analyses of the atmospheric circulation frequency and persistence. The second, more detailed, tier consists of 'circulation types' and can be used to address applied research questions regarding the relationships between large-scale atmospheric circulation characteristics and local climates.

The classification presented here offers further advantages over existing classifications. The circulation patterns of the existing classifications provided limited areal coverage of only parts of the continent (for example, central Europe [Hess-Brezowsky, 1969], the British Isles [Lamb, 1972; Jones et al., 1993]; the Alpine region [Schüepp, 1979], or western Europe [Plaut and Simonnet, 2001; Esteban et al., 2006]). Furthermore, some classification catalogues were developed in relation to a specific country (Hungary [Péczely, 1957], or Greece [Maheras et al., 2000; Kassomenos et al. 2003]). In addition, the classifications developed to date considered regions in Europe that were not relevant to

Bulgaria or to many other areas of the continent. The atmospheric circulation catalogue in this study was developed for a much larger area encompassing the European continent and major portions of the North Atlantic which renders the classification applicable to research agendas concerning any region within the continent.

The derived atmospheric circulation catalogue captures the main centers of action that influence the weather and climate of the European continent and the north Atlantic. The prevalent zonal westerly flow (more intense during the cooler half of the year) is well depicted over the British Isles and the mid-continent in the AL-VBwin, AL-VBspr and AL-VBfal supertypes. The importance and strength of the Icelandic Low during the cooler season is reflected in the ILwin, ILspr and ILfal supertypes, all of which are dominated by a large and intense negative anomaly located in the vicinity of Iceland. The Azores High increases in areal extent and becomes more intense in the summer season. Its larger spatial extent and higher intensity are evident in all of the supertypes for summer. In addition to the annual centers of action (the Icelandic Low, the Siberian High) several seasonal centers of action are captured by the derived circulation supertypes. The cool season center of intense cyclogenesis over the Gulf of Genoa is well evident in the ML-NAHwin, SH-MLwin, SH-MLspr and SH-MLfal supertypes. The Asian thermal cyclone in summer, as represented by the Persian Gulf Low within the map domain, is also captured by the different supertypes. The extension of the Siberian High in winter, as depicted by the high pressure features found over the Russian Plain, is well represented in various

supertypes. The high pressure centers over the continent are also well depicted in the EHwin, ASRspr and ASRsum supertypes.

The distinctiveness of this classification is clearly evident in that the circulation patterns were derived by season, rather than annually, to account for the intra-seasonal differences in atmospheric circulation. In addition, the natural annual progression of the atmospheric circulation processes is well evident in the existence of similar supertypes in almost every season. Time-wise, the classification spans a long time period starting in 1951 and extending into the early 2000s.

The supertypes and types of the classification presented here were named after the physical entities (i.e., European High, Icelandic Low, etc.) which dominate the specific patterns. This approach allows for an easy and clear association to be made between the pattern name and the specific centers of action or sea level pressure anomalies representing the given circulation supertype or type. In contrast, the traditional naming convention is based mostly on the direction of the airflow or the curvature of the circulation entities over a limited area.

Due to the fact that the classification was produced using computer-assisted methods, the methodology is easily transferable to any other region on any other continent. The chosen approach permits all days to be classified (compared to the Hess and Brezowsky [1969] classification, for example, which contains only patterns lasting at least 3 days), thus specifically allowing for transitional patterns.

The frequency and persistence characteristics of the derived atmospheric circulation catalogue validate the findings of previous authors using smaller area patterns, often subsequently aggregated in larger groups. Important characteristics of the atmospheric circulation over Europe during the 20th century determined by previous research were successfully captured by the continental scale classification scheme derived here. More specifically, the increase in frequency of anticyclonic (or dominated by anticyclones) supertypes during the 1951-2004 period and the decrease in frequency of supertypes dominated by cyclonic features during the same period, were established as well in this study.

The seasonal character of the derived classification, the two-tier structure and the larger number of parameters, especially regarding the persistence of events of different length, permitted further details of the frequency and persistence characteristics of the atmospheric circulation over Europe to be elucidated compared to previous research. Changes in the frequency of occurrence of the supertypes were evident in all seasons, except for spring. For most supertypes, breakpoints in the frequency time series were identified in the 1960s or 1970s, and several supertypes displayed significant temporal trends during the sub-periods determined by the breakpoints.

The persistence of the circulation supertypes was considered in much greater detail than previous studies by focusing not only on the average event length but also on the interannual changes in the number of single day (transitional day) events, events lasting 2-4 days and events lasting longer than 4 days. The findings in this study are in disagreement with previous research by

Kysely and Domonkos (2006), who studied the persistence characteristics of the Hess-Brezowsky subjective catalogue, and established an increase in persistence for most groups of circulation types and in all seasons. Three supertypes (dominated by cyclonic features or negative anomalies) indicated a decrease in persistence during 1951-2004 reflected in the negative trend of the average event length. In addition, if only the events lasting longer than 4 days were considered, again some of the supertypes (those dominated by cyclonic features or negative anomalies) indicated a decrease in persistence. Only the supertypes dominated by anticyclonic features or positive anomalies exhibit increasing trends in all or some of these parameters, i.e., an increase in persistence in accordance with previous research.

1.2. Historical changes of temperature extreme events in Bulgaria

The historical changes in temperature extreme events in Bulgaria were explored in terms of temporal trends and changes in estimated return levels for two historical periods. The early historical period 1951-1979 and the late historical period 1973-1999 were determined based on data availability and homogeneity. The basis for this part of the research were the daily maximum and minimum temperature data from four stations extracted from the Bulgarian Meteorological Yearbooks and from one station obtained from the NCDC data base.

Significant changes in the temperature extremes were determined during the early and the late period. The contributions of this part of the study are

related to the comprehensive set of indices of temperature extremes used in the analysis, compared to previous research. In addition to the trend analysis, changes of temperature extremes indices were assessed based on differences in their return levels between the early and late periods. The results concerning Bulgaria expand the knowledge regarding historical changes in temperature extremes in Europe on a single state scale.

Most of the findings regarding changes in temperature extremes in Bulgaria between the early and late periods confirm the results established by past research on a continental, regional and a single country scales. Similarly to previous research, the highest maximum temperature in Bulgaria does not change on annual or seasonal scales in the early period, except in fall when this index indicates a decrease at two of the stations in 1951-1979. In the late period, however, an increase in the absolute highest maximum temperature values is evident in winter and spring as expected based on existing research. In Bulgaria, in agreement with previous reports for other regions in Europe, the lowest daily minimum temperature changed significantly. The absolute minimum temperature increased on annual scale at two of the stations and on a seasonal scale at all stations, but only in spring. During the early period, the daily temperature range (DTR) decreased in the year as a whole and in summer for two stations (Plovdiv and Pleven) similarly to the observed changes in daily temperature range in other regions. The 5- and10-day inter-period differences in maximum and minimum temperature either did not change or decreased for the year as a whole, in winter and in spring during 1951-1979 for some stations (Obraztsov Chiflick, Plovdiv

and Varna) similarly to existing research. Frost period severity declined at all stations in March in 1951-1979, in agreement with the research to date for other regions. In addition, frost period severity increased at two stations in October during the early period in parallel with the observed decreasing trend of lowest minimum tempearture found in this study and reported also by Hundecha and Bardossy (2005) for Western Germany. In 1973-1999 a significant decrease in the frost period duration was established in Bulgaria. A decrease in the number and average length of heat waves was observed in 1951-1979 for all stations except for Varna, similar to the findings of Kysely (2002a) and Domonkos et al. (2003). In contrast, the late period, 1973-1999, was characterized by an increased frequency and duration of heat waves (based on Pleven NCDC) in accordance with the findings of Kysely (2002a), Domonkos et al. (2003), and of Hundecha and Bardossy (2005). The average length of the cold spells decreased in the early period, but only at one station (Obraztsov Chiflick).

Some findings were not in agreement with those of the research to date. In contrast to previous studies, the changes (more specifically, the increase) in the absolute lowest minimum temperature were evident only during the early period (1951-1979) and not during the late period (1973-1999). In addition, no significant trends in extreme summer maximum or minimum temperatures were observed in Bulgaria during the second half of the 20th century. During the early period, contrary to previous findings, the daily temperature range increased for one station (Varna) in spring. Significant increasing trends in annual, winter and summer daily temperature range for the late period were also evident (based on

Pleven NCDC). Positive trends in spring and winter for 1973-1999 (based on Pleven NCDC) were determined for the 5- and 10-day inter-period differences of minimum temperature, contrary to research to date. The frost period length did not change during the early period, and no changes in frost period severity were observed during the late period. The number of cold spells and their maximum excess did not indicate any changes during the early or the late periods. The average length of the cold spells increased at Pleven NCDC in the late period. All of these findings indicate that more research is needed in order to determine if some of the results for the late period and the differences reported here from previous studies depict actual climate variations in Bulgaria or if they are related to the limitations of the data and the set of stations used in the study.

The existing research concerning cooling and heating degree days has been quite limited and the results of this study expand the knowledge regarding these indices. During 1951-1979, the cooling degree days decreased at two stations (Obraztsov Chiflick and Pleven) while in 1973-1999 a significant increasing trend is evident at Pleven NCDC. Changes in the heating degree days were evident only during the late period. The significant negative trend at Pleven NCDC indicated warming during the cooler part of the year for this station.

The results obtained in this study contribute to the existing knowledge regarding historical changes in extreme temperature events, since the use of extreme value analysis in a historical context has been limited. Furthermore, the comparison of return levels from two separate historical periods has not been used as a means of assessing the changes in the indices of interest. The return

levels determined for Pleven NCDC from the late period (1973-1999) were found to be always higher than those for Pleven for the maximum temperature extremes and lower for the minimum temperature extremes on annual and seasonal scales, except for spring. The results from the modeling of the summer exceedances over 32°C with the Generalized Pareto distribution indicated that the return levels were higher at Pleven NCDC from the late period compared to Pleven from the early period. The return levels of the deficiencies below -5°C at Pleven NCDC were lower compared to Pleven.

1.3. Relationships between atmospheric circulation and temperature extreme events in Bulgaria

The relationships between the atmospheric circulation patterns and temperature extreme events in Bulgaria were explored for the 1951-1979 and 1973-1999 periods. This research expands the knowledge regarding the associations between the atmospheric circulation over Europe and the occurrence of temperature extreme events in Bulgaria due to the use of a detailed catalogue of circulation type patterns. A variety of circulation situations, represented by the second-tier of the classification, the circulation types, were established to be favorable for the occurrence of extreme temperature events in the country.

The distinctiveness of the studied relationships between atmospheric circulation and temperature extremes is due to the spatial position of Bulgaria in relation to the circulation entities (cyclones, anticyclones, for example) that characterize each circulation type. Although previous studies exist regarding

association between large-scale circulation and extreme temperature events for regions located in the mid-continent, or in immediate proximity to Bulgaria (i.e., Hungary, Czech Republic, south central Europe, Greece), the comparison of the extreme events recorded in Bulgaria to atmospheric circulation patterns has not been explored and it offers a unique perspective. Different direction of the surface airflow and characteristic weather patterns are observed in Bulgaria compared to the neighboring regions, depending on the size of the circulation features and the position of Bulgaria relative to the center of the circulation entity, in combination with the specific geomorphologic characteristics of the country.

Physically plausible relationships between the atmospheric circulation patterns and temperature extremes in Bulgaria were identified. A comparison of the circulation types with the temperature extremes indicated that heat waves in summer occur: a) when Bulgaria is located within an unorganized zone of higher pressure between two cyclonic features and near the edge of the Azores High and weak pressure gradients and weak winds are evident (AL-PGL1sum, AL-PGL2sum, AL-PGL4sum, AL-PGL5sum and Al-PGL6sum); b) when an extension of the Persian Gulf thermal low is evident over the country (ASR5sum); c) under lower pressure (perhaps a thermal low) present over central and western Europe and extending over the country (ASR4sum and AL-PGL/ASR/WPGLsum). These results are an important addition to previous research which considered central (Kysely, 2002a), south central Europe (Domonkos et al., 2003) or Greece (Katsoulis et al. 2005), and concluded that for the respective areas prolonged periods with high maximum temperatures

occurred under persistent anticyclonic conditions, or under southerly or easterly surface airflow.

Similarly to past studies, the absolute highest temperature extremes occur predominantly (for any season, at all stations) under circulation types that produce southerly or southwesterly flow over Bulgaria. In all occasions this southerly low-level airflow is associated with low pressure systems (IL1win, SH-ML1spr, SH-ML3spr, PGL4fal). Further detail is added by establishing that absolute high temperatures occur also when a trough of lower pressure extends from Scandinavia to North Africa and Bulgaria is under the influence of southerly flow, ahead (east) of the trough axis (AL-VB/ELspr). Absolute highest temperatures have been also recorded when the country is under the influence of a mild high pressure system (AL-VB2win), or with a trough of lower pressure extending northwestward from the thermal low over the Persian Gulf and the Arabian Peninsula (ASR2sum, PGL1fal).

Regarding low temperature extremes, existing research has established that extreme low temperature events in Hungary have occurred predominantly under anticyclonic conditions (Domonkos, 1998). In addition, Domonkoes et al. (2003) determined, using the Hess-Brezowsky classification, that in south central Europe extreme cold temperature events were favored by "northerlies" and "easterlies", "meridional" and "anticyclonic" circulation patterns. The findings in this study complement the existing research by indicating that winter cold spells in Bulgaria occurred: a) during northerly, northeasterly surface airflow around an anticyclone situated over western and central Europe (ML-NAH/EHwin); and b)

under easterly surface airflow around an anticyclone located over Scandinavia and the Russian Plain (SH-ML1win, ML-NAH/SH-MLwin, SH-ML2win). Furthermore, absolute extreme low temperatures in any season were observed when: a) surface anticyclones over central Europe extend over Bulgaria and produce northerly flow (SH-ML2fal, AL-VB3spr, IL/ASRspr, AL-VB1fal); b) an anticyclone over the Russian Plain or Scandinavia extends over the country and produces weak pressure gradients and weak winds, often from an easterly direction (ASR2spr, EL-ILspr, IL2spr, IL1fal); c) Bulgaria is under the influence of easterly or northeasterly air flow, north of a warm front or around an anticyclone (ML-NAH1win, SH-ML1fal, ASR1spr, ASR2sum); d) the Persian Gulf Low is weaker than normal (a positive anomaly exists) and a weak flow is experienced over the country (WPGL1sum, WPGL2sum, WPGL3sum); and e) a surface anticyclone is located over Bulgaria (IL3fal).

The derived classification presented useful insights on the circulation patterns responsible for temperature extremes in Bulgaria. The results for all the stations showed consistency: opposite types of extremes were favored by different circulation types, and a good correspondence between the circulation types contributing to the threshold, as well as the singular extremes, was found.

2. Limitations of the study

Some of the limitations of this study are related to the application of the principal component and cluster analyses for the atmospheric circulation

classification. In this study, however, steps were taken to minimize the subjective input needed in these procedures. Another limitation was imposed on this study by the inhomogeneity of the data for three of the NCDC stations. The set of locations in the late period, used for inter-period comparison, was reduced to one, Pleven NCDC. Limitations in the results interpretation also ensued from the use of two different stations at Pleven for the comparison of the early and late periods. In addition, the large amount of missing data for Pleven NCDC also affected some of the final results for this station. In the last portion of the analysis, in the comparison of the absolute seasonal extremes to the circulation types, mostly one value per year for any season was used. Given that the study periods are relatively short at each station, the contribution coefficients were based on a very small number of values.

3. Future work

In the future, a more detailed quantitative comparison will be performed between the classification derived in this study and available atmospheric circulation catalogues, by assessing the day by day overlap of the circulation types from the different classifications. In addition, the derived classification will be applied to assess the relationships between temperature extreme events and circulation types in other regions of Europe in order to validate quantitatively the classification performance in other parts of the continent. Future research will include also the application of the classification to global circulation model data in order to investigate potential future changes in atmospheric circulation over

Europe. In addition, the classification methodology will be applied to a different continent around the globe, more specifically North America. Subsequently, the relationships between the historical changes in the circulation patterns derived for Europe and the ones derived for North America will be explored. Future research plans also include the investigation of the frequency and persistence of the circulation patterns over North America, their relationships to local weather and climate extremes, and potential future changes in these atmospheric circulation characteristics and the relationships between large-scale circulation and local climate. In the future, a possible acquisition of data for additional stations in Bulgaria for a longer period, in order to extend further the spatial and temporal comparison portion of this study is also envisioned. An exploration of the relationships between circulation patterns and precipitation extremes in Bulgaria, if data are acquired, is also of interest. An exploration of potential future changes in the temperature and precipitation extremes in Bulgaria, and their relationship to the large-scale atmospheric circulation will also be considered in future research.

APPENDIX to Chapter 2

Appendix Table 1 Comparison table of the obtained SLP circulation patterns

	Current study	Hess Brezowsky 1969	Lamb's 'Airflow Types' over the British Isles 1972
Analysis method	Nonhierarchical cluster analysis based on PCA scores.	Subjective classification.	Subjective classification of weather maps according to pressure distribution, winds or weather.
Variable	SLP	SLP and Z500	SLP and Z500
Region	777 grid points between 40 deg W and 50 deg E, and 20-70 deg N	Approx. 35-70 deg N, 50 deg W – 40 deg E.	50-60 deg N, 2 deg E – 10 deg W.
Data source	NCEP/NCAR Reanalysis		Based on maps from the Daily Weather Reports of the Met Office and from 5 other sources.
Period of record	1951-2004	1881-1998	1861-1995
Sampling period	1-day	3-day	Charts from every 6 hours at the end of period or at least 3 charts in the beginning.
Annual/Seasonal	Seasonal values – winter (DJF), spring (MAM), summer (JJA), fall (SON).	Annual (29 patterns identified)	Annual - 8 major directional types: Westerly, Northerly, Northeasterly, Northwesterly, Easterly, Southeasterly, Southwesterly, Southerly; 3 non-directional types – Cyclonic, Anticyclonic and Unspecified.
Data preprocessing	Time standardization of data.		

Appendix Table 1 continued

	Current study	Hess Brezowsky 1969	Lamb's 'Airflow Types' over the British Isles 1972
Correspondence between circulation patterns	*Winter:*		
	Voeikov Belt-Arctic Low	BM, SA	Westerly
	Mediterranean Low-North Atlantic High	----------	Anticyclonic
	European High	HB, HM	Southerly
	Scandinavian High-Mediterranean Low	WW, HFA, HFZ, SZ	Easterly
	Icelandic Low	WS, SWZ, SEZ , SWA	Cyclonic
			Northerly, North-westerly – not seen.
	Spring:		
	Scandinavian High-Mediterranean Low	HFZ, HNFA	Easterly
	Arctic Low-Voeikov Belt	----------	Westerly
	Azores-Scandinavian Ridge	NEA, NEZ, HNFZ, TM	Anticyclonic
	European Low	TRM, NZ, HNZ	North-westerly, Northerly
	Icelandic Low	TB, SEA	Cyclonic
		HNA, NA – not seen.	Southerly – not seen.
	Summer:		
	Weak Persian Gulf Low	NA (somewhat similar)	----------
	Azores-Scandinavian Ridge	HNA, NEA, TRW	Anticyclonic, Easterly (somewhat)
	Arctic Low-Persian Gulf Low	NWA, NWZ	Cyclonic, Westerly, North-Westerly

Appendix Table 1 continued

	Current study	Hess Brezowsky 1969	Lamb's 'Airflow Types' over the British Isles 1972
Correspondence between circulation patterns		TB, HNFA, NZ, WZ, WA – not seen.	Northerly, Southerly – not seen.
	Fall:		
	Persian Gulf Low	----------	Westerly
	Arctic Low-Voeikov Belt	HM, HB, WA	Anticyclonic, Southerly
	Scandinavian High-Mediterranean Low	WW, HFZ	Easterly
	Icelandic Low	SWA, SWZ , SEA	Cyclonic
		HNZ, SA, BM, TRM – not seen.	Northerly, North-westerly – not seen.
Footnotes	None	None	About 4% unclassified (ranging from 2-7% in individual years).
	Current study	**Jenkinson and Collinson (1977), Jones et al. (1993), from Goodess and Palutikof, 1998**	**Schüepp's synoptic classification (1979) from Stefanicki et al., 1998**
Analysis method	Nonhierarchical cluster analysis based on PCA scores.	Automated version of the Lamb Weather Type classification, based on resultant wind flow and total shear vorticity.	Semi-objective classification which takes into account the surface pressure, geostrophic wind direction, wind speed and direction at 500 hPa, Z500, and baroclinicity.
Variable	SLP	SLP	Surface pressure and Z500.
Region	777 grid points between 40 deg W and 50 deg E, and 20-70 deg N	Approximately 40 – 67.5 N, 24 W – 14 E	444 km diameter area in central Alps around 46 deg 30 min N, 9 deg E.
Data source	NCEP/NCAR Reanalysis	Mean SLP gridded data	
Period of record	1951-2004	1880-1989	1945-1994

Appendix Table 1 continued

	Current study	Jenkinson and Collinson (1977), Jones et al. (1993), from Goodess and Palutikof, 1998	Schüepp's synoptic classification (1979) from Stefanicki et al., 1998
Sampling period	1-day	1-day	1-day (12 UTC)
Annual/Seasonal	Seasonal values – winter (DJF), spring (MAM), summer (JJA), fall (SON).	Annual - 14 circulation types. Only maps (anomaly maps also) for winter and summer are shown in GP (1998).	Annual - 40 weather types aggregated into 7 subclasses and 3 main types – convective, advective and mixed weather type.
Data preprocessing	Time standardization of data.		
Correspondence between circulation patterns	*Winter:*		
	Arctic Low-Voeikov Belt	----------	----------
	Mediterranean Low-North Atlantic High	E/NE	----------
	European High	A/HYA , UA	High
	Scandinavian High-Mediterranean Low	----------	----------
	Icelandic Low	W/NW/SW/N group	Southerly
		C, UC, HYC, S/SE – not seen.	Low, W, N, E, Mixed, Flat - not seen
	Spring:		
	Scandinavian High-Mediterranean Low		----------
	Arctic Low-Voeikov Belt		(High)
	Azores-Scandinavian Ridge		Easterly
	European Low		Low
	Icelandic Low		Southerly
			W, N, Flat, Mixed – not seen.

Appendix Table 1 continued

	Current study	Jenkinson and Collinson (1977), Jones et al. (1993), from Goodess and Palutikof, 1998	Schüepp's synoptic classification (1979) from Stefanicki et al., 1998
Correspondence between circulation patterns	*Spring:*		
	Scandinavian High-Mediterranean Low		----------
	Arctic Low-Voeikov Belt		(High)
	Azores-Scandinavian Ridge		Easterly
	European Low		Low
	Icelandic Low		Southerly
			W, N, Flat, Mixed – not seen.
	Summer:		
	Weak Persian Gulf Low	UA (possibly)	Northerly
	Azores-Scandinavian Ridge	C, HYC, E/NE, S/SE	Easterly
	Arctic Low-Persian Gulf Low	A/HYA	----------
		UC, W/NW/SW/N group- not seen.	W, S, High, Low, Flat, Mixed – not seen.
	Fall:		
	Persian Gulf Low		Northerly
	Arctic Low-Voeikov Belt		High
	Scandinavian High-Mediterranean Low		----------
	Icelandic Low		Low
			W, E, S, Flat, Mixed – not seen.
Footnotes	None	None	None

Appendix Table 1 continued

	Current study	Automatic classification Maheras et al., 2000	Plaut G. and E. Simonnet, 2001
Analysis method	Nonhierarchical cluster analysis based on PCA scores.	Automatic classification of circulation types relevant to Greece, using spatial methods of topology and geometry.	PCA, and dynamical clustering algorithm – ANAXV package.
Variable	SLP	SLP and Z500	SLP
Region	777 grid points between 40 deg W and 50 deg E, and 20-70 deg N	20-65 deg N, 20 deg W – 50 deg E	640 grid points, 100 deg longitude by 40 deg lat centered at 50 deg N, 10 deg W.
Data source	NCEP/NCAR Reanalysis	NCEP/NCAR Reanalysis	CRU
Period of record	1951-2004	1958-1997	1880-1997
Sampling period	1-day	6 hrs, 1-day	1-day
Annual/Seasonal	Seasonal values – winter (DJF), spring (MAM), summer (JJA), fall (SON).	Annual 20 circulation types – 6 anticyclonic, 8 cyclonic, 2 mixed and 4 special types (only winter and summer maps shown; Z500 anomalies maps available)	Winter (November-March) 5 patterns (anomaly maps available)
Data preprocessing	Time standardization of data.		Subtracted winter mean fields at each grid point.
Correspondence between circulation patterns	*Winter:*		
	Arctic Low-Voeikov Belt	A4, A5, Cn	Atlantic Ridge (somewhat similar)
	Mediterranean Low-North Atlantic High	C, Cs	West Blocking
	European High	A1, A3, A6, Mt1	Blocking

Appendix Table 1 continued

	Current study	Automatic classification Maheras et al., 2000	Plaut G. and E. Simonnet, 2001
Correspondence between circulation patterns	Scandinavian High-Mediterranean Low	A2	Greenland Anticyclone (somewhat similar)
	Icelandic Low	Cw	Zonal
		Mt2, Cne, Cnw, Csw – not seen.	
	Spring:		
	Scandinavian High-Mediterranean Low		
	Arctic Low-Voeikov Belt-		
	Azores-Scandinavian Ridge		
	European Low		
	Icelandic Low		
	Summer:		
	Weak Persian Gulf Low	Cse, Dsec (upper air circulation somewhat differs), MB1	
	Azores-Scandinavian Ridge	Dor	
	Arctic Low-Persian Gulf Low	MB2 (somewhat)	
	Fall:		
	Persian Gulf Low		
	Arctic Low-Voeikov Belt		
	Scandinavian High-Mediterranean Low		
	Icelandic Low		
Footnotes	None	None	None

Appendix Table 1 continued

	Current study	Kassomenos et al., 2003	Esteban P., J.M. Vide, M. Mases, 2006
Analysis method	Nonhierarchical cluster analysis based on PCA scores.	FA and k-means cluster analysis. The classification combines surface air mass characteristics and the synoptic conditions over an area.	PCA and cluster analysis
Variable	SLP	Surface meteorological data for Athens and SLP.	SLP
Region	777 grid points between 40 deg W and 50 deg E, and 20-70 deg N	315 grid points, 25-60 deg N, 10 deg W – 40 deg E.	30 – 60 deg N, 30 deg W – 15 deg E
Data source	NCEP/NCAR Reanalysis	SLP from NCEP/NCAR reanalysis.	NCEP/NCAR Reanalysis
Period of record	1951-2004	1954-1999	1960-2001
Sampling period	1-day	1-day (12 h UTC)	1 day (18:00 GMT)
Annual/Seasonal	Seasonal values – winter (DJF), spring (MAM), summer (JJA), fall (SON).	Warm period (Apr-Oct, 6 types), cold period (Oct-Apr, 8 types) of the year.	Annual
Data preprocessing	Time standardization of data.		Spatial standardization
Correspondence between circulation patterns	*Winter:* Arctic Low-Voeikov Belt	----------	West-northwest advection (CL7, somewhat similar), Anticyclone Bridge (CL19)
	Mediterranean Low-North Atlantic High	----------	Mediterranean Low/northerly advection (CL6, somewhat similar)

Appendix Table 1 continued

	Current study	Kassomenos et al., 2003	Esteban P., J.M. Vide, M. Mases, 2006
Correspondence between circulation patterns	European High	2W, 7W	Central Europe High (CL15)
	Scandinavian High-Mediterranean Low	1W	Southerly flow (CL8)
	Icelandic Low	----------	Winter westerly (CL1)
		4W – not seen.	British High (CL4), North Atlantic Low (CL9), North-west Iberian Low (CL12), Trough (CL18) – not seen.
	Spring: Scandinavian High-Mediterranean Low	----------	Southerly flow (CL8)
	Arctic Low-Voeikov Belt	2W, 8W	West-northwesterly advection (CL7), Anticyclone Bridge (CL19)
	Azores-Scandinavian Ridge	6S	----------
	European Low	5W, 1S	Mediterranean Low/northerly advection (CL6), Central Europe Low/northerly advection (CL16)
	Icelandic Low	----------	----------
			North Atlantic Low (CL9), North-west advection in Atlantic façade (CL10), North-west Iberian Low (CL12), British Low (CL14) – not seen.

Appendix Table 1 continued

	Current study	Kassomenos et al., 2003	Esteban P., J.M. Vide, M. Mases, 2006
Correspondence between circulation patterns	*Summer:* Weak Persian Gulf Low	3S	Azores Anticyclone II (CL20)
	Azores-Scandinavian Ridge	6S	North Atlantic Ridge (CL2), Azores Ridge (CL13)
	Arctic Low-Persian Gulf Low	----------	Summer westerly in Atlantic façade (CL3), West-northwest advection (CL7), North-west advection in the Atlantic façade (CL10), Azores Anticyclone I (CL11),
			Iberian Thermal Low (CL17) – not seen.
	Fall: Persian Gulf Low	5S	----------
	Arctic Low-Voeikov Belt	3W, 8W, 2S	Anticyclone bridge (CL19)
	Scandinavian High-Mediterranean Low	1W	Southerly flow (CL8)
	Icelandic Low	6W	British Low (CL14 somewhat similar)
		4S – not seen	Mediterranean High (CL5), Mediterranean Low/northerly advection(CL6), West-northwest advection (CL7), North Atlantic Low (CL9), North-west advection in the Atlantic façade (CL10), North-west Iberian low (CL12), Trough (CL18), Azores Ridge (CL13) – not seen.
Footnotes	None	None	None

APPENDIX to Chapter 3

In this Appendix to Chapter 3, all the figures from the GEV and GPD fit are presented as well as the tables containing the details about the parameters of the fitted models. First, the GEV model fit plots to the highest TMAX for the year and by season are given and the stations are ordered as follows: Obraztsov Chiflick, Pleven, Plovdiv, Varna and Pleven NCDC. The tables with the parameters of the fitted models for the highest TMAX follow. Next, the GEV model fit plots to the lowest TMIN for the year and by season are presented, followed by the tables with details about the parameters of the fitted model. The Mean Residual Life plots and the GPD fit to a set of thresholds are presented first for summer and then for winter by station. After that, the GPD model fit to the exceedances over 32°C in summer are presented for all stations. The tables with the details of the parameters follow. Last, the GPD model fit of the deficiencies below 0°C in winter are given by station, followed by the table with the parameters details.

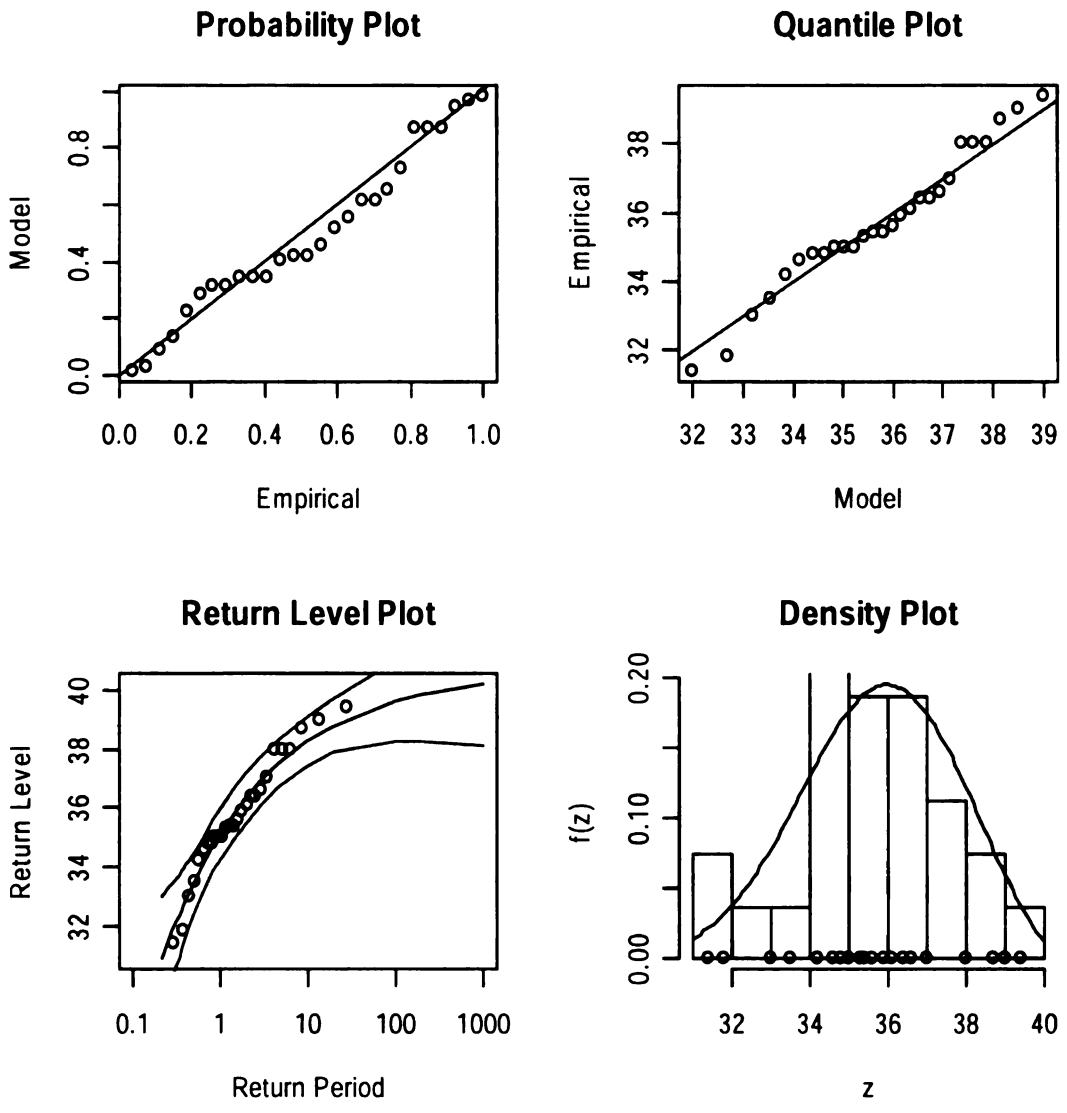

Appendix Figure 1 GEV model fit plots for Annual Highest TMAX for Obraztsov Chiflick, 1953-1979

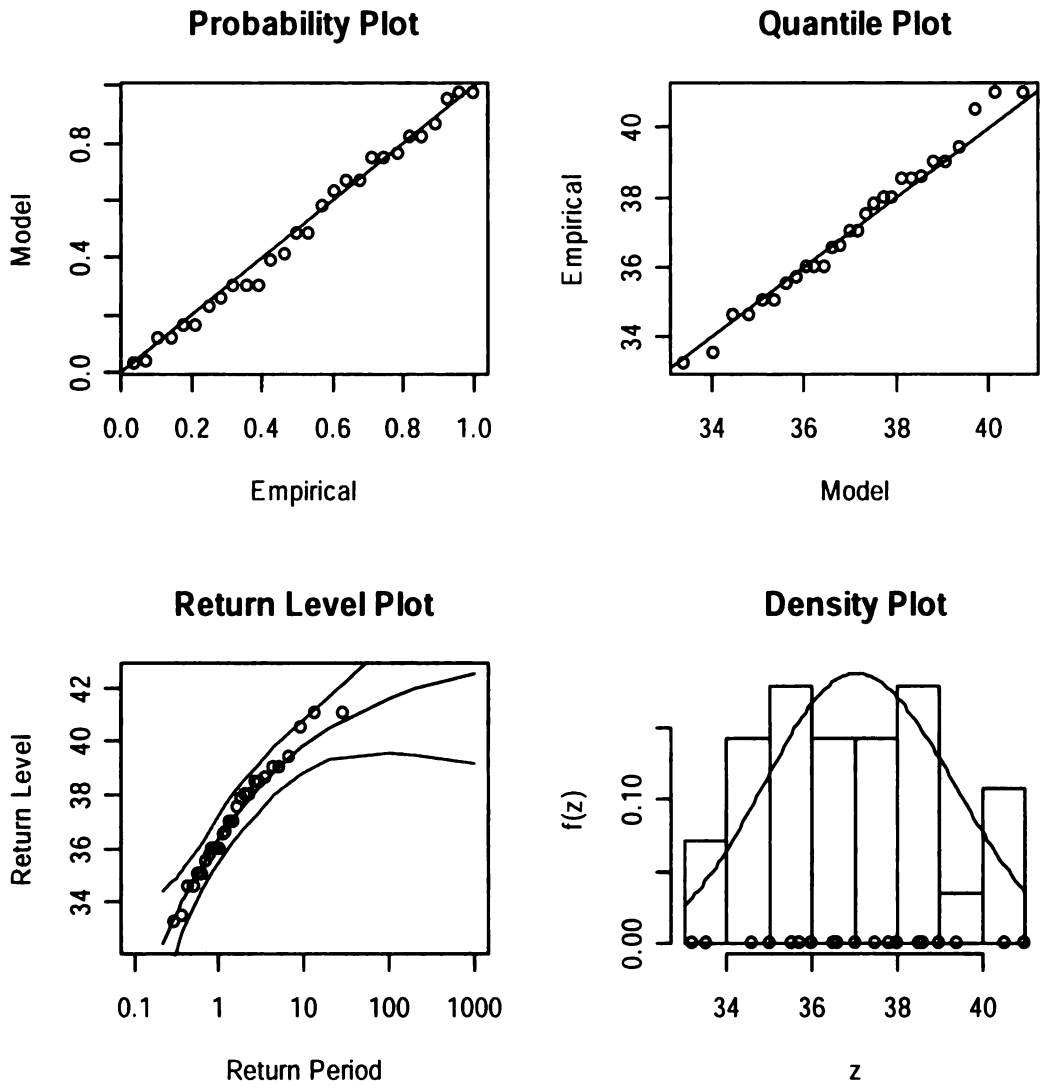

Appendix Figure 2 GEV model fit plots for Annual Highest TMAX for Pleven, 1951-1979

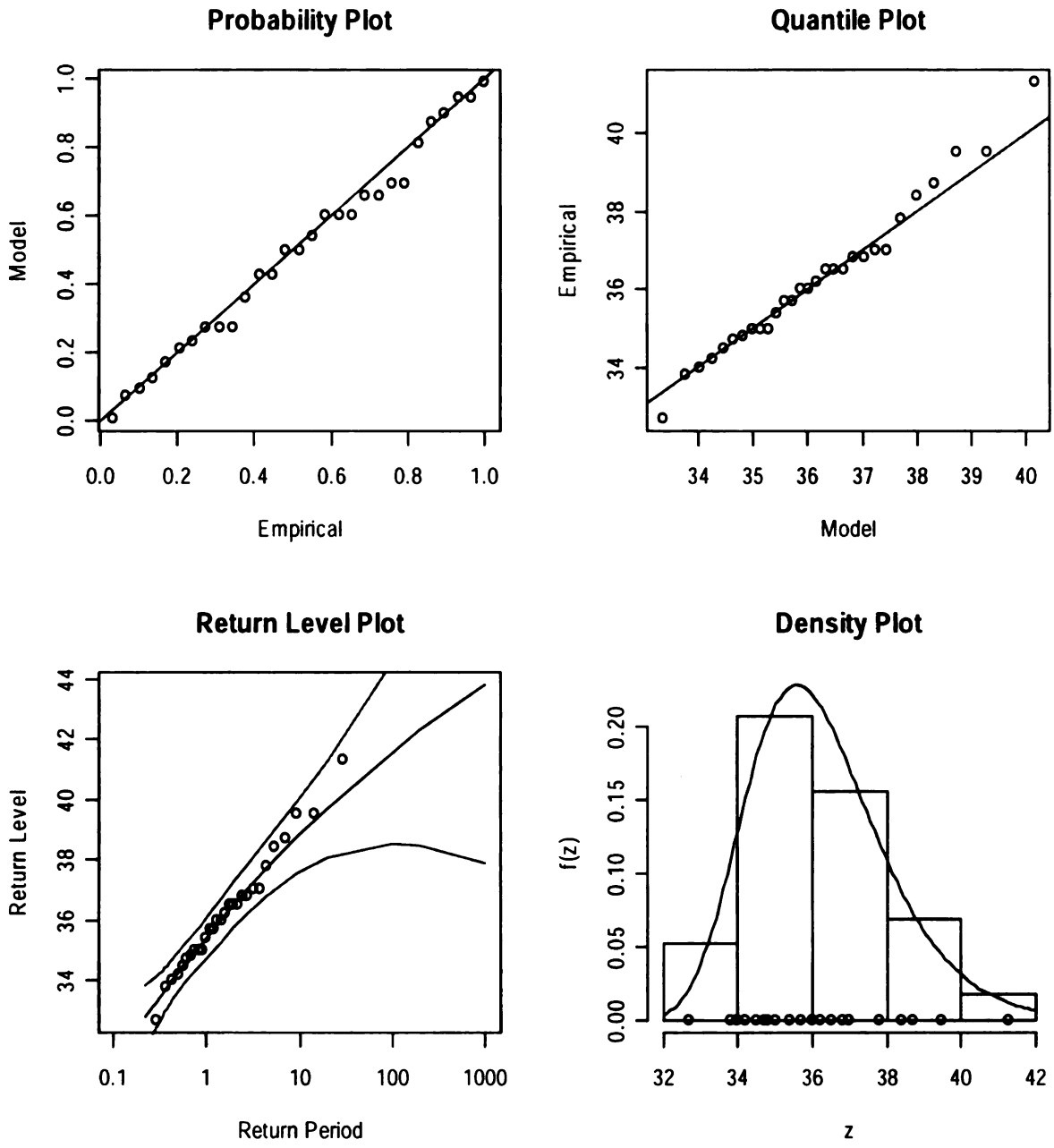

Appendix Figure 3 GEV model fit plots for Annual Highest TMAX for Plovdiv, 1951-1979

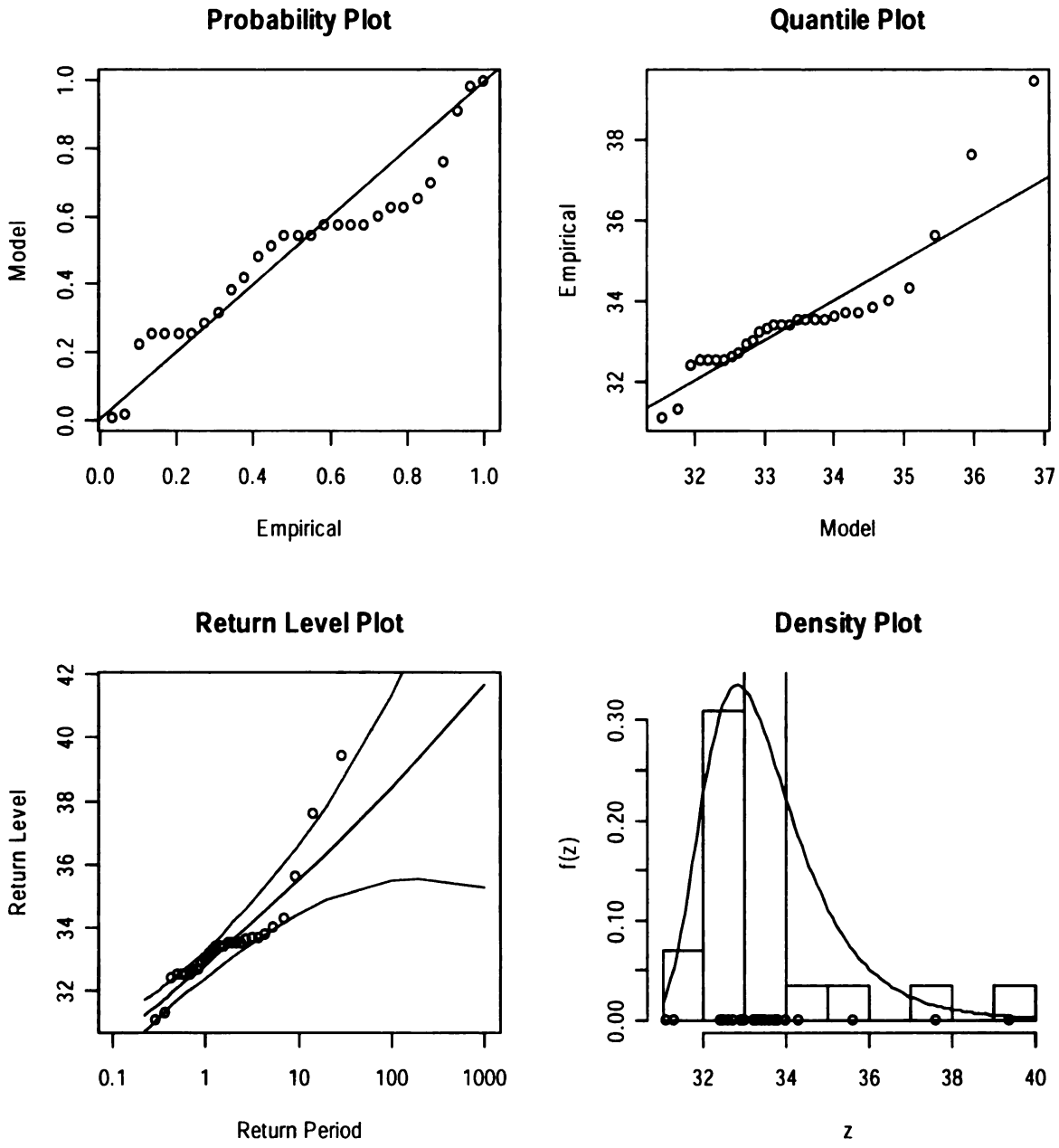

Appendix Figure 4 GEV model fit plots for Annual Highest TMAX for Varna, 1951-1979

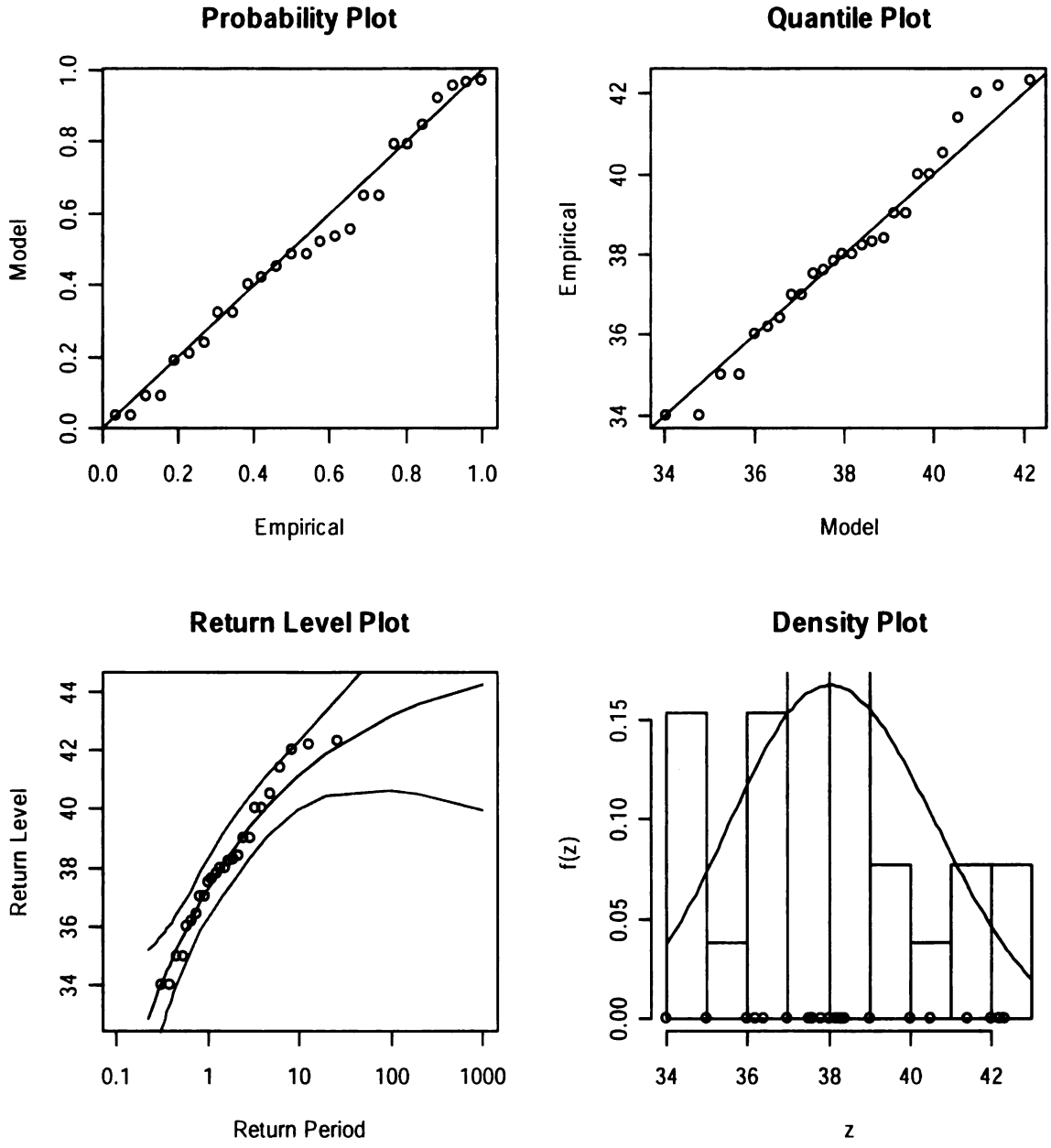

Appendix Figure 5 GEV model fit plots for Annual Highest TMAX for Pleven NCDC, 1973-1999

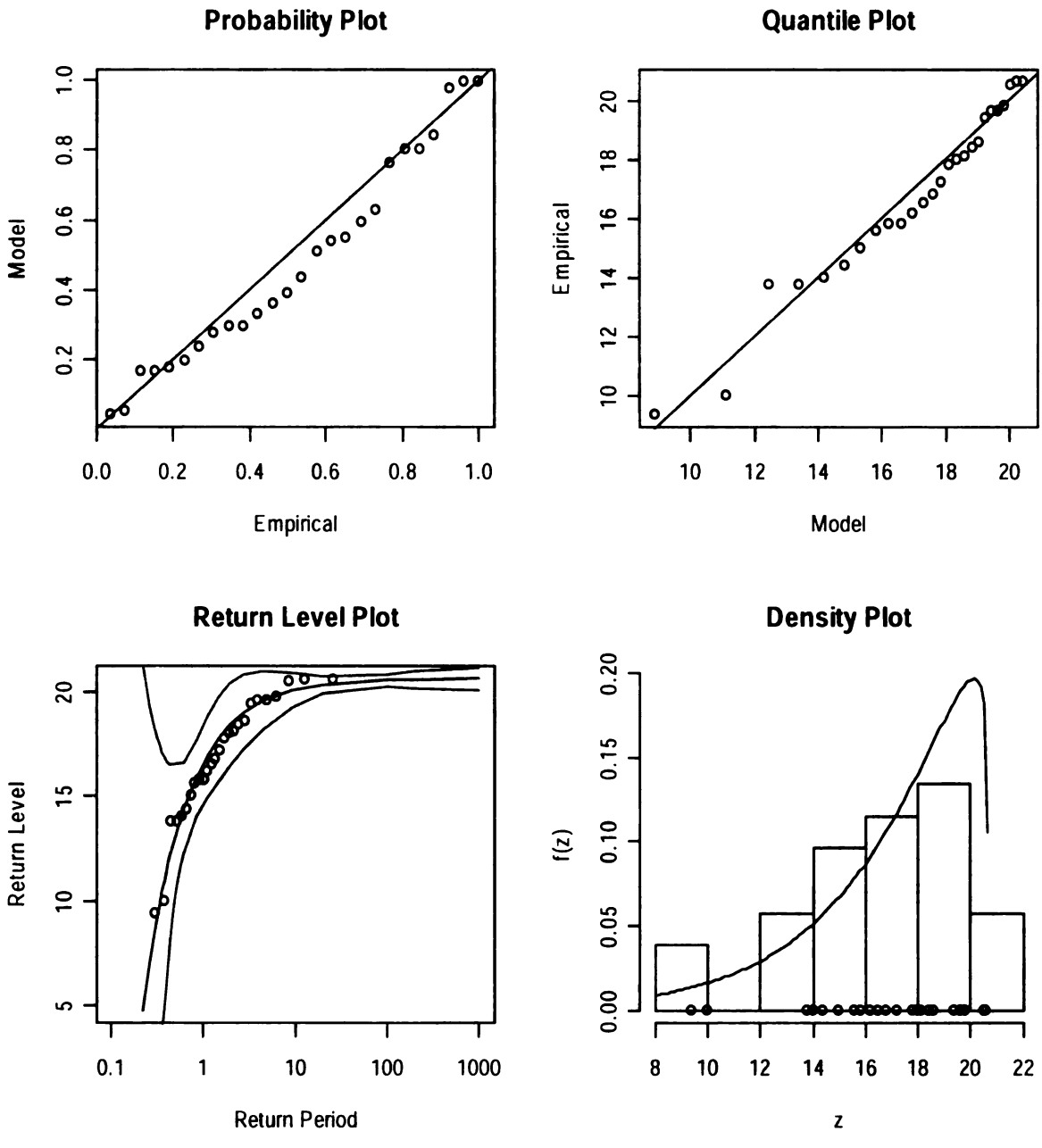

Appendix Figure 6 GEV model fit plots for Winter Highest TMAX for Obraztsov Chiflick, 1953-1979

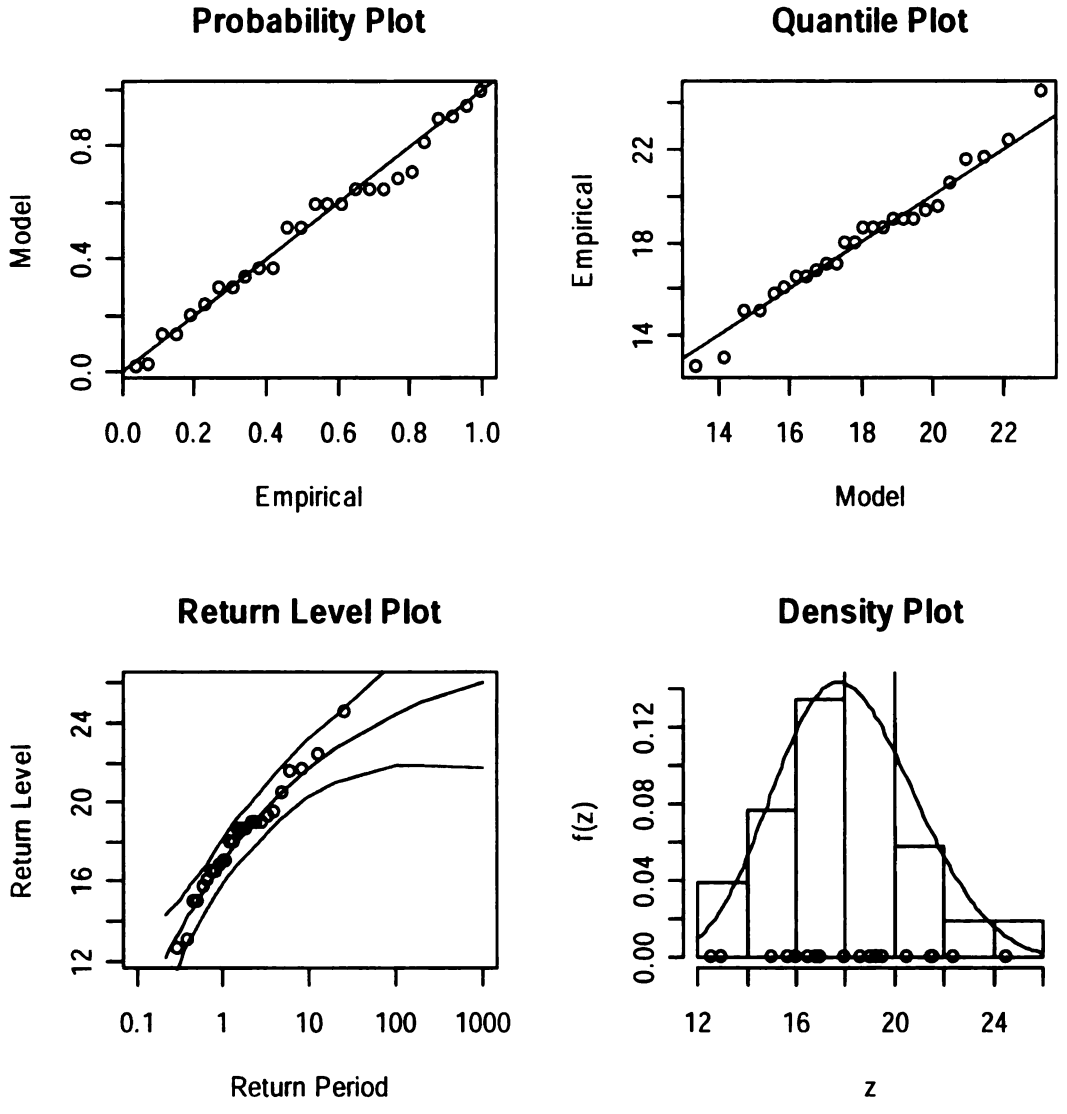

Appendix Figure 7 GEV model fit plots for Winter Highest TMAX for Pleven, 1951-1979

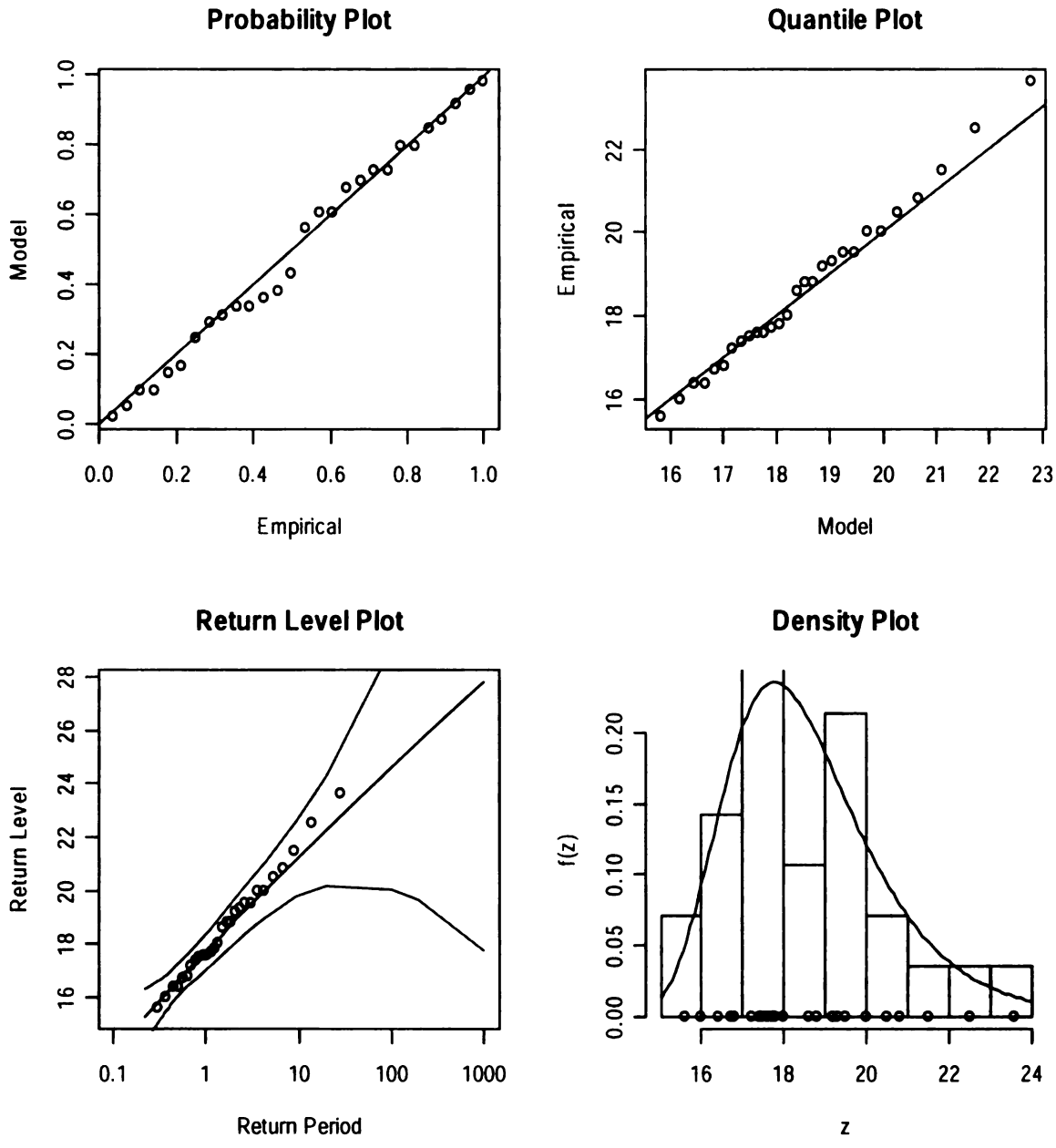

Appendix Figure 8 GEV model fit plots for Winter Highest TMAX for Plovdiv, 1951-1979

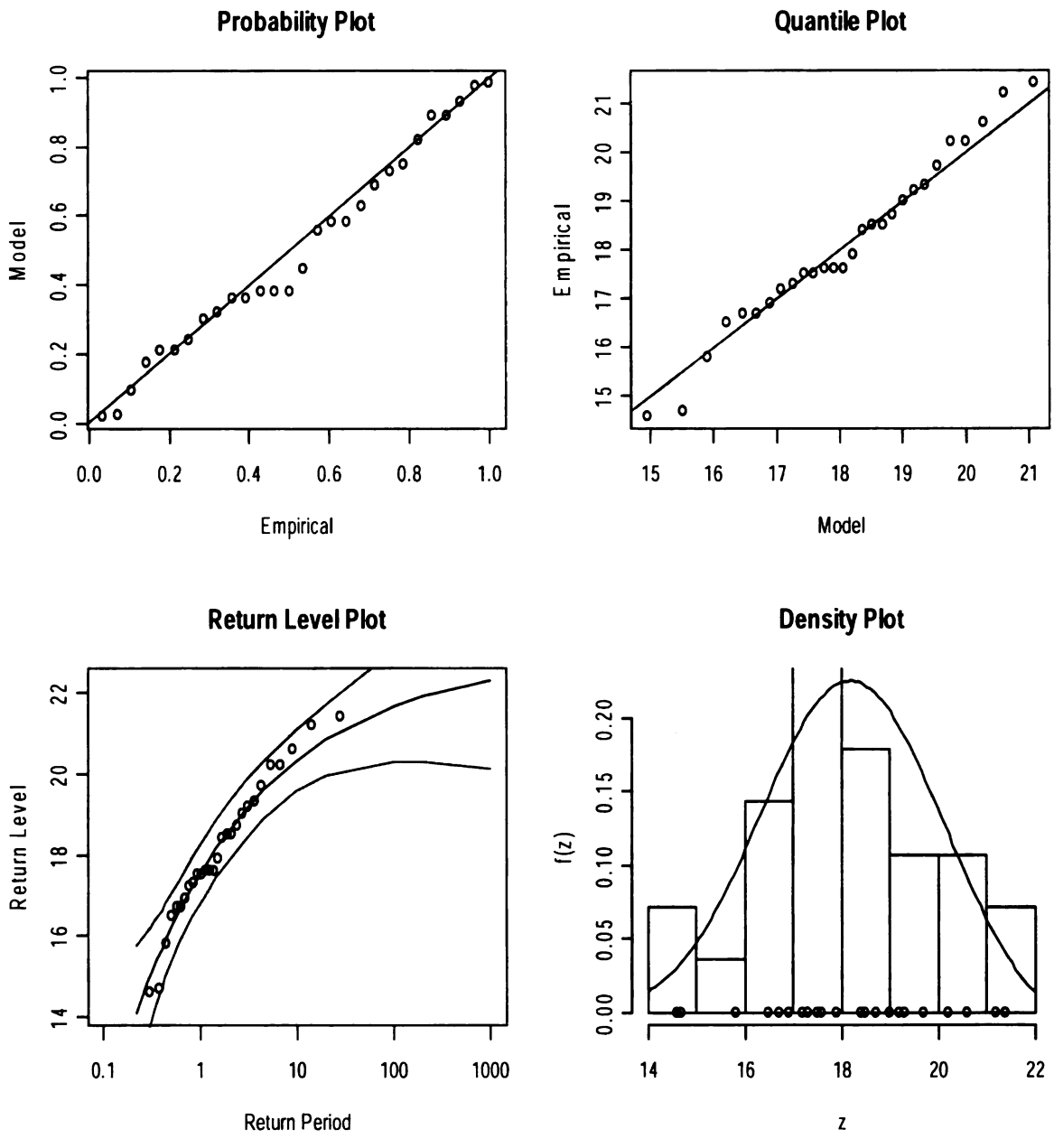

Appendix Figure 9 GEV model fit plots for Winter Highest TMAX for Varna, 1951-1979

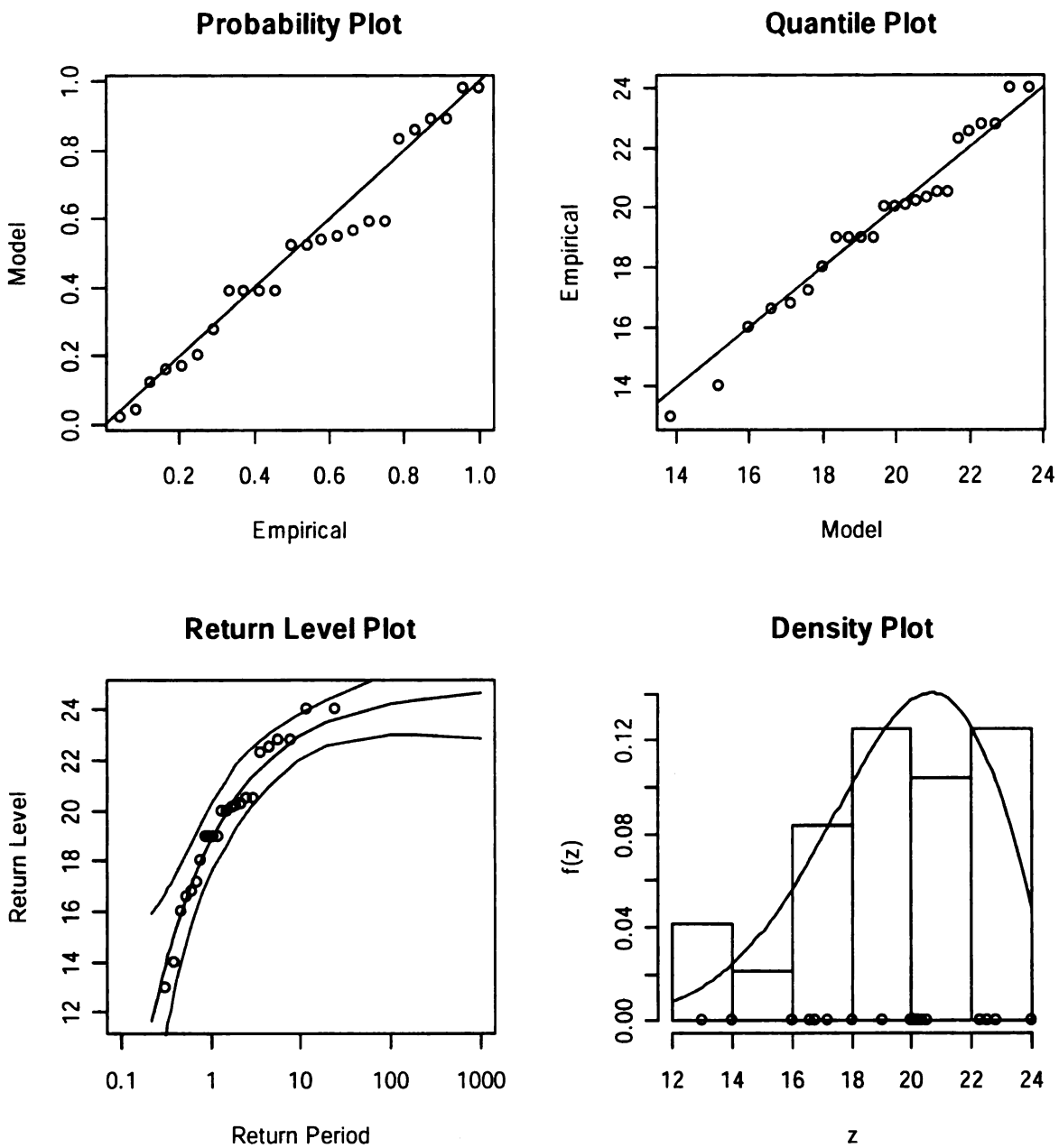

Appendix Figure 10 GEV model fit plots for Winter Highest TMAX for Pleven NCDC, 1973-1999

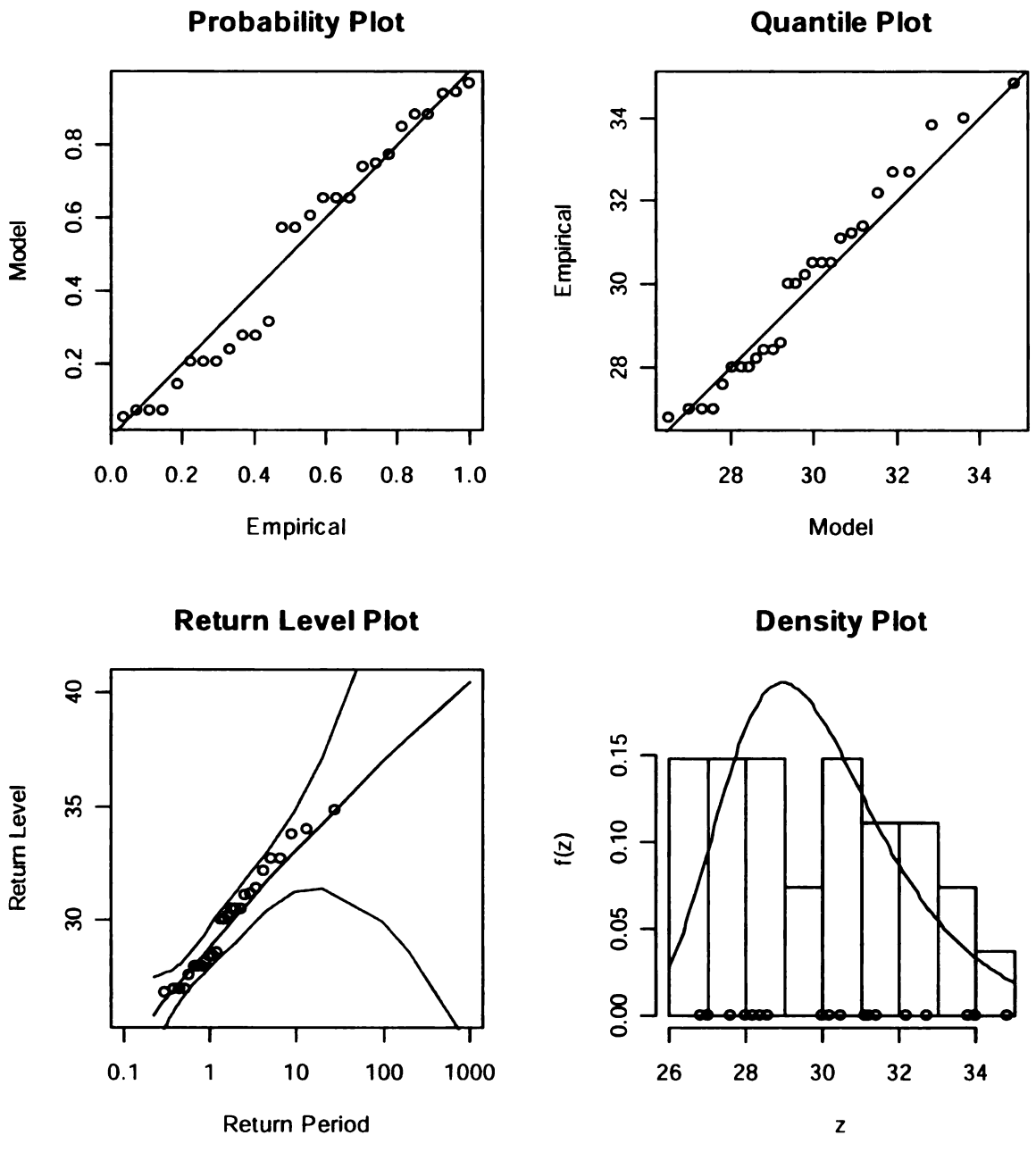

Appendix Figure 11 GEV model fit plots for Spring Highest TMAX for Obraztsov Chiflick, 1953-1979

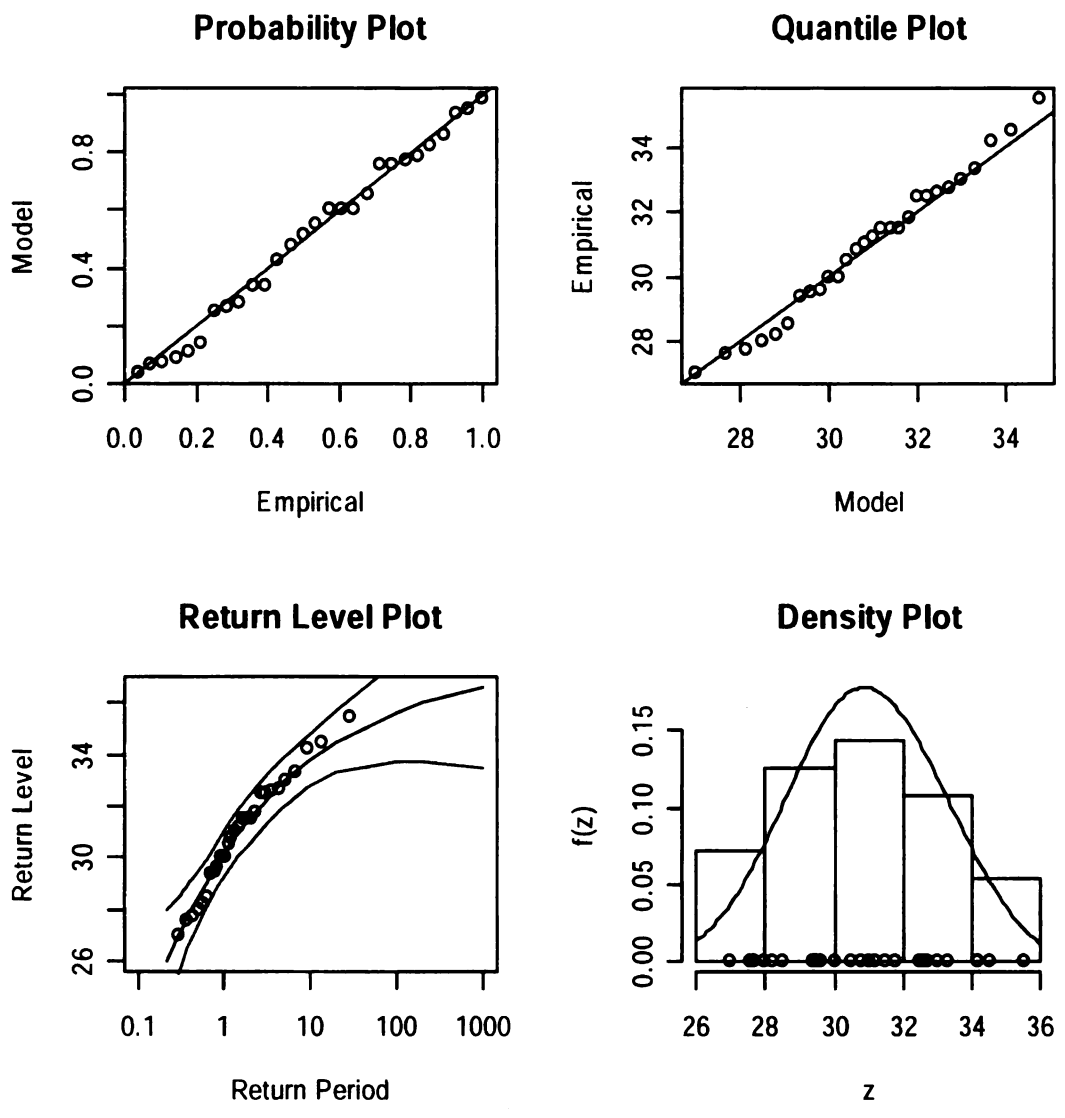

Appendix Figure 12 GEV model fit plots for Spring Highest TMAX for Pleven, 1951-1979

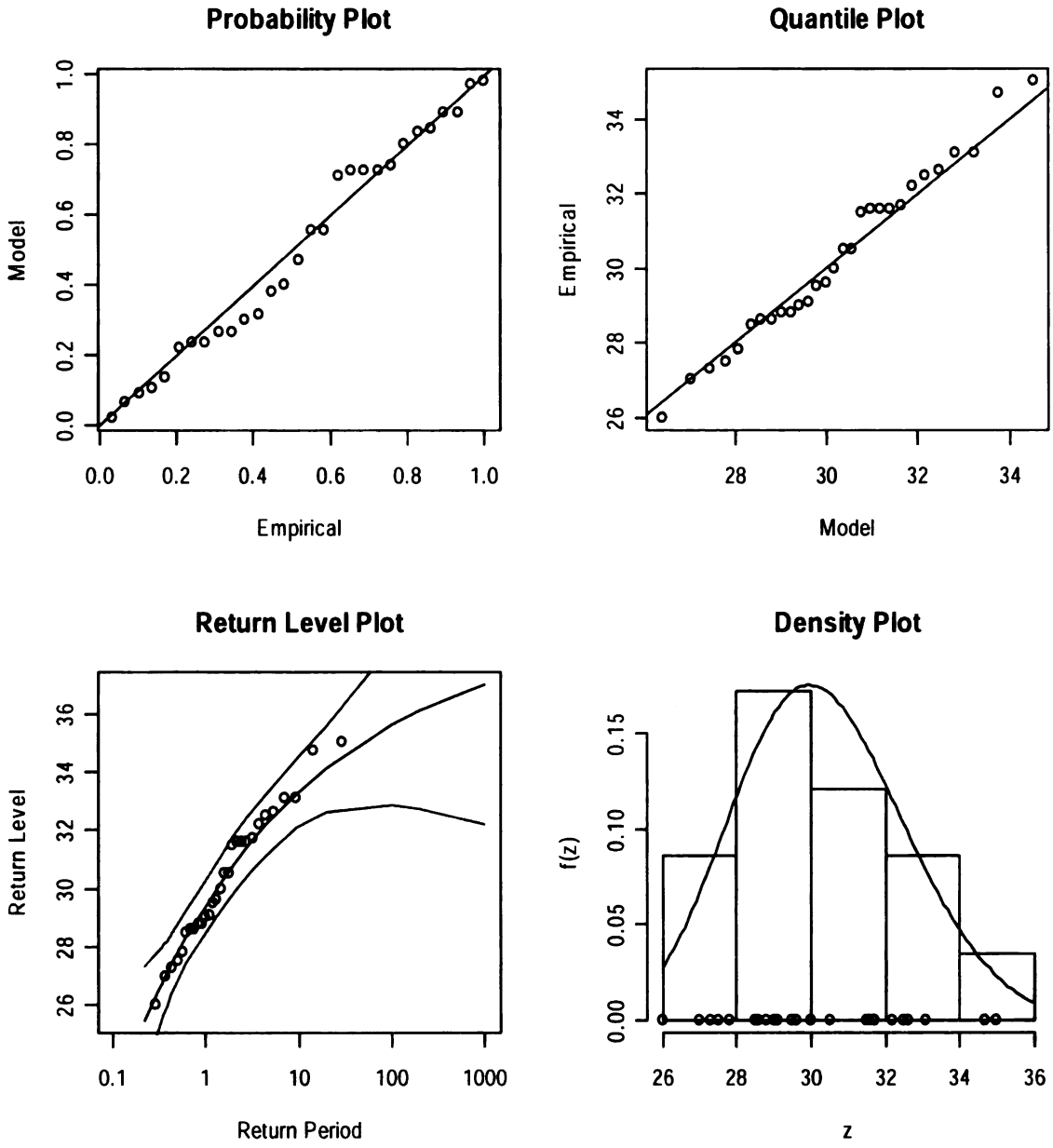

Appendix Figure 13 GEV model fit plots for Spring Highest TMAX for Plovdiv, 1951-1979

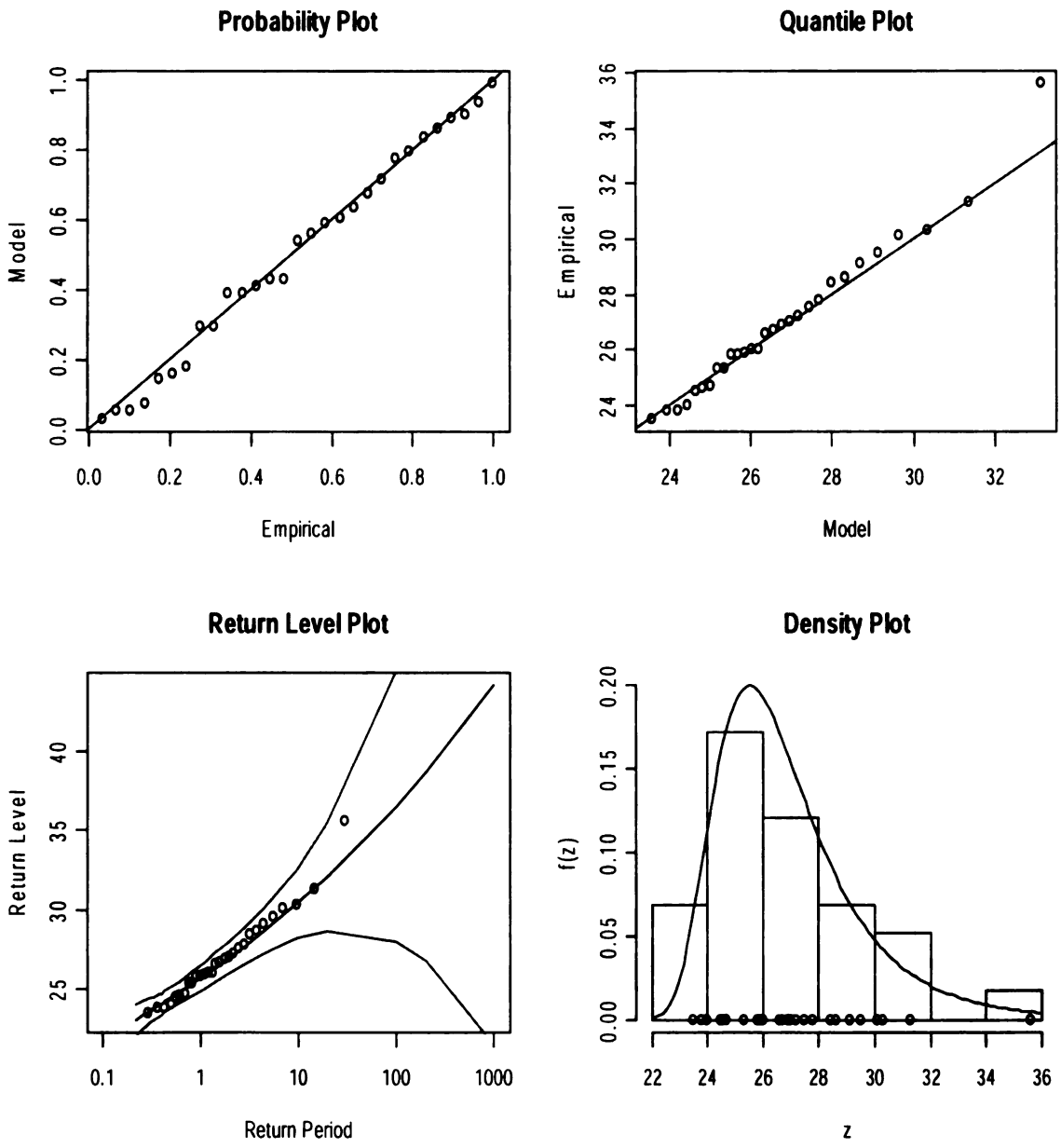

Appendix Figure 14 GEV model fit plots for Spring Highest TMAX for Varna, 1951-1979

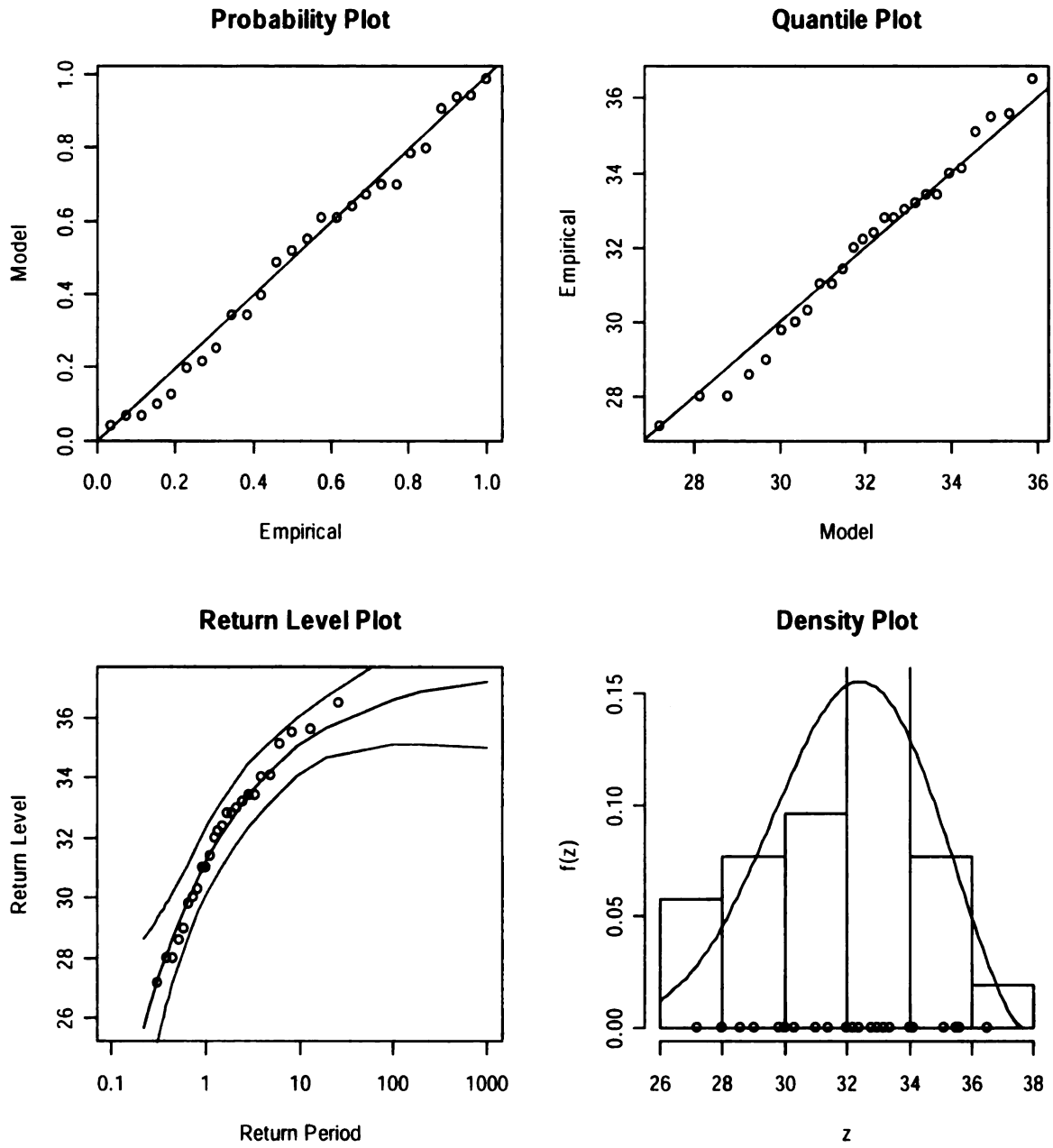

Appendix Figure 15 GEV model fit plots for Spring Highest TMAX for Pleven NCDC, 1973-1999

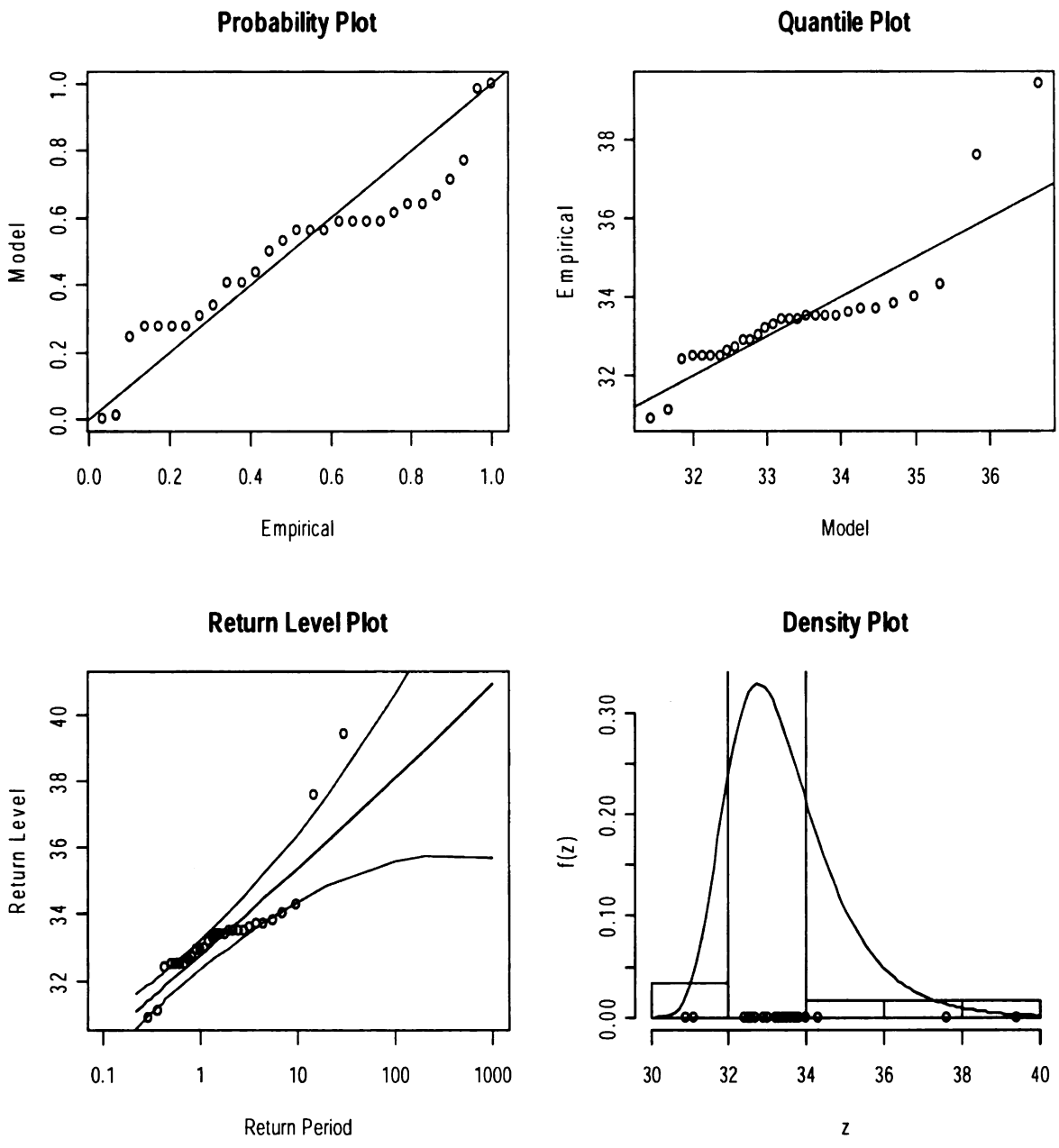

Appendix Figure 16 GEV model fit plots for Summer Highest TMAX for Varna, 1951-1979

GEV plots for the fall highest TMAX

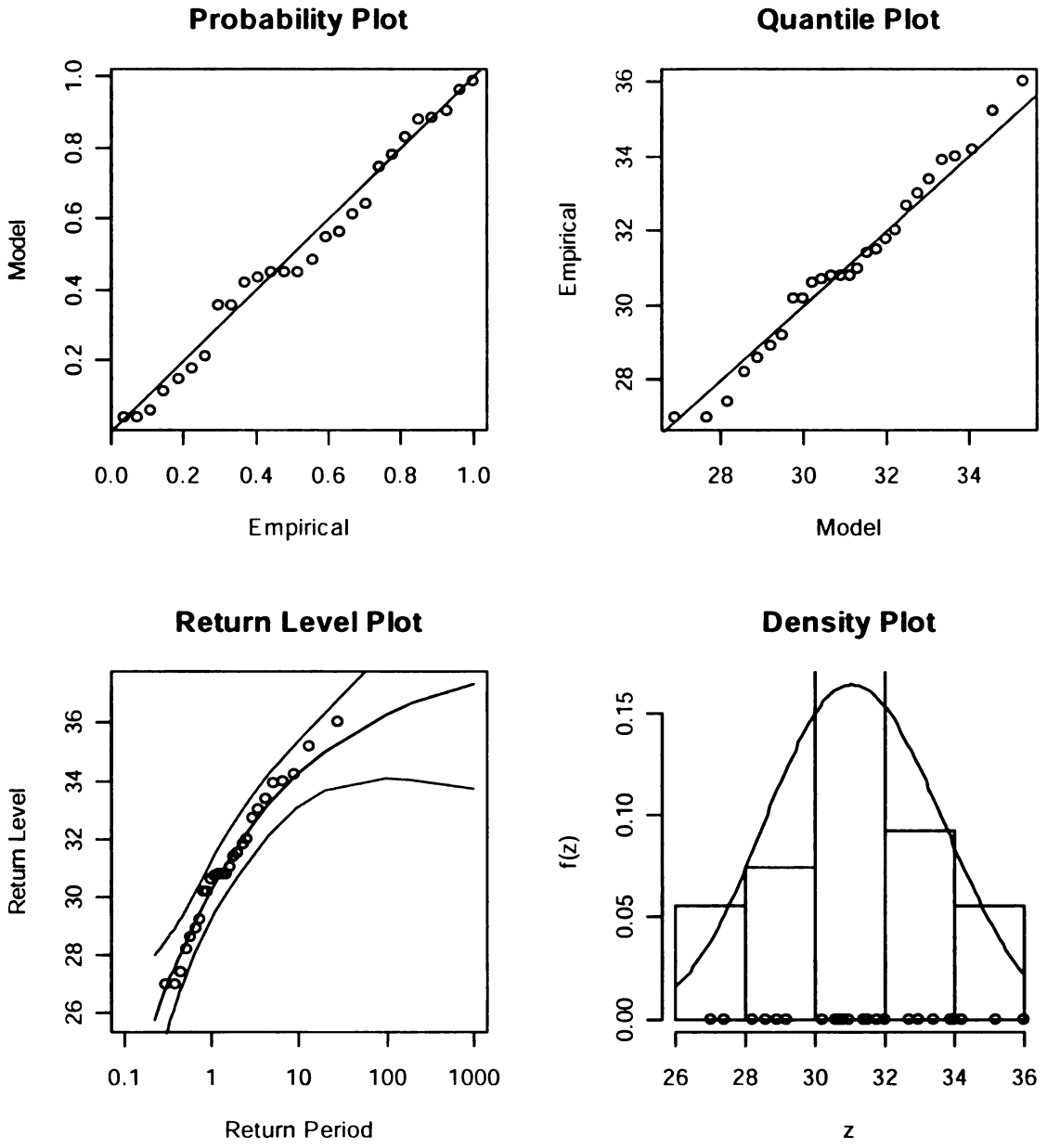

Appendix Figure 17 GEV model fit plots for Fall Highest TMAX for Obraztsov Chiflick, 1953-1979

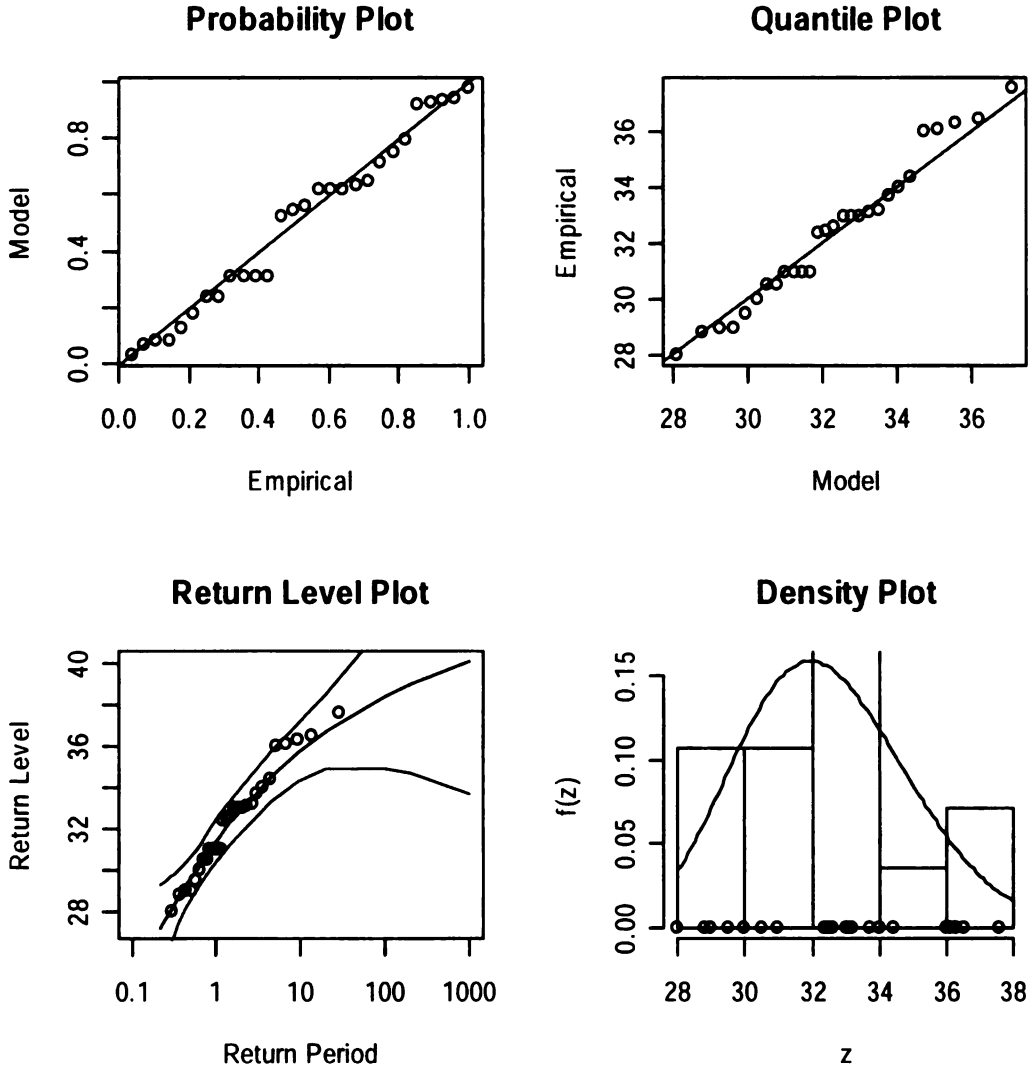

Appendix Figure 18 GEV model fit plots for Fall Highest TMAX for Pleven, 1951-1979

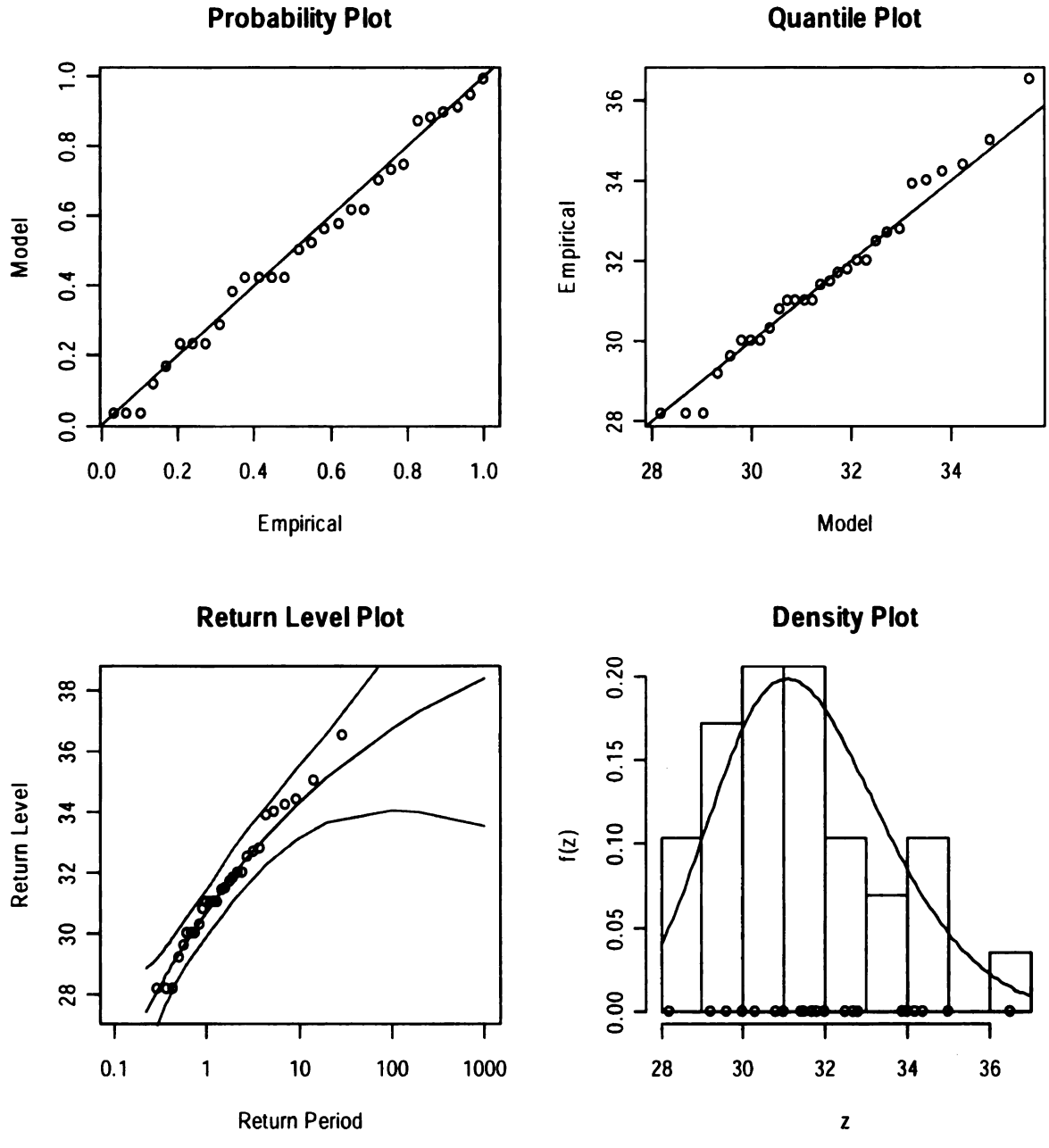

Appendix Figure 19 GEV model fit plots for Fall Highest TMAX for Plovdiv, 1951-1979

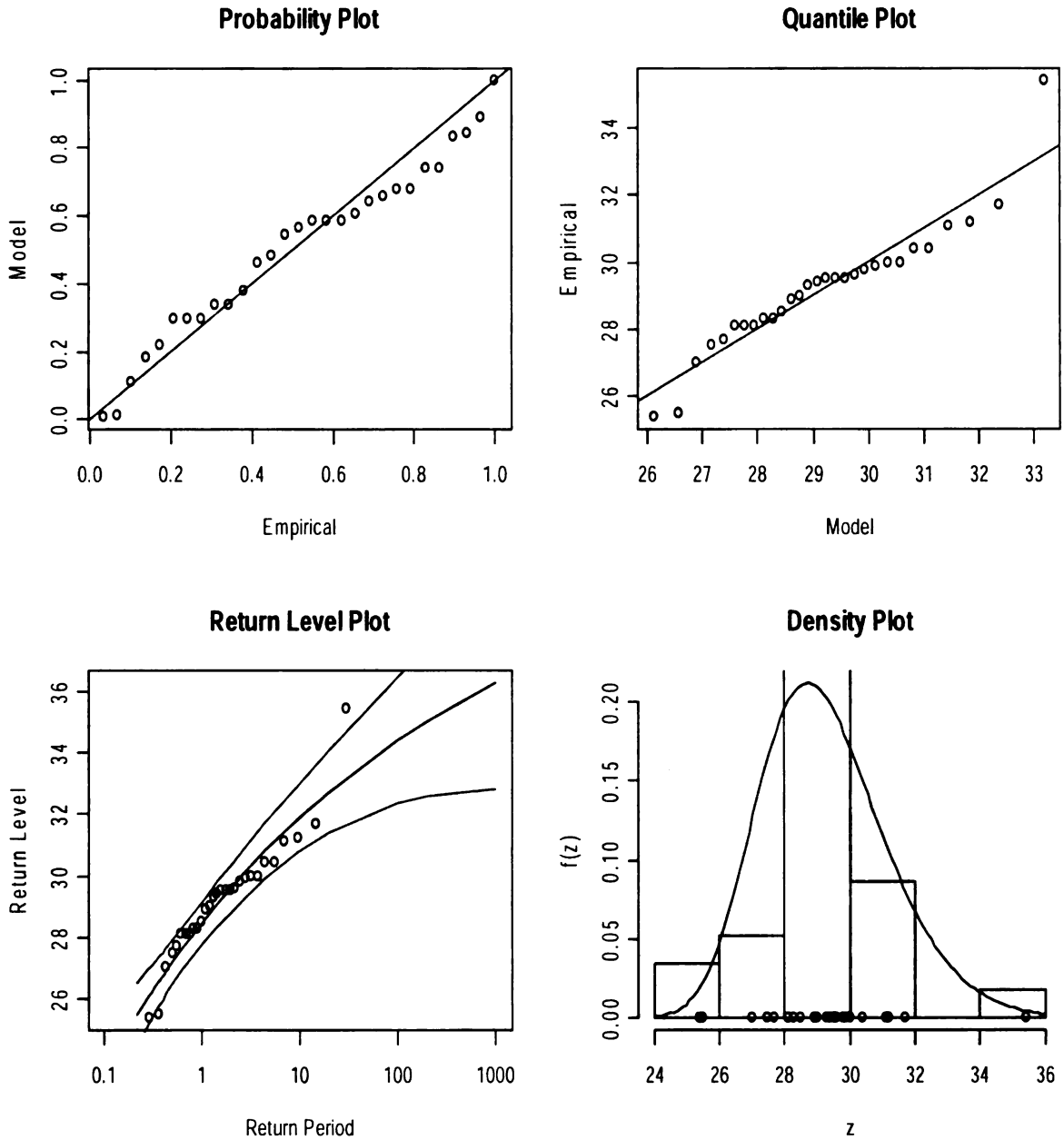

Appendix Figure 20 GEV model fit plots for Fall Highest TMAX for Varna, 1951-1979

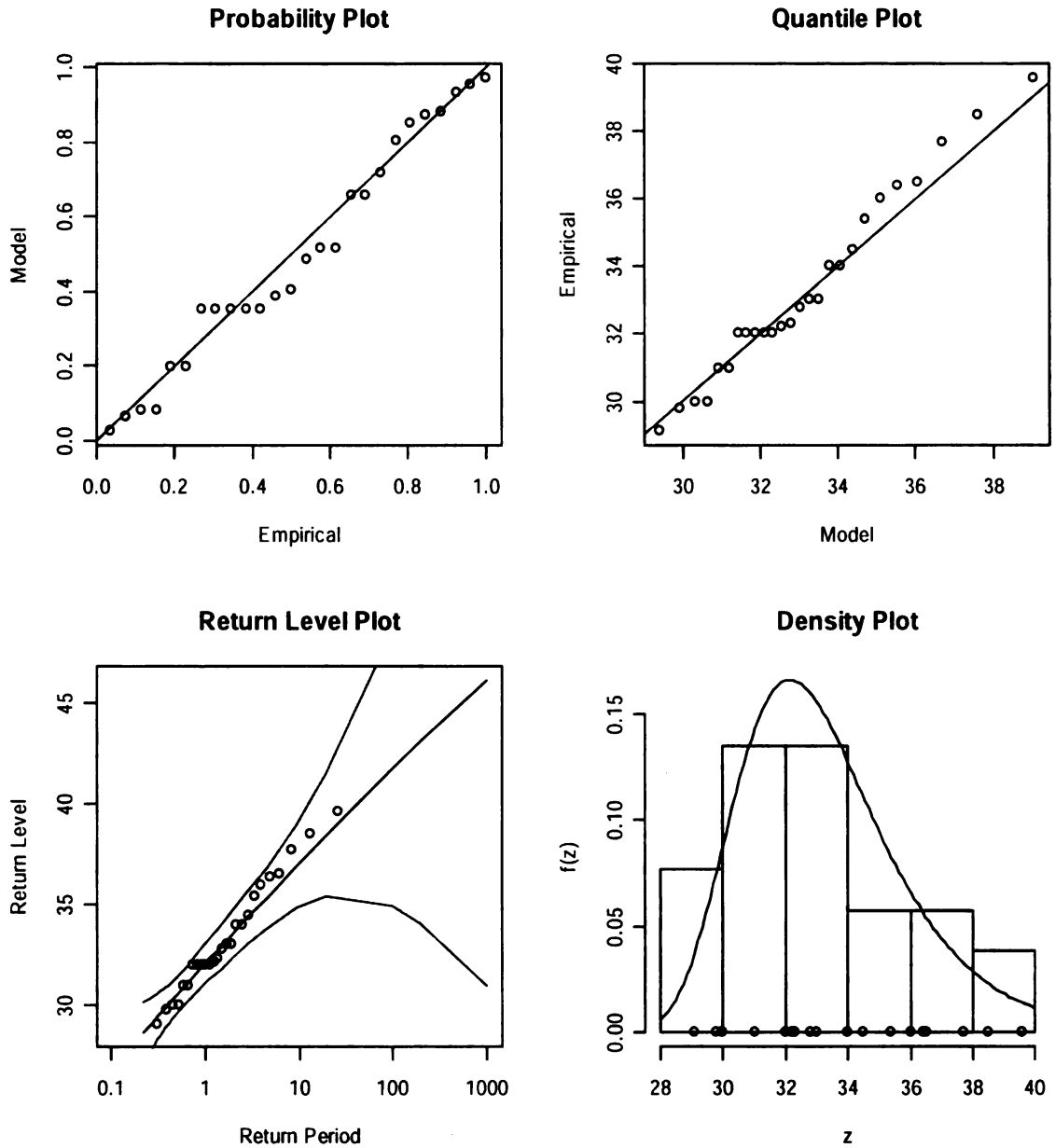

Appendix Figure 21 GEV model fit plots for Fall Highest TMAX for Pleven NCDC, 1973-1999

Appendix Table 2 Highest Annual Daily Maximum Temperature GEV fit details

Station	Obraztsov Chiflick		Varna		Plovdiv		Pleven		Pleven NCDC	
Para-meters	MLE*	Stand. Error	MLE	Stand. Error	MLE	Stand. Error	MLE	Stand. Error	MLE	Stand. Error
Location	35.1	0.4	32.9	0.2	35.4	0.3	36.4	0.4	37.3	0.5
Scale	2.1	0.3	1.1	0.2	1.6	0.2	2.1	0.3	2.3	0.4
Shape	-0.37	0.15	0.04	0.1	-0.09	0.13	-0.29	0.16	-0.29	0.18

MLE means Maximum Likelihood Estimate; Stand. Error means standard error of the estimated parameters of the model

Appendix Table 3 Highest Winter Daily Maximum Temperature GEV fit details

Station	Obraztsov Chiflick		Varna		Plovdiv		Pleven		Pleven NCDC	
Para-meters	MLE	Stand. Error	MLE	Stand. Error	MLE	Stand. Error	MLE	Stand. Error	MLE	Stand. Error
Location	16.6	1.0	17.5	0.4	17.7	0.3	17.0	0.6	18.8	0.7
Scale	3.6	1.2	1.7	0.3	1.6	0.3	2.6	0.4	3.1	0.6
Shape	-0.90	0.47	-0.33	0.14	-0.02	0.17	-0.24	0.12	-0.51	0.17

Appendix Table 4 Highest Spring Daily Maximum Temperature GEV fit details

Station	Obraztsov Chiflick		Varna		Plovdiv		Pleven		Pleven NCDC	
Para-meters	MLE	Stand. Error	MLE	Stand. Error	MLE	Stand. Error	MLE	Stand. Error	MLE	Stand. Error
Location	28.9	0.5	25.7	0.4	29.4	0.5	30.2	0.5	31.2	0.6
Scale	1.9	0.4	1.8	0.3	2.2	0.3	2.2	0.3	2.6	0.4
Shape	-0.04	0.25	0.10	0.17	-0.22	0.16	-0.29	0.15	-0.41	0.15

Appendix Table 5 Highest Summer Daily Maximum Temperature GEV fit details

Station	Obraztsov Chiflick		Varna		Plovdiv		Pleven		Pleven NCDC	
Para-meters	MLE	Stand. Error	MLE	Stand. Error	MLE	Stand. Error	MLE	Stand. Error	MLE	Stand. Error
Location	35.0	0.5	32.8	0.2	35.4	0.3	36.4	0.4	37.2	0.5
Scale	2.1	0.3	1.1	0.2	1.6	0.2	2.1	0.3	2.3	0.4
Shape	-0.38	0.15	0.01	0.09	-0.09	0.13	-0.29	0.16	-0.29	0.18

Appendix Table 6 Highest Fall Daily Maximum Temperature GEV fit details

Station	Obraztsov Chiflick		Varna		Plovdiv		Pleven		Pleven NCDC	
Para-meters	MLE	Stand. Error	MLE	Stand. Error	MLE	Stand. Error	MLE	Stand. Error	MLE	Stand. Error
Location	30.3	0.5	28.5	0.4	30.7	0.4	31.4	0.5	32.1	0.5
Scale	2.4	0.4	1.8	0.2	1.9	0.3	2.4	0.4	2.2	0.4
Shape	-0.29	0.15	-0.14	0.08	-0.17	0.14	-0.21	0.18	-0.03	0.18

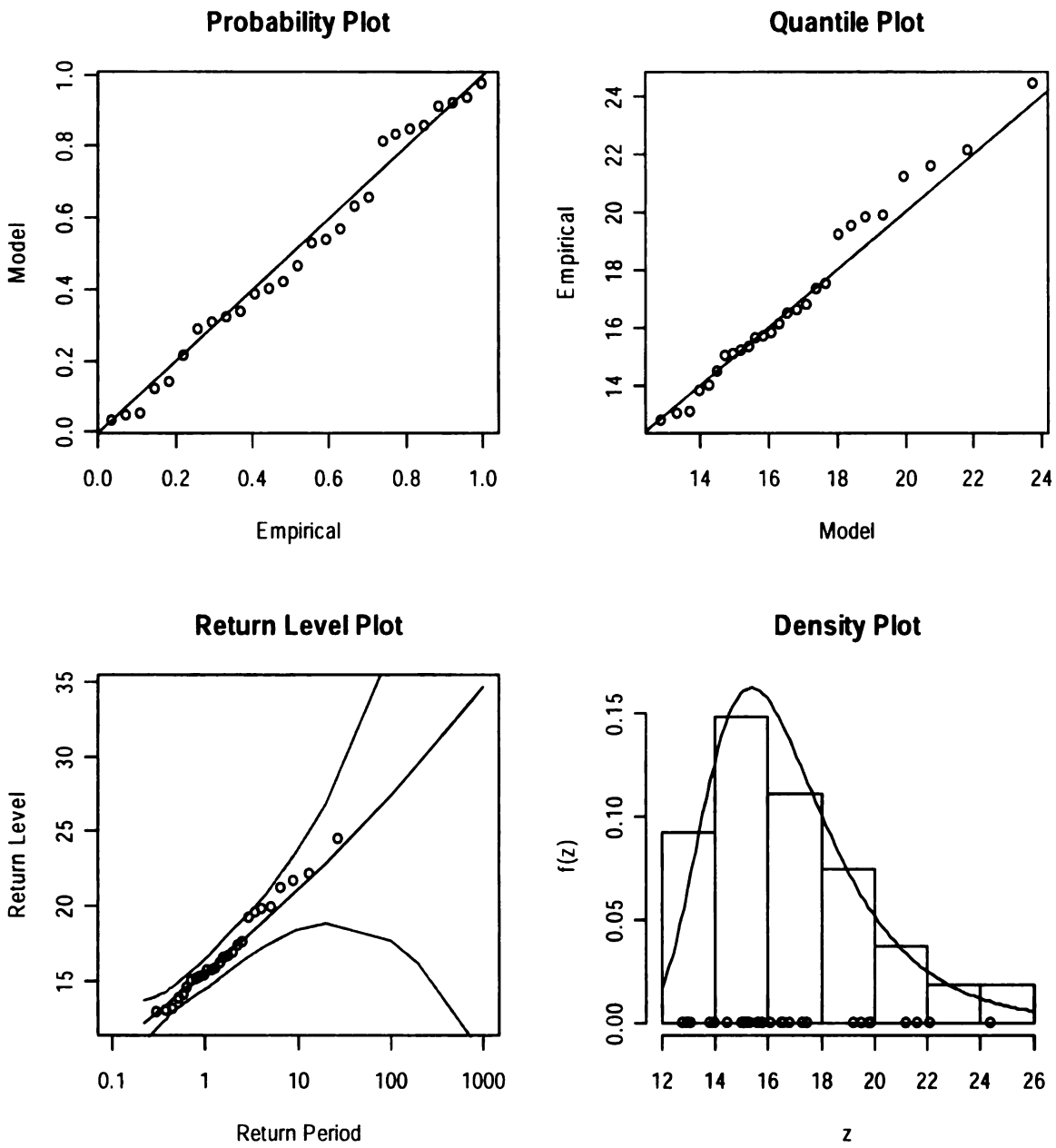

Appendix Figure 22 GEV model fit plots for Annual Lowest TMIN for Obraztsov Chiflick, 1953-1979

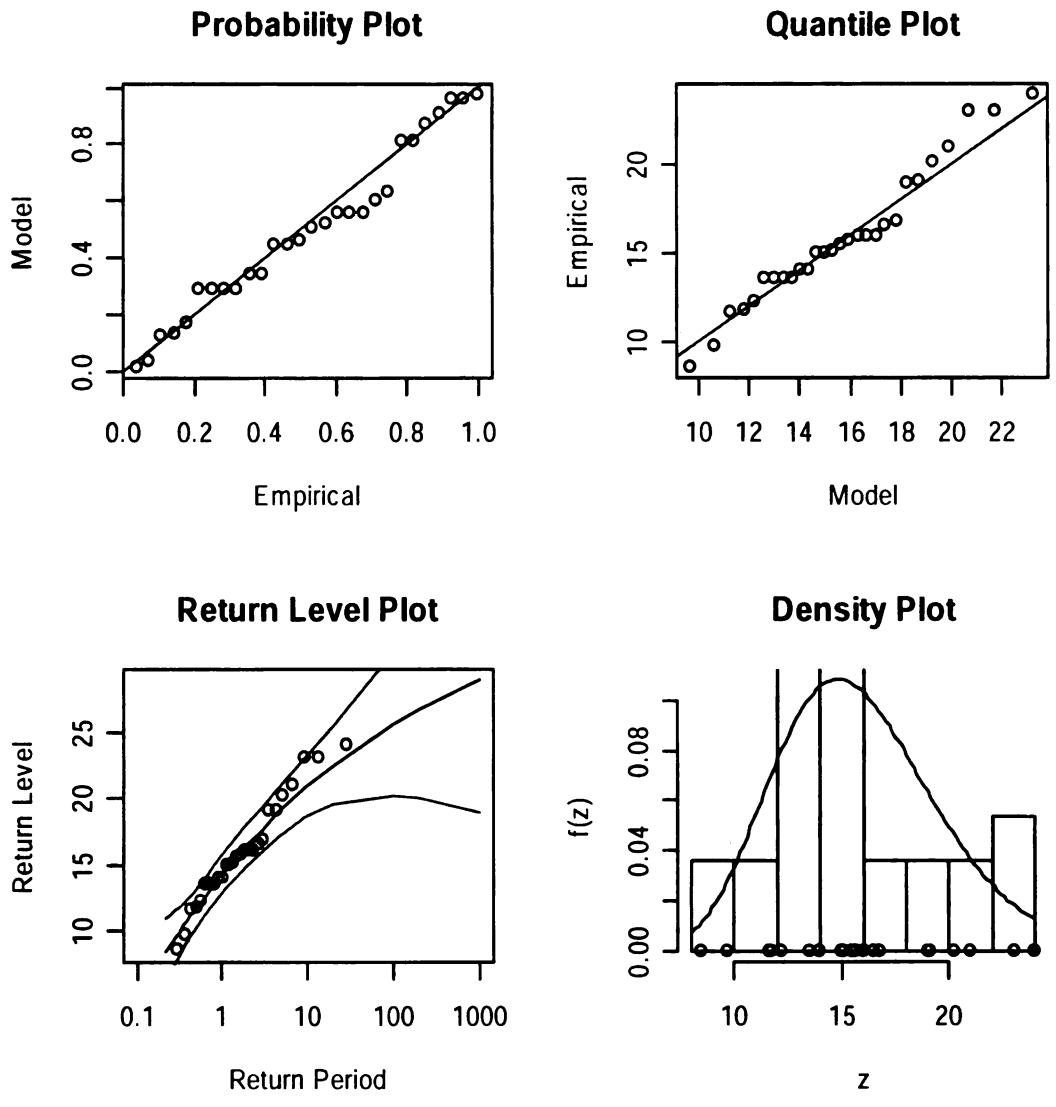

Appendix Figure 23 GEV model fit plots for Annual Lowest TMIN for Pleven, 1951-1979

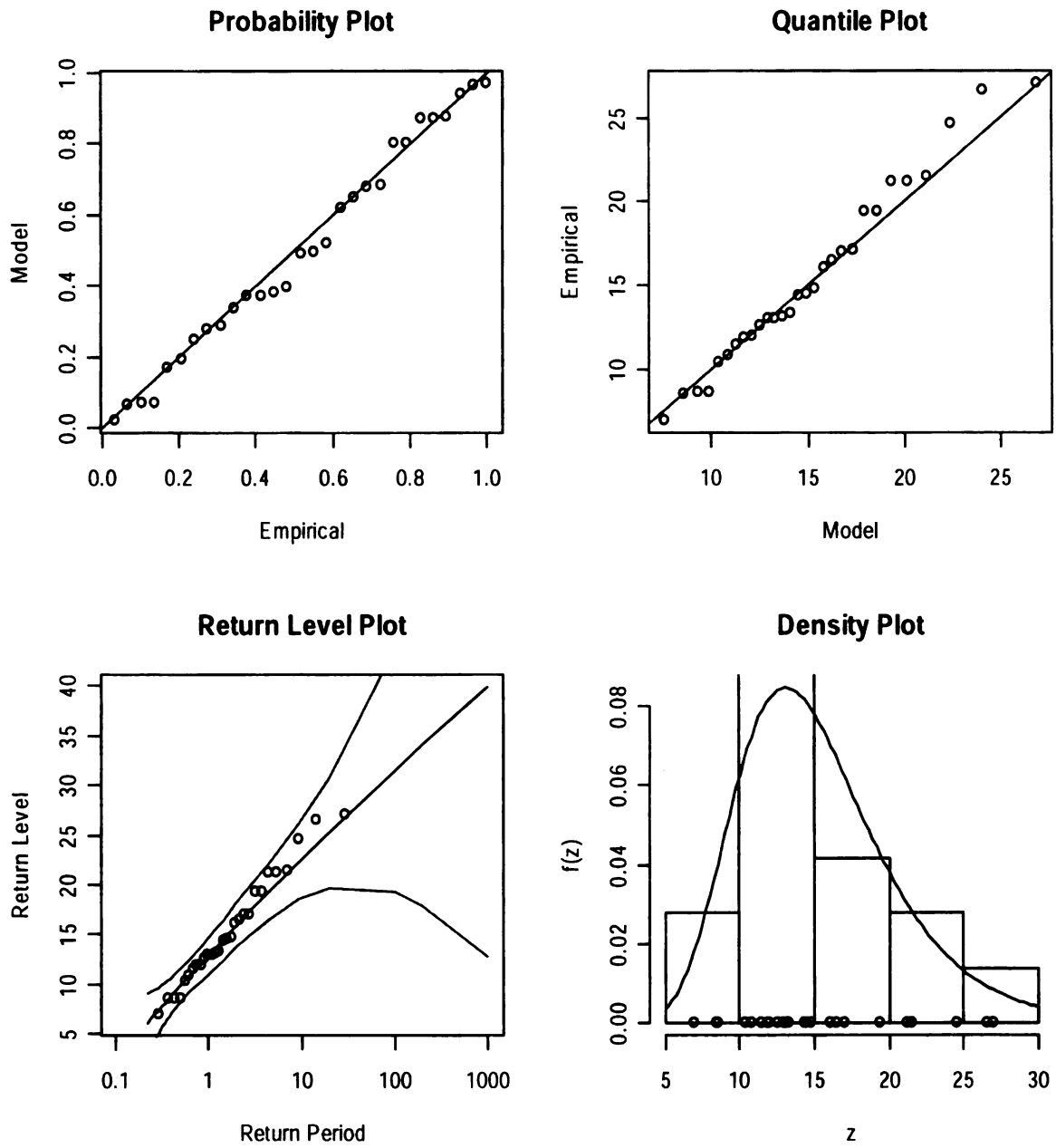

Appendix Figure 24 GEV model fit plots for Annual Lowest TMIN for Plovdiv, 1951-1979

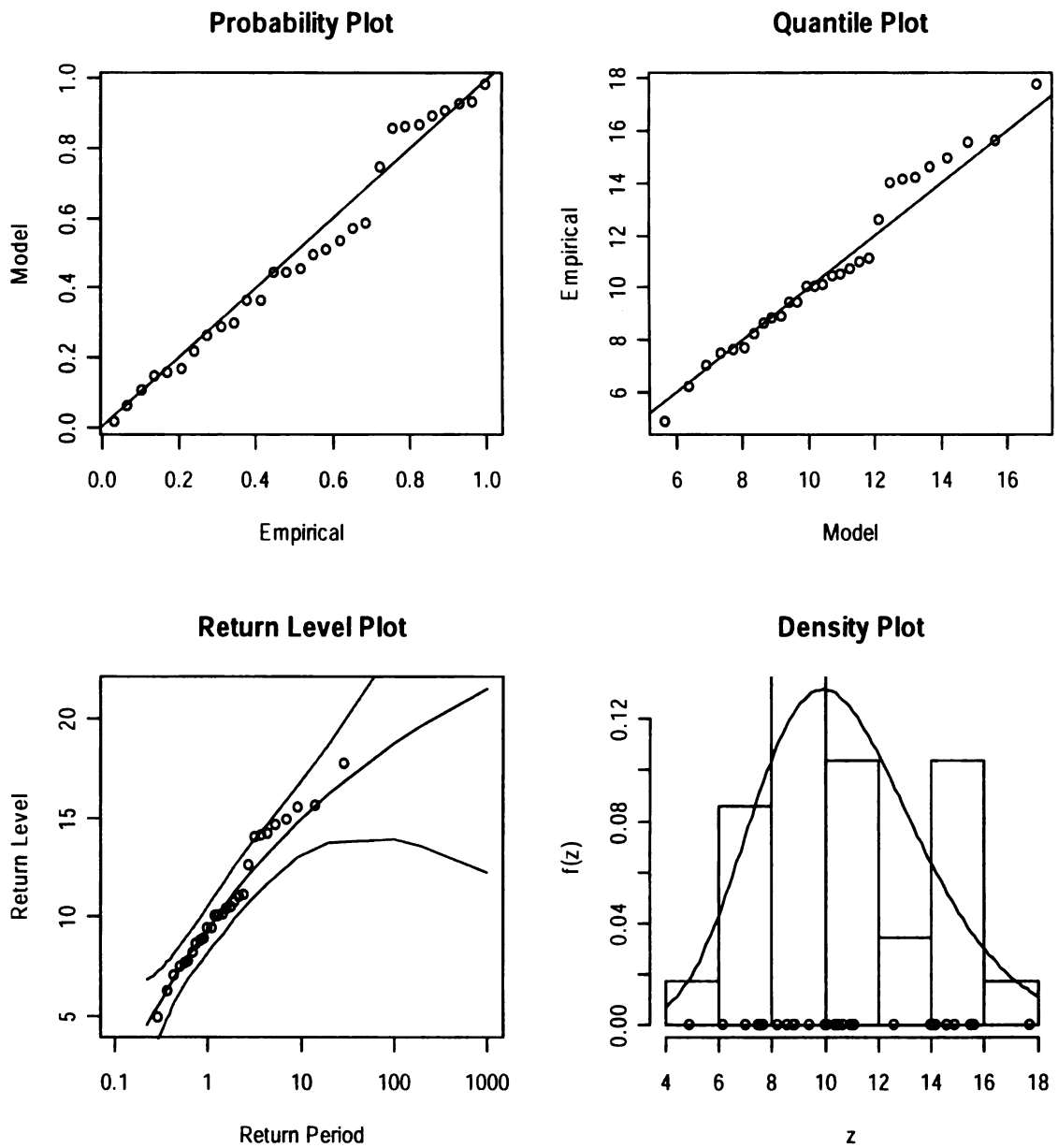

Appendix Figure 25 GEV model fit plots for Annual Lowest TMIN for Varna, 1951-1979

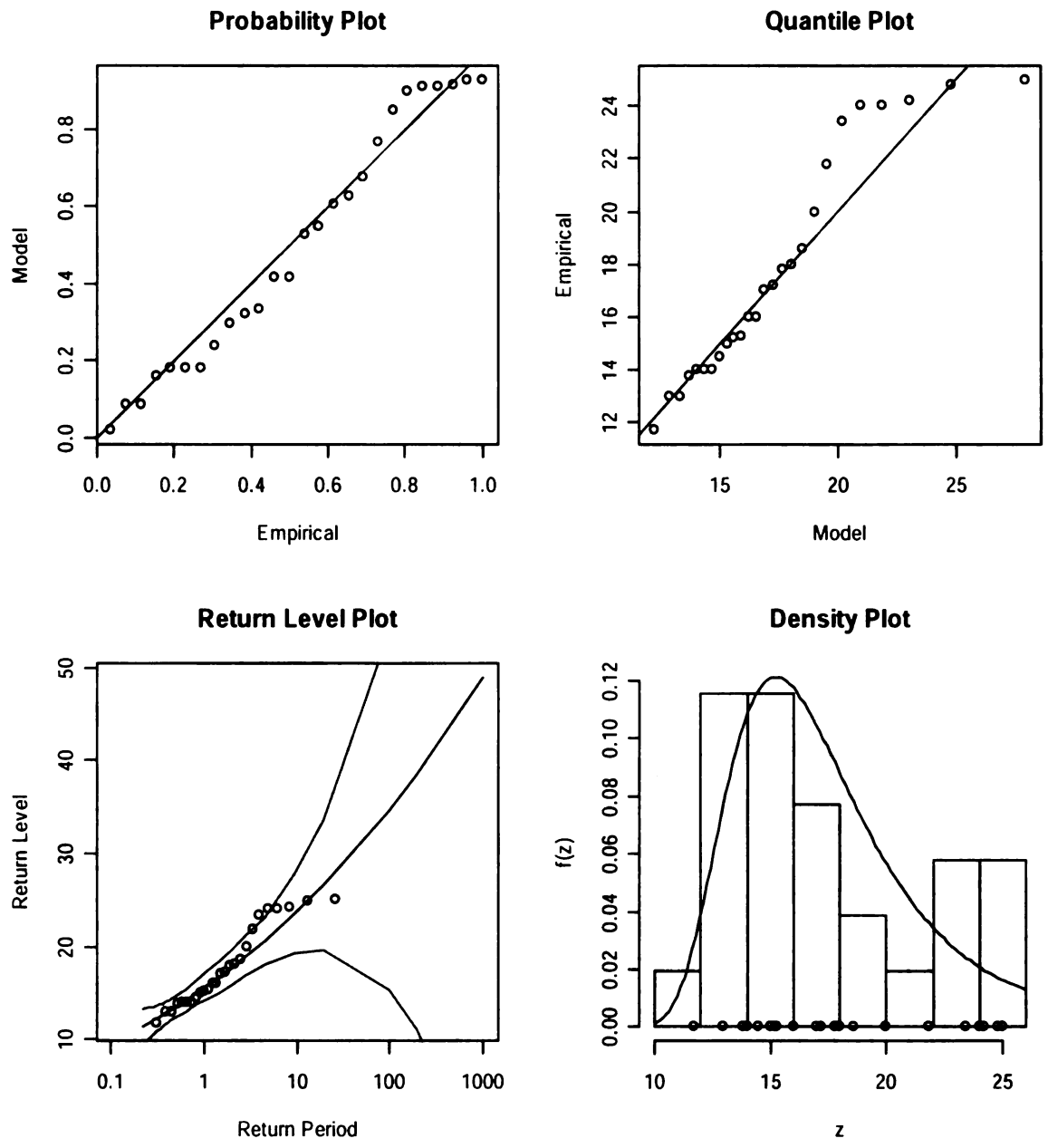

Appendix Figure 26 GEV model fit plots for Annual Lowest TMIN for Pleven NCDC, 1973-1999

GEV pots for winter lowest TMIN (Pleven NCDC only)

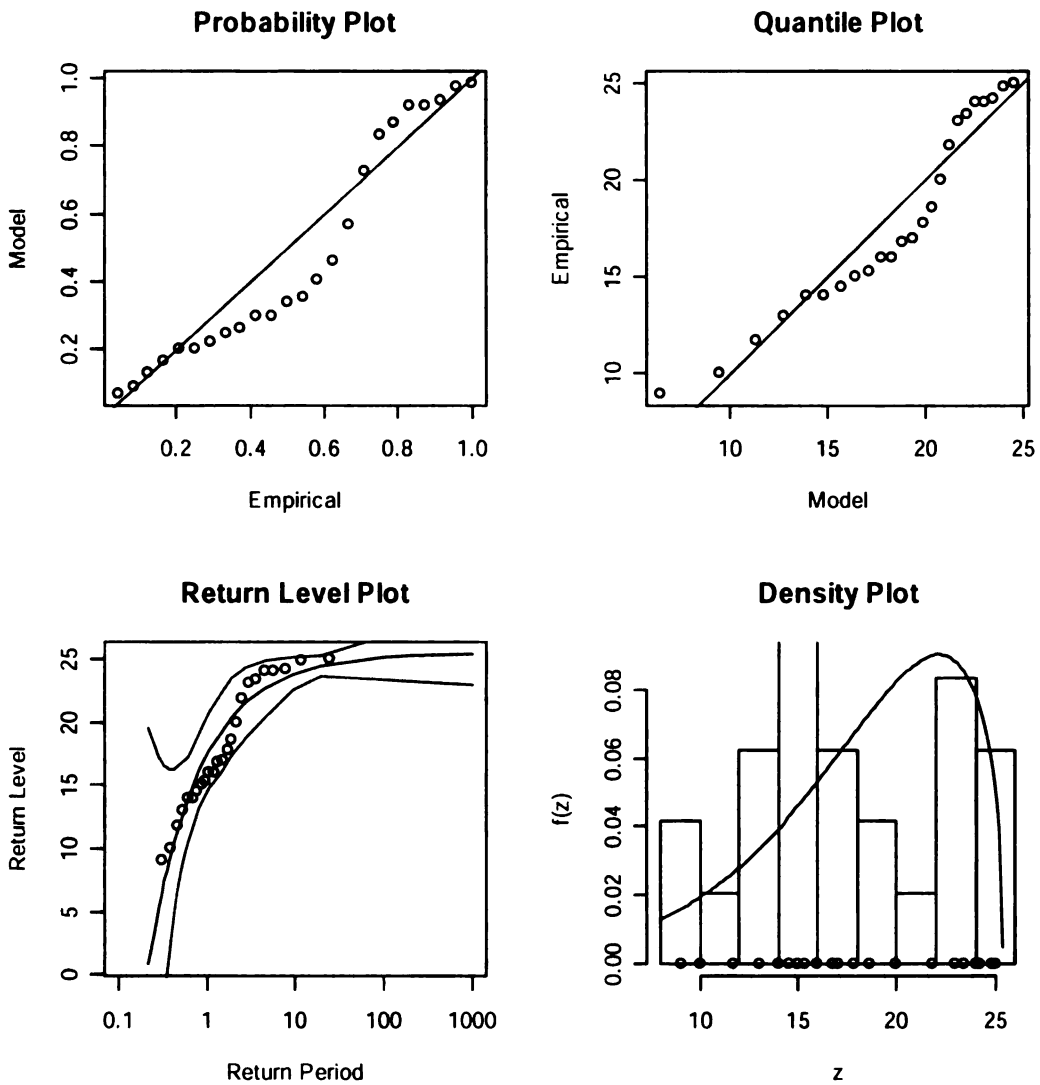

Appendix Figure 27 GEV model fit plots for Winter Lowest TMIN for Pleven NCDC, 1973-1999

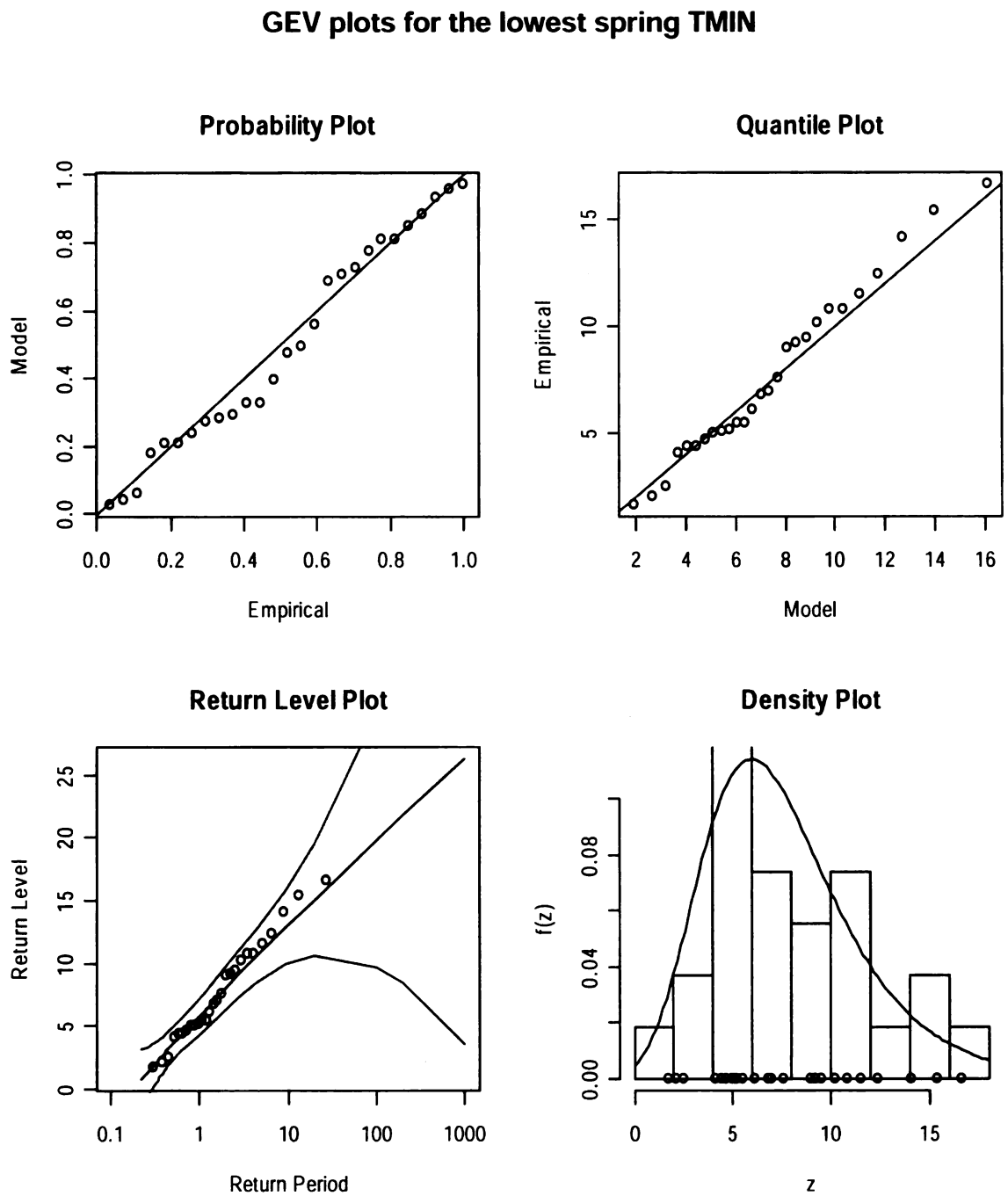

Appendix Figure 28 GEV model fit plots for Spring Lowest TMIN for Obraztsov Chiflick, 1953-1979

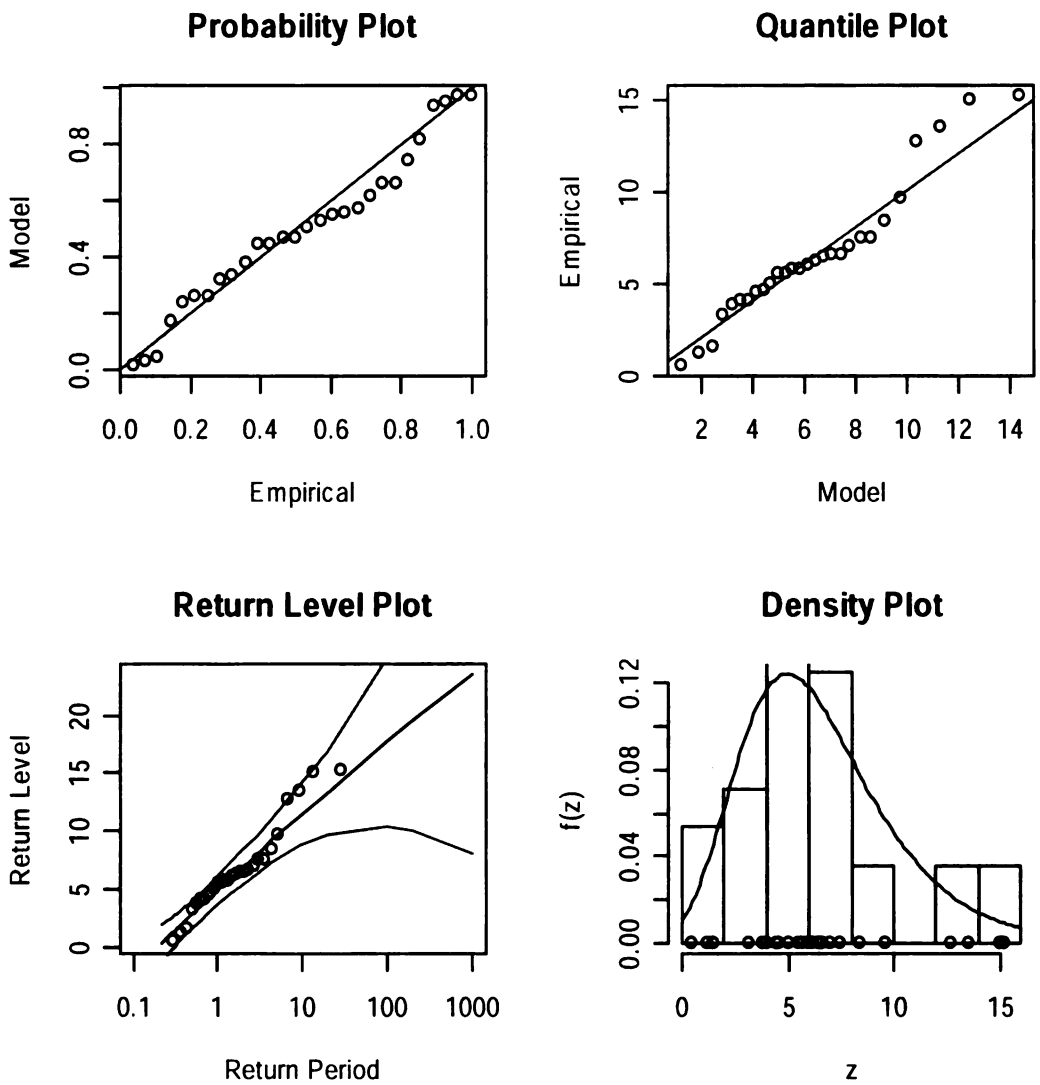

Appendix Figure 29 GEV model fit plots for Spring Lowest TMIN for Pleven, 1951-1979

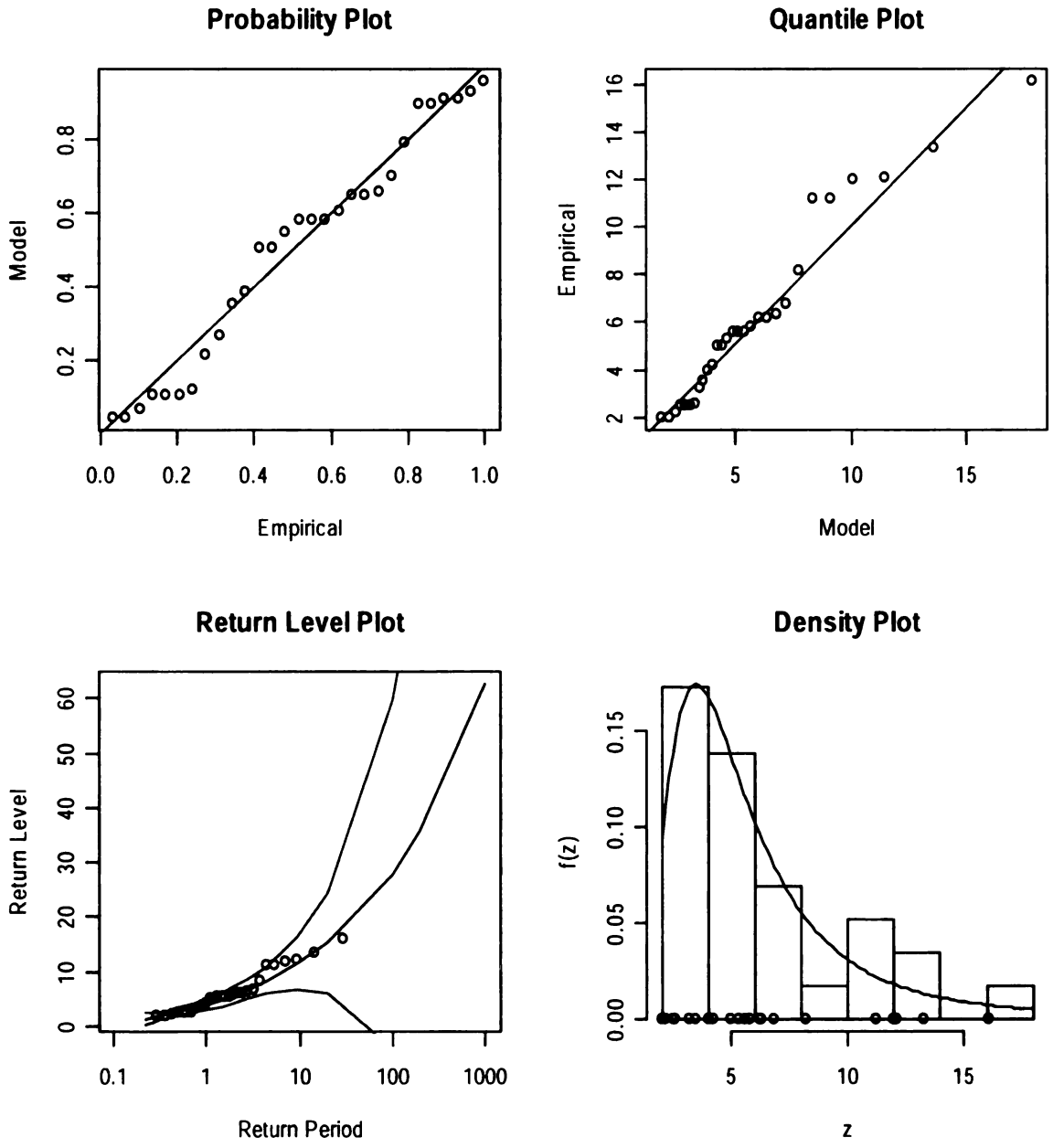

Appendix Figure 30 GEV model fit plots for Spring Lowest TMIN for Plovdiv, 1951-1979

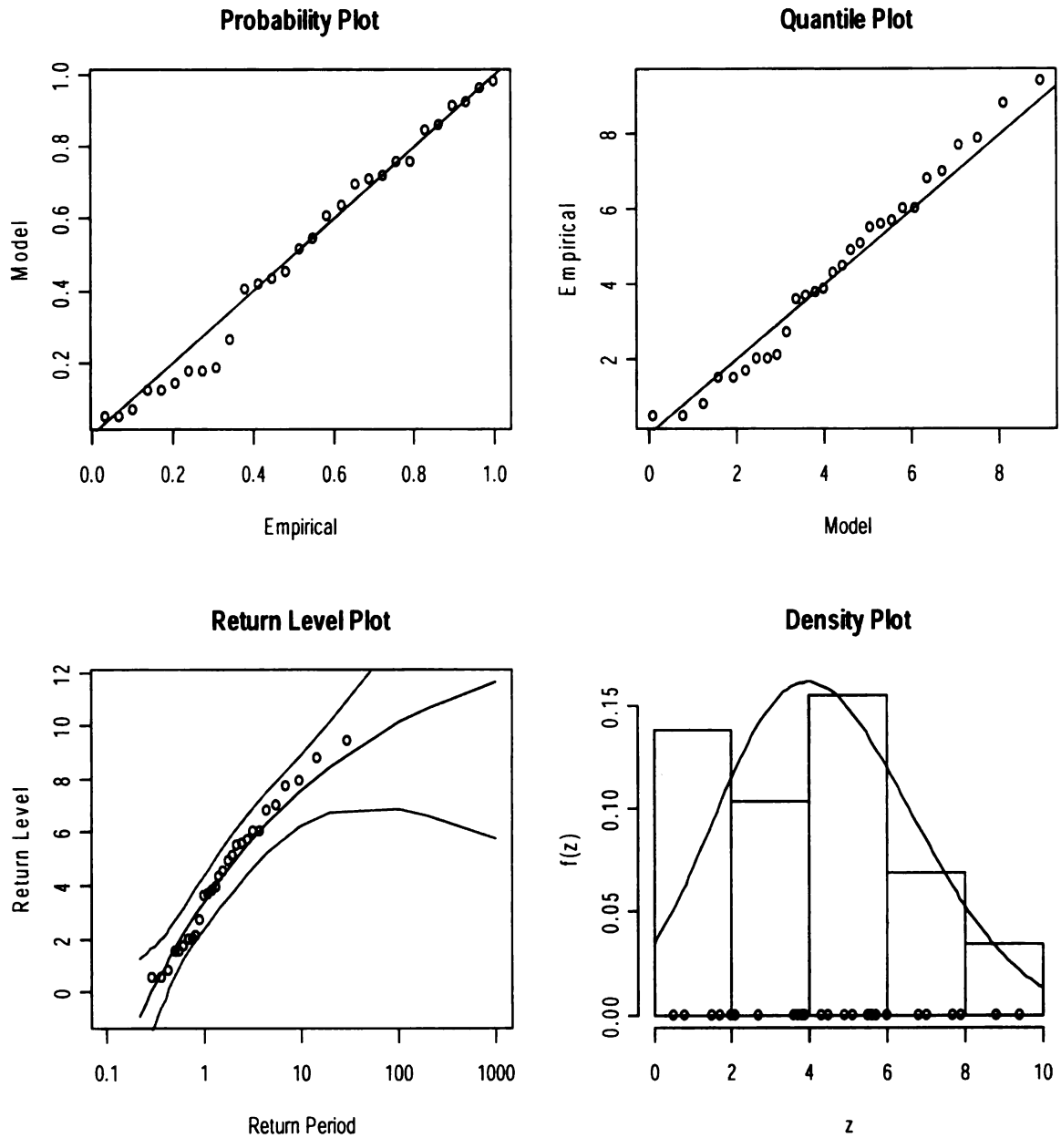

Appendix Figure 31 GEV model fit plots for Spring Lowest TMIN for Varna, 1951-1979

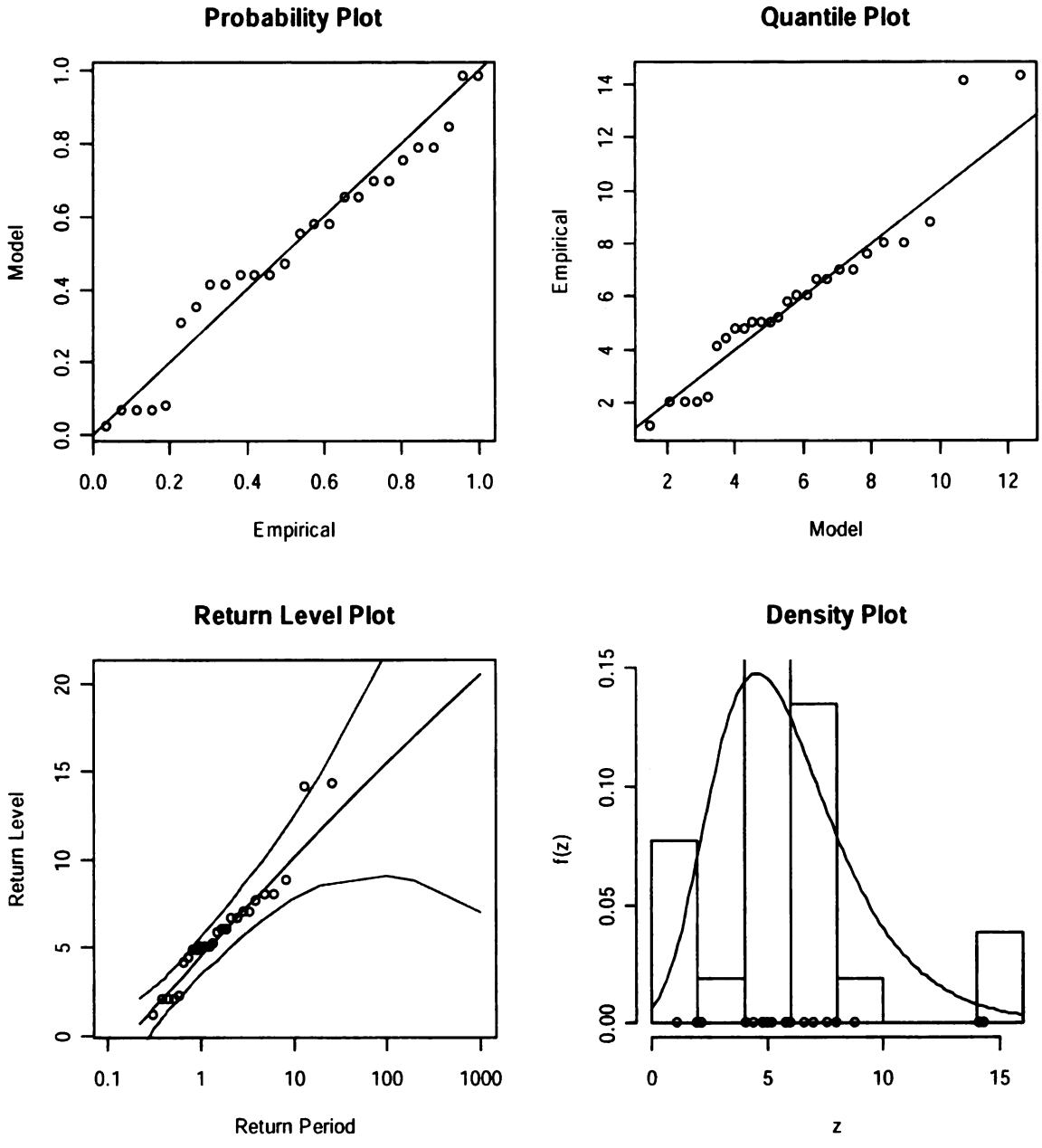

Appendix Figure 32 GEV model fit plots for Spring Lowest TMIN for Pleven NCDC, 1973-1999

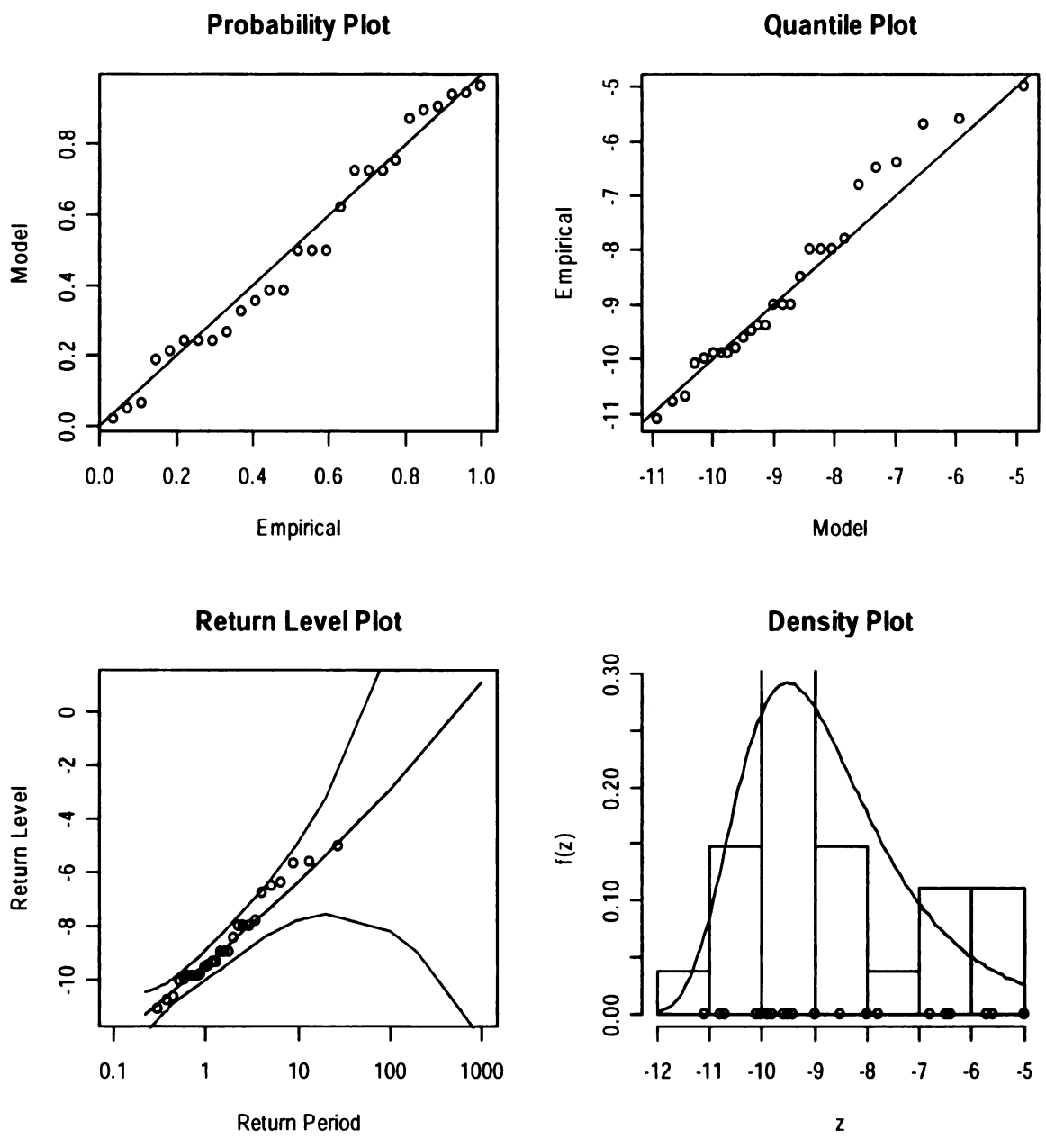

Appendix Figure 33 GEV model fit plots for Summer Lowest TMIN for Obraztsov Chiflick, 1953-1979

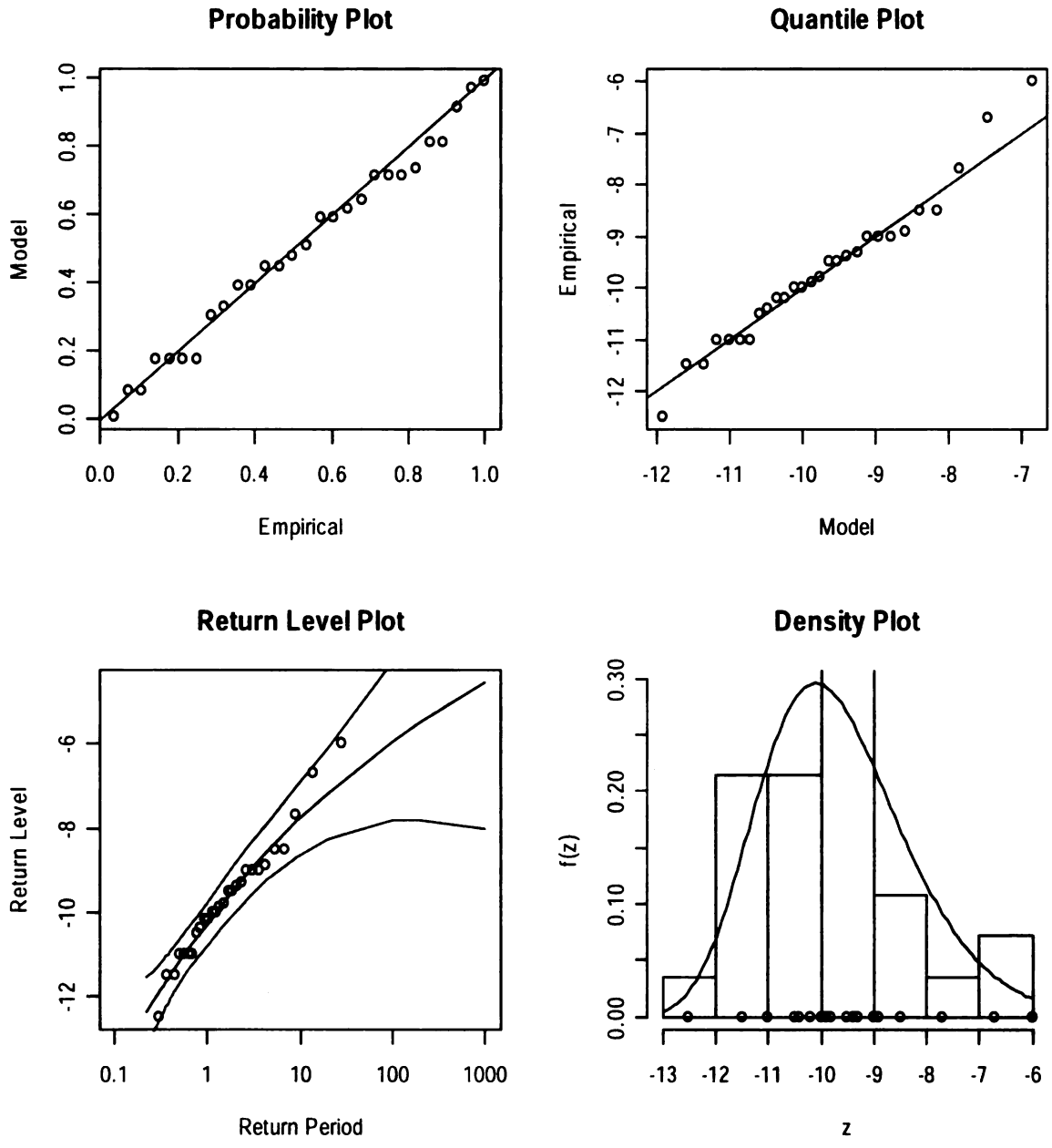

Appendix Figure 34 GEV model fit plots for Summer Lowest TMIN for Pleven, 1951-1979

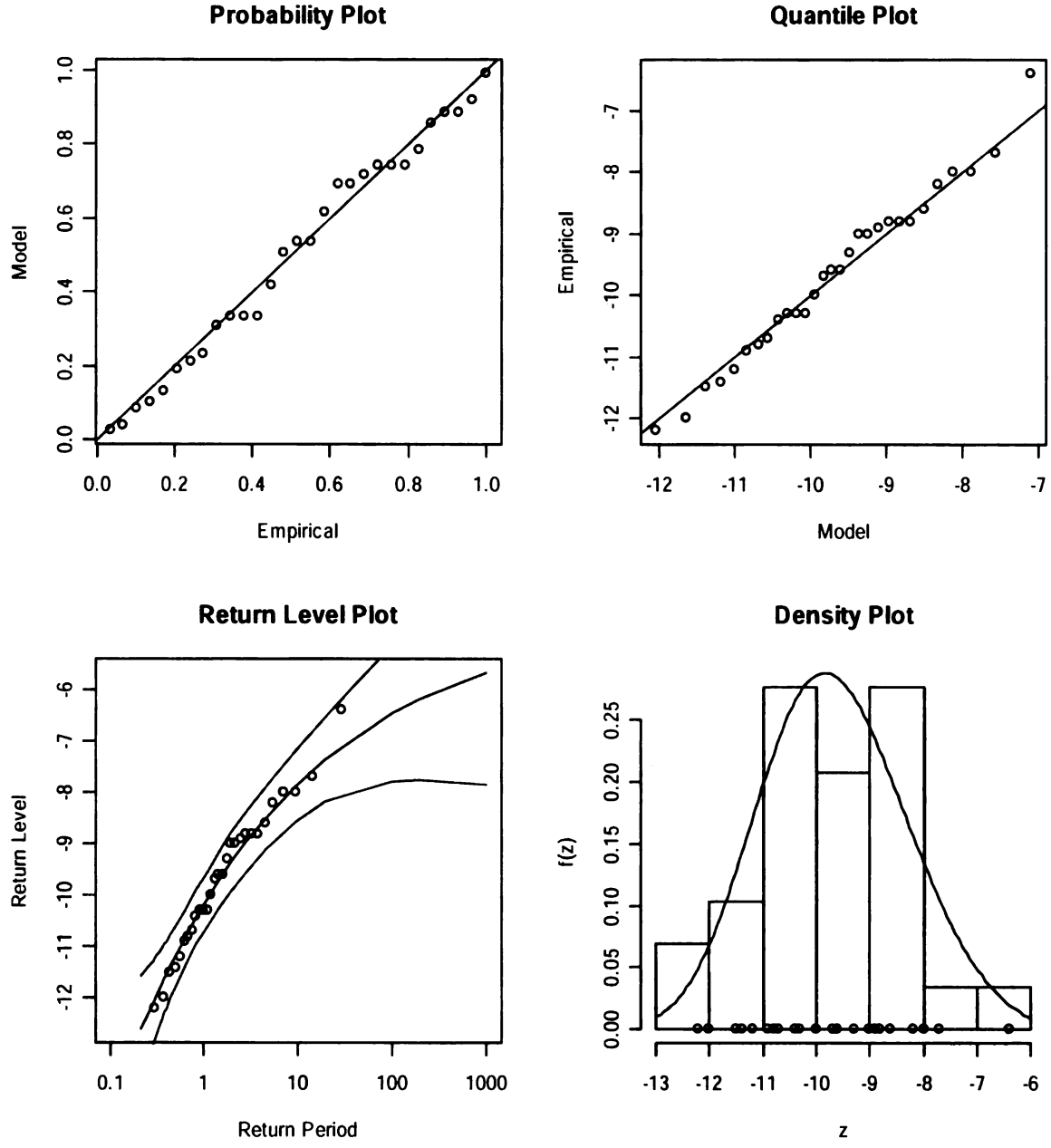

Appendix Figure 35 GEV model fit plots for Summer Lowest TMIN for Plovdiv, 1951-1979

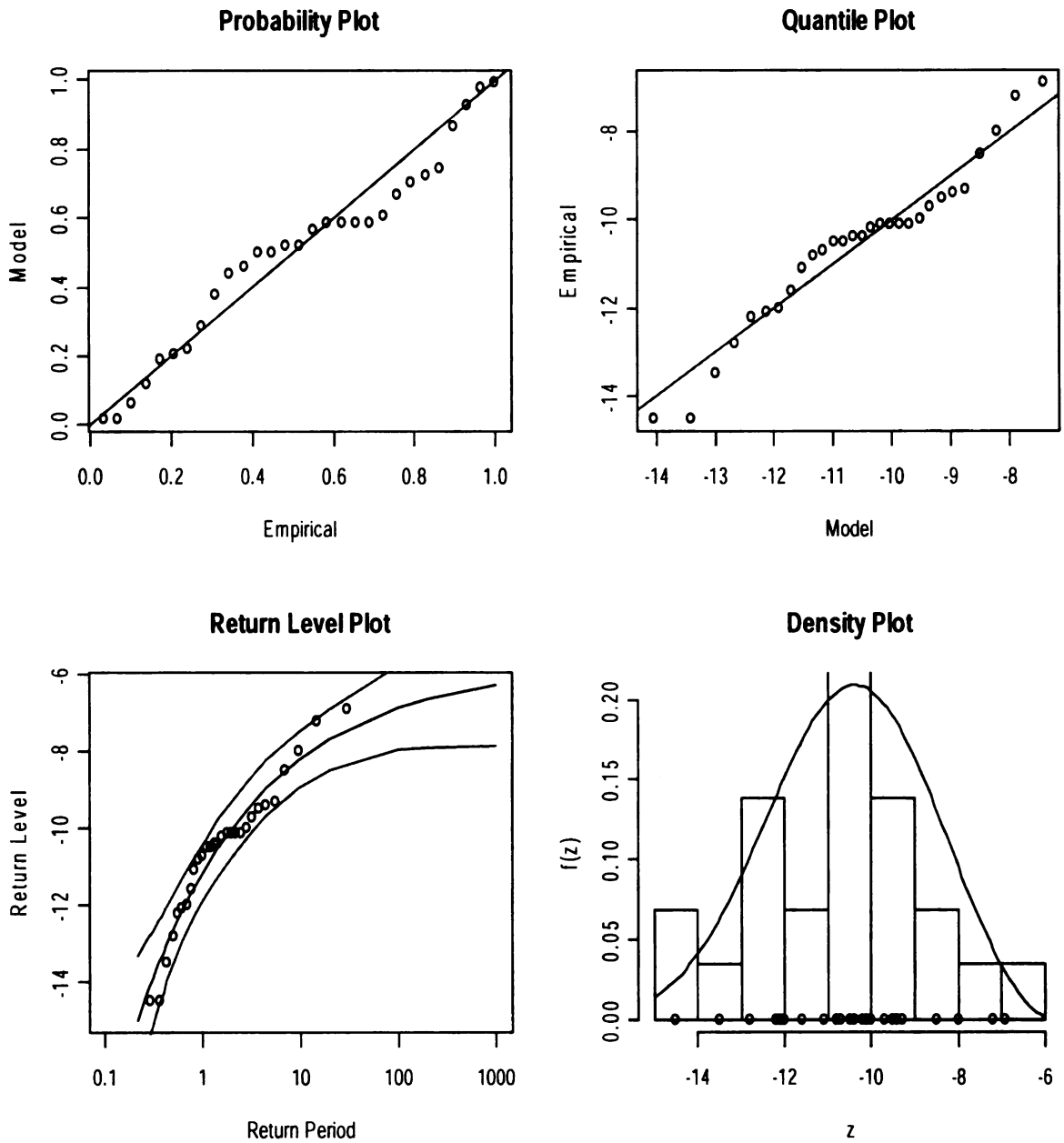

Appendix Figure 36 GEV model fit plots for Summer Lowest TMIN for Varna, 1951-1979

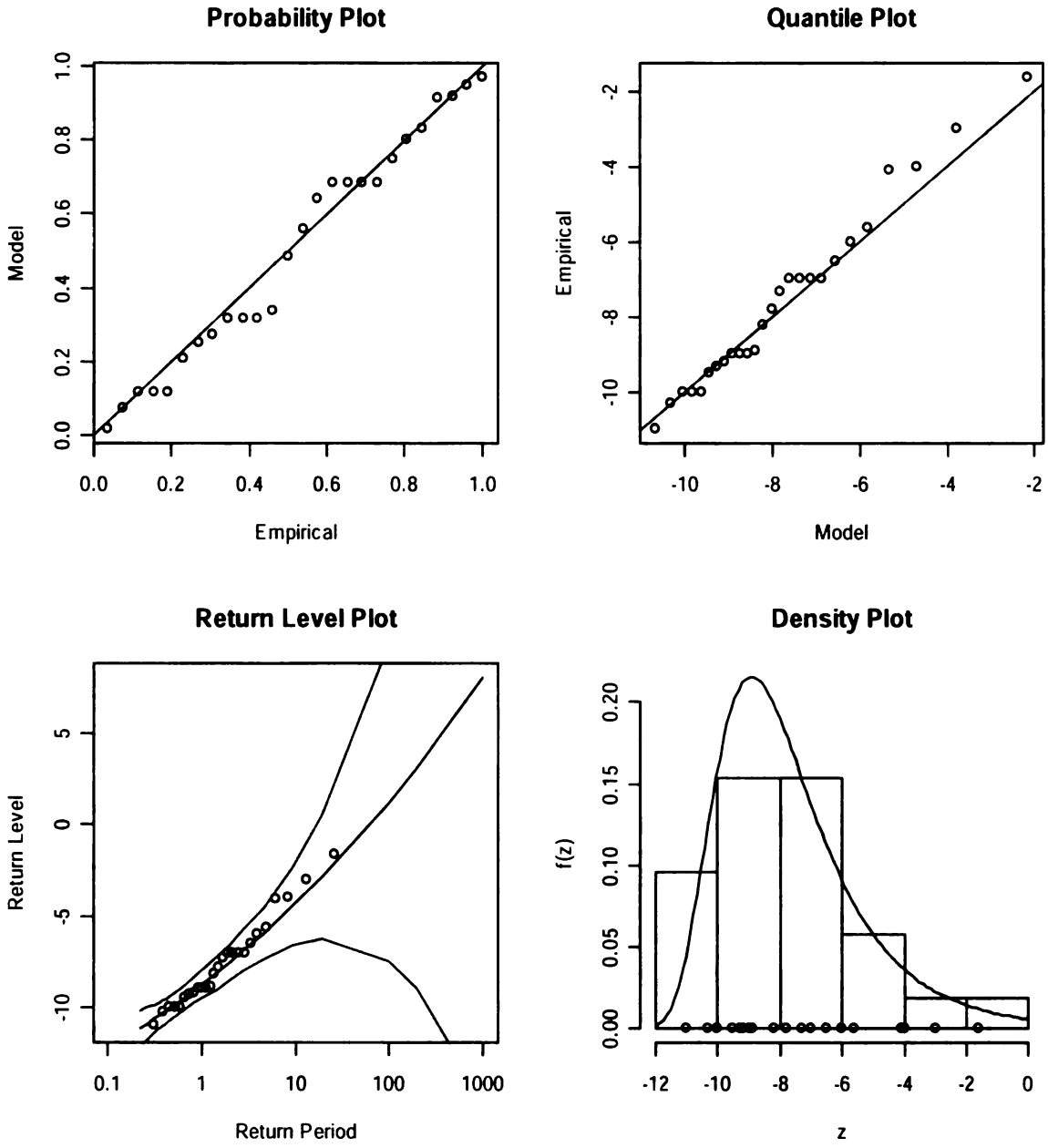

Appendix Figure 37 GEV model fit plots for Summer Lowest TMIN for Pleven NCDC, 1973-1999

GEV plots for fall lowest TMIN

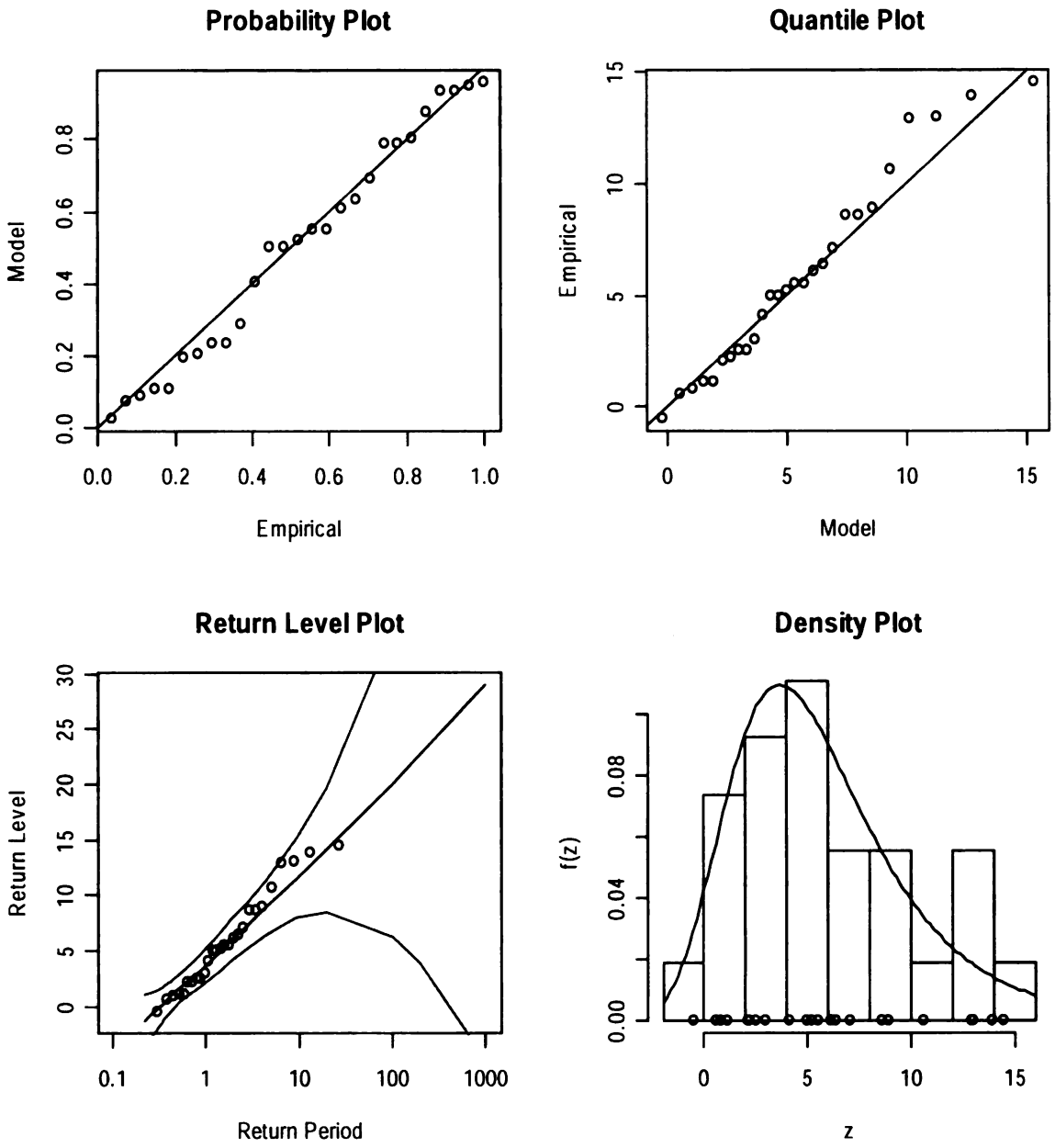

Appendix Figure 38 GEV model fit plots for Fall Lowest TMIN for Obraztsov Chiflick, 1953-1979

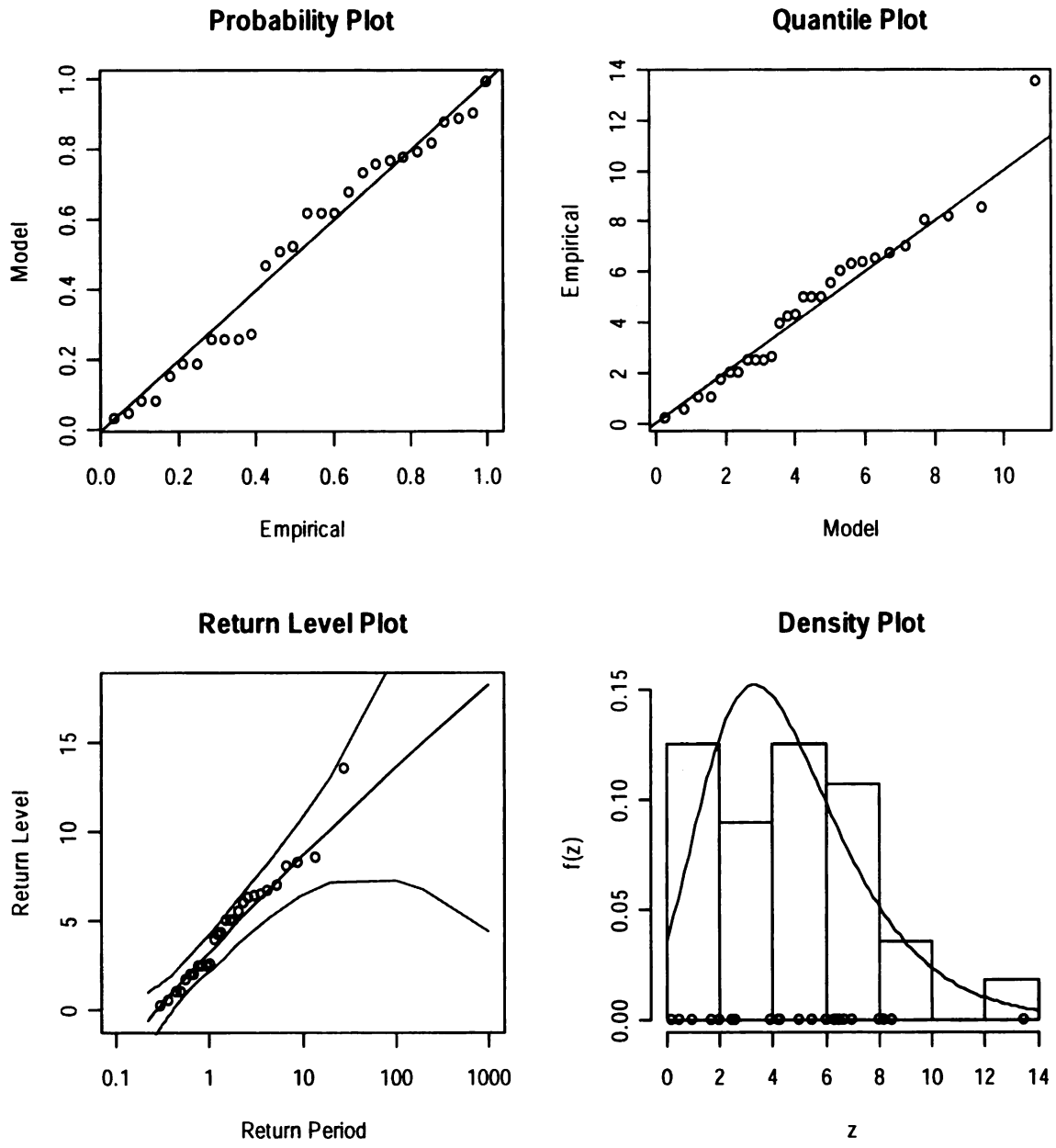

Appendix Figure 39 GEV model fit plots for Fall Lowest TMIN for Pleven, 1951-1979

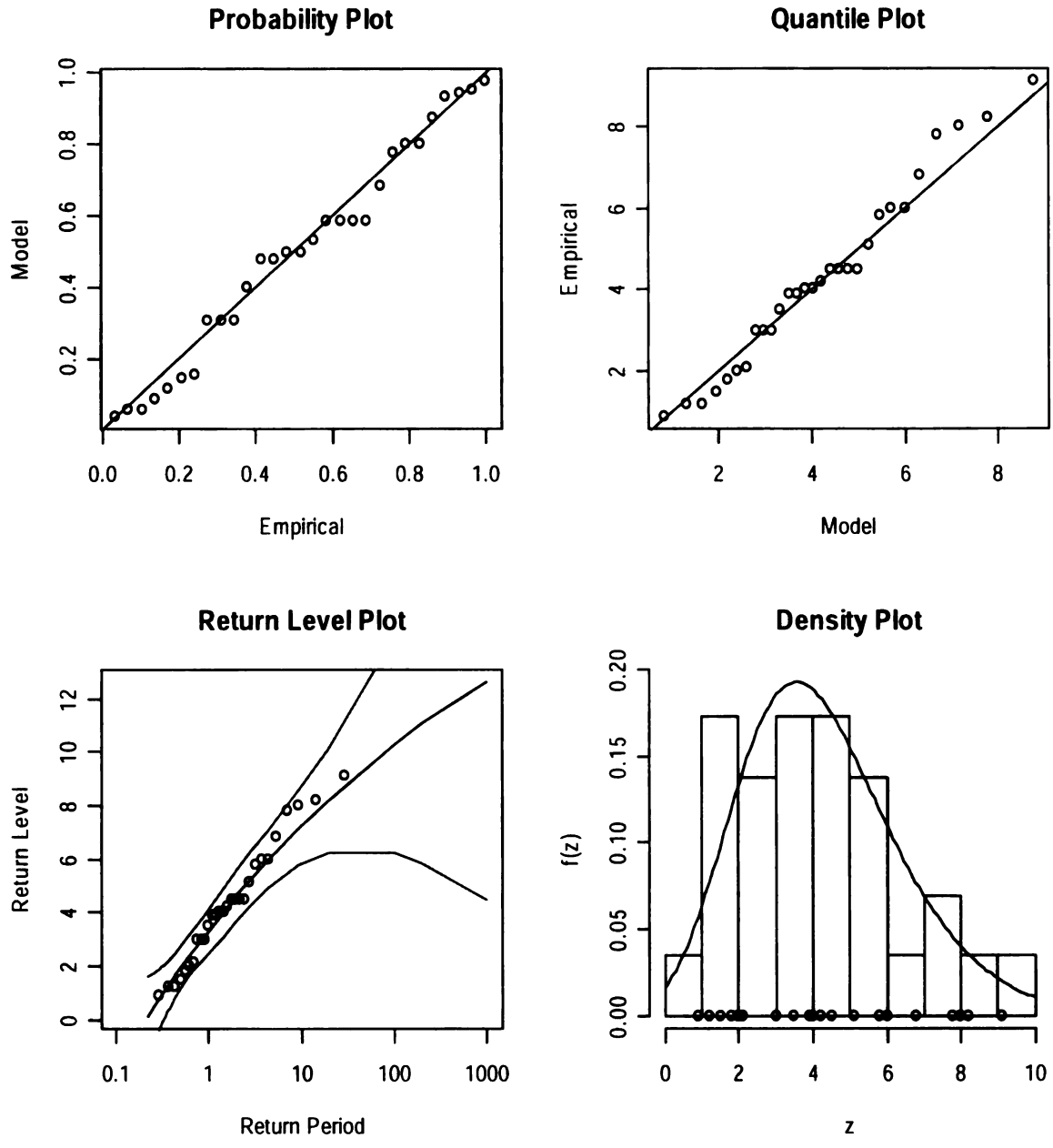

Appendix Figure 40 GEV model fit plots for Fall Lowest TMIN for Plovdiv, 1951-1979

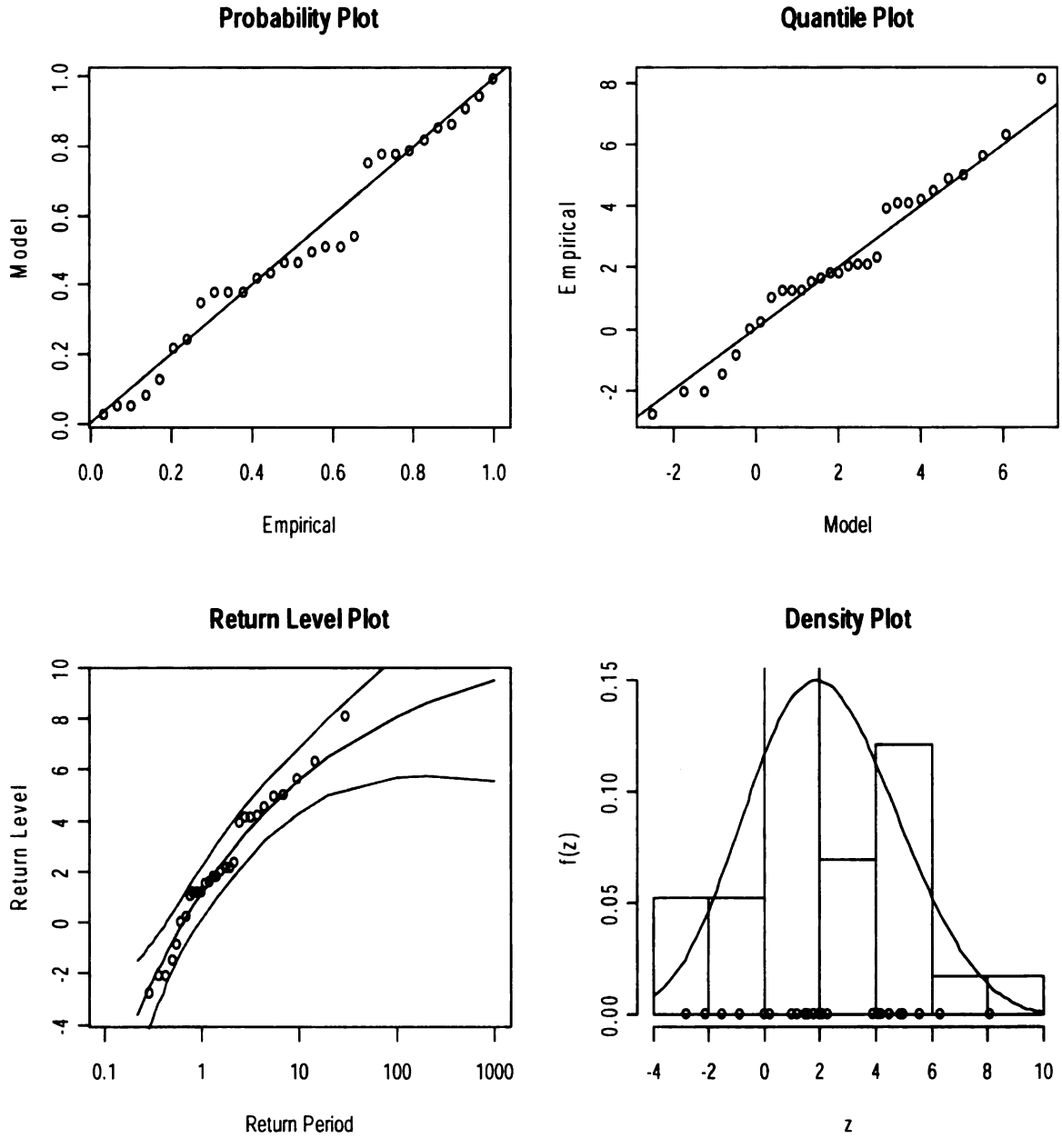

Appendix Figure 41 GEV model fit plots for Fall Lowest TMIN for Varna, 1951-1979

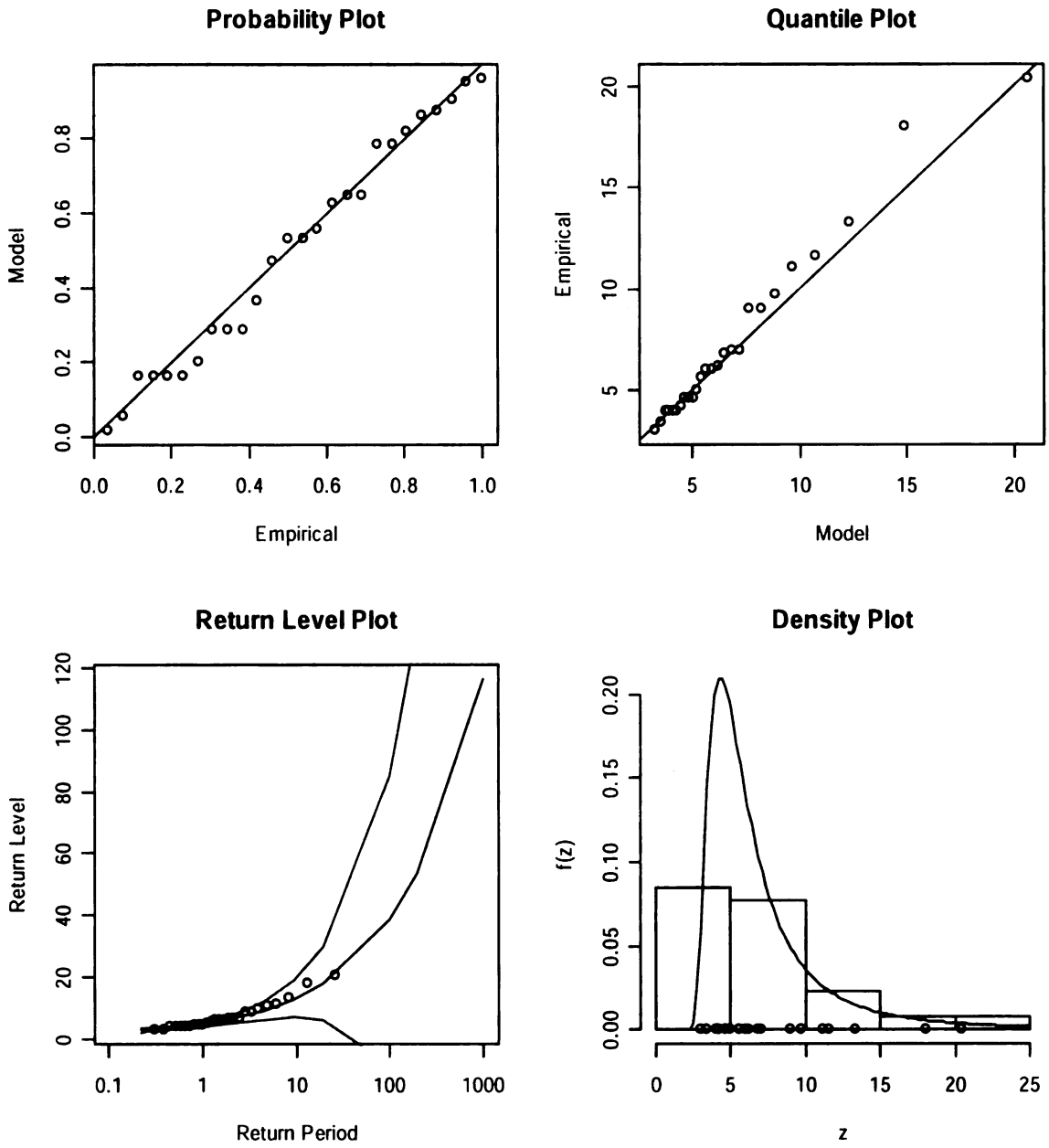

Appendix Figure 42 GEV model fit plots for Fall Lowest TMIN for Pleven NCDC, 1973-1999

Appendix Table 7 Lowest Annual Daily Minimum Temperature GEV fit details

Station	**Obraztsov Chiflick**		**Varna**		**Plovdiv**		**Pleven**		**Pleven NCDC**	
Period	1953-1979		1951-1979		1951-1979		1951-1979		1973-1999	
Para-meters	MLE	Stand. Error	MLE	Stand. Error	MLE	Stand. Error	MLE	Stand. Error	MLE	Stand. Error
Location	15.5	0.5	9.4	0.6	13.0	0.9	14.3	0.7	15.6	0.7
Scale	2.3	0.4	2.8	0.4	4.3	0.7	3.4	0.5	3.1	0.6
Shape	0.06	0.19	-0.15	0.17	-0.03	0.17	-0.15	0.14	0.12	0.23

Appendix Table 8 Lowest Winter Daily Minimum Temperature GEV fit details

Station	**Obraztsov Chiflick**		**Varna**		**Plovdiv**		**Pleven**		**Pleven NCDC**	
Period	1953-1979		1951-1979		1951-1979		1951-1979		1973-1999	
Para-meters	MLE	Stand. Error	MLE	Stand. Error	MLE	Stand. Error	MLE	Stand. Error	MLE	Stand. Error
Location	14.9	0.6	9.2	0.7	11.9	1.1	13.6	0.9	17.2	1.5
Scale	2.5	0.4	3.0	0.5	5.2	0.8	4.1	0.7	5.9	1.7
Shape	0.02	0.18	-0.16	0.20	-0.1	0.17	-0.22	0.16	-0.72	0.38

Appendix Table 9 Lowest Spring Daily Minimum Temperature GEV fit details

Station	**Obraztsov Chiflick**		**Varna**		**Plovdiv**		**Pleven**		**Pleven NCDC**	
Period	1953-1979		1951-1979		1951-1979		1951-1979		1973-1999	
Para-meters	MLE	Stand. Error	MLE	Stand. Error	MLE	Stand. Error	MLE	Stand. Error	MLE	Stand. Error
Location	5.9	0.7	3.4	0.5	4.1	0.5	4.9	0.6	4.5	0.5
Scale	3.2	0.5	2.3	0.4	2.2	0.4	3.0	0.4	2.5	0.4
Shape	-0.03	0.19	-0.22	0.18	0.33	0.26	-0.02	0.13	-0.02	0.14

Appendix Table 10 Lowest Summer Daily Minimum Temperature GEV fit details

Station	**Obraztsov Chiflick**		**Varna**		**Plovdiv**		**Pleven**		**Pleven NCDC**	
Period	1953-1979		1951-1979		1951-1979		1951-1979		1973-1999	
Para-meters	MLE	Stand. Error	MLE	Stand. Error	MLE	Stand. Error	MLE	Stand. Error	MLE	Stand. Error
Location	-9.4	0.3	-11.2	0.4	-10.2	0.3	-10.3	0.3	-8.8	0.4
Scale	1.3	0.2	1.9	0.3	1.3	0.2	1.3	0.2	1.7	0.3
Shape	0.05	0.19	-0.35	0.11	-0.23	0.12	-0.13	0.12	0.1	0.2

Appendix Table 11 Lowest Fall Daily Minimum Temperature GEV fit details

Station	**Obraztsov Chiflick**		**Varna**		**Plovdiv**		**Pleven**		**Pleven NCDC**	
Period	1953-1979		1951-1979		1951-1979		1951-1979		1973-1999	
Para-meters	MLE	Stand. Error	MLE	Stand. Error	MLE	Stand. Error	MLE	Stand. Error	MLE	Stand. Error
Location	3.7	0.8	1.2	0.5	3.3	0.4	3.3	0.5	5.0	0.4
Scale	3.4	0.6	2.6	0.4	1.9	0.3	2.4	0.4	1.9	0.4
Shape	0.02	0.21	-0.25	0.13	-0.11	0.18	-0.03	0.16	0.49	0.22

Mean Residual Life plots and plots of the GP distribution parameters fit to a series of thresholds at all stations

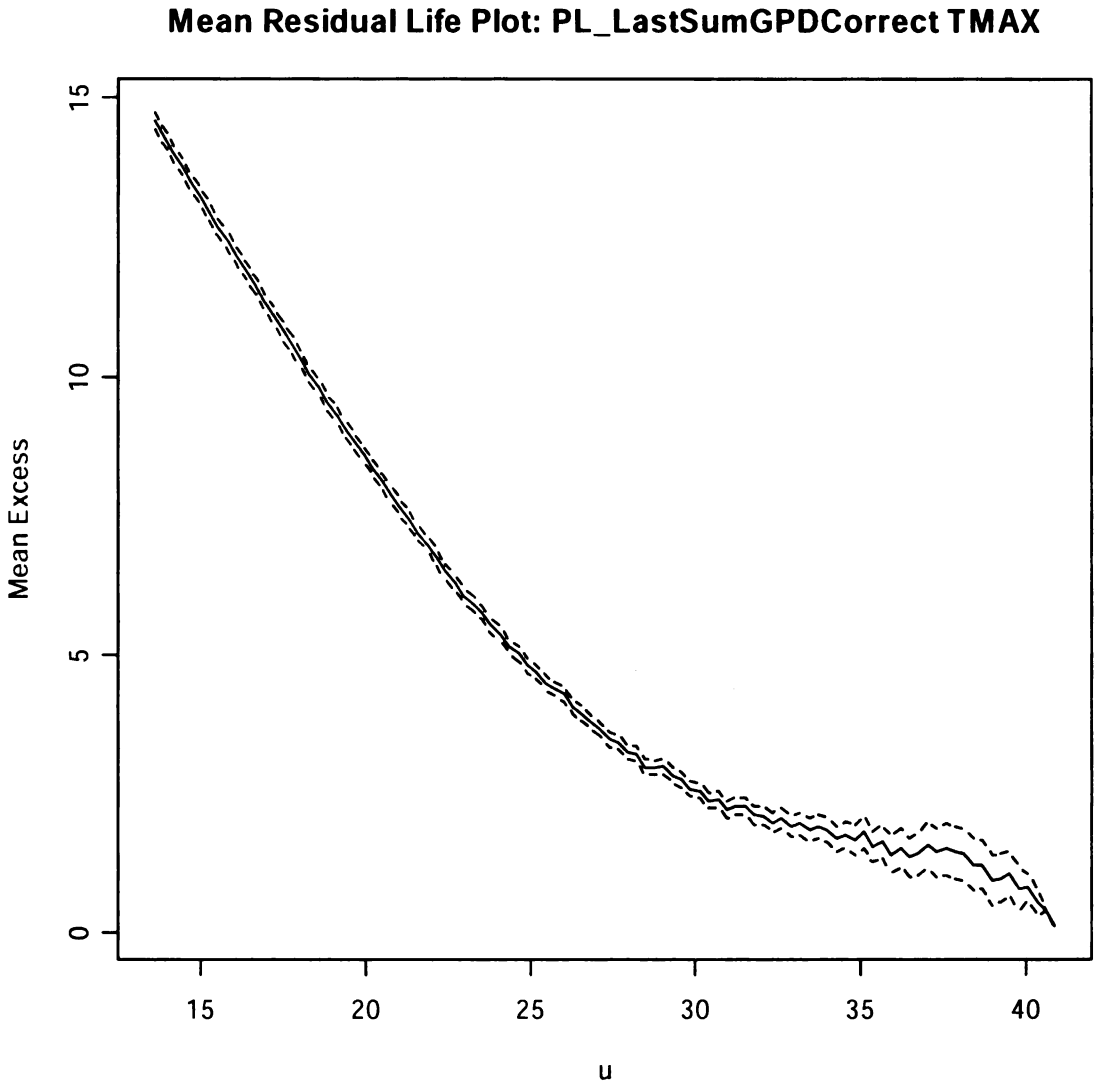

Appendix Figure 43 Pleven, Mean Residual Life Plot for summer TMAX, 1951-1979

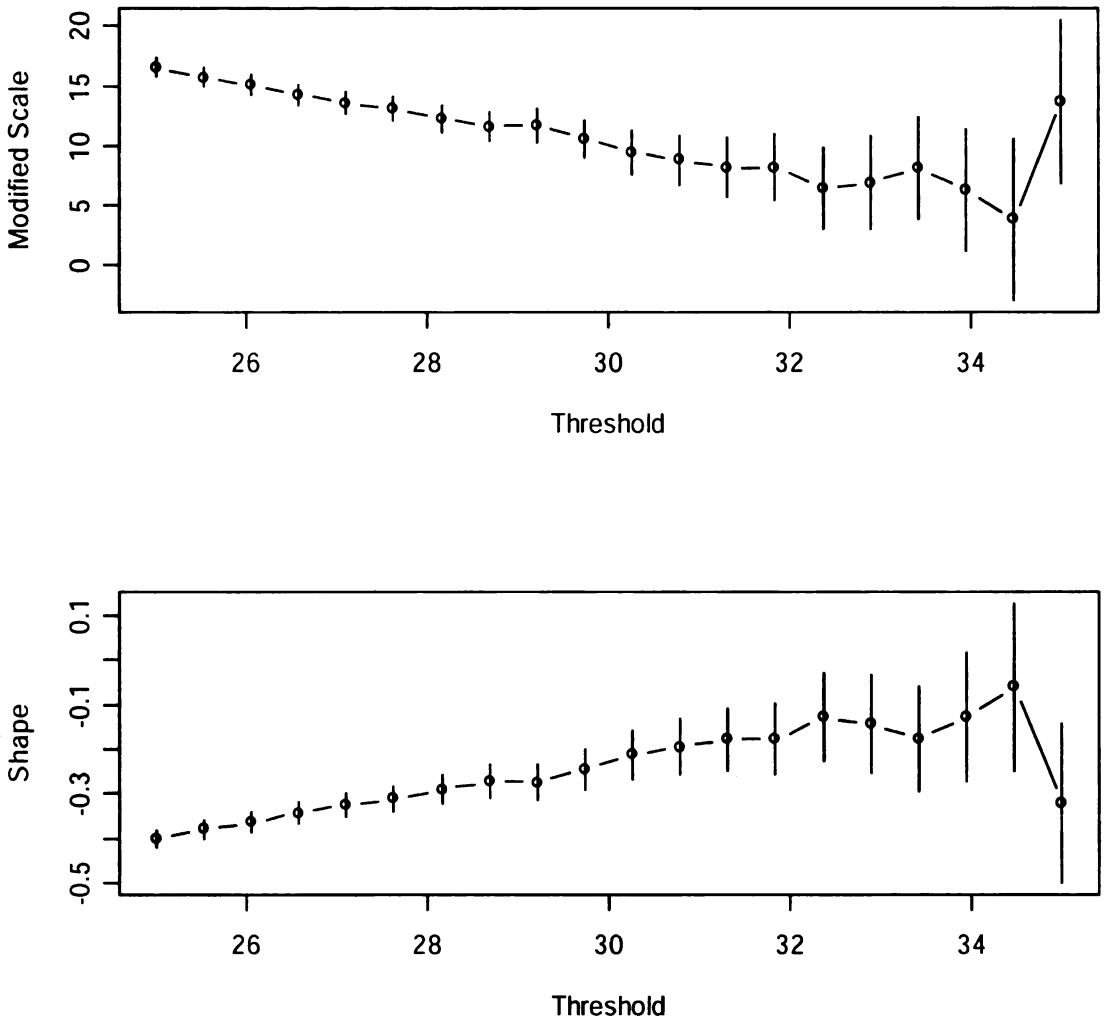

Appendix Figure 44 Pleven GPD fit to thresholds plots for summer TMAX, 1951-1979

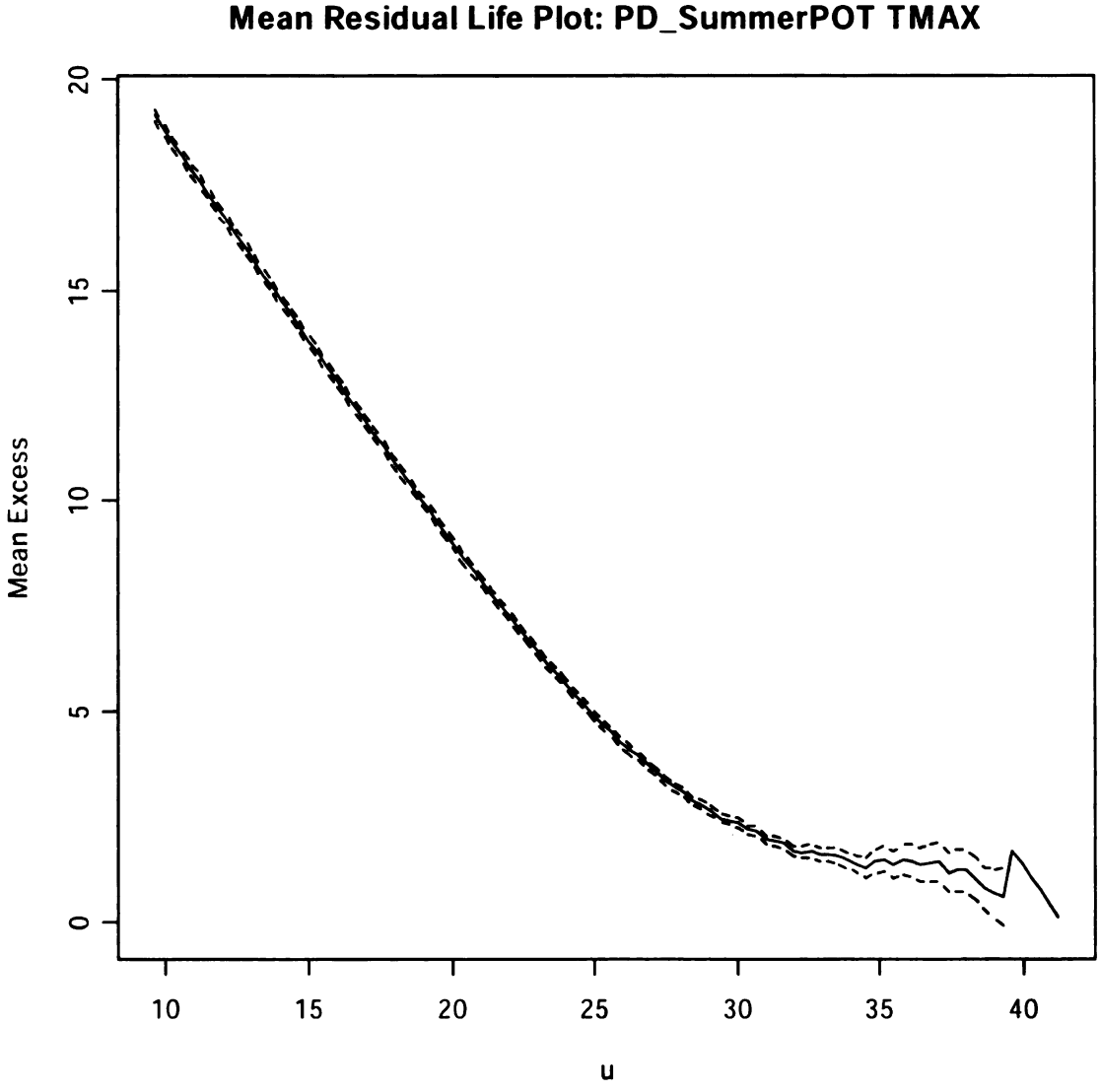

Appendix Figure 45 Plovdiv, Mean Residual Life Plot for summer TMAX, 1951-1979

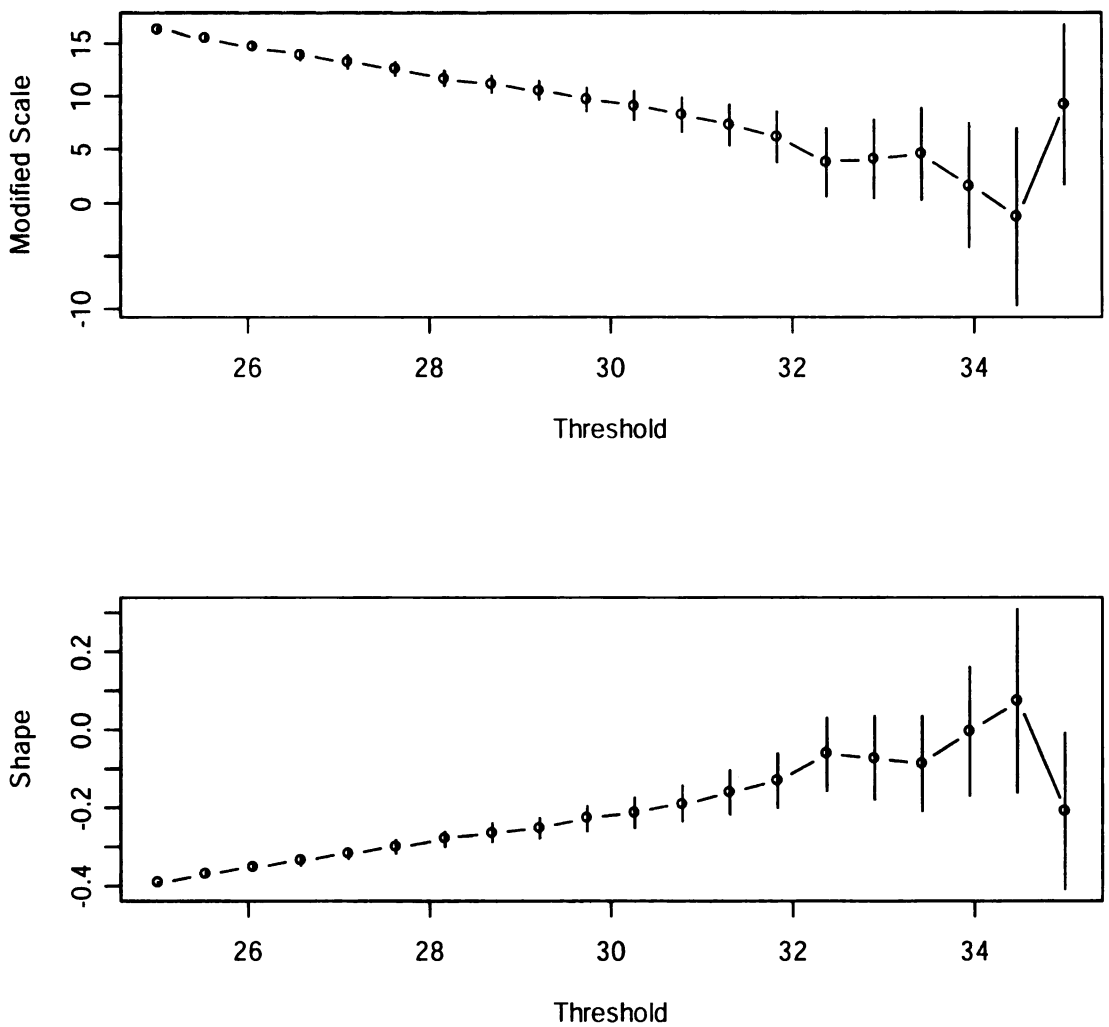

Appendix Figure 46 Plovdiv, GPD fit to thresholds plots for summer TMAX, 1951-1979

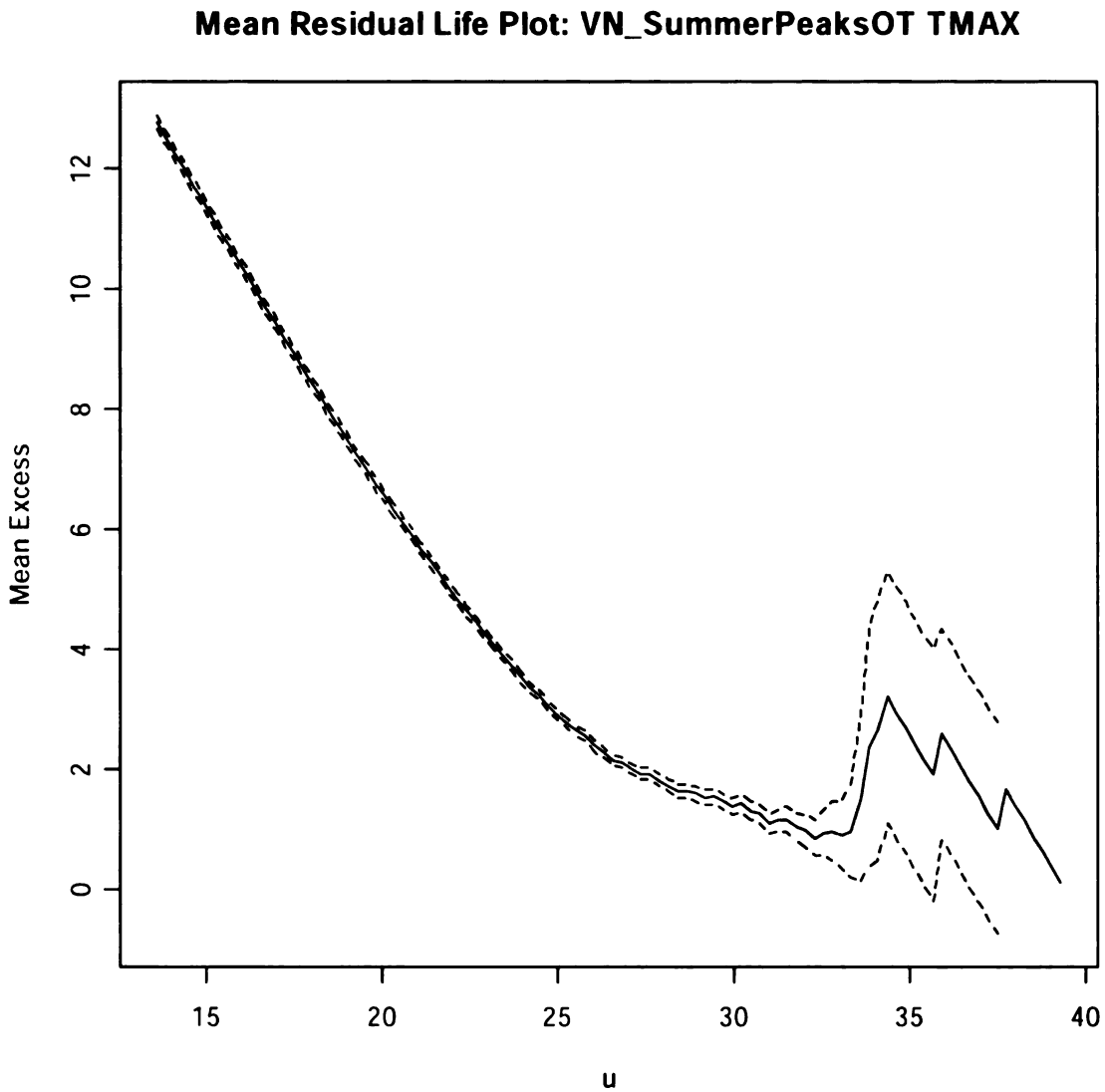

Appendix Figure 47 Varna, Mean Residual Life Plot for summer TMAX, 1951-1979

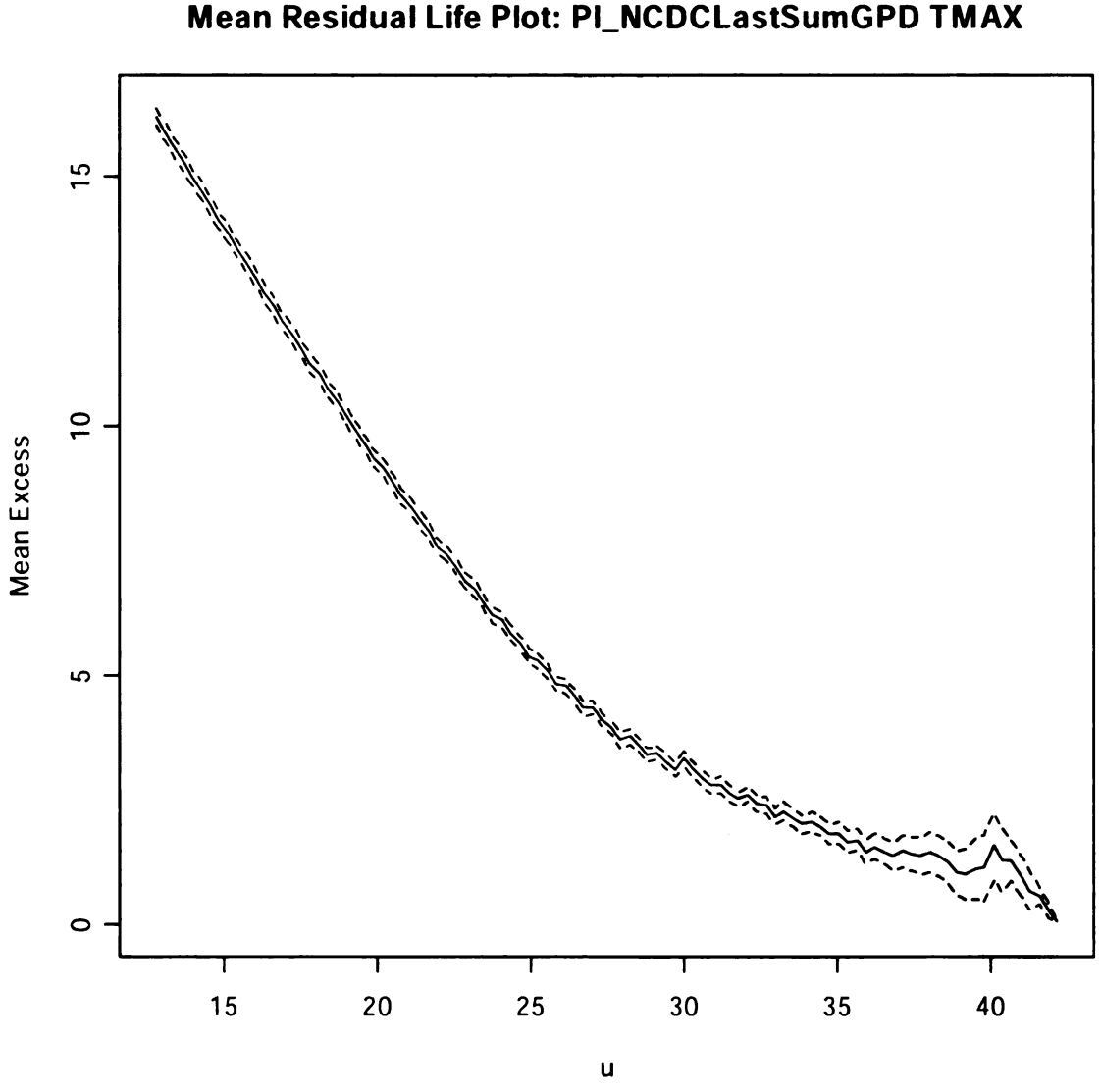

Appendix Figure 48 Pleven NCDC, Mean Residual Life Plot for summer TMAX, 1973-1999

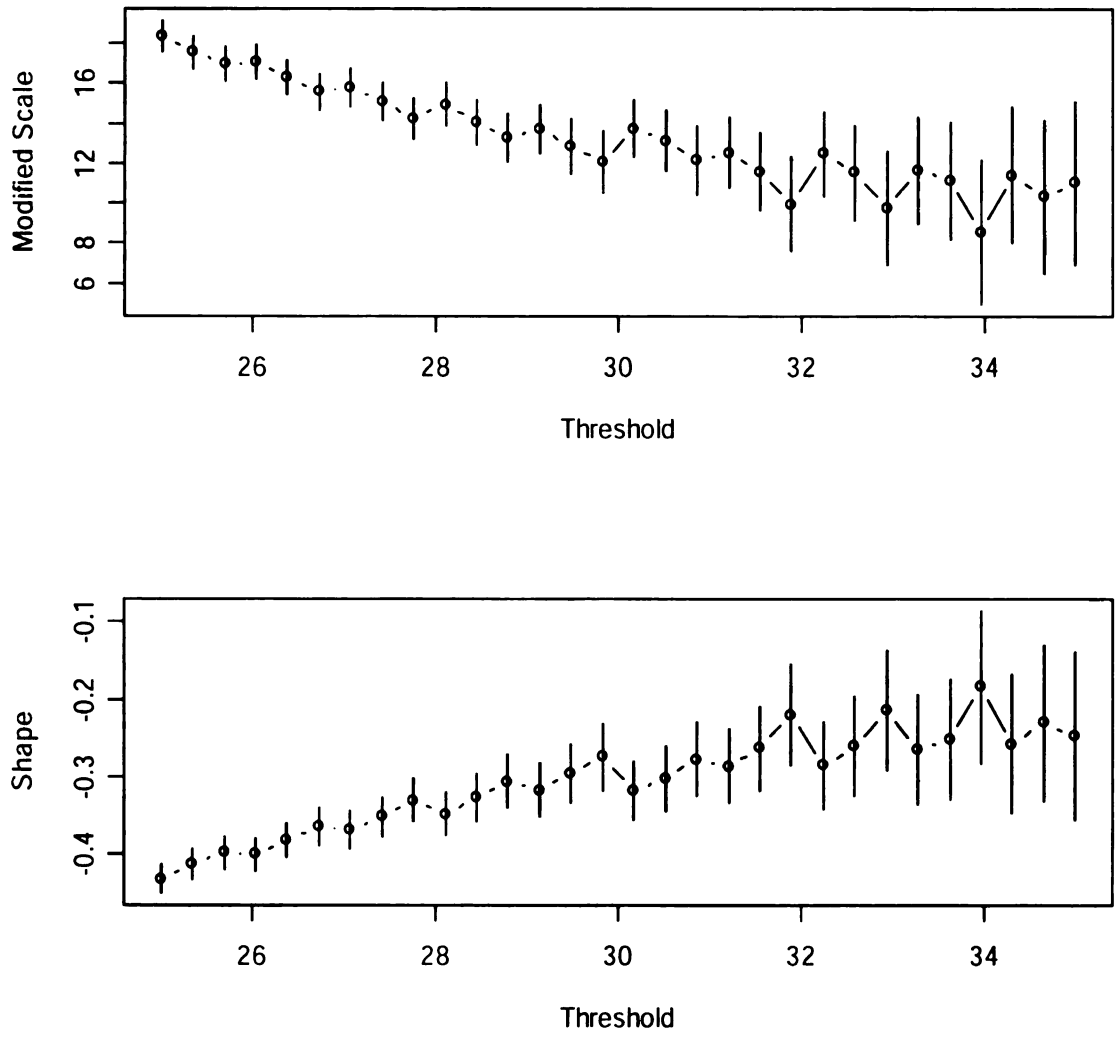

Appendix Figure 49 Pleven NCDC, GPD fit to thresholds plots for summer TMAX, 1973-1999

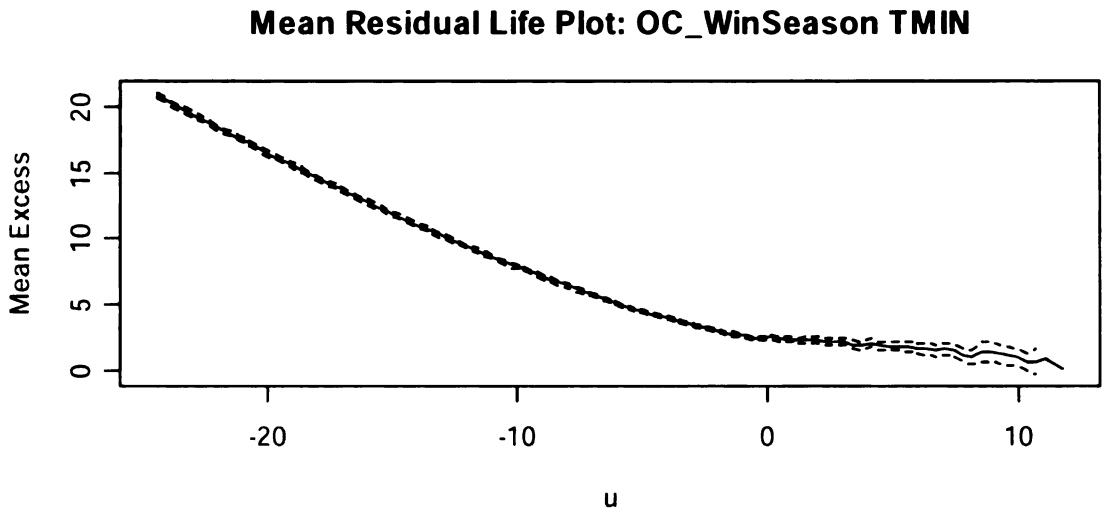

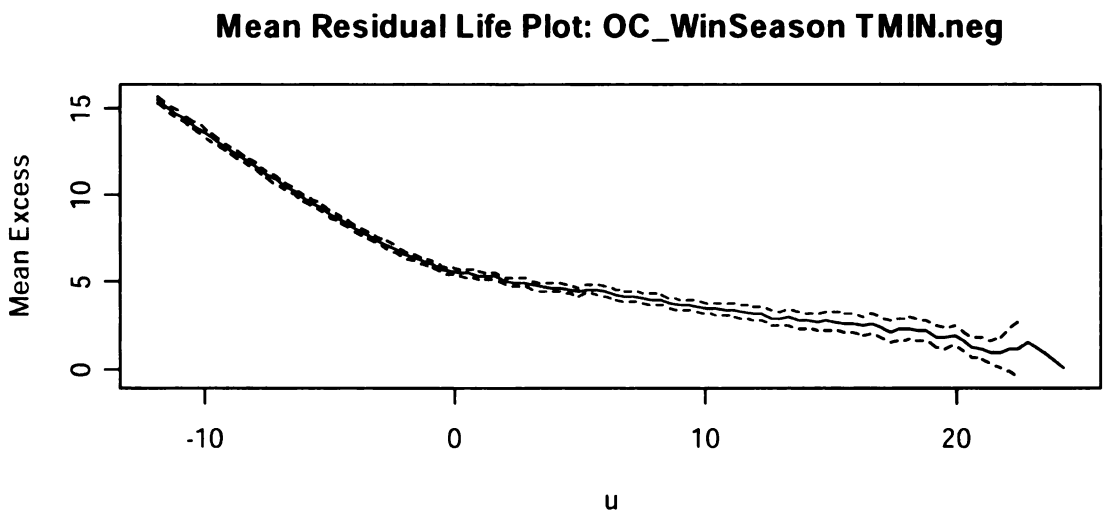

Appendix Figure 50 Obraztsov Chiflick, Mean Residual Life Plot for winter TMIN, 1953-1979 (negative data)

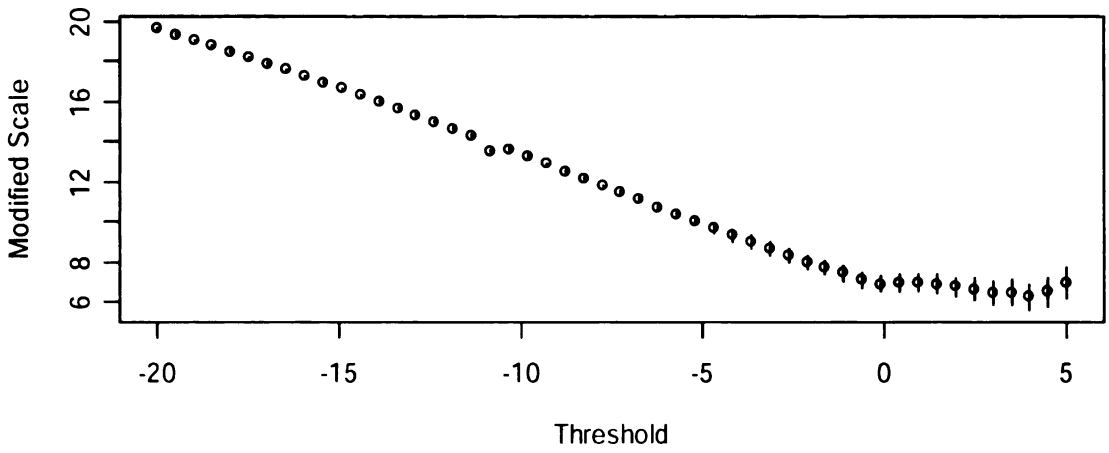

Appendix Figure 51 Obraztsov Chiflick, GPD fit to thresholds plots for winter TMIN, 1953-1979 (negative data)

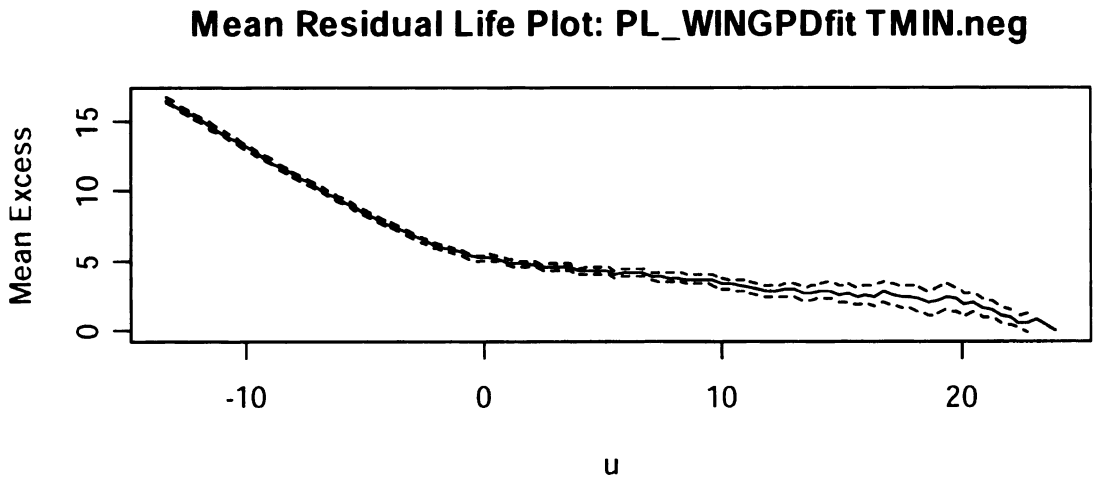

Appendix Figure 52 Pleven, Mean Residual Life Plot for winter TMIN, 1951-1979 (negative data)

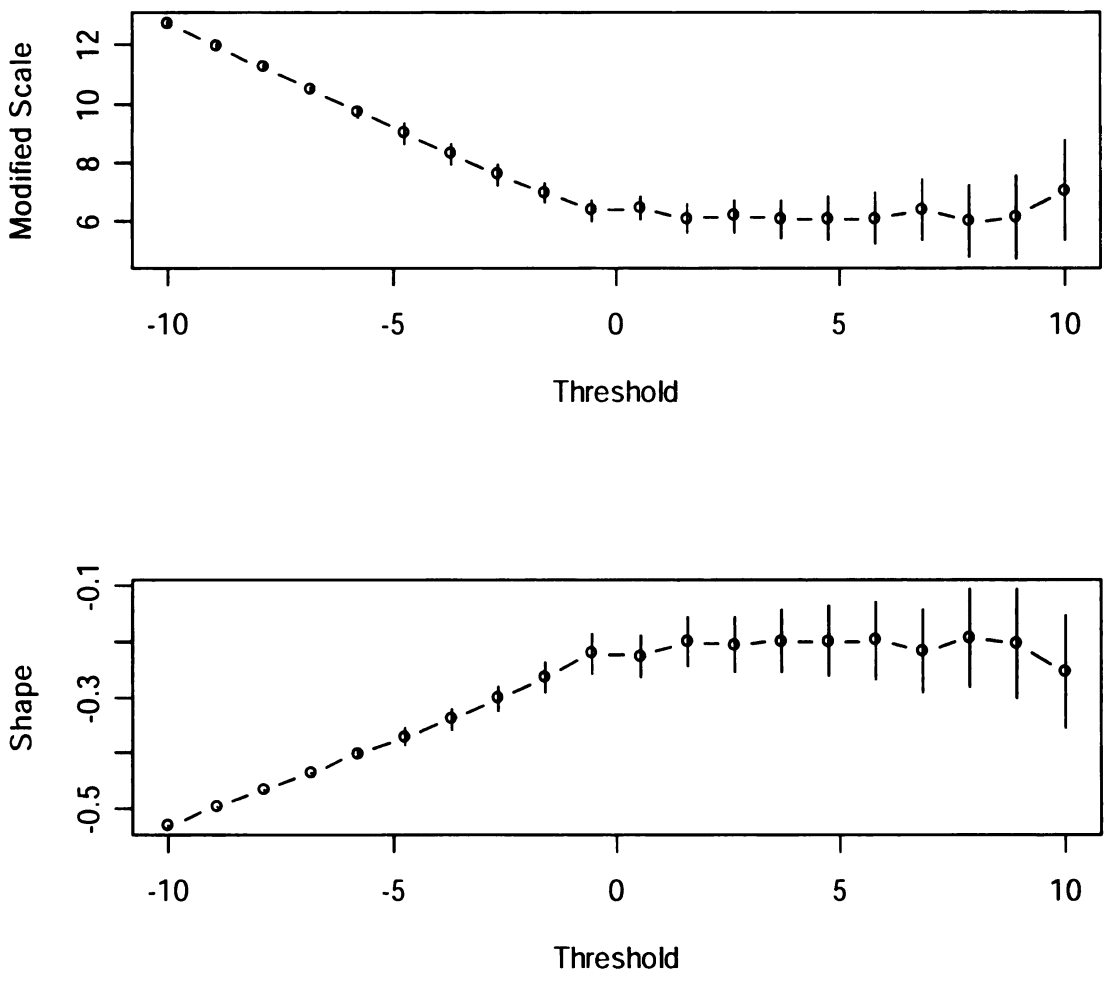

Appendix Figure 53 Pleven, GPD fit to thresholds plots for winter TMIN, 1951-1979 (negative data)

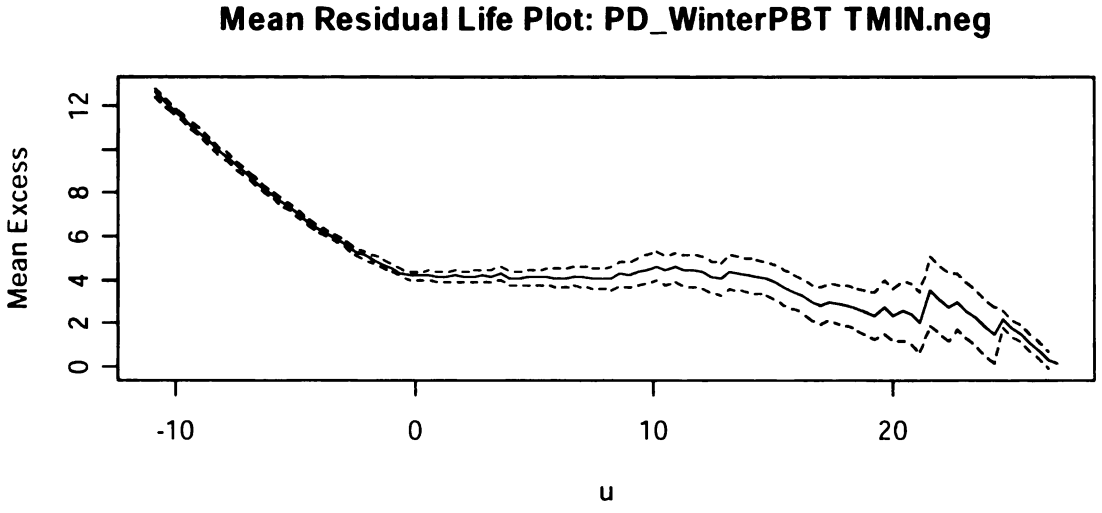

Appendix Figure 54 Plovdiv, Mean Residual Life Plot for winter TMIN, 1951-1979 (negative data)

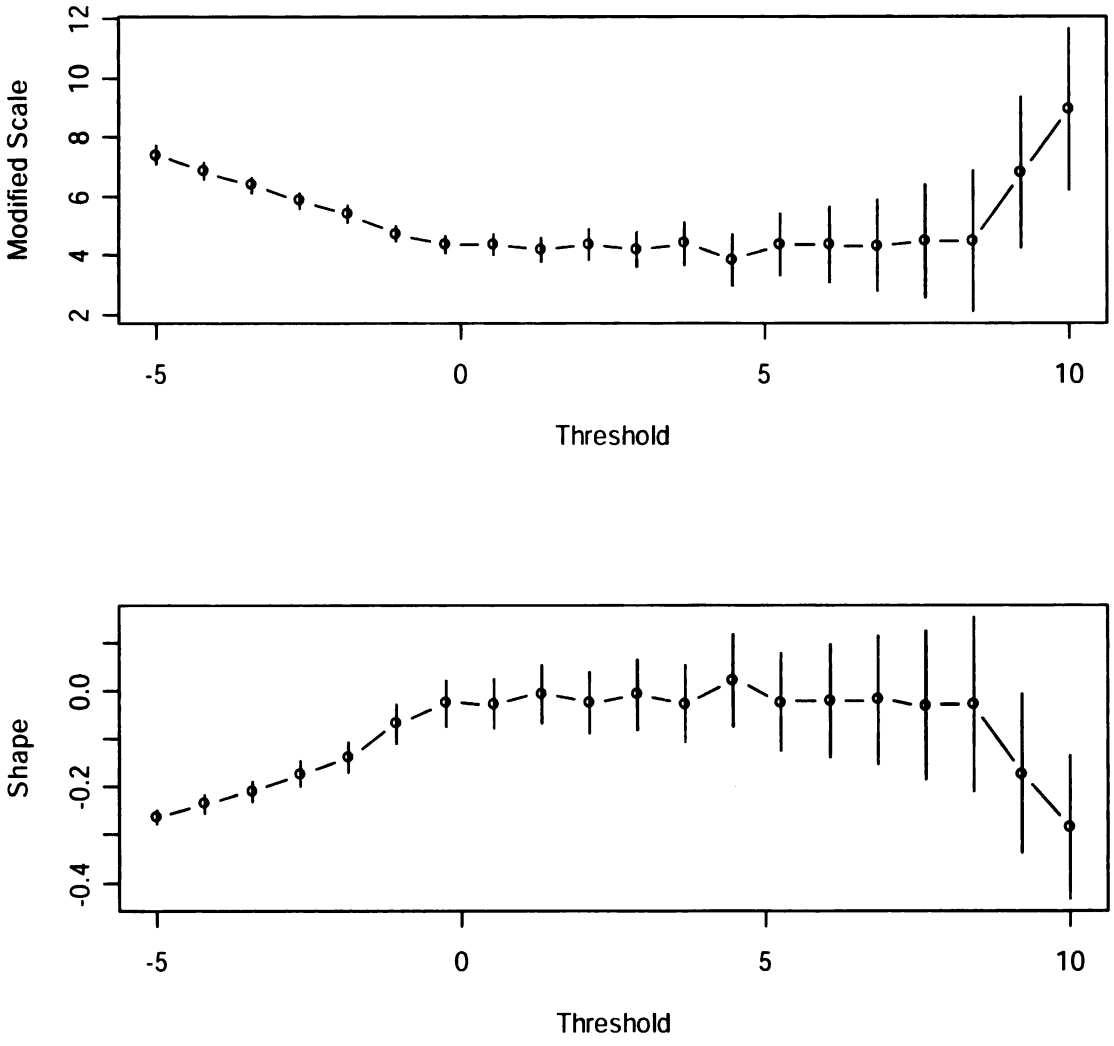

Appendix Figure 55 Plovdiv, GPD fit to thresholds plots for winter TMIN, 1951-1979 (negative data)

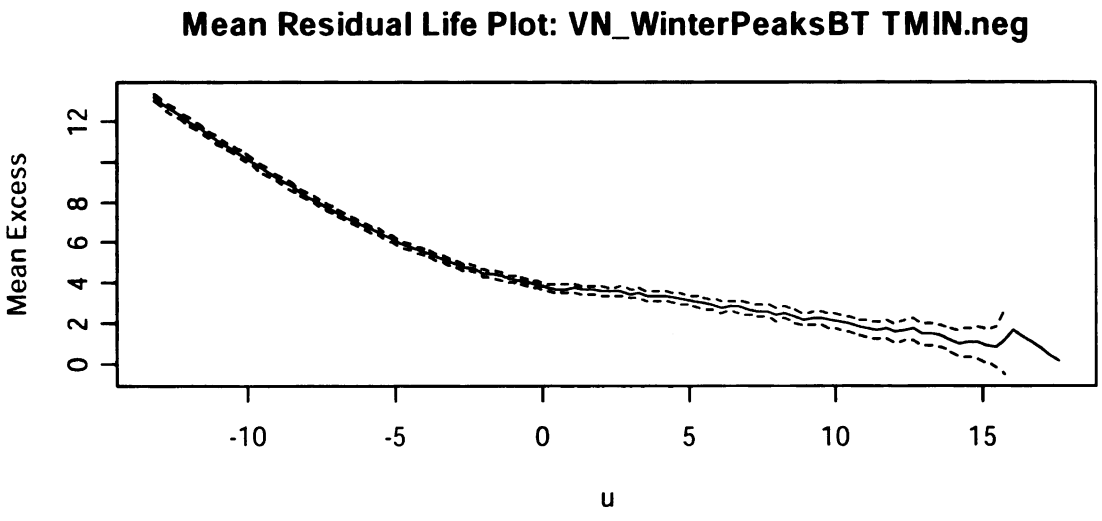

Appendix Figure 56 Varna, Mean Residual Life Plot for winter TMIN, 1951-1979 (negative data)

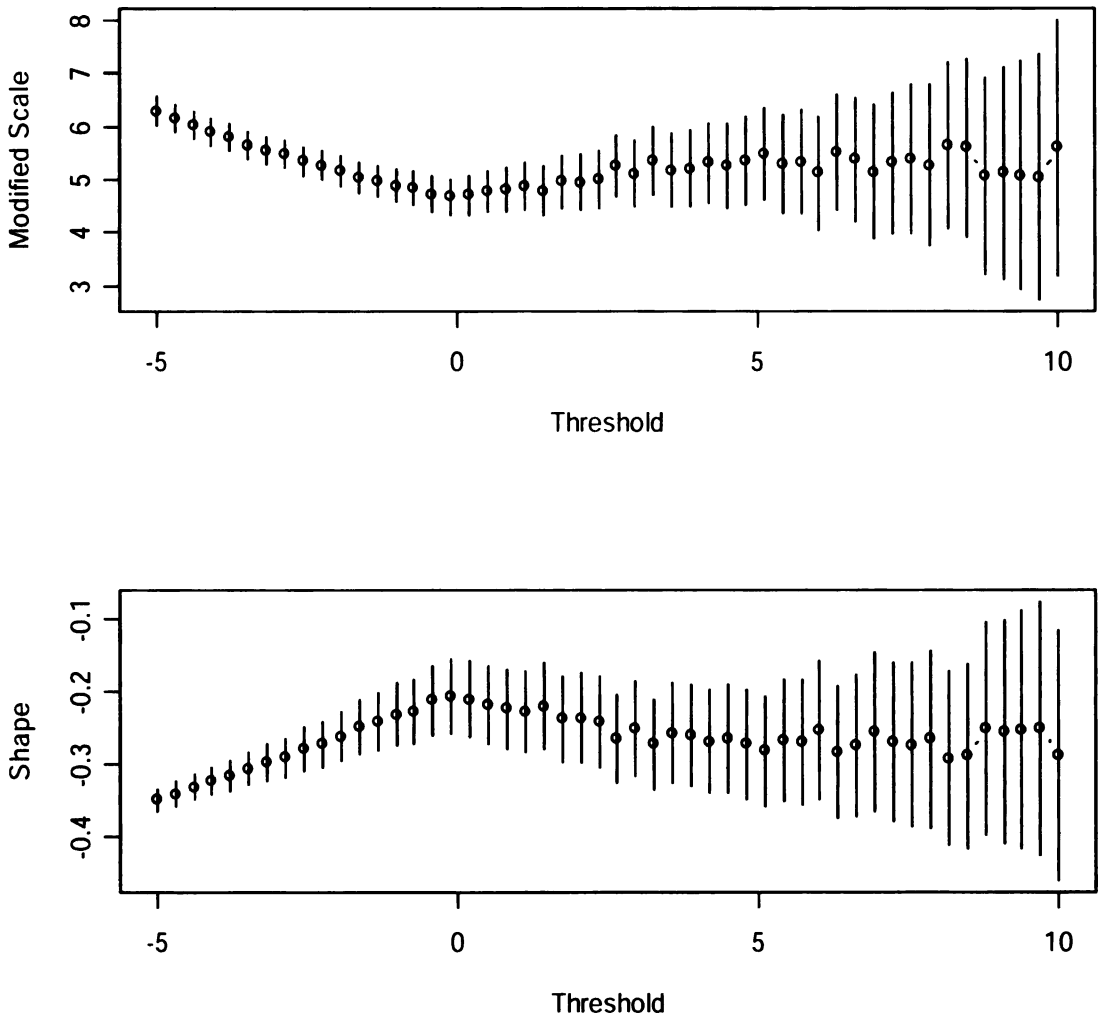

Appendix Figure 57 Varna, GPD fit to thresholds plots for winter TMIN, 1951-1979 (negative data)

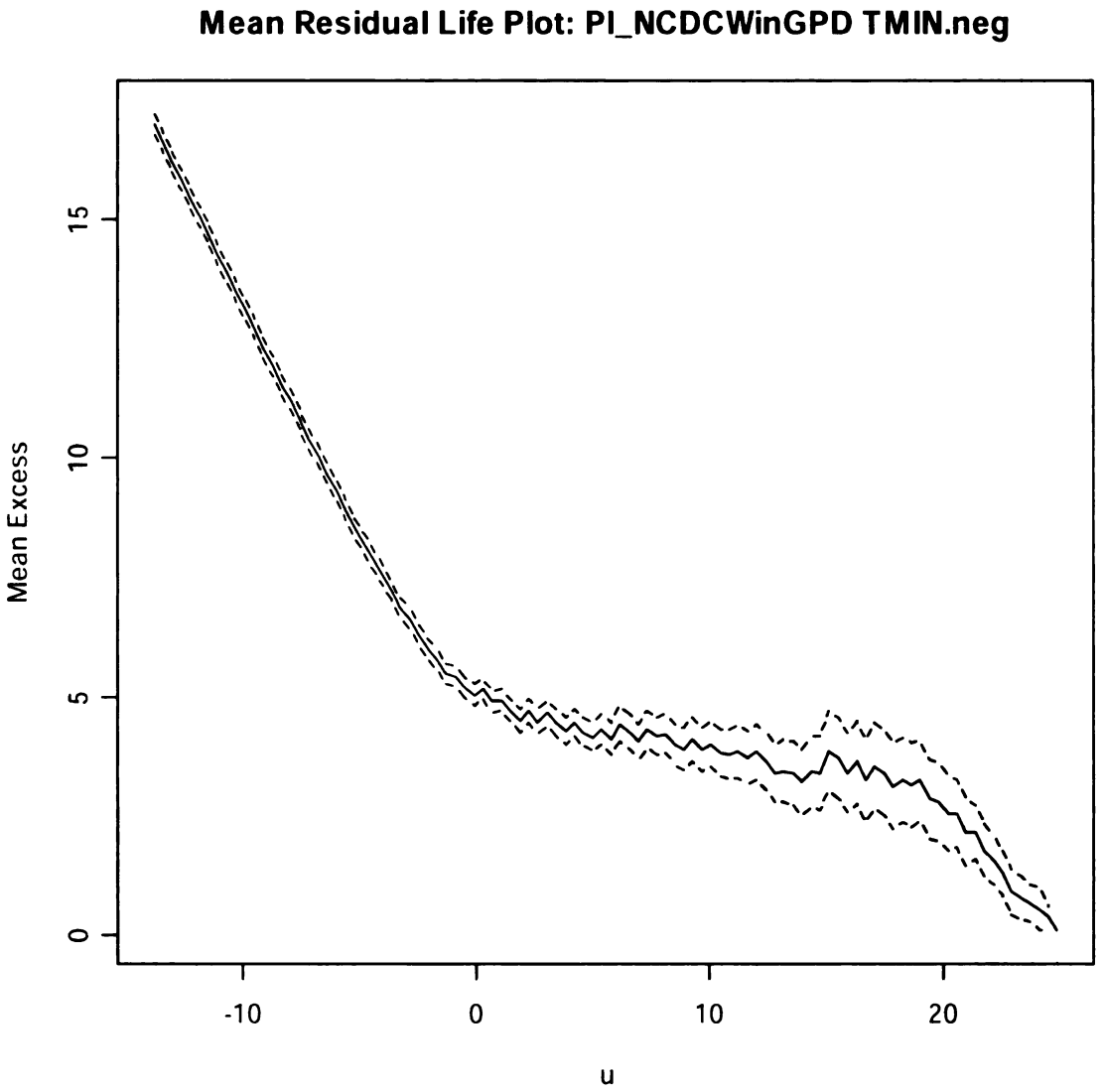

Appendix Figure 58 Pleven NCDC, Mean Residual Life Plot for winter TMIN, 1973-1999 (negative data)

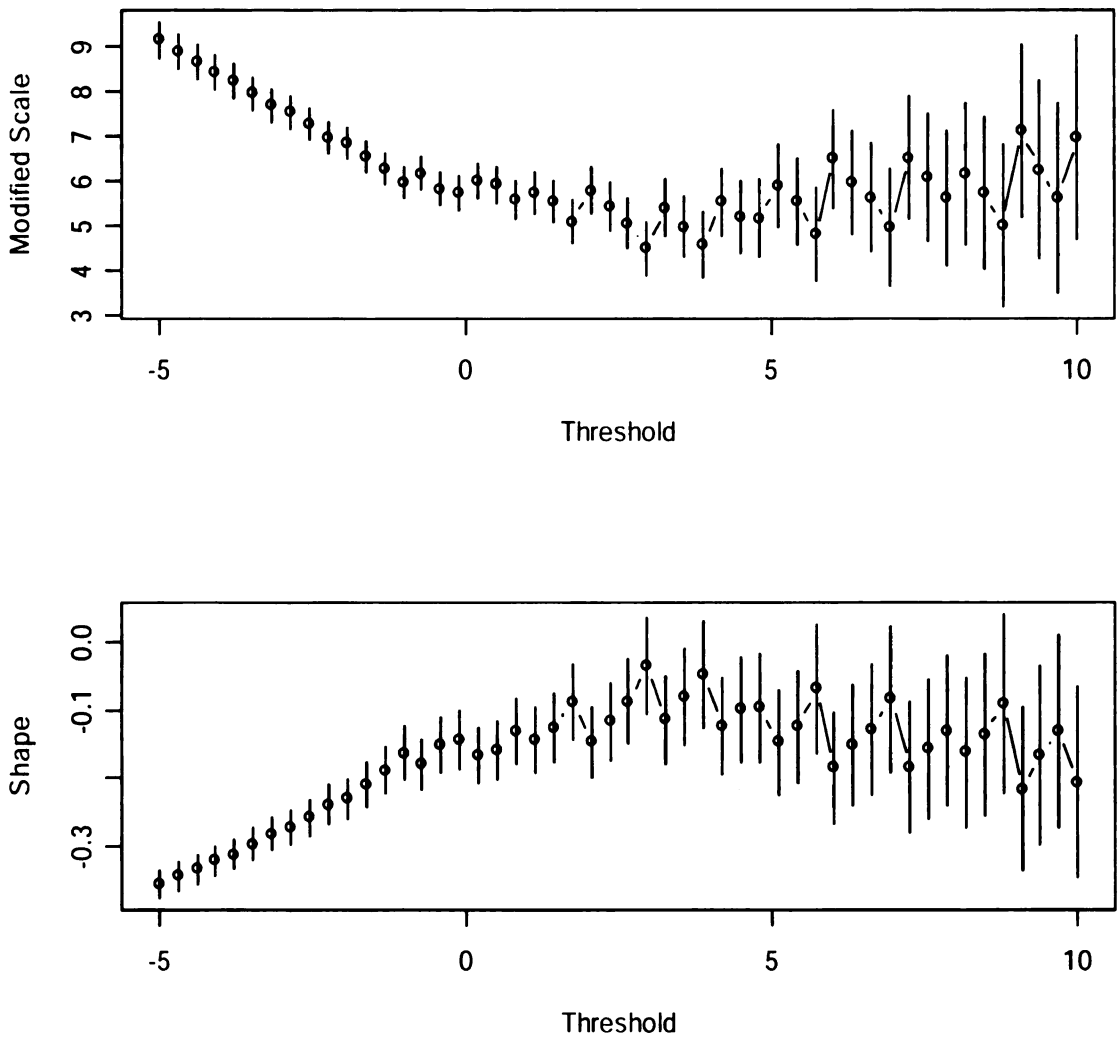

Appendix Figure 59 Pleven NCDC, GPD fit to thresholds plots for winter TMIN, 1973-1999 (negative data)

GPD model fit to all the exceedances over 32°C in summer

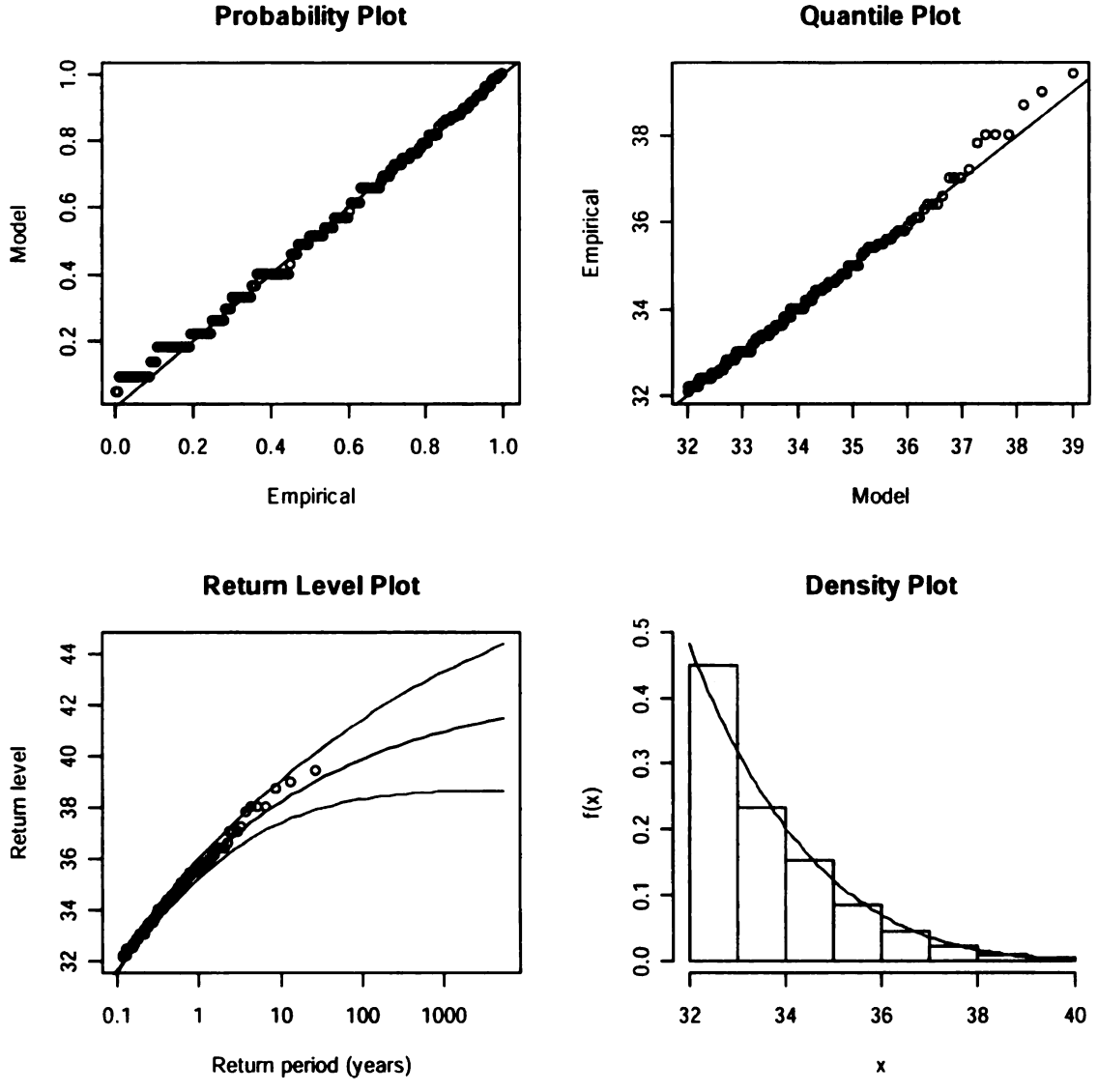

Appendix Figure 60 GPD model fit to summer TMAX exceedances over a 32°C threshold, Obraztsov Chiflick 1953-1979

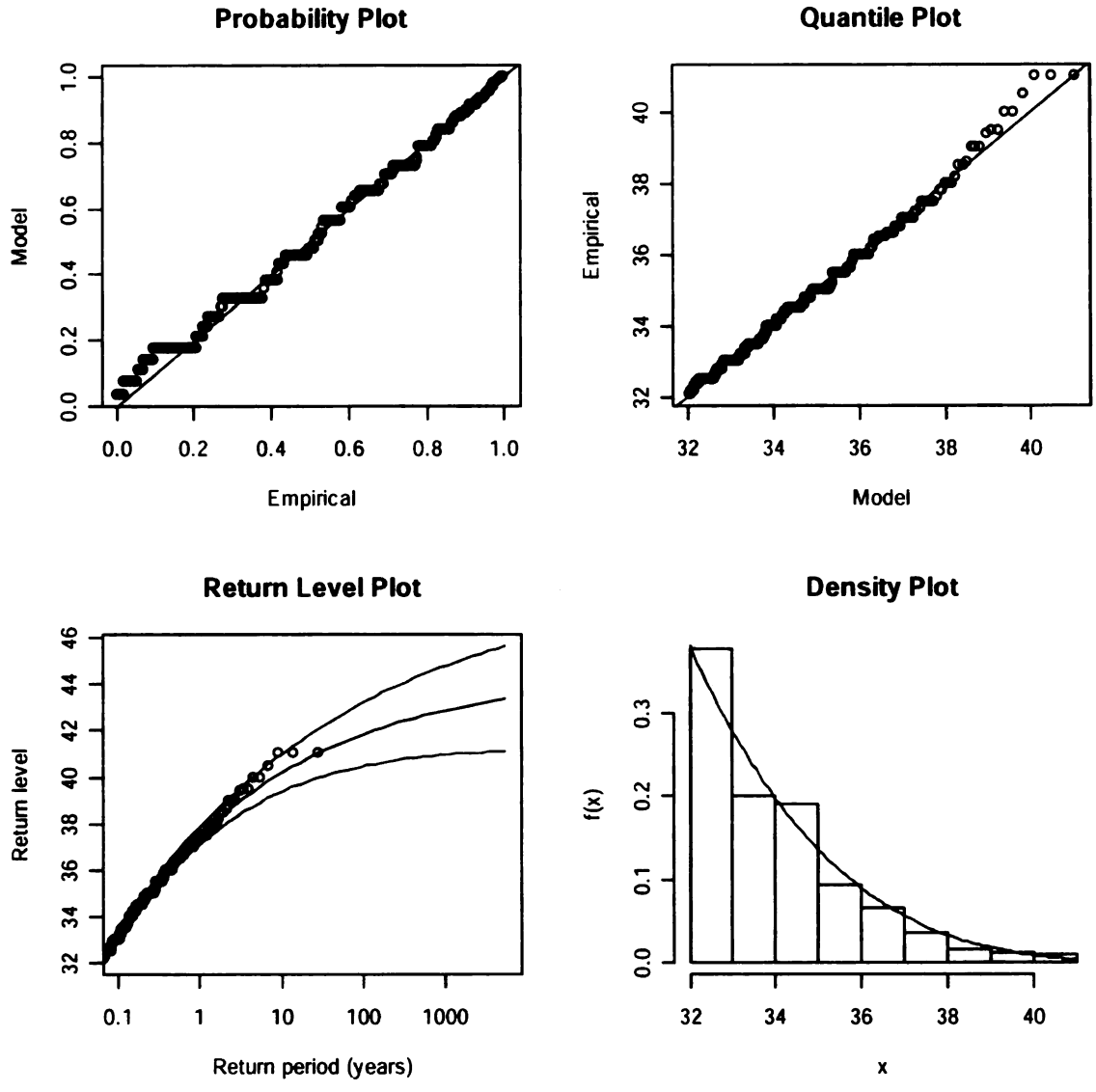

Appendix Figure 61 GPD model fit to summer TMAX exceedances over a 32°C threshold, Pleven 1951-1979

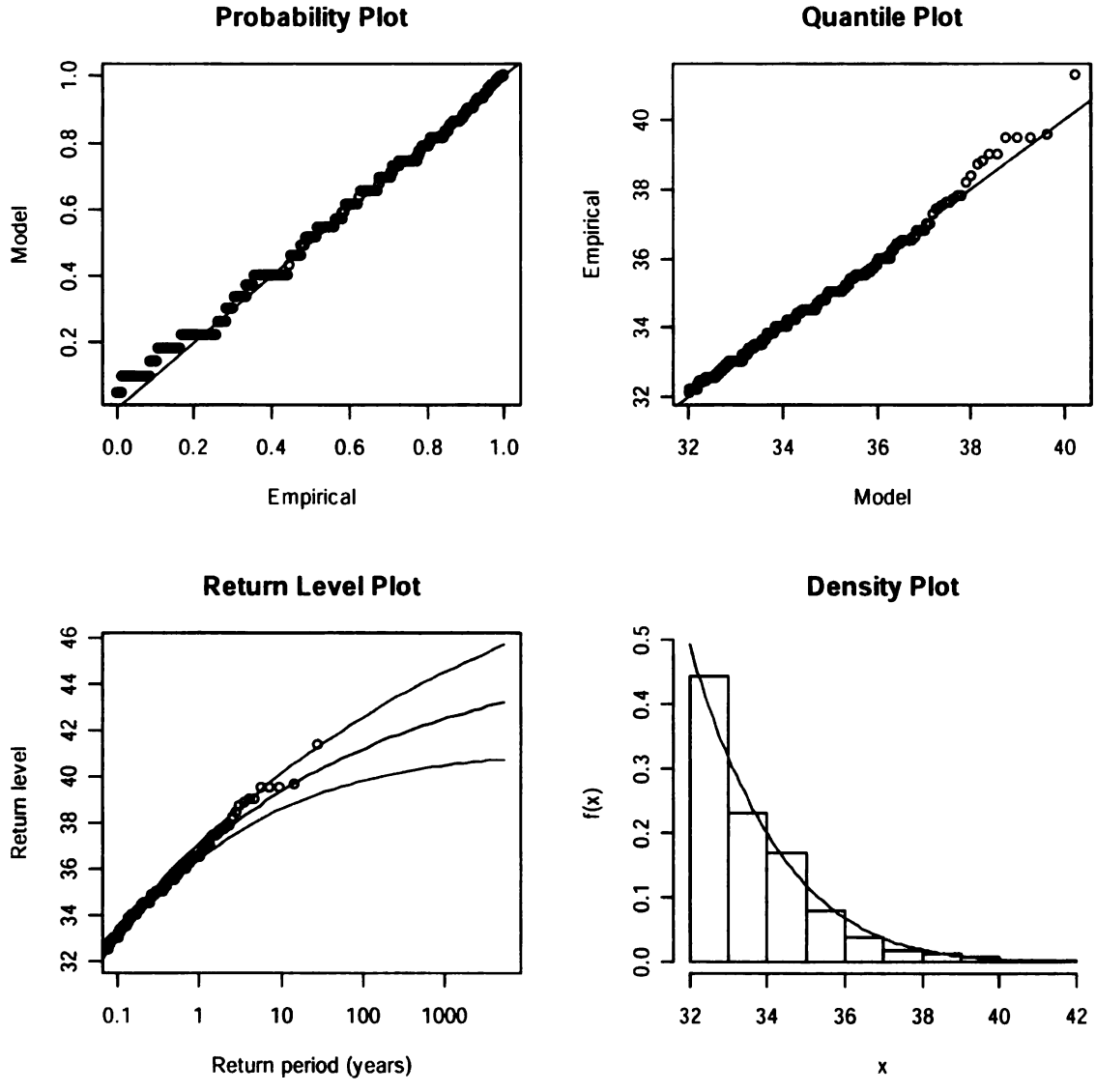

Appendix Figure 62 GPD model fit to summer TMAX exceedances over a 32°C threshold, Plovdiv 1951-1979

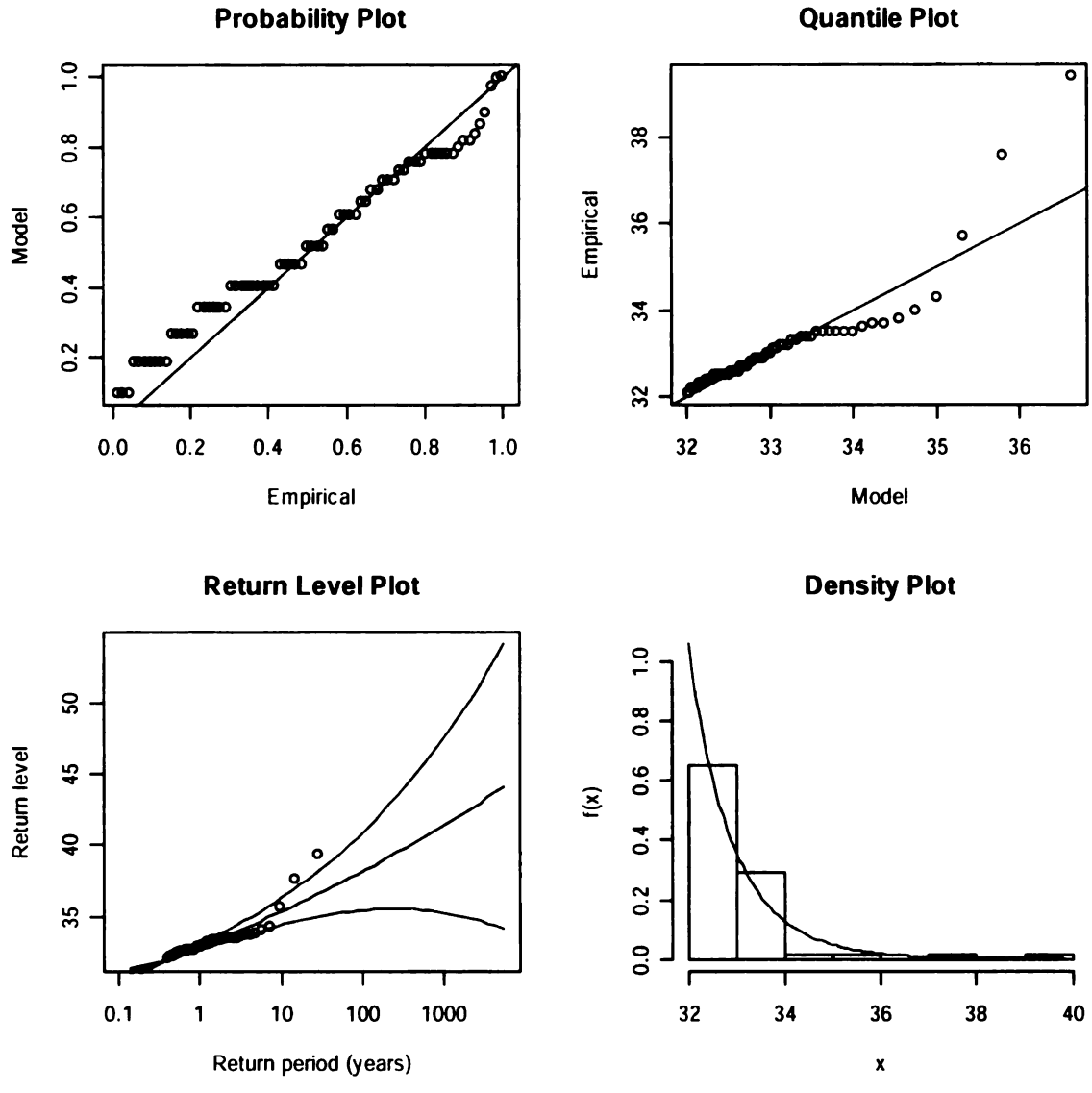

Appendix Figure 63 GPD model fit to summer TMAX exceedances over a 32°C threshold, Varna 1951-1979

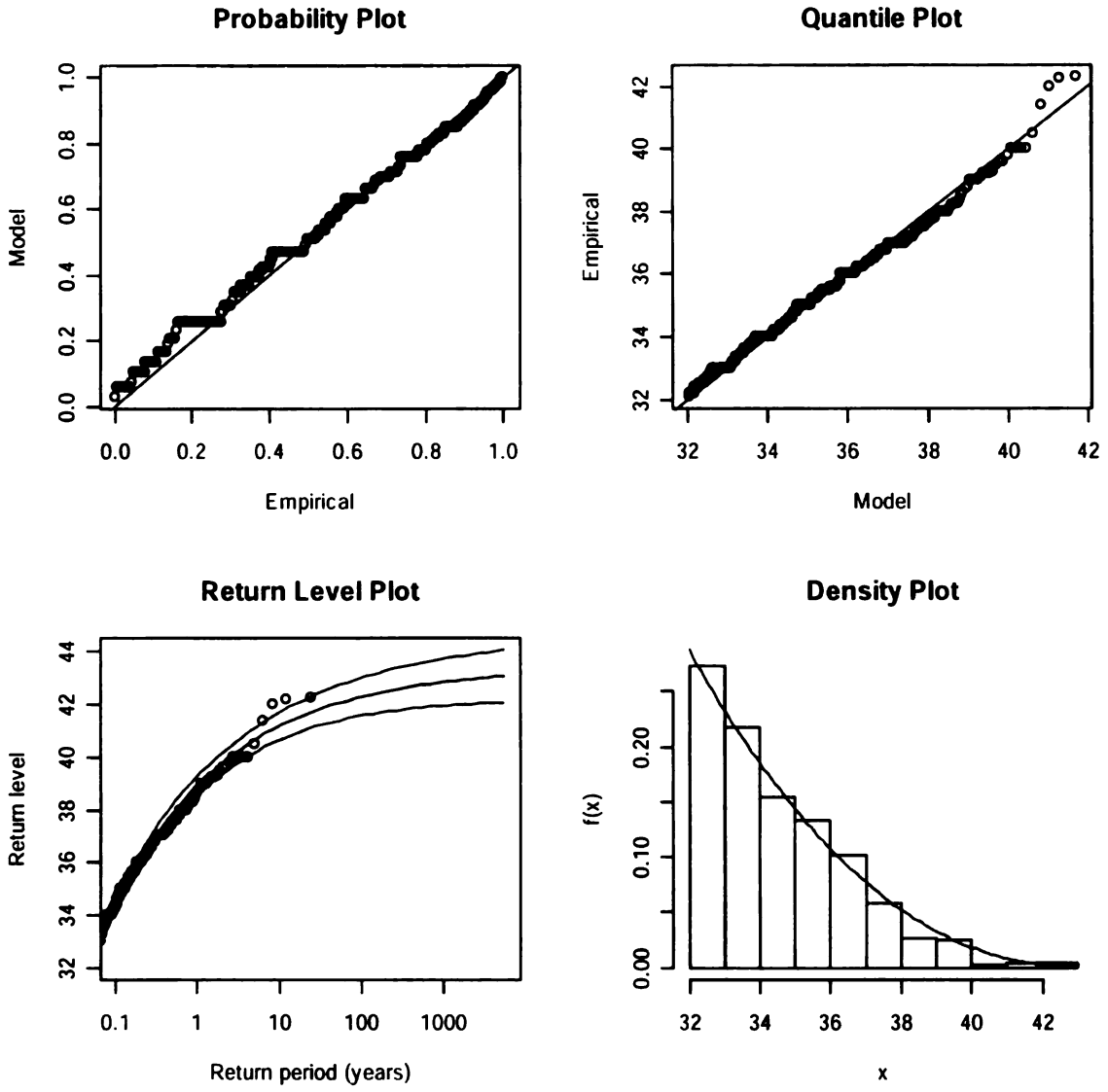

Appendix Figure 64 GPD model fit to summer TMAX exceedances over a 32°C threshold, Pleven NCDC, 1973-1999

Appendix Table 12 Summer TMAX exceedances over a 32°C threshold, GPD fit details

Station	Obraztsov Chiflick		Varna		Plovdiv		Pleven		Pleven NCDC	
Para-meters	MLE	Stand. Error	MLE	Stand. Error	MLE	Stand. Error	MLE	Stand. Error	MLE	Stand. Error
Scale	2.08	0.18	0.95	0.14	2.03	0.12	2.6	0.16	3.5	0.17
Shape	-0.19	0.06	0.06	0.09	-0.15	0.04	-0.2	0.04	-0.3	0.03
Number of excee-dances	223		72		501		433		530	

GPD fit plots for winter TMIN deficiencies below -5°C threshold

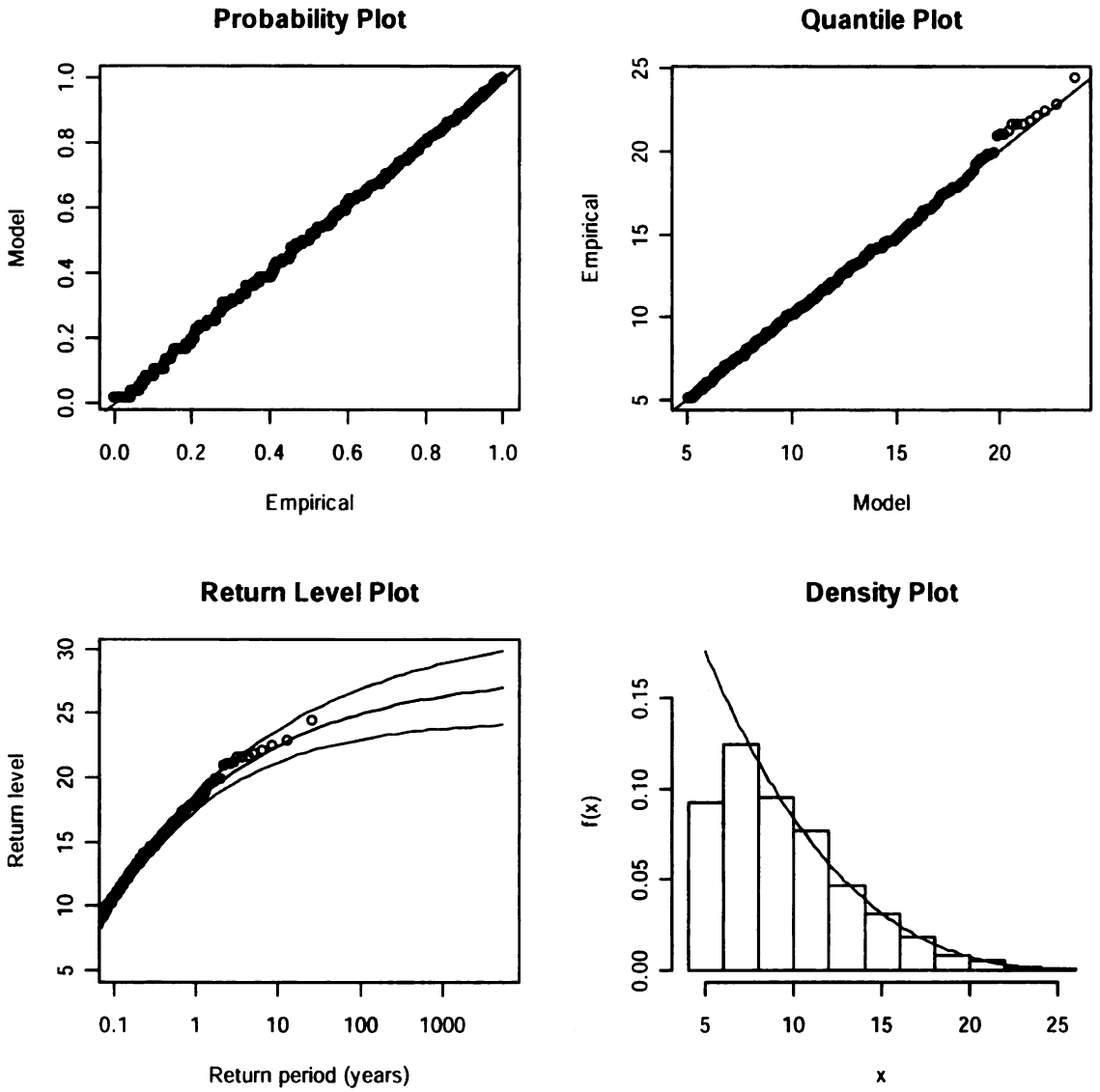

Appendix Figure 65 GPD model fit to winter TMIN deficiencies below a -5°C threshold, Obraztsov Chiflick 1953-1979

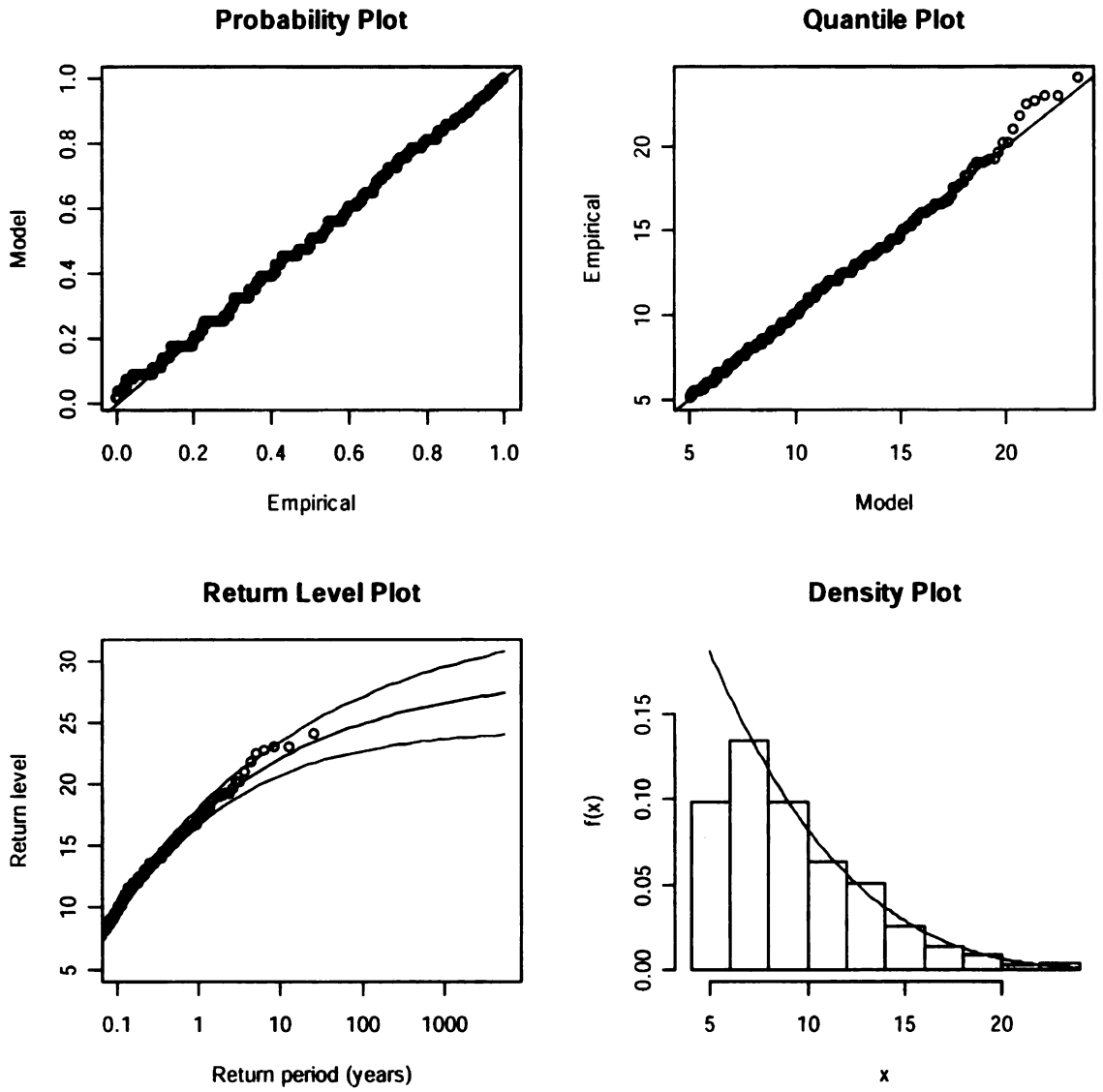

Appendix Figure 66 GPD model fit to winter TMIN deficiencies below a -5°C threshold, Pleven 1951-1979

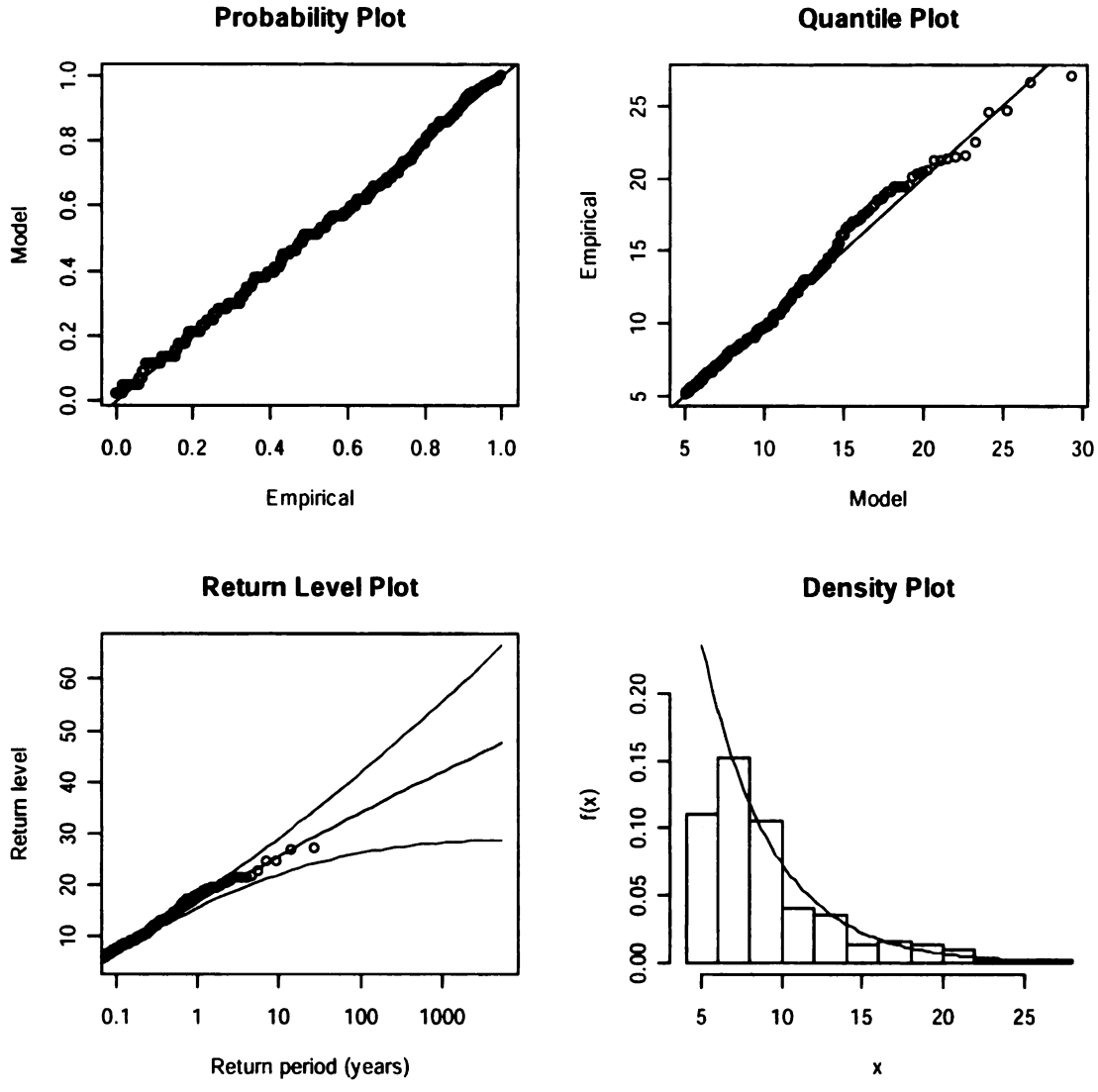

Appendix Figure 67 GPD model fit to winter TMIN deficiencies below a -5°C threshold, Plovdiv 1951-1979

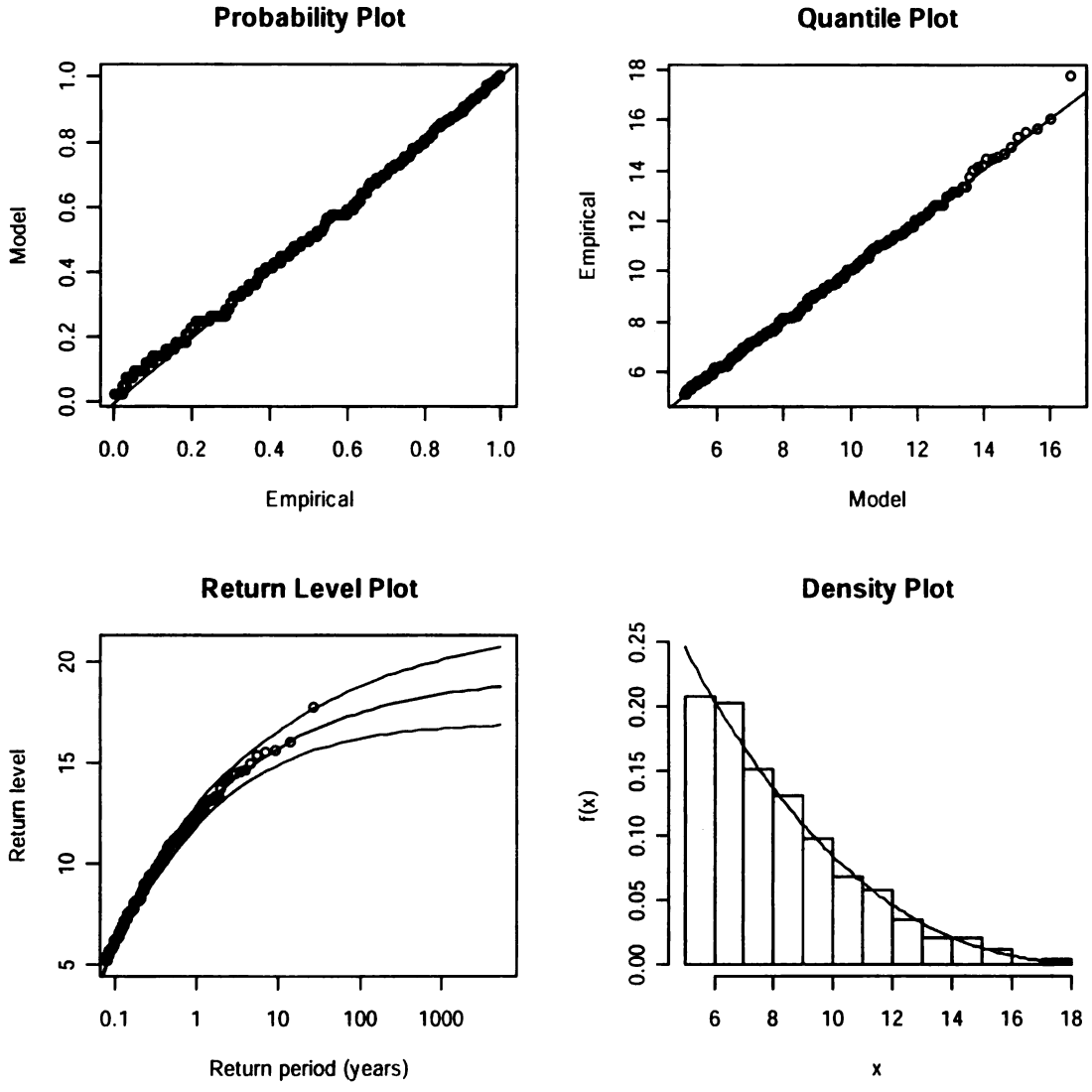

Appendix Figure 68 GPD model fit to winter TMIN deficiencies below a -5°C threshold, Varna 1951-1979

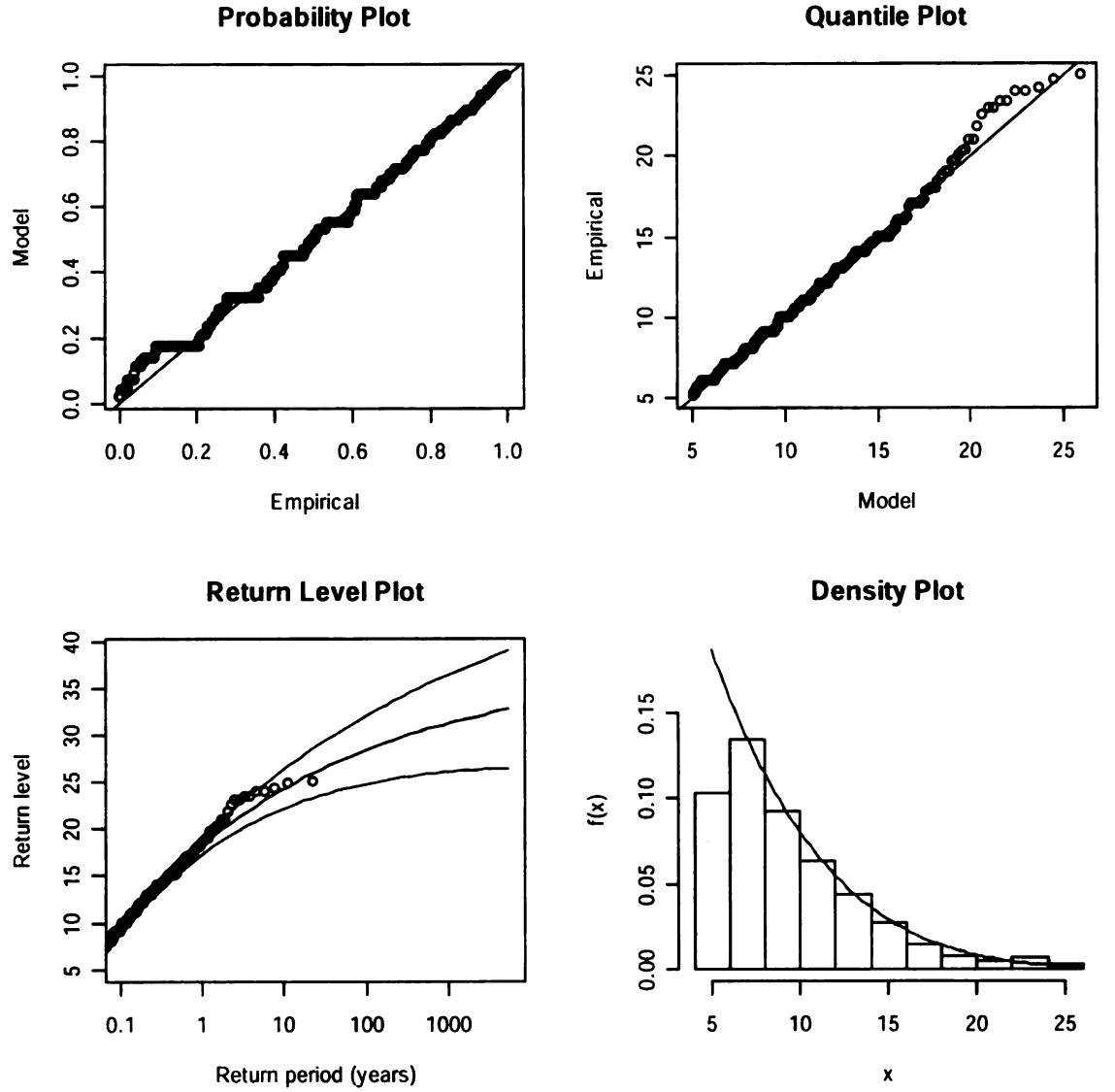

Appendix Figure 69 GPD model fit to winter TMIN deficiencies below a -5°C threshold, Pleven NCDC 1973-1999

Appendix Table 13 Winter TMIN deficiencies below a -5°C threshold, GPD fit details

Station	Obraztsov Chiflick		Varna		Plovdiv		Pleven		Pleven NCDC	
Para-meters	MLE	Stand. Error	MLE	Stand. Error	MLE	Stand. Error	MLE	Stand. Error	MLE	Stand. Error
Scale	5.7	0.3	4.1	0.3	4.3	0.3	5.3	0.3	5.3	0.3
Shape	-0.25	0.03	-0.28	0.04	-0.02	0.05	-0.22	0.03	-0.17	0.04
Number of excee-dances	786		352		480		688		565	

BIBLIOGRAPHY

Alexandersson, H., 1986 – A homogeneity test applied to precipitation data. J Climatol. 6: 661-675.

Bardossy A, Caspary HJ. 1990. Detection of climate change in Europe by analyzing European atmospheric circulation patterns from 1881-1989. Theor. Appl. Climatol. 42: 155-167.

Barnston AG, Livezey RE. 1987. Classification, seasonality and persistence of low-frequency atmospheric circulation patterns. Mon. Wea. Review 115: 1083-1126.

Barry RG, Carleton AM. 2001. Synoptic and dynamic climatology, Routledge, London, 402 pp.

Barry RG, Chorley RJ. 2003. Atmosphere, weather and climate. London, Routledge, 421 pp.

Björnsson H, Venegas SA. 1997. A manual for EOF and SVD analyses of climate data. McGill University.

Brazdil R, et al. 1996. Trends of maximum and minimum daily temperatures in Central and Southeastern Europe. Int. J. Climatol. 16: 765-782.

Bretherton C. 2000. ASP Colloquium Notes: Dynamics of decadal to centennial climate variability.

Briffa KR, Jones PD, Kelly PM. 1990. Principal component analysis of the Lamb catalogue of daily weather types: Part 2, seasonal frequencies and update to 1987. Int. J. Climatol 10 (6): 549-563.

Buishand, T.A. 1982. Some methods for testing the homogeneity of rainfall records. J. Hydrol. 58: 11-27.

Bulgarian Meteorological Yearbooks, years 1951-1979, Institute of Hydrology and Meteorology, Sofia, Bulgaria (in Bulgarian).

Busuioc A, von Storch H. 1996. Changes in the winter precipitation in Romania and its relation to the large-scale circulation. Tellus, 48A: 538-552.

Calinski RB, Harabasz J. 1974. A dendrite method for cluster analysis. Communications in Statistics 3:1-27.

Changnon SA, Changnon JM. 1992. Temporal fluctuations in weather disasters: 1950-1989. Climatic Change 22: 191-208.

Changnon D. 1993. Variability in high temperature extremes in the southeastern United States. Physical Geography 14 (6): 599-611.

Changnon SA, Kunkel KE, Reinke BC. 1996. Impacts and responses to the 1995 heat wave: A call to action. Bull. Amer. Meteor. Soc. 77 (7): 1497-1506.

Chen G, Balakrishnan N. 1995. The infeasibility of probability weighted moments estimation of some generalized distributions. In *Recent Advances in Life-Testing and Reliability*, ed. N. Balakrishnan, London: CRC Press, pp. 565-573.

Choulakian V, Stephens MA. 2001. Goodness-of-fit tests for the Generalized Pareto distribution. Technometrics 43 (4): 478-484.

Coles S. 2001. An introduction to statistical modeling of extreme values. London: Springer Verlag, 208 pp.

Colombo AF, et al. 1999. Climate variability and the frequency of extreme temperature events for nine sites across Canada: Implications for power usage. J. Climate 12: 2490-2502.

Conrad V, Pollack C. 1950. Methods in Climatology, Harvard University Press, Cambridge, MA, 459 pp.

Cooper MC, Milligan GW. 1984. The effect of error on determining the number of clusters. College of Administrative Science, Working paper.

Cooter EJ, Le Duc SK. 1995. Recent frost date trends in the north-eastern USA. Int. J. Climatol. 15: 65-75.

Craddock JM. 1979. Methods of comparing annual rainfall records for climatic purposes. Weather 34: 332-346.

Cramer W. et al. (eds), 2001: Europe. In McCarthy, J.J. et al. (eds), Climate Change 2001: Impacts, Adaptation and Vulnerability. Cambridge University Press, New York.

Davis RE, Kalkestein LS. 1990. Development of an automated spatial synoptic climatological classification. Int. J. Climatol. 10: 769-794.

Davison AC, Smith RL. 1990. Models for exceedances over high thresholds. Journal of the Royal Statistical Society. Series B (Methodological) 52 (3): 393-442.

DeGaetano AT. 1996. Recent trends in maximum and minimum temperature threshold exceedances in the Northeastern United States. J. Climate 9: 1646-1660.

Domonkos P. 1998. Statistical characteristics of extreme temperature anomaly groups in Hungary. Theor. Appl. Climatol. 59: 165-179.

Domonkos P, Piotrowicz K. 1998. Winter temperature characteristics in Central Europe. Int. J. Climatol. 18: 1405-1417.

Domonkos P, Kyselý J, Piotrowicz K, Petrovic P, Likso T. 2003. Variability of extreme temperature events in south-central Europe during the 20th century and its relationship with large-scale circulation. Int. J. Climatol. 23: 987-1010.

Duda RO, Hart PE. 1973. Pattern classification and scene analysis. New York: Wiley.

Dupuis DJ. 1996. Estimating the probability of obtaining nonfeasible parameter estimates of the Generalized Pareto distribution. Journal of Statistical Computer Simulation. 54: 197-209.

EEA, 2004: Impacts of Europe's changing climate. An indicator based assessment. Luxemburg.

Earickson RJ, Harlin JM. 1994. Geographic measurement and quantitative analysis. New York: Macmillan College Publishing Co. Inc.350 pp.

Easterling D, et al. 1997. Maximum and minimum temperature trends for the globe. Science 277: 364-367.

Easterling D, Meehl GA, Parmesan C, Changnon SA, Karl TR, Mearns LO. 2000a. Climate extremes: Observations, modeling, and impacts. Science 289: 2068-2074.

Easterling D, Evans JL, Groisman PY, Karl TR, Kunkel KE, Ambenje P. 2000b. Observed variability and trends in extreme climate events: A brief overview. Bulletin of American Meteorological Society 81 (3): 417-425.

Easton VJ, McColl JH. 1997. STEPS. Statistics Glossary. V. 1.1. http://www.stats.gla.ac.uk/steps/glossary/

Esteban P, et al. 2005. Atmospheric circulation patterns related to heavy snowfall days in Andorra, Pyrenees. Int. J. Climatol. 25: 319-329.

Esteban P, et al. 2006. Daily atmospheric circulation catalogue for Western Europe using multivariate techniques. Int. J. Climatol. 26: 1501-1515.

Folland CK et al. 1999. Workshop on indices and indicators for climate extremes, Asheville, NC, USA, 3-6 June 1997. Breakout group C: Temperature indices for climate extremes. Climatic Change 42: 31-43.

Fovell RG, Fovell MYC. 1993. Climate zones of the conterminous United States defined using cluster analysis. J. Climate 6: 2103-2135.

Frich P. et al. 2002. Observed coherent changes in climatic extremes during the second half of the twentieth century. Climate Research 19: 193-212.

Galambosi et al., 1996. Evaluation and analysis of daily atmospheric circulation patterns of the 500 HPA pressure field over the southwestern USA. Atmospheric Research 40: 49-76.

Gerstengarbe F-W, Werner PC. 1993. Katalog der Grosswetterlagen Europas nach Paul Hess und Helmuth Brezowsky 1881-1992. Deutscher Wetterdienst, Offenbach am Main, 249 pp.

Gerstengarbe F-W et al. 1999. Katalog der Grosswetterlagen Europas nach Paul Hess und Helmuth Bresowsky 1881-1998. Deutscher Wetterdienst, Offenbach am Main.

Gilbert RO. 1987. Statistical methods for environmental pollution monitoring. New York: Van Nostrand Reinhold Co. Inc. 320 pp.

Giles BD, Balafoutis CJ. 1992. Cold windchill spells in the south Balkans: A study of the synoptic situations. Int. J. Climatol. 12: 305-312.

Gilleland E, Katz RW. 2005. Tutorial for the Extremes Toolkit (extremes): Weather and climate applications of extreme value statistics. Version 1.5. http://www.assessment.ucar.edu/toolkit.

Glossary of meteorology. 1999. Glickman TS (ed.), American Meteor. Soc., 2nd edition, 855 pp.

Global Summary of the Day Dataset. Version 7 ftp://ftp.ncdc.noaa.gov/pub/data/gsod/

Goodess C, Palutikof J. 1998. Development of daily rainfall scenarios for southeast Spain using a circulation-type approach to downscaling. Int. J. Climatol. 18 (10): 1051-1083.

Goodess C, Jones PD. 2002. Links between circulation and changes in the characteristics of Iberian rainfall. Int. J. Climatol. 22: 1593-1615.

Hair et al. 1998. Multivariate data analysis. Prentice Hall. 720 pp.

Hannachi et al., 2006. In search of simple structures in climate: Simplifying EOFs. Int. J. Climatol. 26: 7-28.

Heino R, et al. 1999. Progress in the study of climatic extremes in Northern and Central Europe. Climatic Change 42: 151-181.

Helsel DR, Mueller DK, Slack JR. 2006. Computer program for the Kendall family of trend tests: U.S. Geological Survey Scientific Investigations Report 2005-5275, 4p.

Hennessy KJ, Pittock AB. 1995. Greenhouse warming and threshold temperature events in Victoria, Australia. Int. J. Climatol. 15: 591-612.

Hess P, Brezowsky H .1969. Katalog der Großwetterlagen Europas. Berichte des Deutschen Wetterdienstes. Nr. 113, (Band 15), 55p.

Horel JD. 1981. A rotated principal component analysis of the interannual variability of the Northern Hemisphere 500 mb height field. Mon. Wea. Review 109: 2080-1092.

Horton EB, Follan CK, Parker DE. 2001. The changing incidence of extremes in worldwide and Central England temperatures to the end of the twentieth century. Climatic Change 50: 267-295.

Hosking JRM. 1990. L-moments: Analysis and estimation of distributions using linear combinations of order statistics. J. Royal Statist. Soc. B 52 (1): 105-124.

Huang JP, North GR. 1996. Cyclic spectral analysis of fluctuations in a GCM simulation. J. Atmos. Sci. 53: 370-379.

Hulme M, Barrow E (ed.) .1997. Climates of the British Isles: present, past and future. Routledge, London, 454 pp.

Hundecha Y, Bárdossy A. 2005. Trends in daily precipitation and temperature extremes across Western Germany in the second half of the 20th century. Int. J. Climatol. 25: 1189-1202.

Huth R. 1995. PCA-based classification of circulation and weather patterns; Some methodological considerations. 6th International Meeting on

Statistical Climatology, 19-23 June, 1995, University College, Galway, Ireland.

Huth R. 1997. Continental-scale circulation in the UKHI GCM. J. Climate 10: 1545-1561.

Huth R. 2000. A circulation classification scheme applicable in GCM studies. Theor. Appl. Climatol. 67: 1-18.

Huth R, Kyselý J.Pokorna L. 2000. A GCM simulation of heat waves, dry spells, and their relationships to circulation. Climatic Change 46: 29-60.

Huth R. 2001. Disaggregating climatic trends by classification of cicruclation patterns. Int. J. Climatol. 21: 135-153.

IPCC TAR .2001. Climate Change 2001, Working Group I: The Scientific Basis. Cambridge University Press. New York.

IPCC FAR .2007. Climate Change 2007: The Physical Science Basis. Summary for Policymakers. Cambridge. New York.

Jenkinson AF, Collison P. 1977. An initial climatology of gales over the North Sea. Synoptic Climatology Branch Memorandum No.62, Meteorological Office, London, 18 pp.

Johnson DE. 1998. Applied multivariate methods for data analysis. Duxbury Press. 570 pp.

Jones PD, Hulme M, Briffa KR. 1993. A comparison of Lamb circulation types with an objective classification scheme. Int. J. Climatol. 13: 655-663.

Jones PD, Horton EB, Folland CK, Hulme M, Parker DE, Basnett TA. 1999. The use of indices to identify changes in climatic extremes. Climatic Change 42: 131-149.

Kalkstein et al. 1987. An evaluation of three clustering procedures for use in synoptic climatological classification. J. Climate and Appl. Meteor. 26: 717-730.

Kalnay E. et al. 1996. The NCEP/NCAR 40-year Reanalysis project. Bull. Amer. Meteor. Soc. 77: 437-471.

Karl TR et al. 1991. Global warming: evidence for asymmetric diurnal temperature change. Geophys. Res. Letters 18 (12): 2253-2256.

Karl TR, Knight RW, Plummer N. 1995. Trend in high-frequency climate variability in the twentieth century. Nature 377: 217-220.

Karl TR, Knight RW. 1997. The 1995 Chicago heat wave: How likely is a recurrence? Bull. Amer. Meteor. Soc. 78 (6): 1107-1119.

Karl TR, et al. 1999. Climate extremes: Selected review and future research directions. Climatic Change 42: 309-325.

Karossy Cs. 1987. Péczely catalogue of macrosynoptic types (1983-1987). Légkör, 32 (3): 28-30 (in Hungarian).

Kassomenos PA. et al., 2003. Seasonal variation of the circulatin types occurring over southern Greece: a 50 year study. Climate Research 24: 33-46.

Katsoulis BD. et al. 2005. Analysis of hot spell characteristics in the Greek region. Climate Research 28: 229-241.

Katz RW, Parlange MB, Naveau P. 2002. Statistics of extremes in hydrology. Advances in Water Resources 25: 1287-1304.

Katz RW, Brush GS, Parlange MB. 2005. Statistics of extremes: Modeling ecological disturbances. Ecology 86 (5): 1124-1134.

Kistler et al. 2001. The NCEP-NCAR 50-year Reanalysis: Monthly means CD-ROM and documentation. Bull. Amer. Meteor. Soc. 82 (2): 247-267.

Klein Tank AMG, Können GP. 2003. Trends in indices of daily temperature and precipitation extremes in Europe, 1946-99. J. Climate 16: 3665-3680.

Koleva E. 1987. Multiannual variations in air temperature and precipitation in Bulgaria. Problems of Meteorology and Hydrology 2: 27-40. (In Bulgarian)

Koleva E, et al. 1996. Verification of high resolution climatic simulations. Part I: The state of Bulgaria's climate 1961-1990. Bulgarian Journal of Meteorology and Hydrology, 7 (3-4): 73-83.

Kunkel KE, et al., 1999. Temporal fluctuations in weather and climate extremes that cause economic and human health impacts: A review. Bull. Amer. Meteor. Soc. 80: 1077-1098.

Kyselý J, Huth R. 2001. Extreme temperature events in central Europe: Are climate models able to reproduce them? From http://www.cru.uea.ac.uk/cru/projects/mice/2001_St_Lesna_Kysely.pdf

Kyselý J. 2002a. Temporal fluctuations in heat waves at Prague-Klementinum, the Czech Republic, from 1901-97, and their relationship to atmospheric circulation. Int. J. Climatol. 22: 33-50.

Kyselý J. 2002b. Probability estimates of extreme temperature events: Stochastic modeling approach vs. Extreme value distributions. Studia Geophysica et Geodaetica 46 (1): 93-112.

Kyselý J, Domonkos P. 2006. Recent increase in persistence of atmospheric circulation over Europe: Comparison with long-term variations since 1881. Int. J. Climatol. 26: 461-483.

Kyselý J, Huth R. 2006. Changes in atmospheric circulation over Europe detected by objective and subjective methods. Theor. Appl. Climatol. 85: 19-36.

Lamb HH. 1972. British Isles weather types and a register of daily sequence of circulation patterns, 1861-1971. Geophysical Memoir, 116, HMSO, London, 85 pp.

Leadbetter MR, Lindgren G, Rootzen H.1983. Extremes and Related Properties of Random Sequences and Processes. Springer Verlag.

Luterbacher J, Dietrich D, Xoplaki E, Grosjean M, Wanner H. 2004. European seasonal and annual temperature variability, trends, and extremes since 1500. Science 303: 1499-1503.

Maheras P., et al. 1999. Wet and dry monthly anomalies across the Mediterranean basin and their relationship with circulation, 1860-1990. Theor. Appl. Climatol. 64: 189-199.

Maheras P., et al. 2000. Automatic classification of circulation types in Greece: methodology, description, frequency, variability and trend analysis. Theor. Appl. Climatol. 67: 205-233.

Maheras P., et al. 2001. A 40 year objective climatology of surface cyclones in the Mediterranean region: Spatial and temporal distribution. Int. J. Climatol. 21: 109-130.

Maheras P., et al. 2004. On the relationships between circulation types and cnanges in rainfall variability in Greece. Int. J. Climatol. 24: 1695-1712.

McGinnis DL. 2000. Synoptic controls on Upper Colorado river basin showfall. Int. J. Climatol. 20: 131-149.

Mearns L. et al., 1984. Extreme high-temperature events: Changes in their probability with changes in mean temperature. J. Climate and Appl. Meteorol., 23: 1601-1613.

Meehl GA, et al. 2000. Trends in extreme weather and climate events: Issues related to modeling extremes in projections of future climate change. Bull. Amer. Meteor. Soc. 81 (3): 427-436.

Milligan GW, Cooper MC. 1985. An examination of procedures for determining the number of clusters in a data set. College of Administrative Science, Working paper.

Moberg A, et al. 2000. Day-to-day temperature variability trends in 160- to 275-year-long European instrumental records. J. Geophys. Res. 105: 22849-22868.

Moberg A, Jones PD. 2005. Trends in indices for extremes in daily temperature and precipitation in Central and Western Europe, 1901-99. Int. J. Climatol. 25: 1149-1171.

National Statistical Institute (NSI). 2004. Statisticheski spravochnik (Statistical Yearbook), Sofia.

O'Hare GO, Sweeney J. 1993. Lamb's circulation types and British Weather: An evaluation. Geography 78 (1): 43-60.

O'Lenic EA, Livezey RE. 1988. Practical considerations in the use of rotated principal component analysis (RPCA) in diagnosis studies of upper-air height fields. Mon. Wea. Review. 116: 1682-1689.

Palutikof JP, Holt T, Brabson BB, Lister DH. 1998. Methods to calculate extremes in climate change studies. From www.cru.uea.ac.uk/cru/projects/mice/extremes_description.pdf

Péczely G. 1957. Groswetterlagen in Ungarn. Kleinere Veröffentlichungen der Zentralanstalt für Meteorologie. No. 30. Budapest.

Peterson TC, et al. 1998. Homogeneity adjustments of *in situ* atmospheric climate data: A review. Int. J. Climatol. 18: 1493-1517.

Pettit AN. 1979. A non-parametric approach to the change-point detection. Applied Statistics, 28: 126-135.

Pickands J. 1975. Statistical inference using extreme order staitsitcs. Ann. Stat. 3: 119-131.

Plaut G, Simmonnet E. 2001. Large-scale circulation classification, weather regimes, and local climate over France, the Alps and Western Europe. Climate Ressearch 17: 303-324.

Plummer N, et al. 1999. Changes in climate extremes over the Australian region and New Zealand during the twentieth century. Climatic Change, 42: 183-202.

Preisendorfer RW. 1988. Principal component analysis in meteorology and oceanography. New York, Elsevier. 425 pp.

Quadrelli et al. 2001. Wintertime variability of Mediterranean precipitation and its links with large-scale circulation anomalies. Climate Dynamics 17: 457-466.

R Development Core Team (2006). R: A language and environment for statistical computing. R Foundation for Statistical Computing, Vienna, Austria. ISBN 3-900051-07-0, URL http://www.R-project.org.

Ray AA (ed.) .1982. SAS User's guide: Statistics, Cary, NC: SAS Institute.

Richman, M.B., 1986 – Rotation of principal components. Journal of Climatol. 6: 293-335.

Rohli RV, Keim BD. 1994. Spatial and temporal characteristics of extreme-high-summer-temperature events in the south-central United States. Physical Geography, 15 (4): 310-324.

Rummel, RJ. 1967. Understanding factor analysis. Journal of Conflict Resolution, 11 (4): 75-111.

Sahsamanoglou HS. 1990. A contribution to the study of action centers in the North Atlantic. Int. J. Climatol. 10: 247-261.

Salinger MJ, Griffiths GM. 2001. Trends in New Zealand daily temperature and rainfall extremes. Int. J. Climatol. 21: 1437-1452.

SAS. 1995. SAS User's Guide: Statistics. Cary, NC, SAS Institute.

Schüepp M. 1979. Klimatologie der Scweiz, Band III: Witterungsklimatologie. Zürich: Schweizerische Meteorologische Anstalt, 93 pp.

Sen PK. 1968. Estimates of the regression coefficient based on Kendall's tau. J. Amer. Statstical Assoc. 63: 1379-1389.

Serreze et al., 1997. Icelandic Low cyclone activity: Climatological features, linkages with the NAO, and relationships with recent changes in the Northern Hemisphere circulation. J. Climate10: 453-464.

Slonosky VC et al., 2000. Variability of the surface atmospheric circulation over Europe, 1774-1995. Int. J. Climatol. 20: 1875-1897.

Slonosky VC, Graham E. 2005. Canadian pressure observations and circulation variability: Links to air temperature. Int. J. Climatol. 25: 1473-1492.

Smith RL. 2003. Environmental statistics. Version 5.0 http://www.stat.unc.edu/postscript/rs/envnotes.ps

Soule PT, Suckling PW. 1995. Variations in heating and cooling degree-days in the south-eastern USA, 1960-1989. Int. J. CLimatol. 15: 355-367.

Stefanicki G, et al. 1998. Frequency changes of weather types in the Alpine region since 1945. Theor. Appl. Climatol. 60: 47-60.

Stone, RC. 1989. Weather types at Brisbane, Queensland: An example of the use of principal components and cluster analysis. Int. J. Climatol. 9: 3-32.

Tabony RC. 1983. Extreme value analysis in meteorology. The Meteorological Magazine, No. 1329, vol. 112: 77-98.

Thatcher WW. 1974. Effects of season, climate and temperature on reproduction and lactation. J. Dairy Sci. 57: 360-368.

Theil H. 1950. A rank-invariant method of linear and polynomial regression analysis, Part 3. Proceedings of Koninalijke Nederlandse Akademie van Weinenschatpen A. 53: 1397-1412.

Tomozeiu et al., 2002. Changes in seasonal mean maximum air temperature in Romania and their connection with large scale circulation. Int. J. Climatol. 22: 1181-1196.

Trigo et al., 2004. Climate impact of the European winter blocking episodes from the NCEP/NCAR Reanalyses. Climate Dynamics 23: 17-28.

Tuomenvirta H. 2001. Homogeneity adjustments of temperature and precipitation series – Finnish and Nordic data. Int. J. Climatol. 21: 495-506.

Van Bebber WJ, Köppen W. 1885. Die isobarentypen des Nordatlantischen ozeans und Westeuropas. Arch. Deutsch. Seewarte, 18, 27 pp.

Velev S. 1990. The climate of Bulgaria. (Klimatut na Bulgaria) "Narodna Prosveta", Sofia, 180 pp.

Velev S. 1996. Is Bulgaria becoming warmer and drier? GeoJournal 40, (4): 363-370.

Velev S. 1998. Trends in air temperature and precipitation changes in Bulgaria (Tendentsii na izmenenie na temperaturata na vuzduha I valejite v Bulgaria). Proceedings from the International Conference "100 years of Geography in Sofia University", Nature and natural resources, Sofia University Press, Sofia, 1998 (100 godini Geografia v Sofiiskia Universitet, Prirodna Sreda i prirodni resursi, Mejdunarodna Nauchna Konferentsia, Sofia, 1998)

Velev S. 2000. Global change and Bulgarian climate (Globalnite promeni i klimatut na Bulgaria). Proceedings from the International Scientific Session for the 50th anniversary of the Geographical Insitute, Sofia, Bulgaria. (Sbornik dokladi ot Mejdunarodna Nauchna sesia za 50-godshnina na Geografskia Institut, Sofia, Bulgaria).

Von Mises R. 1936. La distribution de la plus grande de *n* valeurs. Reprinted in *Selected Papers*, II, Amer. Math. Soc., Providence, R.I. (1954), 271-294.

Von Neumann J. 1941. Distribution of the ratio of the mean squre successive difference to the variance. Annals of Math. Statistics, 13: 367-395.

Werner PC, et al. 2000. Recent climate change in the North Atlantic/European sector. Int. J. Climatol. 20: 463-471.

Wibig J. 1999. Precipitation in Europe in relation to circulation patterns at the 500 hPa level. Int. J. Climatol. 19: 253-269.

Wijngaard JB, Klein Tank AMG, Können GP. 2003. Homogeneity of 20th century European daily temperature and precipitation series. Int. J. Climatol. 23: 679-692.

Wilks, D.S., 1995 – Statistical Methods in the Atmospheric Sciences. Academic Press.

Winkler J. 2004. The impact of technology upon in situ atmospheric observations and climate science. In Geography and Technology. St. Brunn, S. Cutter and JW Harringotn Jr. (eds.) Kluwer Academic Publishers.

Xoplaki et al., 2000. Connection between the large-scale 500 hPa geopotential height fields and precipitation over Greece during wintertime. Climate Research 14: 129-146.

Yarnal B. 1993. Synoptic climatology in environmental analysis. A Primer. London, Belhaven Press, 195 pp.

Zwiers FW, Ross WH. 1991. An alternative approach to the extreme value analysis of rainfall data. Atmosphere-Ocean 29 (3):437-461.

Zwiers FW, Kharin VV. 1998. Changes in the extremes of the climate simulated by CCC GCM2 under CO_2 doubling. J. Climate 11: 2200-2222.

Zwiers FW, von Storch H. 1999 – Statistical Analysis in Climate Research. Cambridge University Press, Cambridge.